The role of biodiversity for ecosystem functions in polar sea-ice ecosystems

Julia Ehrlich

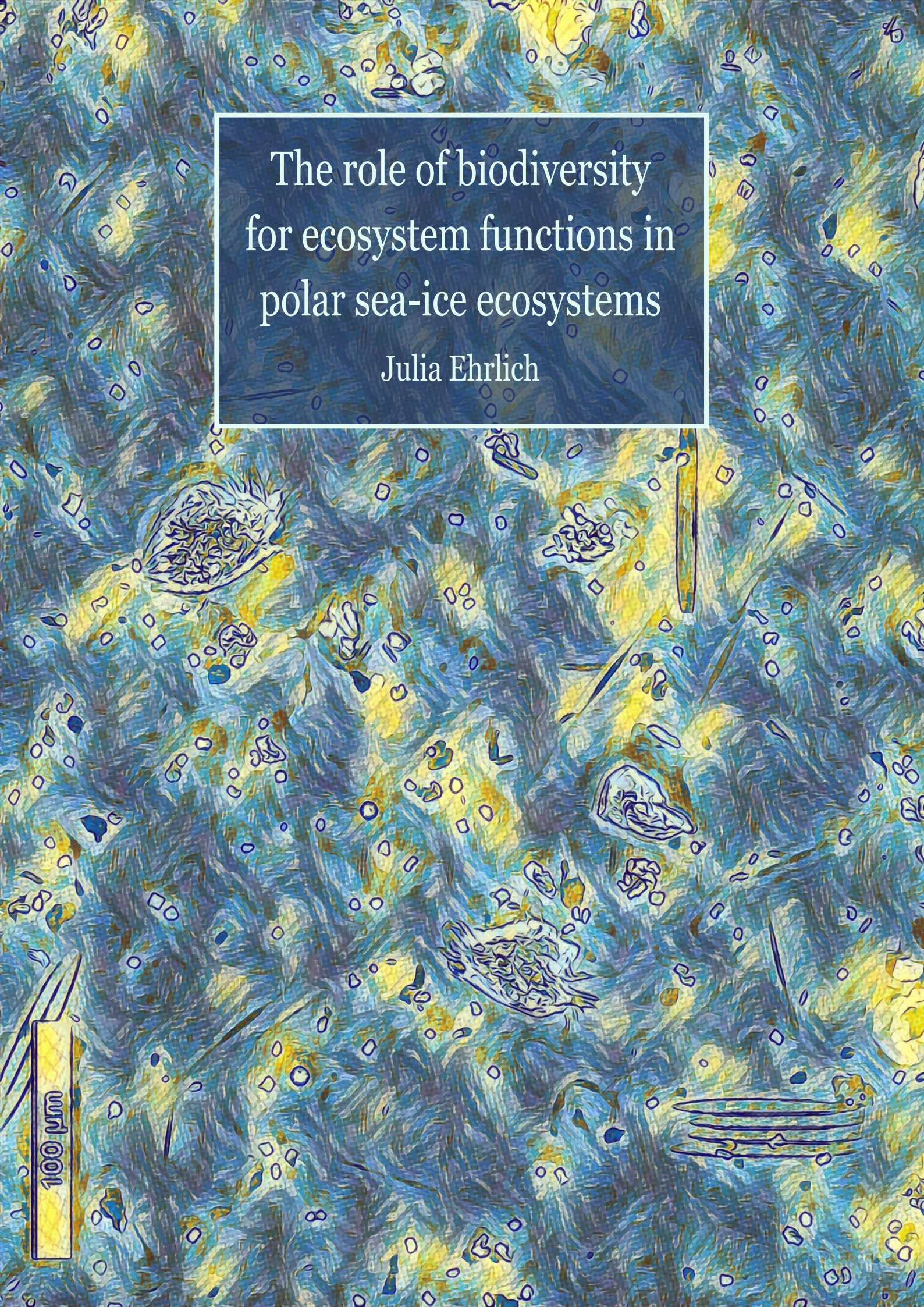

The role of biodiversity for ecosystem functions in polar sea-ice ecosystems

Dissertation

with the aim of achieving a doctoral degree
at the Faculty of Mathematics, Informatics and Natural Sciences
Department of Biology
University of Hamburg

submitted by

Julia Ehrlich

M.Sc. Marine Ecosystem and Fisheries Science
B.Sc. Biology

Hamburg 2021

Universität Hamburg
DER FORSCHUNG | DER LEHRE | DER BILDUNG

ALFRED-WEGENER-INSTITUT
HELMHOLTZ-ZENTRUM FÜR POLAR- UND MEERESFORSCHUNG

POLMAR
HELMHOLTZ GRADUATE SCHOOL FOR POLAR AND MARINE RESEARCH

UNIVERSITY OF TROMSØ

OGS
ISTITUTO NAZIONALE DI OCEANOGRAFIA E DI GEOFISICA SPERIMENTALE

PhD thesis defense date: 06.05.2021

PhD thesis defense committee members:

1. Chair **Prof. Christian Möllmann**
University Hamburg, Faculty of Mathematics, Informatics and Natural Sciences,
Institute of Marine Ecosystem and Fishery Science
Große Elbstrasse 133, 22767 Hamburg, Germany

2. Evaluator **Prof. Angelika Brandt**
Senckenberg Research Institute and Natural History Museum
Senckenberganlage 25**,** 60325 Frankfurt, Germany

3. Evaluator **Dr. Hauke Flores**
Alfred Wegener Institute Helmholtz Centre for Polar and Marine Research,
Am Handelshafen 12, 27570 Bremerhaven, Germany

4. Evaluator **Prof. Jörg Ganzhorn**
University Hamburg, Faculty of Mathematics, Informatics and Natural Sciences,
Institute of Zoology
Martin-Luther-King-Platz 3, 20146 Hamburg, Germany

5. Evaluator **Dr. Rolf Koppelmann**
University Hamburg, Faculty of Mathematics, Informatics and Natural Sciences,
Institute of Marine Ecosystem and Fishery Science
Große Elbstraße 133, 22767 Hamburg, Germany

Evaluators of the written PhD thesis:

1. Evaluator **Prof. Angelika Brandt**
Senckenberg Research Institute and Natural History Museum
Senckenberganlage 25**,** 60325 Frankfurt, Germany

2. Evaluator **Dr. Hauke Flores**
Alfred Wegener Institute Helmholtz Centre for Polar and Marine Research,
Am Handelshafen 12, 27570 Bremerhaven, Germany

“Difficulties are just things to overcome after all.”
— Ernest Shackleton

I dedicate this thesis to the past, present, and future women of my family.

Table of contents

Summary

In the Arctic Ocean, changes caused by global climate warming have been the focus of research for about two decades. Especially the decline and loss of sea ice, but also the increasing inflow of Atlantic Water into the Arctic Ocean or the northward shift of sea-ice formation, are studied processes related to climate change. Those physical changes will undoubtedly affect the Arctic marine ecosystem. Our knowledge of this unique ecosystem, though, is still incomplete, which makes it difficult to assess the consequences of ongoing climate change. More recently, the research focus has been on the importance of ice algae and phytoplankton for the Arctic marine food web. As the main primary producers, they constitute an important food source for many ice-associated (sympagic) species that rely on the ice-algal bloom in spring and the phytoplankton bloom in summer. Sympagic species are important transmitters of carbon from the sea-ice to pelagic and benthic communities. In order to assess the consequences of environmental changes for sympagic communities, we need to broaden our basic understanding of underlying ecosystem functions, such as biomass or carbon cycling.

Following this goal, we used a unique approach to measure physical parameters and sample sympagic organisms of the sea-ice and under-ice environment in the Eurasian Basin. We combined sea-ice coring and trawling with the Surface and Under-ice Trawl. The latter is equipped with an array of sensors to measure environmental parameters, e.g., sea-ice thickness, water temperature, salinity, and chlorophyll *a* concentration, whilst collecting fauna.

The **overarching aim** of this study is to further our understanding of the Arctic sympagic ecosystem regarding its biodiversity and related ecosystem functions in the Eurasian Basin. Specific objectives are to *1)* generate a quantitative inventory of the biodiversity, community structure, and abundance of sea-ice meiofauna and under-ice fauna, *2)* characterize physical habitat properties over large scales to identify environmental parameters of the sympagic environment that structure both sympagic communities, *3)* assess ecosystem functions (biomass, production, consumption) of the sympagic communities with a focus on carbon budgets and food web efficiency.

Chapter I adresses objectives *1)* and *2)* as it provides a quantitative inventory of sea-ice meiofauna and under-ice fauna taxa in the Eurasian Basin in spring 2015. The dominating taxa were Harpacticoida for the sea-ice and *Calanus* species for the under-ice community. Except for a hyperabundance event, also other changes in community composition compared to earlier studies could be detected. Geographical regions were identified as the

most relevant parameter in structuring both sympagic communities. ***Chapter II*** focuses on objective *2)*. It provides a set of large-scale physical and biological sea-ice and under-ice water properties of both hemispheres. The results of the two relevant expeditions for this thesis constituted the base for the assessment of correlations between environmental parameters and community composition of the sympagic fauna for ***Chapter I*** and ***Chapter IV***. ***Chapter III*** addresses objective *3)* as it provides a compilation of the carbon budget (carbon biomass, demand, and production rates) of the sympagic community in the Eurasian Basin in spring 2015. The carbon produced by ice algae and phytoplankton was more than sufficient to cover the demand of the sympagic grazers. The under-ice fauna, especially *Calanus* species, was the main contributor to the cryo-pelagic carbon flux, whereas sea-ice meiofauna played a minor role. The secondary production was hardly sufficient for the carnivorous under-ice fauna, mainly Chaetognatha, in this study and could therefore force them to evade to deeper layers to fulfill their carbon demand. ***Chapter IV*** complements objective *3)* as it summarizes the findings of another SUIT study from the Eurasian Basin in summer 2012 and gives estimations on the total carbon budget of the under-ice fauna. Geographical regions were identified as the main parameter in structuring the under-ice community, which addresses objective *2)* and supports our findings in ***Chapter I***. ***Chapter V*** addresses objective *3)*. The generation of important allometric equations of key taxa of the sympagic ecosystem constituted the groundwork of ***Chapter V***, which was used for some of the biomass estimations in ***Chapter III*** and ***Chapter IV***. The equations can be used in future studies and warrant accurate biomass estimates.

In **summary**, our results show that the sympagic fauna comprises a mixture of taxa of sea-ice, pelagic, or benthic origin. The under-ice fauna indicated a switch to predominantly boreal Atlantic species attributed to the ongoing Atlantification. Loss of former abundant or dominant taxa was detected for both sympagic communities, likely caused by environmental changes due to climate warming. The sympagic community was mainly structured by geographical regions, but also sea-ice thickness played a role. Primary production was sufficient to fulfill the carbon needs of the sympagic grazers and sea-ice algae constituted an important carbon source. The secondary production was hardly sufficient for the demand of carnivorous under-ice taxa, leading to the assumption that predators need to evade to deeper layers to fulfill their carbon demand. Due to the close connectivity of the sympagic and the pelagic communities, the mentioned changes will consequently impact the entire ecosystem.

Zusammenfassung

Im Arktischen Ozean stehen die durch die globale Klimaerwärmung verursachten Veränderungen seit etwa zwanzig Jahren im Fokus der Forschung. Die Abnahme der Meereisausdehnung und -dicke, aber auch die Zunahme des Einstroms von atlantischen Wassermassen in den Arktischen Ozean sind wichtige Prozesse, die mit dem Klimawandel zusammenhängen. Derartige physikalische Veränderungen werden sich zweifellos auf das marine Ökosystem der Arktis auswirken. Unser Wissen über dieses einzigartige Ökosystem ist jedoch unvollständig. Dadurch sind die Folgen des Klimawandels nur schwer abzuschätzen. In jüngster Zeit wird vor allem die Bedeutung von Eisalgen und Phytoplankton für das marine Nahrungsnetz erforscht. Als Hauptprimärproduzenten bilden sie eine wichtige Nahrungsquelle für die eisassoziierte (sympagische) Fauna. Diese ist auf die Eisalgenblüte im Frühjahr und die Phytoplanktonblüte im Sommer angewiesen. Die sympagische Fauna ist essentiell für den Kohlenstofftransport vom Meereis zu den pelagischen- und benthischen Gemeinschaften. Um die Folgen der Umweltveränderungen für das sympagische Ökosystem abschätzen zu können, müssen wir unser Wissen über grundlegende Ökosystemfunktionen, zum Beispiel über den Kohlenstoffkreislauf, erweitern. Dieser Absicht folgend, haben wir einen innovativen Ansatz zur Messung physikalischer Parameter sowie zur Beprobung sympagischer Organismen gewählt, indem wir Eiskernbohrungen und die Verwendung des Surface and Under-Ice Trawl (SUIT) kombinierten. Letzteres nutzt eine Reihe von Sensoren zur Messung von Umweltparametern während es gleichzeitig die Fauna beprobt.

Ziel dieser Dissertation ist die Wissenserweiterung über die Biodiversität und die damit verbundenen Ökosystemfunktionen des sympagischen Ökosystems im Eurasischen Becken. Spezifische Ziele sind: *1)* die Erstellung eines quantitativen Inventars der Biodiversität sowie der Abundanz der Ineis- und Untereisfauna, *2)* die Charakterisierung der physikalischen Habitateigenschaften und die Ermittlung der bedeutendsten Habitateigenschaften für die Strukturierung der sympagischen Fauna, *3)* die Analyse von Ökosystemfunktionen der sympagischen Gemeinschaft mit Fokus auf das Kohlenstoffbudget und den Kohlenstoffffluss.

Kapitel I adressiert die Ziele *1)* und *2)*, da es eine quantitative Bestandsaufnahme der Ineis- und Untereisfauna des Eurasischen Beckens im Frühjahr 2015 enthält. Die dominierenden Taxa waren Harpacticoida für die Ineisfauna und *Calanus* spp. für die Untereisfauna. Neben einem Hyperabundanz-Ereignis konnten auch andere Veränderungen in der Gemeinschaftsstruktur im Vergleich zu früheren Studien festgestellt werden. Geografische Regionen wurden als relevantester strukturierender Parameter

beider sympagischer Gemeinschaften identifiziert. ***Kapitel II*** konzentriert sich auf Ziel *2)*. Hier werden eine Reihe von großräumigen physikalischen und biologischen Eis- und Oberflächenwassereigenschaften analysiert. Die Ergebnisse der beiden, für diese Arbeit relevanten, Expeditionen, bilden die Grundlage für die Korrelationsanalyse zwischen ausgewählten Umweltparametern und der Gemeinschaftsstruktur der sympagischen Fauna in ***Kapitel I*** und ***Kapitel IV***. ***Kapitel III*** adressiert Ziel *3)*. Hierin wird ein Kohlenstoffbudget der sympagischen Gemeinschaft des Eurasischen Beckens im Frühjahr 2015 erstellt. Der von Eisalgen und Phytoplankton produzierte Kohlenstoff überstieg den Bedarf sympagischer Herbivorer deutlich. Die von *Calanus*-Arten dominierte Untereisfauna trug hauptsächlich zum kryo-pelagischen Kohlenstofffluss bei, während die Ineisfauna eine untergeordnete Rolle spielte. Für die karnivore Untereisfauna war die sympagische Sekundärproduktion kaum ausreichend. Dies könnte deren Ausweichen in tiefere Schichten erzwingen. ***Kapitel IV*** ergänzt Ziel *3)*. Hierin werden die Ergebnisse einer weiteren SUIT-Studie aus dem Eurasischen Becken im Sommer 2012 zusammenfasst und Abschätzungen zum Gesamtkohlenstoffbudget der Untereisfauna gegeben. Auch hier waren geografische Regionen der Hauptparameter für die Strukturierung der Untereisgemeinschaft (Ziel *2)*). ***Kapitel V*** bezieht sich auf Ziel *3)*. In diesem Kapitel wurden wichtige allometrische Gleichungen für sympagische Schlüsseltaxa erstellt, welche die Grundlage für einige der Biomasseschätzungen in ***Kapitel III*** und ***Kapitel IV*** bildeten. Diese Gleichungen gewährleisten die Genauigkeit zukünftiger Biomassenberechnungen.

Zusammengefasst zeigen unsere Ergebnisse, dass die sympagische Fauna aus Organismen eisassoziierter, pelagischer und benthischer Herkunft zusammengesetzt war. Die Untereisfauna wurde von boreal-atlantischen Arten dominiert. Dies weist auf die fortschreitende Atlantifizierung hin. In beiden sympagischen Gemeinschaften wurde ein Rückgang ehemals dominanter Taxa festgestellt. Ursache hierfür könnten veränderte Eisbedingungen sein. Die Struktur der sympagischen Gemeinschaft wurde durch geografische Regionen und die Meereisdicke bestimmt. Die Primärproduktion war ausreichend, um den Kohlenstoffbedarf sympagischer Herbivorer zu decken. Meereisalgen stellten eine wichtige Kohlenstoffquelle dar. Die Sekundärproduktion deckte nur knapp den Bedarf der karnivoren Untereisfauna. Aufgrund der engen Verflechtung sympagischer und pelagischer Lebensgemeinschaften können sich die beschriebenen Veränderungen auf das gesamte Ökosystem auswirken.

Abbreviations

AW	Atlantic Water
C	Carbon
Chl *a*	Chlorophyll *a*
DOC	Dissolved organic carbon
FYI	First-year sea ice
Ind.	Individuals
MYI	Multi-year sea ice
PAR	Photosynthetically active radiation
POC	Particulate organic carbon
PP	Primary production
PSW	Polar Surface Water
ROV	Remotely Operated Vehicle
SP	Secondary production
SIE	Sea-ice extent
SUIT	Surface and Under-Ice Trawl

1 General introduction into the research field

1.1 The Arctic Ocean

The Arctic Ocean is a mediterranean sea surrounded by the European, Asian, and North American continents. Its only deep gateway to the world oceans is the Fram Strait between Svalbard and Greenland with depths of up to 2.6 km and a width of 600 km (Aagard and Greisman, 1975). Other, shallower, gateways to the Arctic Ocean are the Bering Strait, the Barents Sea Opening, and the channels of the Canadian Arctic Archipelago. The Arctic Ocean covers an area of ~ 14 Mio. km² and is surrounded by extensive shelves that make up 53% of its area (Jakobsson et al., 2004). The deep central region of the Arctic Ocean is separated by the Lomonosov Ridge (with a sill depth of ~ 1600 m) into two major basins, the Eurasian Basin and the Amerasian Basin. While the Amerasian Basin includes the Makarov Basin (~ 4000 m deep) and the Canada Basin (~ 3800 m deep), the Eurasian Basin, is divided by the Gakkel Ridge into two basins named Nansen Basin (~ 4000 m deep) and Amundsen Basin (~ 4500 m deep) (Rudels, 2015). Upper-ocean water in the Amerasian Basin originates from the inflow of Pacific Water via Bering Strait, whereas the water in the Eurasian Basin originates from the inflow of Atlantic Water (AW) via the Barents Sea and Fram Strait. The region of the AW inflow north of Svalbard represents the main area of interest of this thesis.

Nutrient-rich and warm AW is carried into the Arctic Ocean by a warmer and saline Fram Strait inflow branch and a cooler and fresher Barents Sea inflow branch (Rudels et al., 2013; Carmack et al., 2015). The former branch enters the Arctic Ocean via eastern Fram Strait with the West Spitsbergen Current, the latter branch flows into the Barents Sea and enters the deep Arctic Ocean through the St. Anna Trough in the Kara Sea (Figure 1) (Aagaard et al., 1973). The two AW branches flow together in the northern Kara Sea where they follow the Eurasian continental slope with the Arctic Circumpolar Boundary Current (Figure 1) (Jones et al., 1998; Carmack et al., 2015). When entering the Arctic Ocean, the AW is cooled down and gets isolated from the sea ice by a layer of nutrient-depleted, less saline, and cooler Polar Surface Water (PSW) (Anderson et al., 1994). The PSW is found in the upper 50 m of the Arctic Ocean, whereas the (intermediate) AW layer can be detected throughout the Arctic Ocean in ~ 150 to 900 m depth below a pronounced cold halocline (Rudels et al., 1994; Carmack et al., 2015; Polyakov et al., 2020b). This halocline is either formed by brine-driven convection or by injection of cold salty shelf waters (Steele and Boyd, 1998). Two major surface current systems determine the drift of the PSW and the sea ice: the Beaufort Gyre and the Transpolar Drift (Figure 1). The latter advects surface water and sea ice from the Siberian shelves towards the Fram Strait, where they are carried out of the Arctic Ocean

into the North Atlantic via the East Greenland Current (Nansen, 1905; Krumpen et al., 2019). The deepest parts of the Arctic Ocean basins (> 1,000 m depth) are filled with very saline Arctic Deep Water (ADW, not shown). The exchange of ADW between the Eurasian Basin and the Makarov Basin is restricted by the Lomonosov Ridge, which results in significant differences in temperature and salinity between both basins (Anderson et al., 1994).

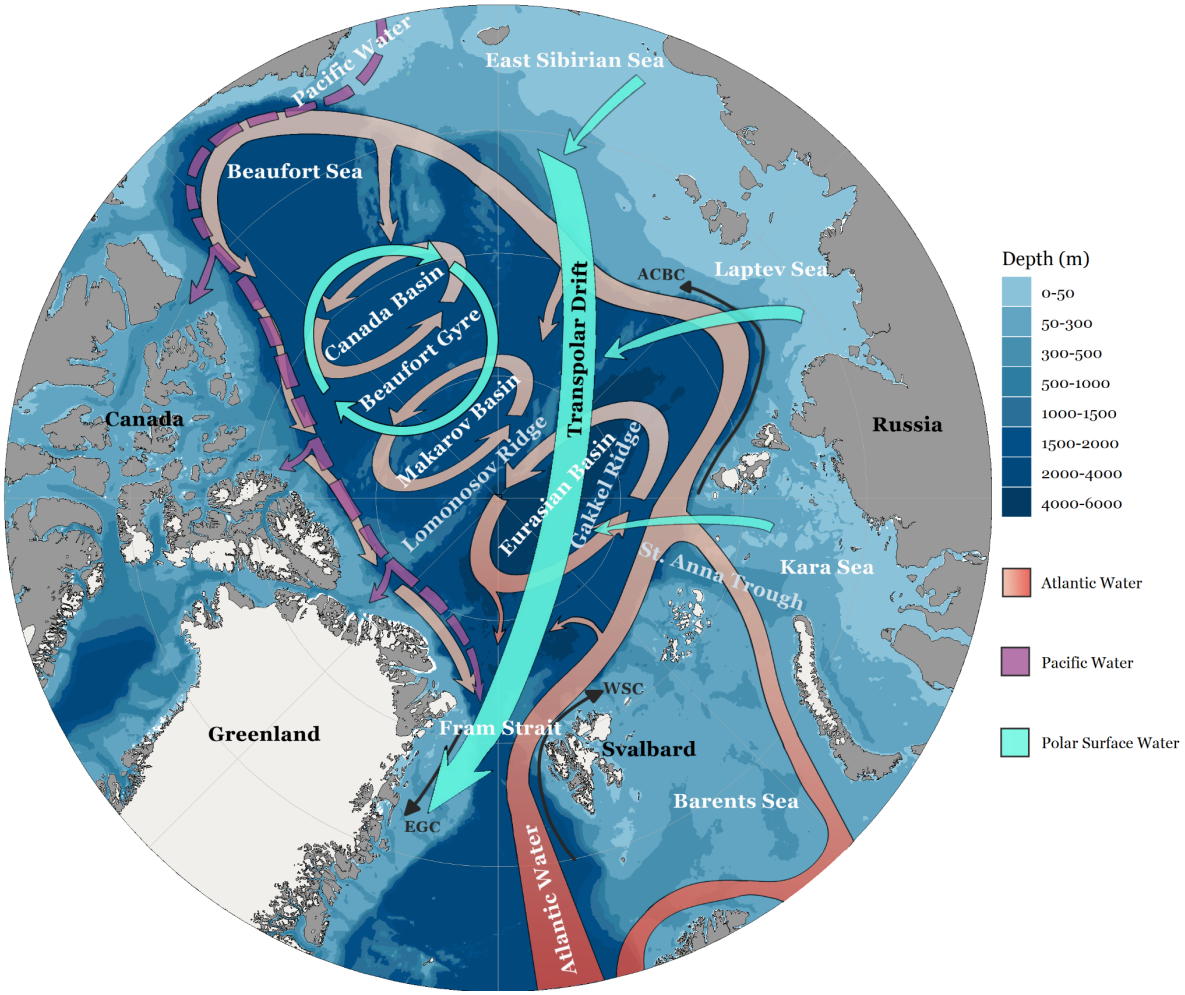

Figure 1. Map of the Arctic Ocean summarizing the major basins, marginal seas, and surface currents as well as the inflows of AW and PW and the Transpolar Drift (The map was modified after Carmack et al., 2015). EGC=East Greenland Current, WSC= West Spitzbergen Current, ACBC= Arctic Cyclonic Boundary Current.

A unique characteristic of the polar oceans is sea ice. In the Arctic Ocean, part of the sea ice is formed along the shelves before it is pushed by winds and surface currents from shallower coastal zones into the deep basins (Pfirman et al., 1997). Sea ice that is attached to the coastline, to the sea floor, or to grounded icebergs is referred to as 'landfast ice', whereas sea ice that drifts with wind and currents is referred to as 'pack-ice'. The extent of the Arctic sea ice reaches its minimum in summer and its maximum in winter but shows a strong reduction in the last decades (Serreze et al., 2007; Haas et al., 2008; Kwok et al., 2009), together with a loss of older and thick ice (Kwok et al., 2009; Comiso, 2012; Rabenstein et al., 2010). When First-year ice (FYI) survives the annual cycles of freezing in

winter and melting in summer, it becomes Multi-year ice (MYI). Today, a high occurrence of MYI can primarily be found in high Arctic deep-sea regions (> 78°N in the Eurasian Basin) with bottom depths of more than 4000 m, which are permanently ice covered, while the remaining Arctic Ocean is covered with FYI in winter months. The growth, melt, horizontal transport, and deformation processes of the sea ice make it a highly dynamic feature of the Arctic Ocean. By insulating the subjacent ocean from the cold polar atmosphere, sea ice reduces the convective heat exchange between ocean and atmosphere. Because of its bright color, sea ice reflects more incoming solar radiation than the open water. The ratio between the reflected and the incoming solar radiation is called 'albedo'. Consequently, sea ice has a higher albedo than the ocean. An increased area or longer periods of open water would, therefore, decrease the albedo and result in (further) sea-ice melting and warming of the Arctic Ocean (Pistone et al., 2014). Sea ice also plays a role in the regulation of uptake and emission of climate-relevant gases, such as carbon dioxide. It acts, for example, as a sink for carbon dioxide during spring and summer mainly due to brine dilution and as a source during winter (Lannuzel et al., 2020). All these processes are important for the exchange of energy and transport of mass in the Arctic Ocean and play a major role in recent Arctic changes.

1.2 The New Arctic

The Arctic Ocean is facing drastic environmental changes caused primarily by climate warming (Meredith et al., 2019). Temperatures are rising much faster than at lower latitudes and climate-driven changes appear first in the Arctic region (Broccoli and Manabe, 1987; Landrum and Holland, 2020), a phenomenon which is referred to as 'polar amplification'. Retreat and thinning of the sea ice are attributes of the changing Arctic in the past decades (Kwok et al., 2009; Comiso, 2012; Polyakov et al., 2017). In the past 13 years, the annual minimum sea-ice extent (SIE) has been lower than in any other year since the beginning of the satellite era (Landrum and Holland, 2020). From 1979 - 2012 the September SIE has been decreasing at a rate of 14% per decade in almost the entire Arctic Ocean (Overland and Wang, 2013), which is forecast to be ice free in summer by latest 2100 (Landrum and Holland, 2020; 'Ice-free' is generally defined as when SIE falls below 1 Mio. km²). In September 2012, Arctic sea-ice extent and thickness reached a record low since satellite observations started (Parkinson and Comiso, 2013). Due to enhanced melt of sea-ice in the marginal zones of the Arctic Ocean, less sea ice survives the transport with the Transpolar Drift. Instead, the sea-ice is released already in the northern Laptev Sea or in the central Arctic Ocean because the thinning ice cover results in a faster break up by winds and waves (Krumpen et al., 2019). The ice, which reaches the Fram Strait area, is, therefore, mainly newly formed ice from the central Arctic Ocean (Krumpen et al., 2019).

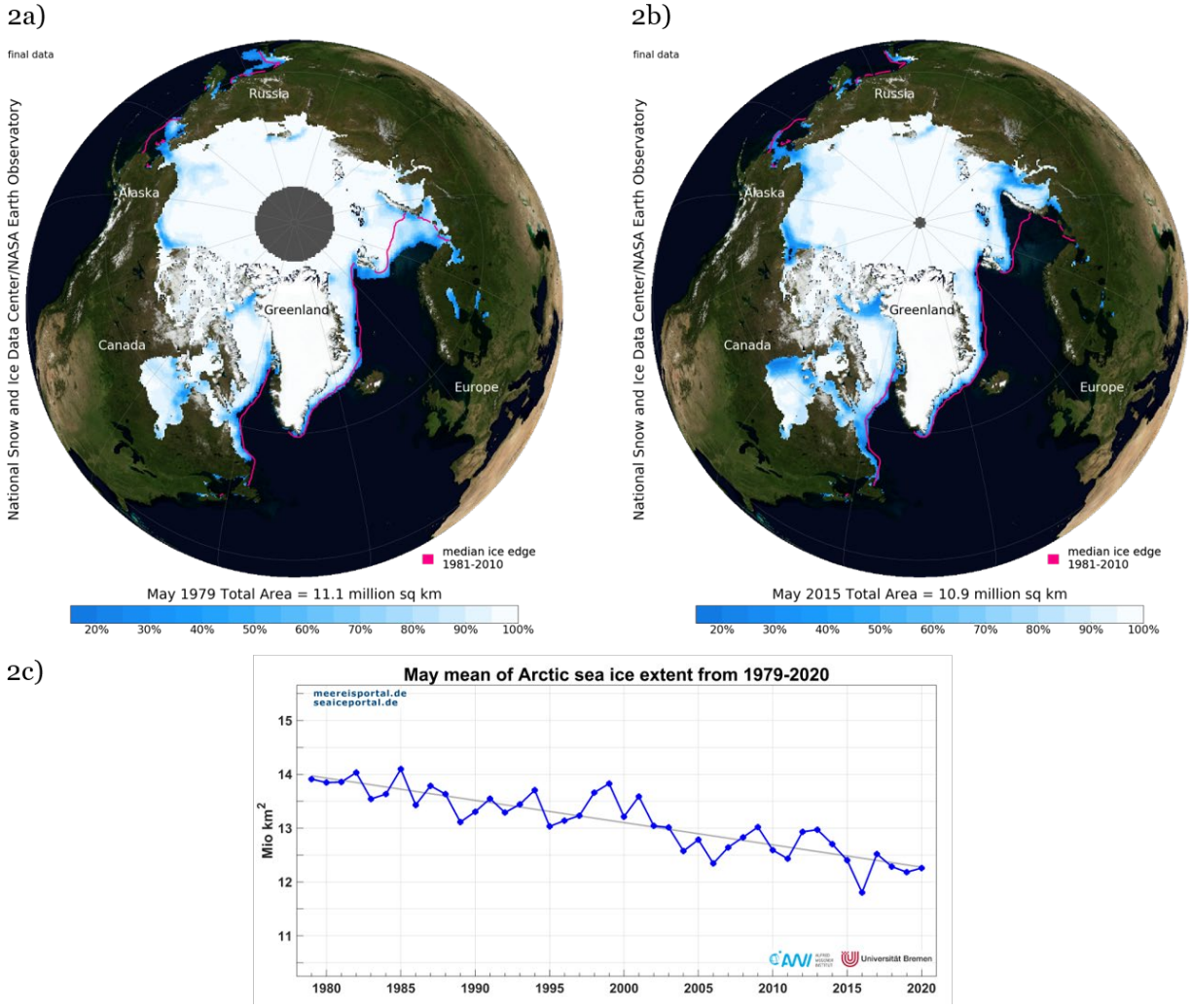

Figure 2. Maps of the Arctic Ocean comparing the mean sea-ice extent for the month May 2a) in 1979 and 2b) in 2015; the red line indicates the median SIE for the period 1981 to 2010 (figures acquired from NSIDC). 2c) shows the trend of the Arctic sea-ice extent as yearly mean for the month May from 1979-2020; the blue line represents measured values in Mio. km²; the grey line represents the approximated linear decline (figure taken from www.meereisportal.de).

The major heat supply to the Arctic Ocean is provided by the inflow of warm AW (Beszczynska-Möller et al., 2012). Enhanced inflow and warming temperatures of the AW have been observed since the 2000's, a phenomenon which is often referred to as 'Atlantification'. An attribute of the Atlantification is the weakening of the halocline as a result of a positive ice/ocean-heat feedback in the Eurasian Basin (Polyakov et al., 2020b): Enhanced melting of sea ice results in increased ventilation of the AW during winter, which weakens the halocline stratification. This, in turn, results in more heat release to the sea surface, which causes further sea-ice melt (Manabe and Stouffer, 1980). In the 2010s, a threshold in the warming trend of the AW was passed and resulted in the loss of the function of the halocline as an effective barrier between the PSW and the AW heat (Polyakov et al., 2017). As a consequence, Atlantification contributes significantly to sea-ice melt in the Arctic Ocean (Kwok et al., 2009; Ivanov et al., 2012; Polyakov et al., 2017). Another attribute of the Atlantification is the positive ice/albedo feedback (Manabe and

Stouffer, 1980): The reduced sea-ice extent results in decreased albedo when solar radiation is no longer reflected at the sea-ice surface but absorbed from open water. Thus, more solar radiation reaches the surface environment in summer and further contributes to a warming ocean. Consequently, the Arctic sea-ice regime has become increasingly seasonal in the 2010s switching from a perennial MYI-dominated system to an annual FYI system (Serreze et al., 2007; Kwok et al., 2009), the so-called 'New Arctic' (Carmack et al., 2015; Granskog et al., 2020).

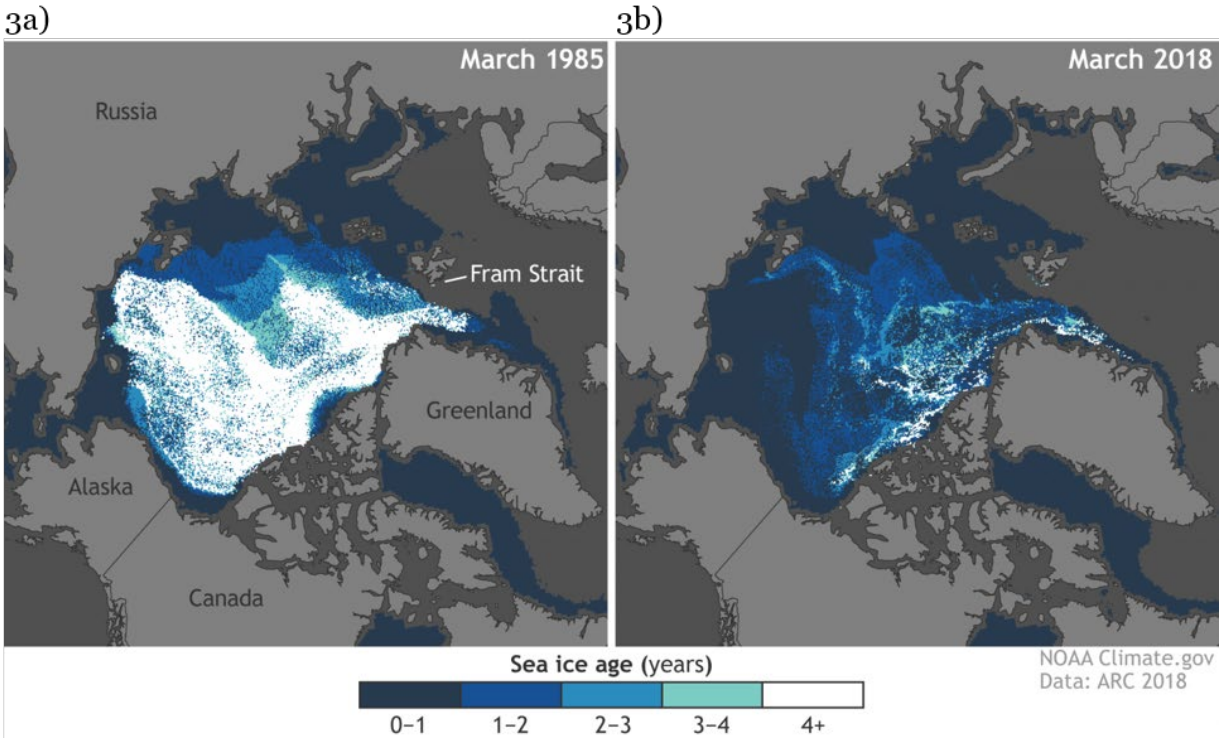

Figure 3. Map of the Arctic Ocean displaying the sea-ice age in March 3a) 1985 and 3b) 2018 (figure acquired from NSIDC, data based on NOAA, 2018).

1.3 The history of sampling the sea-ice environment

For a long time, the sea ice of the Arctic Ocean was considered an inanimate desert. Only in the 19th century, when German naturalist and protozoologist Christian Gottfried Ehrenberg found brown-colored sea ice, the interest in discovering this unique environment awoke (Ehrenberg, 1853). Ehrenberg analyzed the ice and showed that algae, especially diatoms, were responsible for the greenish coloring. Fridtjof Nansen was the first who reported the occurrence of ciliates in Arctic sea ice after his famous FRAM expedition between 1893 and 1896 (Nansen, 1905). While the early studies mainly concentrated on algae, a more intensive study period of the sea-ice meiofauna began in the 1980's (Melnikov and Kulikov, 1980; Carey, 1985; Gulliksen and Lønne, 1989). Since then, there have been various documentations about the biodiversity of sea-ice biota in the Arctic Ocean (Friedrich, 1997; Gradinger, 1999; Nozais et al., 2001; Gradinger et al.,

2005; Bluhm et al. 2010, 2017; Poulin et al., 2011) and recently a quantitative pan-Arctic synthesis of sea-ice meiofauna composition and abundance has been published (Bluhm et al., 2018). However, the Polar Regions are still under-sampled and especially studies on biomass and production rates of sea-ice fauna are still sparse (Gradinger, 1999; Kramer, 2011; Gradinger and Bluhm, 2020), as are studies with a focus on responses of sea-ice biota to the described changes since the 2000's. The sampling of sea-ice meiofauna is based on sea-ice coring and microscopic analysis, a successful combination that has been used for decades, but also on modern technologies like Remotely Operated Vehicles (ROV). Besides microscopy, molecular techniques have been used recently to determine the diversity of sea-ice biota (Collins et al., 2010; Hardge et al., 2017).

During the first ~ 80 years of Arctic zooplankton research, organisms were collected from drifting ice platforms or ships frozen into the ice. Within this period of sporadic data collection, basic knowledge on the major parameters and seasonal dynamics of the zooplankton communities of the Arctic Ocean was obtained (Brodsky, 1967; Matthews and Hestad, 1977; Bradstreet and Cross, 1982; Tande and Båmstedt, 1985). In the last three decades, biological observations on under-ice fauna in the Arctic Ocean have increased markedly (Werner and Arbizu, 1999; Poltermann et al., 2000; Werner and Auel, 2005; Werner, 2006; Bluhm et al., 2010; Hop et al., 2011). Ice-breakers allow access to even permanently ice-covered regions, such that large-scale and efficient sampling can be accomplished nowadays, albeit with major logistical effort. This century's interdisciplinary research has brought a breakthrough in understanding the relationships between the structure of pelagic communities with hydrographic processes and environmental factors (Kosobokova and Hirche, 2009). Investigations of under-ice fauna have largely been based on under-ice pumping systems or semi-quantitative observations by SCUBA divers sampling on relatively small spatial scales (Werner, 2006; Gradinger and Bluhm, 2004). For the last few years, repeated and quantitative mesoscale sampling of the sea-ice underside (3.000-5.000 m^2 per haul) has been possible with the Surface and Under-Ice Trawl (SUIT; van Franeker, 2009; Flores et al., 2012), a tool also used in the present study. Additionally, the SUIT is equipped with a state-of-the-art environmental sensor array to accurately map under-ice habitat properties. The first basin-wide analysis of the relationship of the under-ice community structure with sea-ice properties in the Arctic Ocean was published by David et al. (2015).

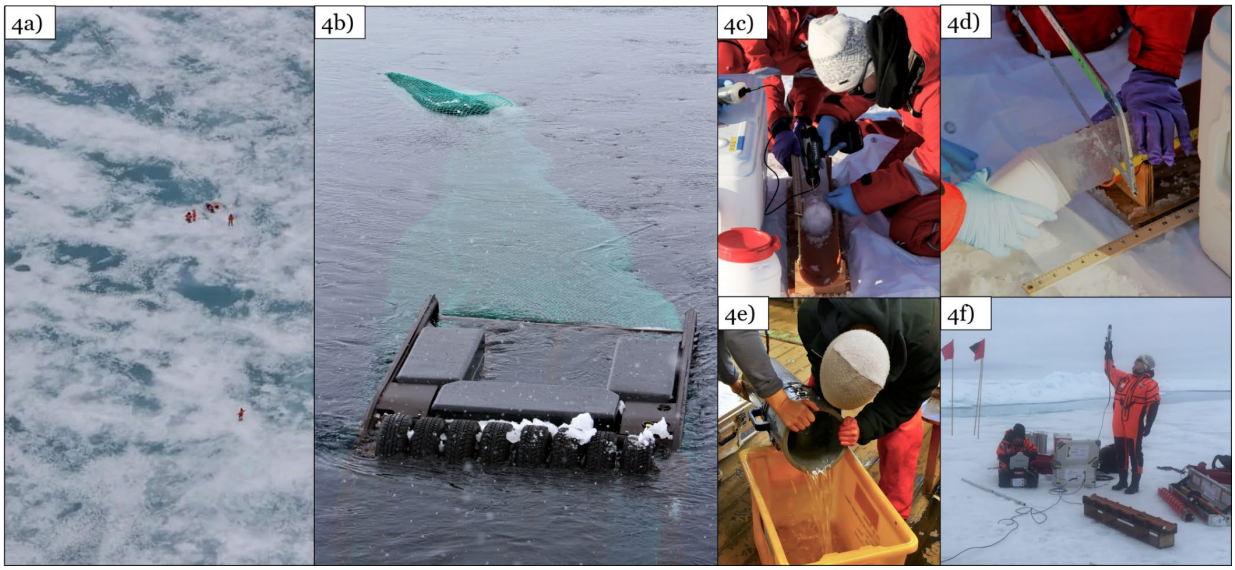

Figure 4. Pictures of different sampling methods of the sympagic environment: 4a) scanning the ice floe for a suitable place, b) SUIT in the water, c)-d) Ice-core processing e) SUIT-catch processing 4f) light measurements on the floe (photo credits: 4a) Bram Fey, 4b) Hans Verdat, 4c)-d) Matthias Gottschalk)

1.4 Sea ice as habitat

Besides its essential role in regulating earth's climate and weather (Liu, 2012; Dethloff et al., 2019; Lannuzel et al., 2020), sea ice constitutes a substrate for sea-ice associated ('sympagic') organisms, which live inside, attached to or associated with the sea ice for at least a part of their life cycles. Their taxonomic range extends from prokaryotes to large marine mammals, though this thesis focuses on invertebrates in the mm to cm range. In the Arctic Ocean, an inventory of invertebrate species counted more than 50 meio- and macrofauna species in the sympagic environment (Bluhm et al., 2010).

During sea-ice formation, salt ions are rejected from the growing ice crystals in form of highly saline brine with very low freezing temperatures. The brine resides in little channels and cavities inside the sea-ice matrix (Weissenberger et al., 1992; Eicken, 2003). Small organisms such as prokaryotes, ice algae, other protists, or very small metazoans can inhabit those channels and cavities (Kramer, 2011). Through phases of sea-ice melt or growth, these organisms can be released back into the water column or refrozen into the newly forming sea ice. For the purpose of this thesis, the term 'sea-ice meiofauna' refers to heterotrophic protists and small metazoans that live inside the brine channels and cavities of the sea ice. The bulk biomass of ice algae and sea-ice meiofauna can be found in the bottom few centimeters of the sea ice, where temperature and nutrient concentration are highest and salinity is lowest (Gradinger et al., 2009; Bluhm et al., 2011). Common protozoan taxa in the sea ice are Ciliophora, Foraminifera, Radiolaria, and heterotrophic Dinoflagellata. The metazoan sea-ice fauna comprises mainly Harpacticoida, Acoela, Rotifera, Nematoda, and, in coastal areas, larvae of Polychaeta and Mollusca (Friedrich,

1997; Schnack-Schiel, 2003; Bluhm et al., 2010; Caron and Gast, 2010; Marquardt et al., 2011). Over the past decade, several first records of sea-ice meiofauna taxa from Arctic sea ice, even at the phylum level, indicate that sea-ice biodiversity research is still in the exploratory phase of science (Kiko et al., 2008; Marquardt et al., 2018).

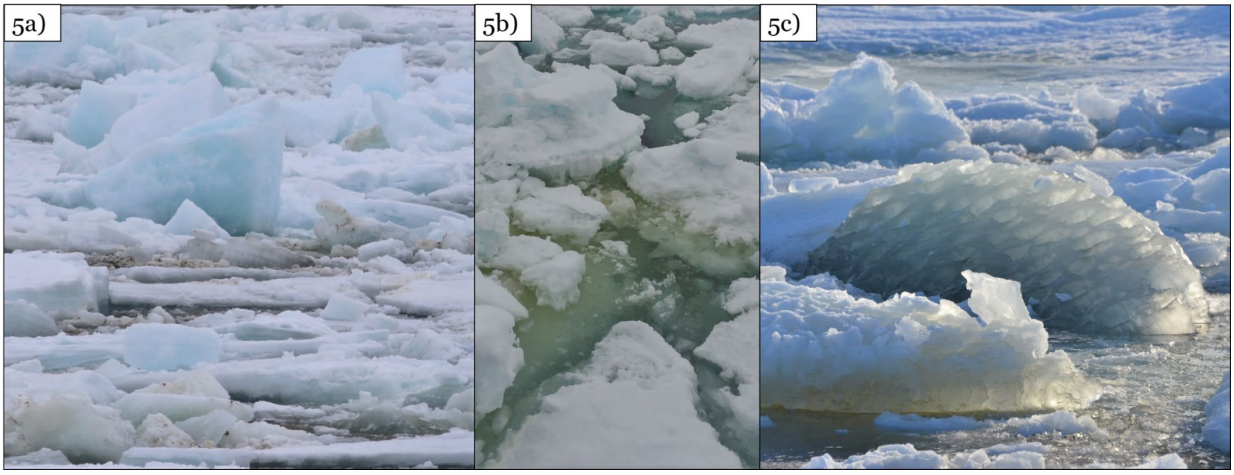

Figure 5. Exemplary pictures of Arctic sea ice in spring 5a-b) with brown-greenish algal coloring, and 5c) with brine channels in the advanced phase of melting (photo credit Fokje L. Schaafsma).

Larger taxa such as large zooplankton species are too large to enter the brine system but still use the sea-ice-water interface as habitat (Gulliksen and Lønne, 1991; Arndt and Swadling, 2006). For the purpose of this thesis, the term 'under-ice fauna' refers to metazoans using the ice-water interface as a habitat, at least temporarily. Common taxa of the under-ice fauna in the Arctic Ocean are copepods (Calanoida, Cyclopoida, Harpacticoida), Amphipoda, Euphausiacea, Chaetognatha, Ctenophora, and Polar cod (*Boreogadus saida*) (Bluhm et al., 2010). Although mostly calanoid copepods dominate the under-ice communities, Amphipoda are the most studied organisms of this habitat (Poltermann et al., 2000; Beuchel and Lønne, 2002; Hop et al., 2011; David et al., 2015; Kunisch et al., 2020). The Arctic Ocean hosts two origins of zooplankton communities: an autochthonous community and an allochthonous community of expatriates of Atlantic or Pacific origin (Kososbokova and Hirche, 2000; Kosobokova et al., 2011). In the region of interest for this thesis, sub-Arctic and boreal North Atlantic zooplankton species are transported through the Norwegian and Greenland Seas towards the Fram Strait and from there into the Arctic Ocean (e.g., zooplankton transport in May 2014 was ~ 34 kg C s^{-1}, Basedow et al., 2018). Consequently, one of the three *Calanus* species, which mostly dominate the under-ice community, is considered to be of Atlantic origin (*Calanus finmarchicus*), whereas two are considered to be of true Arctic origin (*Calanus hyperboreus* and *Calanus glacialis*) (Conover, 1988; Auel and Hagen, 2002; Hirche and Kosobokova, 2007; Wassmann et al., 2015).

Under-ice fauna has developed sophisticated life-history strategies to survive and reproduce in a habitat characterized by frigid temperatures, a perennial or seasonal sea-ice cover, limiting nutrients in the surface layer, and an extremely pulsed cycle of primary production (Conover and Huntley, 1991; Darnis et al., 2012). The main Arctic *Calanus* species (*C. glacialis and C. hyperboreus*) migrate from the upper water masses to deeper layers for overwintering in diapause (Hirche, 1997; Søreide et al., 2010), which results in a shift of zooplankton composition in the surface layer from dominance of large copepods to dominance of small-sized zooplankton during winter (Hansen et al., 1999). Unlike the large *Calanus* spp., small copepods (e.g., *Oithona* spp.) mostly stay active during the long Arctic winter (Madsen et al., 2008) and do not perform extensive seasonal vertical migration in the Arctic Ocean (Fortier et al., 2001). In the following spring, *C. glacialis* and *C. hyperboreus* do use the under-ice environment as a nursing ground and time nauplii development with the springtime peak of primary production (Hirche, 2013). In contrast to *Calanus* species, the amphipod *Apherusa glacialis* is considered to have a semelparous reproduction strategy and the ability to inhabit the water column at any time of the year with no clear seasonal pattern (Kunisch et al., 2020).

1.5 The role of sympagic organisms for ecosystem functions

Marine communities are complex biological networks in which energy flows from primary producers at the base of the food web through intermediate consumers to top predators and back through decomposition or detrital pathways. Consequently, all organisms of an ecosystem are somehow connected to and dependent on each other, whether as prey-predator, as competitors for space, nutrients, or particulate food, or in mutualism. Ecological processes that control the fluxes of energy, nutrients, and organic matter through an environment (e.g., nutrient cycling, primary production, secondary production, and carbon cycling), are usually summarized as ‘ecosystem functions’ (Cardinale et al., 2012).

Sea-ice associated communities play a pivotal role for important ecosystem functions in the Arctic ecosystem, particularly for primary production (PP). PP is based to a significant extent on primary producers in the sea ice (ice algae) and in the pelagic zone (phytoplankton). Both of these groups depend on photosynthetically active radiation (PAR) and on nutrients to grow. In the Arctic Ocean, a strong seasonality of the light cycle determines the timing and extent of ice-algal and phytoplankton blooms. In spring, the growth of ice algae and phytoplankton under the ice is mainly controlled by light availability after the polar night, but also by snow depth which can be seen in a negative relationship between the PP and the depth of the snow (Mundy et al., 2007; Campbell et al., 2015; Leu

et al., 2015). If conditions are favorable, the sympagic environment can produce high chlorophyll *a* (chl *a*) concentrations caused by dense communities of algae in and underneath the sea ice (Lannuzel et al., 2020). In the Eurasian Basin, the average chl *a* concentration in FYI during the historical sea-ice minimum in September 2012 was 14.35 mg m^{-2} for ice algae and phytoplankton in the euphotic zone (Fernández-Méndez et al., 2015). In general, phytoplankton production tends to exceed ice-algal production, yet ice-algal production is proportionally higher in the central Arctic basins than on the shelves (Gosselin et al., 1997). During the above-mentioned study, for example, ice-algal production contributed 30 % of the total PP in FYI (Fernández-Méndez et al., 2015).

As primary producers, ice algae and phytoplankton constitute the nutritional basis for the sympagic ecosystem (Søreide et al., 2006; Budge et al., 2008) (Figure 6). As fast-sinking aggregates, they are also consumed by pelagic and benthic organisms and, thus, play a key role in the export of particulate organic carbon (POC) to the deep ocean and for the so-called 'biological carbon pump' (Riebesell et al., 1991; Dybwad et al., 2021). The biological carbon pump is the part of the oceanic carbon cycle that is responsible for the biological driven carbon sequestration and cycling of organic carbon in form of POC and dissolved organic carbon (DOC) from the surface to the seafloor. Since there is a loss of 75 - 80 % of the organic matter from one to another trophic level, only a small proportion of the primary produced carbon actually reaches the sea floor (Sakshaug, 2004). The amount and composition of the organic material available for the respective trophic levels affect the species composition, spatial distribution, abundance, and biomass of micro- and megafauna (Grebmeier et al., 2006; Doney et al., 2012). Especially sea-ice algae are considered a high-quality food source for many organisms way beyond sea-ice meiofauna (Søreide et al., 2006, 2010; Wang et al., 2015; Kohlbach et al., 2016, 2021).

Although it is known that herbivorous, carnivorous, omnivorous, bacteriovorous, and detritivorous feeding types are common in sea-ice meiofauna, studies on the feeding ecology of these organisms are still limited. Only few studies exist about the diets of sea-ice meiofauna in terms of gut content analyses (Grainger and Hsiao, 1990), feeding experiments (Kramer, 2011), or stable isotope analysis (Gradinger and Bluhm, 2020). The most abundant sea-ice meiofauna taxa, Ciliophora and Harpacticoida, are herbivores, which graze on ice algae (Kramer, 2011; Kohlbach et al., 2016). Sea-ice meiofauna taxa with better swimming capabilities, specifically cyclopoid copepods, Rotifera, and Acoela, are considered to switch between the sea-ice channel system and the under-ice realm to feed also on pelagic food in the under-ice water layer, at least during summer (Bluhm et al., 2010). This implies that sea-ice meiofauna is competing with other under-ice grazers for

ice algae and phytoplankton as food source (Figure 6). Although the few existing estimates on the carbon demand of sea-ice meiofauna are very variable (e.g., 0.1 - 7.9 mg C m^{-2} day^{-1}, Gradinger, 1999), they indicate that the grazing impact of the sea-ice meiofauna is negligible, because it does not substantially reduce ice-algal production (Nozais et al., 2001; Michel et al., 2002; Gradinger et al., 2005).

Being the major consumers of ice-algal carbon in the sympagic environment, grazers among the under-ice fauna play a crucial role for the functioning of Arctic ecosystems (Figure 6). They transfer energy in form of ice-algal produced carbon to pelagic and benthic communities (Budge et al., 2008; Kosobokova et al., 2011; Kohlbach et al., 2016). This process is referred to as cryo-pelagic coupling (Scott et al., 1999; Søreide et al., 2006). Predators, such as *Boreogadus saida* or top predators like birds or mammals, feed on under-ice fauna as well as on zooplankton (and nekton). *B. saida* feeds extensively on calanoid copepods, such as *C. glacialis*, and Amphipoda, such as *A. glacialis* (Scott et al. 1999; Kohlbach et al., 2017). Consequently, the upper trophic levels thrive indirectly on the energy produced by ice algae. Especially the dominance of large calanoid copepods has energetic implications due to their high-energy lipid compounds and essential fatty acids (Darnis et al., 2012). Body size is an important driver of ecosystem functions as it is related to various biological and physiological processes such as metabolic rates, the ability to move or migrate, and the vulnerability to predation (Peters, 1986; Norrko et al., 2013). All of the mentioned processes reflect the fitness of a population. Body size data combined with body weight of a given taxon can be used for allometric relationships to estimate the growth performance or biomass, to evaluate predator-prey relationships, or the impact of environmental parameters on the condition of a given taxon. For the most abundant taxa under Arctic sea ice (e.g., *Calanus* spp., Chaetognatha, Amphipoda, and Euphausiacea) studies on allometric relationships exist (Richter, 1994; Poltermann, 2000; Auel and Werner, 2003; Grigor et al., 2015). Studies on biomass, production or carbon demand, however, are still limited, in spite of their importance for a better understanding of the sympagic ecosystem.

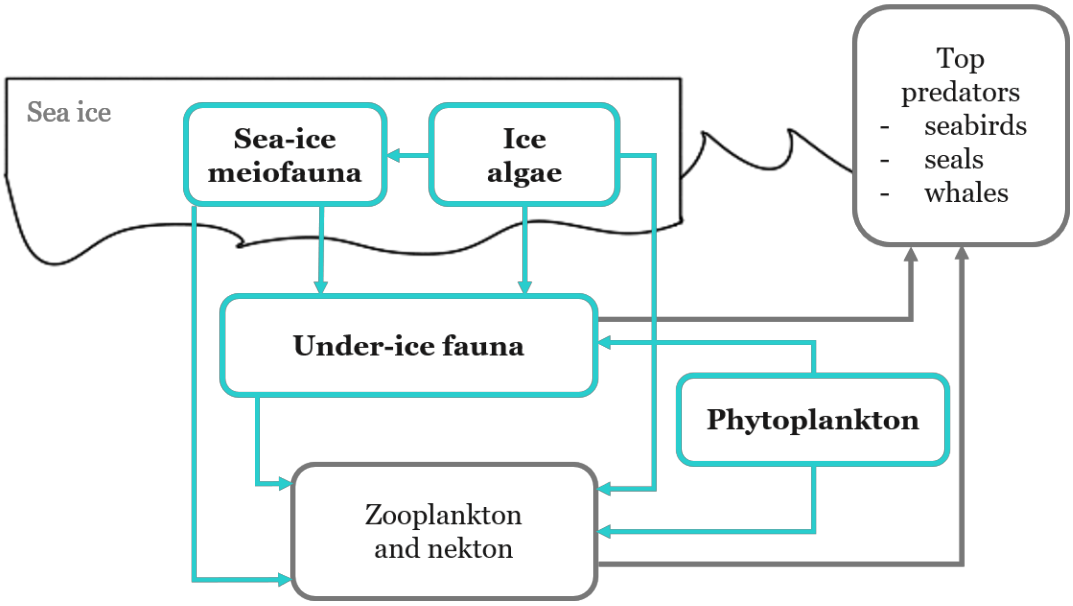

Figure 6. Schematic carbon flux through the polar sympagic ecosystem (in blue) and to pelagic zooplankton and top predator communities (in grey) (modified after Flores, 2009)

A further decline of the Arctic sea-ice cover is expected to have decisive impacts on the cryo-pelagic coupling and therewith on the Arctic food webs (Grebmeier et al., 2010; David et al., 2015; Kohlbach et al., 2016; Lannuzel et al., 2020). Since sea ice directly impacts the availability of light, nutrients, and space for primary producers, sea-ice loss and sea-ice melt have strong effects on sympagic algal communities. Only recently it was hypothesized that in the future ice-algal communities will develop earlier in the season and produce more biomass over a shorter period (van Leeuwe et al., 2018). The weakened stratification of the halocline through Atlantification and the loss of brine through melting enhance mixing of the under-ice environment and nutrient availability, which, in turn, boost primary production (Ardyna et al., 2014; Polyakov et al., 2020a, b). Since the late 1990's phytoplankton primary production over the entire Arctic Ocean has increased by 30 %, mainly due to a decrease in sea-ice extent and thickness, but also due to an increased nutrient supply (Arrigo and van Dijken, 2015; Ardyna and Arrigo, 2020). Recently, a prolonged phytoplankton growing season has been observed as well as massive under-ice phytoplankton blooms in the Arctic Ocean (Arrigo et al., 2012; Arrigo and van Dijken, 2015; Assmy et al., 2017; Ardyna and Arrigo, 2020).

How reduced long-range transport with the Transpolar Drift or the loss and thinning of the sea ice will affect the biodiversity, species composition, abundance, and production of the Arctic sympagic community is unclear. The shift of the sea-ice regime is suspected to favor pelagic species, which can colonize the sea ice from the pelagic realm (Kramer, 2011). Zooplankton species are considered sentinels of climate change because of their short life histories and their sensitivity to environmental changes (Hunt et al., 2014). Some studies

have documented implications of sea-ice decline for certain sympagic species for instance on the gammarid amphipod *Gammarus wilkitzkii*, which shows decreasing abundance since the 1980's, which is considered to be a consequence of the decline of the MYI in Arctic regions (Polyakov et al., 2012; Hop et al., 2000). Other, model-based, studies indicate a northward migration of the smaller Atlantic species *C. finmarchicus* with an increased inflow of Atlantic water into the Arctic Ocean (Richardson, 2008) along with a replacement of the Arctic species *C. glacialis*. Since *C. glacialis* has higher nutritional values than *C. finmarchicus* (Kosobokova and Hirche, 2000), a replacement could cause changes in the zooplankton community of the Arctic Ocean and affect the pelagic food-web structure. A current inventory of abundance and biodiversity of sympagic biota in the Atlantic inflow region where sea-ice decline has been most prominent is therefore timely and necessary.

1.6 Objectives

The overall aim of this thesis was to elucidate the role of biodiversity for ecosystem functions of sympagic communities in the Eurasian Basin of the Arctic Ocean.

The fundamental role of biodiversity for human well-being and as an enhancer and stabilizer of ecosystem functions is principally valid in all biomes on earth, including the marine environment (Stachowicz et al., 2007; Solan et al., 2008). The more diverse a system is, the more resilient it is to environmental changes. Because of the rapid decline of sea ice in the Arctic Ocean, shifts in the biodiversity and with it in ecosystem functions of sea-ice ecosystems are expected. Investigations on the relationship between biodiversity and ecosystem functions have been emerging only in the last decade (Stachowicz et al., 2007; Link et al., 2013a; Kohlbach et al., 2017; Olli et al., 2019). The slow progress in capturing the full diversity of sympagic fauna makes it more and more difficult to identify a baseline of the system against which change can be measured. To understand and evaluate the changes the New Arctic will entail, it is important to assess the current state of sympagic communities. For this reason, I specifically aimed to:

Objective 1) Generate a quantitative inventory of the biodiversity, community structure, and abundance of sea-ice meiofauna and under-ice fauna in the Atlantic inflow region north of Svalbard (***Chapter I***). The main research questions for this objective were: What is the species composition of sea-ice meiofauna and under-ice fauna? What are the most abundant taxa of both faunas? Can we see changes in biodiversity and community composition relative to earlier studies? The quantitative inventory will constitute a baseline for future studies that aim to evaluate community changes. The comparison of biodiversity

and abundance with earlier studies will reveal possible changes that have already occurred. The quantitative inventory will also be the basis for ***Chapter III***.

The strongest evidence for the dramatic changes of the Arctic Ocean in the last decades is the loss and thinning of the sea ice (Serreze et al., 2007; Kwok et al., 2009). Since sea ice constitutes a habitat for a diverse sympagic community (Gradinger 1999; Bluhm et al., 2010), these changes are likely to affect sympagic biota with cascading effects on the entire ecosystem (Kramer et al., 2011; Hop et al., 2020; Lannuzel et al., 2020). Insights into the association of the sympagic fauna with the sea-ice habitat will, therefore, help predict changes under future environmental conditions. To evaluate the most important sea-ice and under-ice water properties (e.g., temperature, salinity, ice thickness, and chl *a* concentration) for structuring the sea-ice meiofauna and under-ice fauna community, it is important to assess a comprehensive dataset of environmental parameters. Therefore I further aimed to:

Objective 2) characterize physical habitat properties over large scales and seasons (***Chapter II***) and to identify environmental drivers of the sympagic community (***Chapter I*** and ***Chapter IV***). The main research questions for this objective were: Which environmental parameters do characterize the sea-ice and under-ice habitat? Do sea-ice properties have a stronger influence on sea-ice meiofauna and surface water properties (hydrography) on under-ice fauna? The outcomes can improve predictions on future biodiversity changes and the subsequent effects on the sympagic ecosystem. They can further be used for habitat mapping and for the validation of large-scale physical models, which are increasingly used to predict changes in Polar Regions.

How sympagic taxa use the sea-ice habitat is sparsely explored until today (Gradinger, 1999; Melnikov and Kulikov, 1980; Fortier et al., 2001; Kohlbach et al., 2017). Predictions forecast that phytoplankton PP will increase in the Eurasian Basin (Ardyna et al., 2014; Polyakov et al., 2020a), but can the sympagic community make use of the surplus organic matter? To investigate the dependency of Arctic key species on ice algae and phytoplankton is of high significance in a time where climate change-induced shrinkage of the sea-ice cover is predicted to decrease ice-algae and increase phytoplankton production in the Arctic Ocean (Lewis et al., 2020). Being the major consumers of ice-algal carbon in the sympagic environment, grazers among the under-ice fauna play a crucial role for the functioning of Arctic ecosystems (Figure 6). They transfer energy in form of ice-algal produced carbon to pelagic and benthic communities (Budge et al., 2008; Kosobokova et al., 2011; Kohlbach et al., 2016). The determination of the cryo-pelagic link in the Arctic

Ocean will help evaluate the effects of continuous ice melt on the Arctic ecosystem. Therefore I finally aimed to:

Objective 3) Quantify ecosystem functions (biomass, production, and consumption) of the sympagic communities with a focus on carbon budgets and food web efficiency (***Chapter III***, ***Chapter IV***, and ***Chapter V***). The main research questions were: Is the PP sufficient for the demand of the sympagic grazers? Do ice algae contribute to a substantial degree to the PP and to the herbivorous consumption? Which taxa are key contributors to the ecosystem functions? Is the sympagic secondary production (SP) sufficient for sympagic carnivores? Which are the key taxa for the cryo-pelagic link? How much carbon is transferred through the different trophic levels of the sympagic environment? How much surplus of the PP and SP remains for pelagic and benthic communities? The comprehensive compilation of the carbon flux through the sympagic ecosystem will give new insights on trophic interactions and dependencies between the different trophic levels and/or taxa. The results will further allow the evaluation of the importance of sympagic biota for underlying communities. The results can also be used to complete and improve food-web models.

To accomplish **Objectives 1) – 3)** and resolve the research questions of this study, a unique interdisciplinary approach was applied by integrating data from different habitats (sea ice and under-ice water) and at various spatial scales (local to km). This thesis is the first one combining concurrent sampling of the sea-ice and the under-ice habitat (0 – 2 m). Relevant samples were obtained during two expeditions to the Arctic Ocean (PS80 in summer 2012 and PS92 in spring 2015).

Sea-ice coring and trawling with the SUIT were used to sample sea-ice meiofauna (here heterotrophs >10 μm) and under-ice fauna (here metazoans >300 μm) respectively. To relate habitat properties to ecological data, environmental parameters of the sea-ice and under-ice water were characterized. Various ice cores were taken to examine ample sea-ice properties (e.g., chl *a*, temperature, salinity). Snow thickness and sea-ice thickness were measured at the coring site. A sensor array mounted on the SUIT was used to collect environmental data during trawling (e.g., chl *a*, temperature, salinity, ice thickness). The taxonomic analysis of sea-ice meiofauna from ice cores was conducted via morphological analysis in collaboration with the Arctic University of Norway (UiT) in Tromsø supervised by Prof. Dr. Bodil Bluhm and the Istituto Nazionale di Oceanografia e Geofisica Sperimentale (OGS) in Trieste supervised by Dr. Marina Monti-Birkenmeier. Taxonomic determination of the under-ice fauna was done morphologically at the Alfred Wegener Institute in Bremerhaven. Both, for sea-ice meiofauna and under-ice fauna different

biodiversity metrics were used to quantify biodiversity (e.g., taxa richness, Shannon diversity, Pielou's evenness). Abundance (ind. m^{-2}) was calculated from raw counting numbers. To assess the carbon flux and food web efficiency of sympagic communities, the carbon biomass (mg C m^{-2}) was calculated by multiplying abundances with the carbon content of the respective taxon. Values for the latter were mainly found in literature. The carbon demand (mg C m^{-2} day^{-1}) was calculated from biomass values and mass-specific ingestion rates taken mainly from literature. Carbon production rates (mg C m^{-2} day^{-1}) were calculated by using production/biomass ratios for each taxon.

This thesis brings together new data on sea-ice and under-ice communities in Arctic sea-ice systems. The improved knowledge on biodiversity, biomass, and productivity of the sympagic environment will serve future studies as a reference point against which they can evaluate or predict impacts of the changing Arctic. The large amount of biological and physical data assessed in this thesis will help improve physical ice-ocean or ecological models. Ultimately, the results of this thesis will be used in a study that aims to comprehensively quantify the carbon budget in the Arctic Ocean (Kedra et al., in preparation).

1.7 Publication outline

This cumulative dissertation presents the research findings of my PhD project that were obtained from October 2015 to March 2021. This project was conducted under the umbrella of the Universität Hamburg with Prof. Angelika Brandt (formerly Universität Hamburg, now Senckenberg Research Institute and Natural History Museum). In cooperation with the Alfred-Wegener-Institute Helmholtz Center for Polar and Marine Research, Bremerhaven, this thesis was part of the Helmholtz Association Young Investigators Group *Iceflux* (Ice-ecosystem carbon flux in Polar Oceans), supervised by Dr. Hauke Flores.

This thesis consists of a general introduction into the research field, followed by five manuscripts: ***Chapter I***, ***Chapter II***, and ***Chapter IV*** were published in peer-reviewed journals, ***Chapter III*** will be accepted after moderate revisions, and ***Chapter V*** is in preparation for submission to a peer-reviewed journal. The objectives of this thesis are addressed in the single chapters and in the synoptic discussion.

Chapter II, and ***Chapter V*** comprise multiple studies from both Polar Oceans. This thesis focuses on the biodiversity and ecosystem functions of the sympagic fauna (sea-ice meiofauna and under-ice fauna) of the Eurasian Basin. Relevant expeditions for this thesis are the Arctic expeditions: PS80 in summer 2012 and PS92 in spring 2015.

Chapter I focuses on **Objective 1),** in that it provides a quantitative inventory of the biodiversity, community structure, and abundance of sea-ice meiofauna and under-ice fauna. Additionally, it describes key environmental variables, such as sea-ice properties and surface-water column properties that define the sympagic communities in the Eurasian Basin. Therefore ***Chapter I*** is also addressing **Objective 2)**. The results of ***Chapter I*** provide the basis for calculations of ***Chapter III*** and are therefore crucial for estimations of the linkage of biodiversity with ecosystem functions in polar sea-ice ecosystems.

Chapter I: Sympagic Fauna in and Under Arctic Pack Ice in the Annual Sea-Ice System of the New Arctic

J. Ehrlich, F.L. Schaafsma, B.A. Bluhm, I. Peeken,
G. Castellani, A. Brandt, H. Flores
(2020)

Frontiers in Marine Science 7:452. doi: 10.3389/fmars.2020.00452

AB, HF, and **JE** designed the sampling of this study. FS, GC, IP, and HF collected the samples of sea-ice meiofauna and under-ice fauna. **JE** and BB analyzed the sea-ice meiofauna samples. **JE** and FS analyzed the under-ice fauna samples. FS and IP contributed to the biological dataset. GC and FS contributed to the environmental dataset. AB contributed to the taxonomical accuracy of the manuscript. **JE** analyzed the data and prepared all figures and tables. BB, FS, and HF contributed to data interpretation. **JE** wrote the manuscript. **All** authors contributed to the discussion of various versions of the manuscript.

Chapter II provides a unique dataset of large-scale physical and biological sea-ice properties collected with the SUIT during different campaigns and seasons. The gained data of this chapter help assess the role of sea-ice and under-ice properties as drivers of distribution and community patterns in ***Chapter I*** and ***Chapter IV***. Thereby, ***Chapter II*** mainly focuses on **Objective 2)**. The results of this chapter can further be used to improve large-scale physical models, which are increasingly used to predict change and manage resources in Polar Regions.

Chapter II: Large-Scale Variability of Physical and Biological Sea-Ice Properties in Polar Oceans

G. Castellani, F. L. Schaafsma, S. Arndt, B. A. Lange, I. Peeken, **J. Ehrlich**,
C. David, R. Ricker, T. Krumpen, S. Hendricks, S. Schwegmann,
P. Massicotte, H. Flores
(2020)

Frontiers in Marine Science 7:536. doi: 10.3389/fmars.2020.00536
GC wrote the paper, processed the data to obtain sea-ice draft and in-ice chl *a*, and prepared most of the figures. SA processed the light data to obtain integrated irradiance and radiance values and also to extract the wavelengths. RR provided the satellite ice-concentration data. PM provided modeled downwelling irradiance data. IP supervised the Arctic sea-ice biology sampling and processed all HPLC samples. FS, HF, and **JE** contributed to developing the structure of the manuscript and FS provided information on the snow depth per each SUIT haul. TK, SH, SS, and BL collected the EM-bird data. BL processed and plotted the EM-data, provided in-ice chl *a* estimates for PS80, and carried out the spatial autocorrelation analysis. GC, HF, **JE**, BL, FS, and CD contributed to SUIT data collection. **JE**, FS, CD, and HF contributed to data interpretation in connection with biological data. HF supervised the construction of the SUIT and designed the sampling for all the campaigns and conducted statistical analyses. **All** co-authors contributed to the discussion of results and to the preparation of the manuscript.

Chapter III quantifies biomasses, carbon production, and carbon demand of sea-ice meiofauna and under-ice fauna. Furthermore, it provides a comprehensive compilation of trophic interactions in form of carbon flow through the sympagic ecosystem. It is, thereby, the main chapter which addresses **Objective 3)**. ***Chapter IV*** refers mainly to ***Objective 3)*** as it quantifies biomasses, carbon production, and carbon demand of under-ice fauna during the historical sea-ice minimum in 2012. Since this chapter is also discussing the influence of nutrient and sea-ice properties on shaping the under-ice community, it also addresses **Objective 2)**. ***Chapter V*** focuses on the calculation and compilation of allometric relationships of key under-ice taxa. These are highly valuable for the quantification of biomasses and other traits. As such, this chapter contributes also to **Objective 3)**. The results of these chapters enable future researchers to track changes of sympagic communities in terms of carbon budget and carbon fluxes.

Chapter III: Sea-ice associated carbon flux in Arctic spring

J. Ehrlich, B.A. Bluhm, I. Peeken, P. Massicotte, F.L. Schaafsma, G. Castellani, A. Brandt, H. Flores

Accepted after 'moderate revisions' in Elementa: Science of the Anthropocene.

JE, HF, AB, and BB designed the study. HF, FS, GC, and IP conducted the fieldwork and sample collection. **JE** and BB analyzed the meiofauna samples. **JE** and FS analyzed the under-ice fauna samples. IP determined the chlorophyll *a* concentration in the sea-ice samples. GC modeled chl *a* concentration in the ice and the 0-2 m water column for all

SUIT stations. **JE** calculated the biomass of ice algae and phytoplankton for all stations. PM calculated the primary production of ice algae and phytoplankton for all stations. **JE** calculated the biomass, carbon demand, and secondary production of sea-ice meiofauna and under-ice fauna for all stations. **JE** analyzed the data, wrote the manuscript and prepared all figures and tables. **JE**, BB, HF, and IP contributed to data interpretation. **All** authors contributed to different versions of the manuscript.

Chapter IV: Sea-ice properties and nutrient concentration as drivers of the taxonomic and trophic structure of high-Arctic protist and metazoan communities

H. Flores, C. David, **J. Ehrlich**, K. Hardge, D. Kohlbach, B.A. Lange, B. Niehoff, E.-M. Nöthig, I. Peeken, K. Metfies
(2019)

Polar Biology 42:1377. doi: 10.1007/s00300-019-02526-z

HF was the main author of this paper, supervised the collection of environmental data, under-ice metazoan and epipelagic metazoan samples, and accomplished the data analyses. CD conducted laboratory analyses of under-ice metazoans. **JE** conducted laboratory analyses of epipelagic metazoan samples and provided online resources. KH provided protist community data based on OTU analysis and contributed to data analysis. DK provided size and weight data of under-ice metazoans. BAL collected and validated environmental data and provided Fig. 1. BN supervised epipelagic metazoan analysis. E-MN provided count data of phytoplankton samples and advised on aspects of phytoplankton ecology. IP provided chlorophyll and other environmental datasets. KM initiated the study and advised on aspects of molecular-based biodiversity and ecology. **All** authors contributed significantly to the drafting of this research article.

Chapter V: Allometric measurements of Arctic and Antarctic zooplankton and nekton

F. L. Schaafsma, C. David, D. Kohlbach, M. Vortkamp, A. Meijboom, **J. Ehrlich**, G. Castellani, B. A. Lange, A. Immerz, H. Cantzler, A. van de Putte, J. A. van Franeker, H. Flores

In preparation for submission to Polar Biology.

Samples were collected by FS, CD, DK, MV, AM, **JE**, GC, BL, AI, HC, AP, JF, HF. Samples were analyzed by FS, CD, DK, MV, AI, HC, HF, and **JE**. MK and NZ analyzed

samples under supervision of HF. The data were analyzed by FS. **JE** provided sources about taxonomic information. **All** authors contributed to data validation. The figures were created by FS, HF, AP, and **JE**. The first manuscript was written by FS with contributions from **all** authors.

2 Thesis chapters

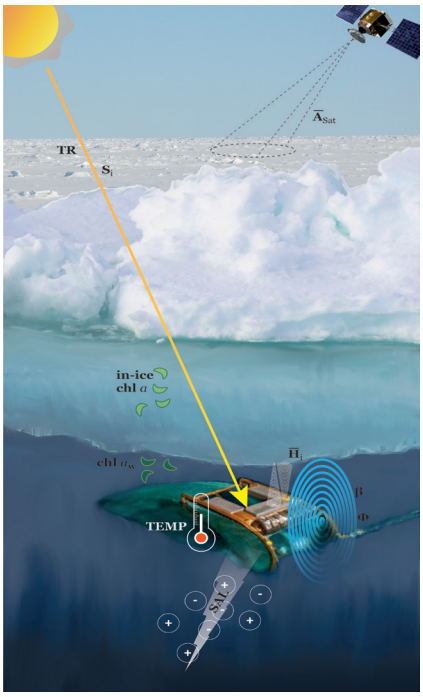

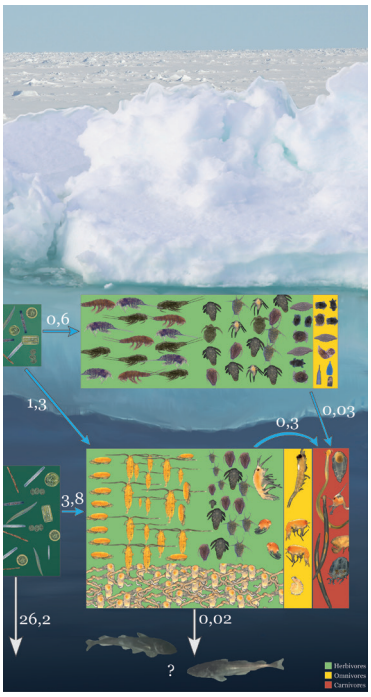

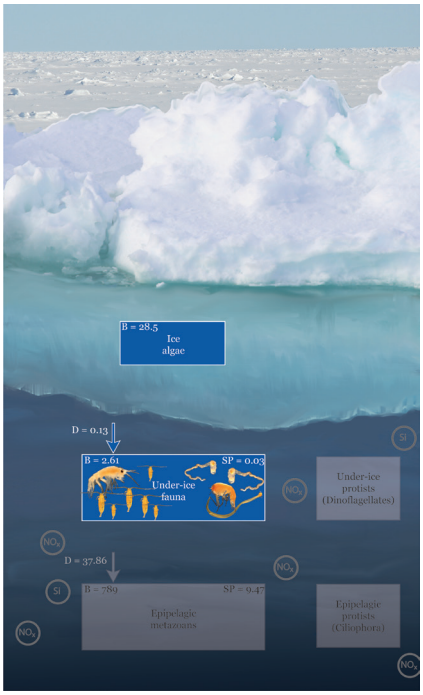

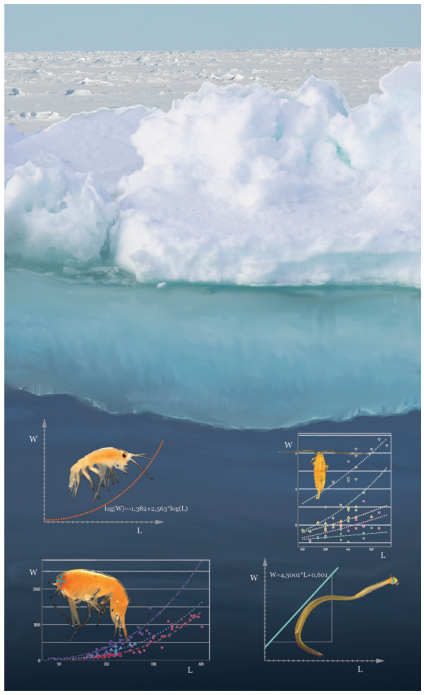

Chapter I

Sympagic Fauna in and Under Arctic Pack Ice in the Annual Sea-Ice System of the New Arctic

J. Ehrlich[1,2], F.L. Schaafsma[3], B.A. Bluhm[4], I. Peeken[2], G. Castellani[2], A. Brandt[5,6], H. Flores[2]
(2020)

[1] Centre of Natural History (CeNak), University of Hamburg, Hamburg, Germany
[2] Alfred Wegener Institute, Helmholtz Centre for Polar and Marine Research, Bremerhaven, Germany
[3] Wageningen Marine Research, Den Helder, Netherlands
[4] Institute of Arctic and Marine Biology, UiT – The Arctic University of Norway, Tromsø, Norway
[5] Senckenberg Research Institute and Natural History Museum, Frankfurt am Main, Germany
[6] Institute of Ecology, Diversity and Evolution, Goethe University,Frankfurt am Main, Germany

Front. Mar. Sci. 7:452. doi: 10.3389/fmars.2020.00452

frontiers in Marine Science

ORIGINAL RESEARCH
published: 19 June 2020
doi: 10.3389/fmars.2020.00452

Sympagic Fauna in and Under Arctic Pack Ice in the Annual Sea-Ice System of the New Arctic

Julia Ehrlich[1,2], Fokje L. Schaafsma[3], Bodil A. Bluhm[4], Ilka Peeken[2], Giulia Castellani[2], Angelika Brandt[5,6] and Hauke Flores[2]*

[1] Centre of Natural History (CeNak), University of Hamburg, Hamburg, Germany, [2] Alfred Wegener Institute, Helmholtz Centre for Polar and Marine Research, Bremerhaven, Germany, [3] Wageningen Marine Research, Den Helder, Netherlands, [4] Institute of Arctic and Marine Biology, UiT – The Arctic University of Norway, Tromsø, Norway, [5] Senckenberg Research Institute and Natural History Museum, Frankfurt am Main, Germany, [6] Institute of Ecology, Diversity and Evolution, Goethe University, Frankfurt am Main, Germany

A strong decline and thinning of the Arctic sea-ice cover over the past five decades has been documented. The former multiyear sea-ice system has largely changed to an annual system and with it the dynamics of sea-ice transport across the Arctic Ocean. Less sea ice is reaching the Fram Strait and more ice and ice-transported material is released in the northern Laptev Sea and the central Arctic Ocean. This trend is expected to have a decisive impact on ice associated ("sympagic") communities. As sympagic fauna plays an important role in transmitting carbon from the ice-water interface to the pelagic and benthic food webs, it is important to monitor its community composition under the changing environmental conditions. We investigated the taxonomic composition, abundance and distribution of sea-ice meiofauna (here heterotrophs >10 μm; eight stations) and under-ice fauna (here metazoans >300 μm; fourteen stations) in Arctic 1.5 year-old pack ice north of Svalbard. Sampling was conducted during spring 2015 by sea-ice coring and trawling with a Surface and Under-Ice Trawl. We identified 42 taxa associated with the sea ice. The total abundance of sea-ice meiofauna ranged between 580 and 17,156 ind.m^{-2} and was dominated by Ciliophora (46%), Copepoda nauplii (29%), and Harpacticoida (20%). In contrast to earlier studies in this region, we found no Nematoda and few flatworms in our sea-ice samples. Under-ice fauna abundance ranged between 15 and 6,785 ind.m^{-2} and was dominated by Appendicularia (58%), caused by exceptionally high abundance at one station. Copepoda nauplii (23%), *Calanus finmarchicus* (9%), and *Calanus glacialis* (6%) were also very abundant while sympagic Amphipoda were comparatively rare (0.35%). Both sympagic communities showed regional differences in community composition and abundance between shelf and offshore stations, but only for the under-ice fauna those differences were statistically significant. Selected environmental variables moderately explained variations in abundances of both faunas. The results of this study are consistent with predictions of diversity shifts in the new Arctic.

Keywords: Arctic Ocean, Svalbard, sea-ice meiofauna, under-ice fauna, zooplankton, biodiversity, community composition, environmental conditions

OPEN ACCESS

Edited by:
Zhijun Dong,
Yantai Institute of Coastal Zone Research (CAS), China

Reviewed by:
Xiubao Li,
Hainan University, China
Juan Andrés López,
University of Alaska Fairbanks, United States

****Correspondence:***
Julia Ehrlich
julia.ehrlich@awi.de

Specialty section:
This article was submitted to Marine Evolutionary Biology, Biogeography and Species Diversity, a section of the journal Frontiers in Marine Science

Received: *02 March 2020*
Accepted: *22 May 2020*
Published: *19 June 2020*

Citation:
Ehrlich J, Schaafsma FL, Bluhm BA, Peeken I, Castellani G, Brandt A and Flores H (2020) Sympagic Fauna in and Under Arctic Pack Ice in the Annual Sea-Ice System of the New Arctic. Front. Mar. Sci. 7:452. doi: 10.3389/fmars.2020.00452

INTRODUCTION

Arctic pack ice is drift ice which moves with the agitation of winds and currents. It is either annual and reaches a maximum thickness of ∼2 m, or perennial with a thickness of 3–4 m (Haas, 2003; Kwok and Cunningham, 2015). Because sea-ice extent and thickness have been decreasing rapidly over the past five decades, the Arctic Ocean is gradually changing from a perennial sea-ice system to a system dominated by annual sea ice (Serreze et al., 2007; Comiso, 2012; Melnikov, 2018). This shift combined with associated ecosystem changes has coined the term 'The New Arctic' (Jeffries et al., 2013; Carmack et al., 2015; Granskog et al., 2020). More recently, changes in the Transpolar Drift were also characterized. Less sea ice is now reaching the Fram Strait and more ice and ice-transported material is released in the northern Laptev Sea and the central Arctic Ocean (Krumpen et al., 2019).

Sea ice provides a habitat for sympagic communities, which include microalgae and a diversity of heterotrophic protists and metazoans (Gradinger, 1999; David et al., 2015; Bluhm et al., 2018). Sympagic fauna comprises organisms that complete either their entire life cycle within the sea ice (autochthonous fauna) or spend at least part of their life cycle attached to the ice (allochthonous fauna) (Melnikov and Kulikov, 1980; Carey, 1985; Gulliksen and Lønne, 1989). Of these, the small heterotrophic organisms (>10 μm), which live in the brine channels and cavities within the sea-ice matrix, are referred to as sea-ice meiofauna. Some field studies have estimated the abundance and documented the distribution of sea-ice meiofauna in landfast ice (Carey and Montagna, 1982; Friedrich, 1997; Michel et al., 2002), but only few have focused on Arctic pack ice (Gradinger et al., 1992, 2005; Gradinger, 1999). While taxonomic composition of sea-ice meiofauna varies between regions, seasons and ice types, Harpacticoida, Nematoda, Rotifera, Acoela, other flatworms, and various nauplii are frequently occurring taxa (Bluhm et al., 2018). Loss and/or reduction of sea-ice meiofaunal taxa, however, has been reported from sea ice in the central Arctic Beaufort Gyre between the 1970s and 1980s and been related to sea-ice change (Melnikov et al., 2001). The highest sea-ice meiofauna densities are usually found in the bottom layer of the sea ice (Friedrich, 1997; Nozais et al., 2001; Marquardt et al., 2011). This is because the bottom layer has a high probability of colonization from pelagic and benthic fauna and is in free exchange with nutrients from the underlying seawater, which sustain the growth of ice algal food for many of these taxa (Arndt and Swadling, 2006). Ice algae can account for 50% of the primary production in the central Arctic Ocean in summer (Gosselin et al., 1997; Fernández-Méndez et al., 2015) and are a high-quality food source for the Arctic food web (Søreide et al., 2006, 2013; Falk-Petersen et al., 2009; Kohlbach et al., 2016). Sea-ice decline increases the light availability (Nicolaus et al., 2012) and thus the primary production over shelf areas (Arrigo et al., 2008; Ardyna et al., 2014; Arrigo and van Dijken, 2015), whereas primary production in the basins may remain low due to nutrient limitation caused by strong stratification through sea-ice melt (Bluhm and Gradinger, 2008; Tremblay and Gagnon, 2009; Tremblay et al., 2015). By grazing on ice algae, sea-ice meiofauna may represent an important link in the carbon transfer from the sea-ice to pelagic and benthic communities. Gradinger et al. (1999) and Nozais et al. (2001) analyzed the potential role of sea-ice meiofauna in controlling algal production, though they drew contradictory conclusions. Gradinger (1999) found significant positive correlations between ice-algal biomass and meiofauna abundance, indicating a strong trophic link between ice algae and sea-ice meiofauna. In contrast, Nozais et al. (2001) found that the grazing impact of sea-ice meiofauna on ice algae was negligible, suggesting a rather limited contribution of sea-ice meiofauna to the carbon flux in the food web.

Larger taxa such as Amphipoda, Calanoida, and Appendicularia are generally excluded from the narrow-channeled ice matrix but tend to concentrate under the ice (Carey, 1985; Gradinger and Bluhm, 2004; Bluhm et al., 2010). Amphipoda are the most studied organisms of this under-ice fauna (Poltermann et al., 2000; Beuchel and Lønne, 2002; Hop et al., 2011). They can regionally occur in high densities of >100 ind.m^{-2}, though decreasing densities have recently been suspected for the study area (Arctic Council Secretariat, 2016), and decreasing species number from the Beaufort Gyre (Melnikov et al., 2001). In contrast, the ice-association of Calanoida has gained much less attention and only few studies report on their species composition in the ice-water interface layer (Werner and Arbizu, 1999; David et al., 2015). Large copepod species are key drivers of the energy transfer through the Arctic marine ecosystem due to their high-energy lipid compounds and essential fatty acids (Søreide et al., 2010; Darnis et al., 2012; Kohlbach et al., 2016). There are three *Calanus* species in the Eurasian Arctic Ocean: *Calanus finmarchicus*, *Calanus glacialis*, and *Calanus hyperboreus*. They resemble one another morphologically, but differ in body size, reproductive strategy, life cycle, and distribution. While *C. hyperboreus* and *C. glacialis* are of true Arctic origin, *C. finmarchicus* is a boreal North Atlantic species (Conover, 1988; Auel and Hagen, 2002; Hirche and Kosobokova, 2007). In addition, *C. glacialis* and *C. hyperboreus* are dependent on ice algae as a food source at least during parts of their life cycle (Søreide et al., 2010; Kohlbach et al., 2016). In the past, under-ice fauna has mostly been sampled by divers (Arndt and Pavlova, 2005; Hop et al., 2011). This method provides a good small-scale resolution of sea-ice habitats, but does not provide insights into the large-scale spatial variability of the under-ice habitat. The SUIT used in this study overcomes that problem since it enables large-scale horizontal sampling of the 0–2 m surface layer, both under the sea ice and in the open water.

The community structure of sympagic fauna is related to ice age and under-ice topography (Hop et al., 2000; Hop and Pavlova, 2008; Flores et al., 2019). A further decline of sea ice may thus have strong effects on the composition, abundance, and biodiversity of sympagic fauna and, because of their role in the energy transfer to higher trophic levels (Budge et al., 2008), on the entire Arctic marine food web. Therefore, an accurate

Abbreviations: *A.*, *Apherusa*; *C.*, *Calanus*; chl *a*, chlorophyll *a*; CTD, Conductivity Temperature Depth probe; *H′*, Shannon diversity; ind., individuals; *J′*, Pielou's evenness; NMDS, non-metric multidimensional scaling; PCA, principal component analysis; PS, Polarstern; PVC, polyvinylchloride; S, taxa richness; SUIT, Surface and Under-Ice Trawl.

quantification of sympagic fauna in the Arctic Ocean along with environmental properties is crucial to provide a baseline for monitoring the effects of environmental changes on Arctic marine ecosystems. In this study, we combined two sampling methods to comprehensively cover a wide range of sympagic fauna from the Arctic Ocean pack ice. Sea-ice meiofauna was sampled by drilling ice cores on Arctic pack ice and under-ice fauna was sampled with the SUIT in the region of Atlantic Water inflow north of Svalbard during springtime 2015. Our study aimed to:

1. Provide a concurrent inventory of the community composition, biodiversity and abundance of sea-ice meiofauna and under-ice fauna, and
2. Identify key environmental variables of sea ice and the surface water that define in-ice and under-ice habitats and structure the different communities.

MATERIALS AND METHODS

Study Area

During the Polarstern expedition TRANSSIZ ('Transitions in the Arctic Seasonal Sea-Ice Zone,' PS92) from May 19 to June 28, 2015 the composition, abundance, and distribution of sea-ice meiofauna and under-ice fauna were examined. Samples were collected during eight ice stations and fourteen SUIT stations between 7.068–19.907°E and 81.007–82.211°N. Two of the eight sea-ice stations were located on the marginal shelf of north Svalbard (19 and 32), four in the Sophia Basin and on its slope (27, 31, 39, and 47), and two at the Yermak Plateau (43 and 46). In close proximity to each ice station a SUIT station was conducted. Five of the fourteen SUIT stations were located on the marginal shelf of north Svalbard (19 and 32), eight were located in the Sophia Basin and on its slope (27, 28, 31, 38, 39, 47, 48, and 49), and four on the Yermak Plateau (43, 44, 45, and 56) (**Figure 1**).

This region of the Arctic Ocean is characterized by a pronounced inflow of Atlantic Water along the West Spitsbergen Current and the Fram Strait branch. The latter is assumed to carry most of the oceanic heat into the Arctic Ocean (Rudels, 1987; Beszczynska-Möller et al., 2012; Rudels et al., 2013). Around 80°N the Atlantic Water inflow bifurcates due to topographic steering. Here, one part of the current propagates eastward while another part follows the topography around the Yermak Plateau. North of Svalbard the Atlantic Water is flowing close to the surface and thus contributing strongly to seasonal sea-ice melt and delays in the refreezing of the ice during fall (Rudels et al., 2004, 2013). In the past decades, observations in Fram Strait have revealed a warming of the Atlantic Water inflow into the Arctic Ocean. This warming trend reached its maximum in 2006 and has slightly decreased since then (Hughes et al., 2011; Beszczynska-Möller et al., 2012).

Environmental Parameters of Sea Ice at Ice Stations

At each ice station several ice cores were drilled for determination of environmental properties with a Kovacs corer (Kovacs Enterprise, Roseburg, OR, United States; inner diameter: 9 cm). To determine the chlorophyll *a* (chl *a*) concentration, one ice core was taken and the bottom 10 cm were cut into two sections of approximately 5 cm length. Those ice-core sections were then put into polyvinyl chloride (PVC) jars and 200 ml of 0.2 μm filtered seawater were added per 1 cm of ice core. Melting took place in a dark room at 4°C. After melting, the volume of the meltwater was determined and subsamples were filtered through Whatman GF/F filters. The filters were put into liquid nitrogen and kept at −80°C for later analysis. In the laboratories of the Alfred Wegener Institute, pigments including chl *a* were extracted from the filters with 100% Acetone and homogenized. The chl *a* concentration was then measured with high performance liquid chromatography (HPLC) as described in Tran et al. (2013) and calculated mean values of chl *a* concentration were used for further analyses. For ice-temperature measurements, one ice core was put into a PVC halfpipe immediately after coring and the temperature of the bottom 10 cm of the ice core was measured with a temperature probe (Testo 720) in 5 cm intervals. Mean values of those measurements were then calculated. In order to determine bulk salinity, one ice core was taken at each ice station and the bottom 10 cm section was cut off. The segment was put into a PVC jar and melted at 4°C in the dark. The salinity of the melted ice section was then measured with a salinometer (WTW Cond.3110) as described by Peeken (2016). Snow thickness was measured at 5 different points on each coring site by using a meter stick. Mean values were calculated and used for further analyses. Sea-ice thickness was measured using an ice thickness gauge (Kovacs Enterprise, Roseburg, OR, United States), which was lowered through one sea-ice meiofauna hole at each ice station.

Sampling and Processing of Sea-Ice Meiofauna

For sampling of sea-ice meiofauna, two replicate ice cores were drilled at each ice station with a Kovacs corer (Kovacs Enterprise, Roseburg, OR, United States; inner diameter: 9 cm) and the lowermost 10 cm of each ice core were cut off for further examination. The 10 cm ice-core sections were put separately into PVC jars. In the ship's laboratory 200 ml 0.2 μm filtered seawater were added per 1 cm of ice core to prevent the fauna from osmotic stress during melting (Garrison and Buck, 1986). Melting took place in a dark room at 4°C. After melting, the total volume was determined and the sample was then concentrated over 10 μm gauze and fixed in 4% buffered formaldehyde solution until later quantitative analysis in the laboratories of The Arctic University of Norway (UiT). The replicates of all eight ice stations were sorted under a stereo- microscope (Zeiss Discovery.V20) and identified to the lowest taxonomic level possible. Taxonomic names were verified for correctness and synonymy using the World Register of Marine Species (WoRMS[1]).

The number of individuals per liter of melted sea ice was determined by dividing the number of individuals in each sample by the volume of the sample (minus the added filtered seawater). From that the number of individuals per m^2 ($ind.m^{-2}$) was

[1]http://www.marinespecies.org

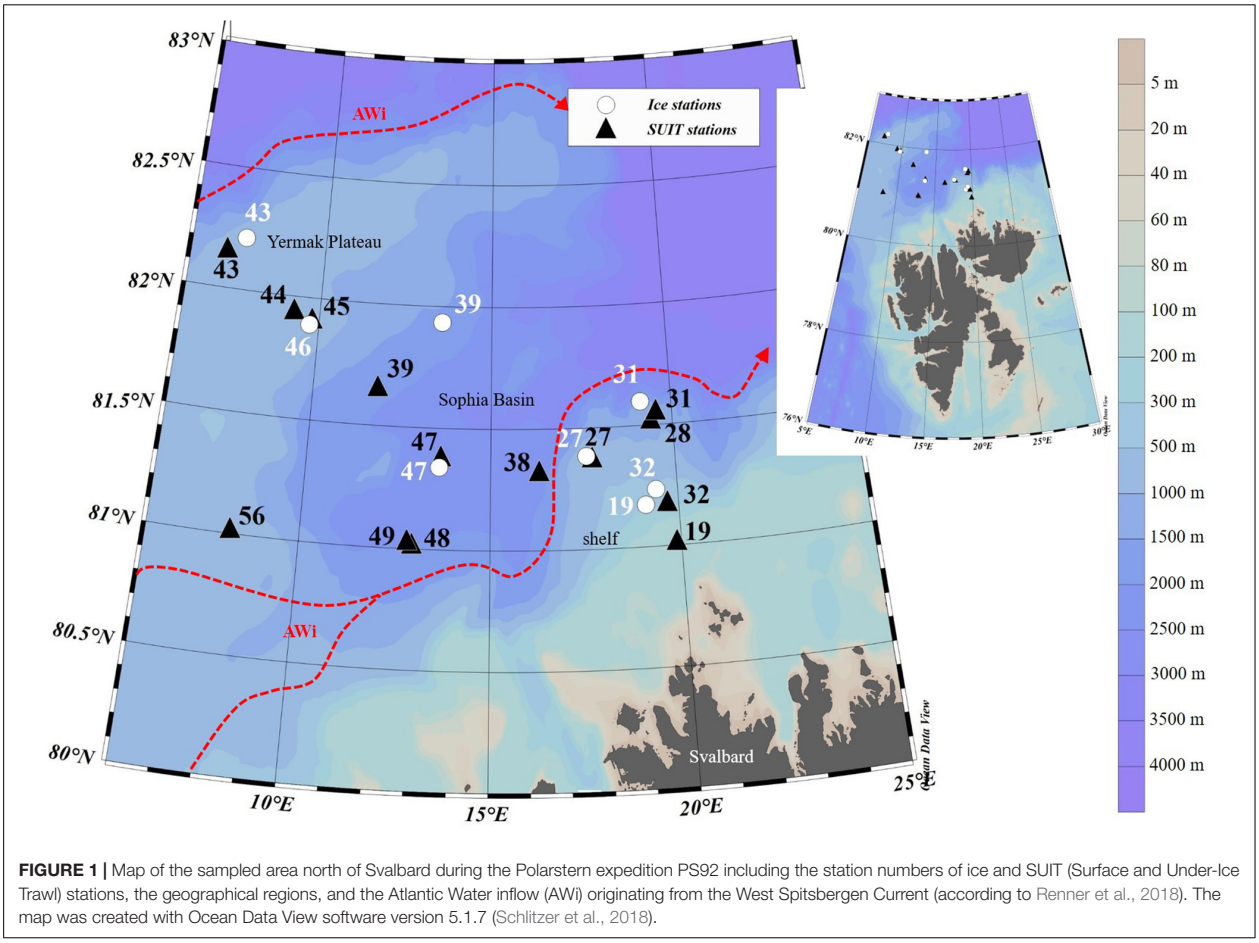

FIGURE 1 | Map of the sampled area north of Svalbard during the Polarstern expedition PS92 including the station numbers of ice and SUIT (Surface and Under-Ice Trawl) stations, the geographical regions, and the Atlantic Water inflow (AWi) originating from the West Spitsbergen Current (according to Renner et al., 2018). The map was created with Ocean Data View software version 5.1.7 (Schlitzer et al., 2018).

then calculated by multiplying by 100, by the height of the ice-core section in meters (0.1 m) and by an ice-to-water density conversion factor of 0.95 (Bluhm et al., 2018). An average was then calculated for the two replicates per station.

Environmental Parameters of Sea Ice and Under-Ice Water at SUIT Stations

An array of sensors was mounted on the SUIT frame in order to collect data on sea-ice and water properties (David et al., 2015; Lange et al., 2016; Castellani et al., in press). It contained an Acoustic Doppler Current Profiler (ADCP, Nortek Aquadopp®, Norway), which measured the velocity and direction of water passing through the net at a frequency of 2 MHZ, and a sampling interval of 1 s, and a CTD (CTD75 M, Sea & Sun Technology, Germany) with built-in fluorometer (Cyclops, Turner Designs, United States), which measured water temperature, salinity and surface water chl *a* concentration every 0.1 s. An altimeter (PA500/6-E, Tritech, United Kingdom) mounted on the CTD probe measured the distance between the net and the sea-ice underside. In combination with pressure data from the CTD, the distance to the sea-ice underside was used to derive ice thickness profiles over the entire SUIT haul (Lange et al., 2016; Castellani et al., in press). For examination of the ridge density the keels of ridges were detected along each profile by using the Rayleigh criterion (Rabenstein et al., 2010; Castellani et al., 2014). For all of the above mentioned parameters mean values were calculated. An observer on deck estimated the snow thickness visually during trawling. These estimates are presented as approximate ranges if variable and are therefore reported in **Table 1**, but were not included in further analyses. Some environmental data were not available at SUIT stations 31 and 32 due to failure of sensors.

Sampling and Processing of Under-Ice Fauna

Sampling of under-ice fauna was performed with the SUIT (van Franeker et al., 2009), which consisted of a steel frame with a 2 m × 2 m opening and two parallel, 15 m long nets attached. One net was a 0.3 mm mesh plankton net covering 0.5 m of the net opening, the other was a 7 mm half mesh covering 1.5 m of the net opening. As this study focused on mesozooplankton (0.3–20 mm), the net used to calculate the abundances of the under-ice fauna was the 0.3 mm zooplankton net. van Franeker et al. (2009), Flores et al. (2012), and David et al. (2015) provided a more detailed description of the SUIT. The catch was concentrated

TABLE 1 | Station table with the general characteristics of the ice stations.

Ice station	Cast number	Date	Lat (N)	Long (E)	Temp [°C]	Sal [PSU]	Chl *a* [$\mu g l^{-1}$]	Chl *a* [$\mu g m^{-2}$]	Btm depth [m]	Ice thick [m]	Snow thick [m]
19	6	28.05.15	81.17	19.13	−2.2	5.1	2.6	255	377	1.1	0.9
27	1	31.05.15	81.39	17.59	−1.6	3.9	2.3	227	877	1.2	0.3
31	2	03.06.15	81.60	19.15	−2.2	5.2	4.8	480	1349	1.2	0.4
32	4	06.06.15	81.24	19.43	−1.7	4.3	7.9	791	462	1.1	0.3
39	9	11.06.15	81.94	13.57	−2.0	5.9	4.7	470	1570	1.3	0.2
43	6	15.06.15	82.21	7.60	−1.4	5.2	2.0	199	806	1.1	0.3
46	3	17.06.15	81.89	9.73	−1.2	4.6	4.1	412	907	1.1	0.1
47	5	19.06.15	81.34	13.61	−1.2	1.7	5.3	529	2173	1.2	0.2

Lat, latitude; Long, longitude; Temp, temperature of the ice; Sal, salinity of the ice; Chl a, chlorophyll a concentration of the ice; Btm depth, bottom depth at ice station; Ice thick, ice thickness; Snow thick, snow thickness at coring site. Temp, Sal, Chl a, and Ice thick are for n = 1; Snow thick is for n = 5.

over a 100 μm sieve and a defined fraction (mostly one half of the original sample) was put in 4% buffered formaldehyde solution for preservation and later quantitative analysis. If the density was still high, the sample was split again with a plankton splitter prior to analysis. The samples of fourteen SUIT stations were sorted and identified to the lowest taxonomic level possible under a stereo- microscope coupled to a digital image analysis system (Leica Model M 205C, image analysis software LAR 4.2 or a Leica Discovery V8 with Axiocam) in the laboratories of the Alfred Wegener Institute. Taxonomic names were verified using the current classification of WoRMS[1]. Classification of *Calanus* spp. individuals to species level (*C. hyperboreus*, *C. glacialis*, and *C. finmarchicus*) was based on length measurements and stage determination according to Madsen et al. (2001). Abundances of ind.m^{-2} were calculated by multiplying the total number of individuals of each taxon in the sample by the respective splitting factor and dividing the result by the water volume sampled by the SUIT at the respective station (measured by the ADCP). The result was then multiplied by the height of the net (2 m) (David et al., 2015).

Data Analysis

A correlation based PCA (Mardia et al., 1979) with Euclidean distance measure was applied to both environmental datasets to reveal habitat typologies of the sea ice and the upper water column (Clarke and Warwick, 2001). Spearman's rank correlation coefficients were used to identify environmental variables with high collinearity (Clarke and Warwick, 2001; Zuur et al., 2007) in order to decide which variables to include in the respective PCA. If pairs of environmental variables had a Spearman's rank correlation coefficient >0.8, only one of the correlated variables was chosen for further analysis based on the relevance of this variable for the scientific question and the comparability to other studies (Zar, 1984). For the ice stations, six environmental variables were analyzed and four were retained for further statistical analysis (**Supplementary Table S1**). For the SUIT stations, seven environmental variables were analyzed and four were retained for further statistical analysis (**Supplementary Table S2**). The PCA was then applied to each normalized environmental dataset.

Three diversity indices were separately calculated for sea-ice meiofauna and under-ice fauna in order to investigate patterns of diversity over the sampled area: (1) Taxa richness (S) (the number of taxa observed per station), (2) Shannon diversity (H), and (3) Pielou's evenness (J') (Shannon and Weaver, 1963; Pielou, 1969). We note that these and subsequent analyses were done separately for sea-ice meiofauna and under-ice fauna communities, because gear types and mesh sizes are not directly comparable.

To visualize community similarity patterns of the sea-ice meiofauna and the under-ice fauna, NMDS (Shepard, 1962; Kruskal, 1964) based on a Bray–Curtis similarity matrix (Bray and Curtis, 1957) was applied to each data set. The four environmental variables selected for the PCA were fitted into the NMDS ordination. The generation of an NMDS is an iterative procedure. It compiles a plot by successively refining the positions of the points until they fit as closely as possible to the dissimilarity relations between the samples (Clarke and

Warwick, 2001). Thus, short distances of sampling sites in the NMDS plot indicate a high similarity in community structure, whereas sampling sites with low similarity are further apart in the ordination plot. The goodness-of-fit of NMDS plots was assessed by Shepard plots and stress values (Clarke and Warwick, 2001; Legendre and Legendre, 2012). A stress value of <0.05 was considered a very good representation with no prospect of misinterpretation (Clarke and Warwick, 2001). We applied the NMDS analysis with different transformations (none to 4th root) of the abundance datasets. The lowest stress values for both sea-ice meiofauna and under-ice fauna datasets were achieved by untransformed abundance data. Based on these untransformed abundance data an analysis of similarity (ANOSIM; Clarke and Ainsworth, 1993) was conducted to test for significant differences of community similarity between *a priori* defined geographical regions (shelf, Yermak Plateau and Sophia Basin with adjacent slope). Again, this analysis was separately performed for sea-ice meiofauna and under-ice fauna. Geographical regions were defined by a combination of water depth and geomorphological structures. Statistical analyses were conducted with the R software Version 3.5.1[2] (R Core Team, 2018) by using the packages: vegan (Oksanen et al., 2018), ggplot2 (Wickham, 2016), dplyr (Wickham and Ruiz, 2018), and scales (Wickham, 2018).

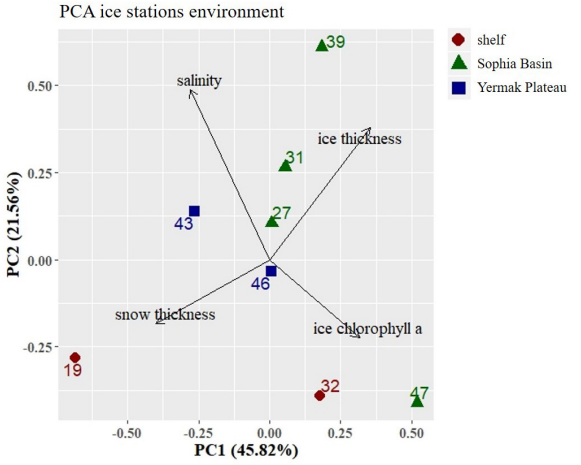

FIGURE 2 | Principal Component Analysis (PCA) plot of environmental parameters at the ice stations. Stations were color-coded according to geographical regions (shelf, Sophia Basin, and Yermak Plateau). Black arrows point into the direction of increasing values of environmental parameters in the ordination. Percentage values in axis annotations indicate the proportion of explained variance of the PCA.

RESULTS

Environmental Conditions at Ice Stations

The ice thickness of the sea-ice cores was very similar among stations and ranged between 1.07 m (station 19) and 1.25 m (station 39) with an average thickness of 1.16 m, reflecting first-year sea ice (**Table 1**). Snow thickness was highest at station 19 with 0.9 m while it ranged for the other stations between 0.13 and 0.4 m, with station 43 having the lowest snow thickness. On average, the stations had a snow thickness of 0.33 m across the sampled area (**Table 1**). The temperature of the sea-ice cores varied between −2.2°C (station 19) and −1.2°C (station 47) with an average temperature of −1.7°C (**Table 1**). Bulk salinity of the bottom 10 cm sea-ice sections stood out at station 47 with a PSU of 1.65. All the other stations ranged in their PSU between 3.88 (station 27) and 5.88 (station 39), with a mean salinity of 4.47 (**Table 1**). Sea-ice chl *a* concentration of the bottom 10 cm of the ice core varied from 199 μgm^{-2} (station 43) to 790 μgm^{-2} (station 32) with an average of 420 μgm^{-2} (**Table 1**).

In the PCA of environmental variables, 67% of variance could be explained by the first two components (**Figure 2**). The first axis (PC1) explained 46% of the variance and was mainly driven by snow thickness. Along this axis there was a distinction between the two shelf stations 19 and 32, with station 19 being strongly influenced by snow thickness (**Figure 2**). The second axis (PC2) explained 22% of the variance and was mainly associated with bulk salinity. Along this axis there was a noticeable, albeit not very strong, regional distinction between the shelf, the Sophia Basin with adjacent slope, and the Yermak Plateau stations (**Figure 2**).

[2]https://www.R-project.org/

Sea-Ice Meiofauna Biodiversity, Taxonomic Composition and Abundance

In total 10 sea-ice meiofauna taxa belonging to five phyla were identified in this study (**Tables 2**, **3** and **Figure 3**). Taxa richness (*S*) ranged from 2 to 8 and Shannon diversity index (H') ranged from 0.60 to 1.53 across ice stations (**Table 2**). The lowest *S* and *H*' were observed at stations in the Sophia Basin and on the Yermak Plateau (stations 39 to 47) (**Table 2**). The ice cores of these stations contained either only Harpacticoida and copepod nauplii (stations 39, 47) or these two taxa and Ciliophora (stations 43, 46) (**Figure 4**). Higher *S* and *H*' were observed at the stations on the Sophia Basin slope and the shelf of Svalbard with station 27 being the station with the highest *S* (8) and H' (1.53) (**Table 2**). Except for Amoebozoa, all phyla were present in the ice cores of this station (**Figure 4**). Pielou's evenness (J') ranged from 0.54 to 0.90 and did not strictly follow the pattern of *S* and H', though values were mostly higher further offshore where stations had low taxa richness and were dominated by Harpacticoida and copepod nauplii (**Table 2** and **Figure 4**). The lowest value of J' was reached at stations closer to the shelf, which were dominated by Ciliophora (**Table 2** and **Figure 4**).

Total abundances of sea-ice meiofauna ranged from 580 ind.m^{-2} (station 39) to 17,156 ind.m^{-2} (station 27) (**Table 2** and **Figure 4**). The most abundant taxon across all stations was Ciliophora with a maximum abundance of 8,562 ind.m^{-2} and an average contribution of 46% to the total sea-ice meiofauna abundance (**Table 3**). Second most abundant were copepod nauplii with a maximum abundance of 7,682 ind.m^{-2} and a share of 29%, and Harpacticoida with a maximum abundance of 4,609 ind.m^{-2} and a share of 20% to the total sea-ice meiofauna

TABLE 2 | List of total abundances and biodiversity indices for sea-ice meiofauna per station.

Sea-ice meiofauna/station	19	27	31	32	39	43	46	47
Total abundance [ind.m^{-2}]	14576	17156	8820	12130	580	3867	3610	6641
Taxa richness (*S*)	7	8	4	7	2	3	3	2
Shannon diversity (*H'*)	1.29	1.53	1.19	1.05	0.60	0.99	0.63	0.62
Pielou's evenness (*J'*)	0.66	0.74	0.86	0.54	0.87	0.90	0.58	0.89

TABLE 3 | List of sea-ice meiofauna taxa with mean abundance and frequency of occurrence across the sample area.

Sea-ice meiofauna taxon	Mean abundance [ind.m^{-2}]	*SD*	Range	Freq. of occurrence [%]	Relative abundance [%]
ARTHROPODA von Siebold, 1848					
Crustacea Brünnich, 1772					
Copepoda Milne Edwards, 1840					
Harpacticoida G.O. Sars, 1903	1710.56	1617.31	0–4609.38	0.88	20.31
Nauplii (copepoda)	2427.70	2336.31	167.41–7681.94	1.00	28.82
ROTIFERA Cuvier, 1817	106.16	216.24	0–593.22	0.25	1.26
CILIOPHORA not documented	3363.15	3414.98	0–8562.06	0.75	39.93
Oligotrichea Bütschli, 1887					
Tintinnina Kofoid and Campbell, 1929	482.75	575.19	0–1525.42	0.63	5.73
MYZOZOA Cavalier-Smith and Chao					
Dinoflagellata not documented					
Dinophyceae Fritsch, 1927					
Protoperidinium Bergh, 1881	123.47	228.84	0–512.13	0.25	1.47
Podolampas Stein, 1883	32.01	90.53	0–256.06	0.13	0.38
Polykrikos Bütschli, 1873 spp.	40.32	85.14	0–237.83	0.25	0.48
Gyrodinium Kofoid and Swezy, 1921	125.75	272.60	0–768.19	0.25	1.49
AMOEBOZOA Lühe, 1913, emend. Cavalier-Smith, 1998	10.59	29.96	0–84.75	0.13	0.13

"Ciliophora" values are excluding "Tintinnina". SD, standard deviation; Freq. of occurrence, frequency of occurrence.

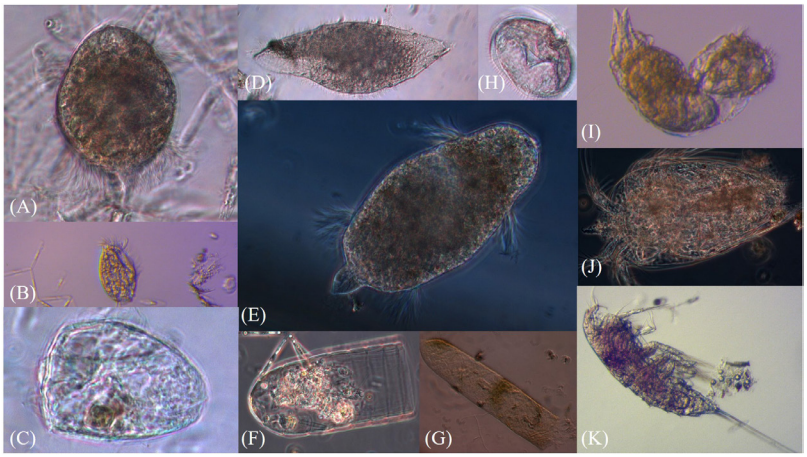

FIGURE 3 | Pictures of sea-ice meiofauna **(A–E)** Ciliophora, **(F,G)** Tintinnina, **(H)** *Protoperidinium* sp., **(I)** Rotifera, **(J)** Nauplius, **(K)** Harpacticoida. Photographs by Julia Ehrlich.

abundance (**Table 3**). The community structure showed some geographical or seasonal/temporal variability, since Rotifera, Dinophyceae, and Amoebozoa occurred solely at the four easternmost stations (stations 19–32) on the shelf of Svalbard and the slope of the Sophia Basin sampled early during the expedition (**Figure 4**). Those stations showed also a higher abundance of Ciliophora compared to the offshore stations (stations 39–47). The NMDS ordination of the sampling stations

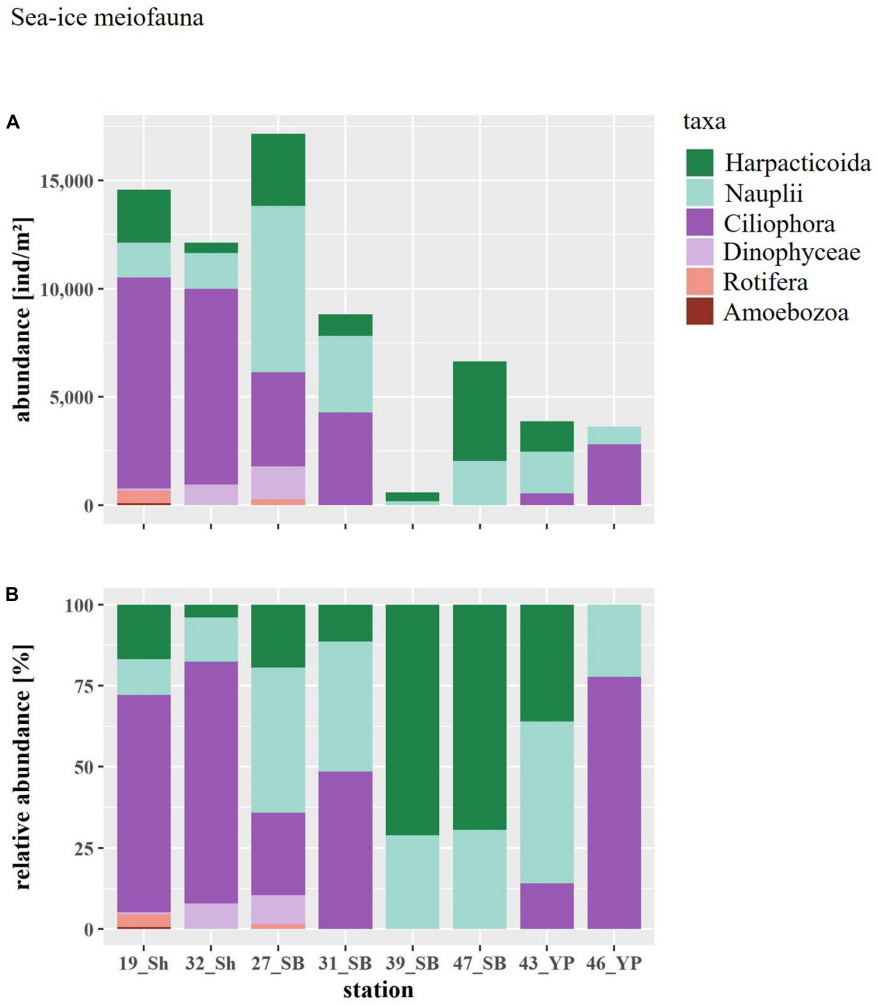

FIGURE 4 | (A) Abundance and **(B)** relative abundance of the sea-ice meiofauna at ice stations arranged by geographical region (Sh, shelf; SB, Sophia Basin; YP, Yermak Plateau).

along ordination axis 1 largely resembled gradual changes in community structure along a quasi-bathymetric gradient from the shelf to the Sophia Basin with adjacent slope and the Yermak Plateau stations (**Figure 5**). However, the conducted ANOSIM showed no significant difference in community similarity between the three regions shelf, Sophia Basin with slope and Yermak Plateau ($\alpha > 0.05$, $R = -0.075$, $p = 0.41$).

Environmental Conditions at SUIT Stations

The bottom depth of the SUIT stations varied considerably during this study from 188 m on the shelf (station 19) to 2,249 m in the Sophia Basin (station 38) (**Table 4**). The average ice coverage in the areas of the under-ice hauls was 51% (**Table 4**). Ice thickness ranged between 1.05 m (station 19) and 3.84 m (station 44), with a mean of 1.70 m across the sampled stations (**Table 4**). The density of sea-ice ridges was highest at station 39 with 11.4 ridges km^{-1} and lowest at station 19 with 1.4 ridges km^{-1}. The average ridge density was 4.9 ridges km^{-1} (**Table 4**). The temperature of the 0–2 m surface water varied between 1.3 and 1.8°C with an average of 1.6°C. Stations on the Svalbard shelf and slope of the Sophia Basin (stations 19, 27, and 28) had lower temperatures (1.3–1.4°C) than stations in the Sophia Basin and on the Yermak Plateau (39–56: 1.6–1.8°C) (**Table 4**). Salinity of the sampled SUIT stations ranged from 33.4 PSU (station 47) to 34.3 PSU (station 45) with a mean salinity of 33.8 PSU (**Table 4**). Chlorophyll *a* concentrations of the surface water varied widely between 540 $\mu g m^{-2}$ at station 43 and 21,158 $\mu g m^{-2}$ at station 47 with an average of 6,967 $\mu g m^{-2}$ (**Table 4**).

The first two components (PC1 and PC2) of the PCA explained 75% of the variance and showed a regional pattern (**Figure 6**). Stations located in the Sophia Basin and adjacent

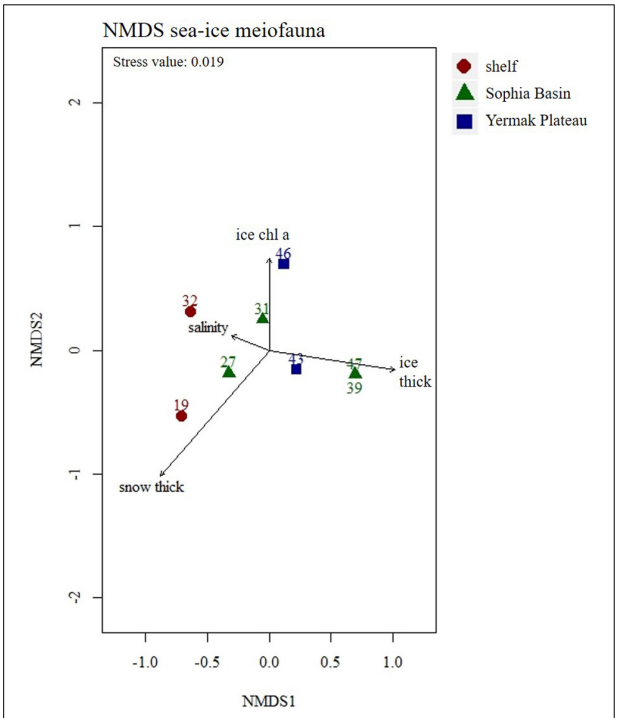

FIGURE 5 | Non-metric Multidimensional Scaling (NMDS) plot of sea-ice meiofauna abundances with four fitted environmental variables. Stations were color coded according to geographical regions (shelf, Sophia Basin, and Yermak Plateau). Ice thick, ice thickness; ice chl *a*, ice chlorophyll *a*; snow thick, snow thickness.

slope grouped together as did those over the Yermak Plateau (**Figure 6**). PC1 explained 50% of the variance and was mainly driven by bottom depth. Along this ordination axis there was a regional distinction between the shelf, the Sophia Basin with adjacent slope, and the Yermak Plateau stations (**Figure 6**). PC2 explained 25% of the variance and was mainly associated with ice thickness. Along this axis there was a clear separation of station 44 from all the other stations, which had an appreciably higher ice thickness than the other stations (**Figure 6**).

Under-Ice Fauna Biodiversity, Taxonomic Composition and Abundance

In total we identified 32 taxa of under-ice fauna from 8 phyla in this study (**Tables 5**, **6** and **Figure 7**). Species richness (*S*) ranged between 7 and 21 with no clear pattern among stations. For example, the lowest and the highest *S* were reached at stations 48 (7 taxa) and 49 (21 taxa), which were geographically closest to each other. Both stations were located in the southern part of the Sophia Basin and dominated by *C. finmarchicus* and *C. glacialis* (**Figure 8**). H' and J' ranged from 0.58 to 1.73 and from 0.21 to 0.80, respectively, again with no clear geographic pattern (**Table 5**). The highest H' and J' were reached at stations 27 and 31 on the slope of the Sophia Basin. Both stations were dominated by equally abundant *C. finmarchicus*, *C. glacialis*, *C. hyperboreus*, and

TABLE 4 | Station table with the general characteristics of the SUIT stations.

SUIT station	Cast number	Date	Lat (N)	Long (E)	Temp [°C]	Sal [PSU]	Chl *a* [$\mu g l^{-1}$]	Chl *a* [$\mu g m^{-2}$]	Btm depth [m]	Ice thick [m]	Snow thick [m]	Filtered vol [m^3]	Ridge dens [km^{-1}]
19	1	27.05.15	81.01	19.89	1.3	33.9	70.3	7032	189	1.1	0.1–0.2	1453	1.4
27	1	31.05.15	81.37	17.75	1.4	33.4	92.2	9218	828	1.1	0.1–0.4	1060	6.3
28	4	02.06.15	81.52	19.42	1.4	34.1	46.0	4600	928	1.3	0.3–0.4	841	4.4
31	1	03.06.15	81.55	19.57	NA	NA	NA	NA	1051	NA	0.2	424	NA
32	12	07.06.15	81.18	19.71	NA	NA	NA	NA	336	NA	0.2	403	NA
38	1	09.06.15	81.32	16.31	1.7	33.7	175.6	17560	2249	1.2	0.1–0.4	1025	4.8
39	17	12.06.15	81.65	11.82	1.8	33.8	9.1	906	1955	1.6	0.1–0.4	657	11.4
43	23	16.06.15	82.16	7.08	1.8	34.1	5.4	540	794	1.8	0.2–0.3	635	1.6
44	1	17.06.15	81.94	9.26	1.8	34.2	7.8	784	814	3.8	0.1–0.2	792	2.6
45	1	17.06.15	81.91	9.80	1.7	34.3	10.4	1044	922	1.8	0.1–0.3	588	3.4
47	1	19.06.15	81.38	13.65	1.7	33.4	211.6	21158	2139	1.5	0.1	551	5.2
48	1	21.06.15	81.02	12.95	1.5	33.5	56.7	5666	2047	1.7	0.1–0.2	1301	5.8
49	1	21.06.15	81.03	12.83	1.6	33.4	111.6	11164	2083	1.9	0.2–0.3	832	4.9
56	2	23.06.15	81.02	8.20	1.7	34.0	39.4	3940	849	2.3	0.05	656	7.2

Lat, latitude; Long, longitude; Temp, temperature of the surface water; Sal, salinity of the surface water; Chl a, chlorophyll a concentration of the surface water; Btm depth, bottom depth; Ice thick, ice thickness; Snow thick, snow thickness; Filtered vol, filtered water volume; Ridge dens, ridge density. Temp, Sal, and Chl a were measured every 0.1 s; Filtered vol was measured every 1 s; Temp, Sal, Chl a, Ice thick, and Ridge dens are averaged measurements over the SUIT transect.

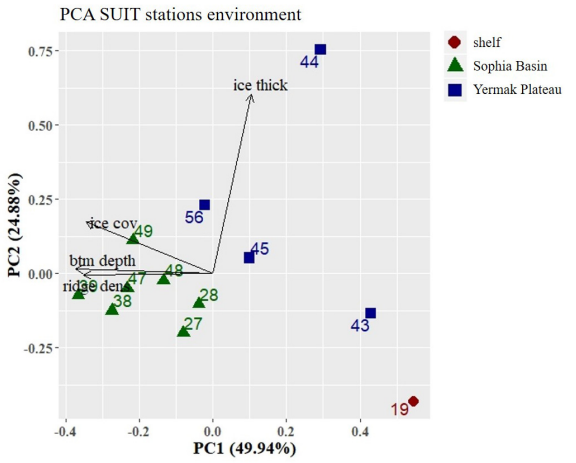

FIGURE 6 | Principal Component Analysis (PCA) plot of environmental parameters at the SUIT stations. Stations were color coded according to geographical regions (shelf, Sophia Basin, and Yermak Plateau). Black arrows point into the direction of increasing values of environmental parameters in the ordination. Percentage values in axis annotations indicate the proportion of explained variance of the PCA. Ice thick, ice thickness; ice cov, ice coverage; btm depth, bottom depth; ridge dens, ridge density.

nauplii. The lowest H' and J' were estimated for the shelf stations 19 and 32, which were dominated by copepod nauplii (**Table 5** and **Figure 8**).

Total abundances of under-ice fauna ranged from 15 ind.m^{-2} (station 44) to 6,785 ind.m^{-2} (station 32) (**Table 5**). The highest total abundances were found at stations in the center of the Sophia Basin (stations 38, 47, and 49) and at the single shelf station, with very high Appendicularia abundance (station 32) (**Figure 8**). The most abundant taxa were Appendicularia with a maximum abundance of 4,915 ind.m^{-2} and an average contribution of 58% to the total under-ice fauna abundance. The high share of Appendicularia to the overall abundance was due to their exceptionally high abundance (4,915 ind.m^{-2}) at station 32. At all other stations, their abundance ranged between 0 and 4 ind.m^{-2} (**Figure 8**). Except for station 32, all other stations were dominated by copepod nauplii with a maximum abundance of 1,747 ind.m^{-2} and a share of 23% to the total under-ice fauna abundance (55% if Appendicularia abundance at station 32 was excluded) (**Table 6** and **Figure 8**). Copepod nauplii were especially abundant at stations, which were sampled early during the expedition (stations 19–39). *C. finmarchicus* was the most abundant copepod species with abundances between 2 and 260 ind.m^{-2} contributing 9% to the total under-ice fauna abundance (20% if Appendicularia at station 32 excluded) (**Table 6** and **Figure 8**). *C. glacialis* ranged between 0.4 and 231 ind.m^{-2} contributing 6% (14% if Appendicularia at station 32 excluded), and *C. hyperboreus* ranged between 0.2 and 49 ind.m^{-2} contributing 2% (5% if Appendicularia at station 32 excluded) to total under-ice fauna abundance (**Table 6** and **Figure 8**). The remaining 27 taxa together made up 2% (6% if Appendicularia at station 32 excluded) of the total under-ice fauna abundance (**Table 6**). The three *Calanus* species were abundant at all fourteen stations and had a constantly high contribution to the under-ice fauna (**Figure 8**). Another taxon with high frequency of occurrence, but mostly low abundances (0–56 ind.m^{-2}) were Cirripedia, which made up 1% of the entire under-ice fauna (3% if Appendicularia at station 32 excluded) (**Table 6** and **Figure 8**). Cirripedia resembled the pattern of copepod nauplii that were mainly abundant at stations sampled early during the expedition (stations 27–39). The NMDS showed no clear separation of distinct communities based on taxa abundances (**Figure 9**). However, the ordination of the sampling stations along ordination axis 2 showed a gradual change in the community similarity from the shelf to the Sophia Basin with adjacent slope and the Yermak Plateau stations (**Figure 9**). This spatial community change was resembled in the conducted ANOSIM showed a significant difference in community similarity between the three regions shelf, Sophia Basin with slope and Yermak Plateau ($\alpha \leq 0.05$, $R = 0.26$, $p = 0.04$).

DISCUSSION

Sea-Ice Meiofauna

During this study, sea-ice meiofauna abundances ranged from 580 to 17,156 ind.m^{-2} in the pack ice north of Svalbard. This abundance range is consistent with that reported from pack ice in the same region two decades earlier (Gradinger et al., 1999). When excluding Ciliophora, which most ice biota studies from the Arctic Ocean do not include, the total abundances of sea-ice meiofauna in this study ranged between 580 and 13,827 ind.m^{-2}. This wide range of abundances is again similar to other pack-ice studies from the geographic area of our study (Schünemann and Werner, 2004; Bluhm et al., 2018) and has also been reported from other locations such as Baffin Bay and the Amerasian Basin (Nozais et al., 2001; Gradinger et al., 2005).

The taxonomic composition showed both similarities and differences to earlier sea-ice meiofauna studies. After Ciliophora, Harpacticoida and copepod nauplii were the most abundant groups, both of which have been consistently reported to occur in sea ice. Harpacticoida are common sea-ice residents and tolerant to extreme conditions such as freezing into solid ice for short periods (Damgaard and Davenport, 1994). Their capability to reproduce several times a year with no interruption during winter (Carey, 1992; Friedrich, 1997) may contribute to their high abundance in our and other studies. For pack ice in the region northwest of Svalbard, similar relative abundances for Copepoda (including Harpacticoida) were reported by Gradinger et al. (1999) and Schünemann and Werner (2004), but nauplii abundances were much lower in those studies. For the pan-Arctic, Bluhm et al. (2018) synthesized 23 studies on sea-ice meiofauna and estimated a mean abundance across all ice types and seasons of 341 ind.m^{-2} for Harpacticoida and 1,141 ind.m^{-2} for nauplii, recognizing that nauplii abundances are highly seasonal. Calanoid copepod nauplii

TABLE 5 | List of total abundances and biodiversity indices for under-ice fauna per station.

Under-ice fauna/station	19	27	28	31	32	38	39	43	44	45	47	48	49	56
Total abundance [ind.m^{-2}]	55	125	61	77	6785	277	25	27	15	57	216	39	548	186
Taxa richness (*S*)	15	9	10	11	14	13	8	10	7	10	17	21	7	11
Shannon diversity (*H'*)	0.58	1.73	1.71	1.93	0.69	1.62	1.58	1.23	1.31	1.21	1.38	1.34	0.99	1.02
Pielou's evenness (*J'*)	0.21	0.79	0.74	0.80	0.26	0.63	0.76	0.53	0.67	0.53	0.49	0.44	0.51	0.42

tend to be encountered in sea ice in highest abundances in springtime (Bluhm et al., 2018) matching the sampling time in this study. In addition, Nozais et al. (2001) suggested that copepods (including Harpacticoida and Cyclopoida) reproduce inside the bottom ice layer itself. Consistent with these findings we suggest that the high densities of nauplii were a result of successful reproduction of copepods inside the sea-ice in our study.

The taxonomic composition of the sea-ice meiofauna in this study, however, also shows some marked differences to earlier studies. Nematoda, Acoela, and platyhelminth flatworms (in earlier studies reported as 'Turbellaria') were among the most abundant taxa in earlier Arctic pack-ice studies (Gradinger, 1999; Nozais et al., 2001; Gradinger et al., 2005) including the region north of Svalbard (Gradinger et al., 1999; Schünemann and Werner, 2004), but neither of these taxa were observed in this study. Essentially the same pattern (absence of flatworms and nematodes except for a single ice core) was found in a parallel study in the same area that extended over six months comprising the entire ice-covered period (N-ICE data set in Bluhm et al., 2018; Granskog et al., 2018) suggesting our finding was not barely a bias of our limited sample size or the time point of our sampling. As Nematoda are thought to colonize the sea ice in shallow waters from the sediment, where they dominate the meiofauna of the benthic interstitial (Carey and Montagna, 1982), they are predominantly found in land-fast ice or pack ice formed on shallow shelves. So far, it was assumed that Nematoda are allochthonous and do not reproduce in sea ice (Riemann and Sime-Ngando, 1997). However, recently reproduction of Nematoda was reported from shallow Arctic land-fast ice of Alaska's north coast (Gradinger and Bluhm, 2020). Colonization patterns of ice fauna of benthic origin may change as climate driven sea-ice formation shifts. In a recent analysis of sea-ice meiofauna communities in different types of Arctic sea ice, Kiko et al. (2017) suggested that pack ice of the new Arctic will favor pelagic-sympagic species (e.g., Ciliophora) over benthic-sympagic species (e.g., Nematoda), because the now dominant first-year pack ice tends to form farther offshore and multi-year ice vanishes. For our study region, recent backtracking analyses suggest that less sea ice formed on the Siberian shelves now actually reaches the Fram Strait area (Krumpen et al., 2019). In addition, much of the ice in our research area was formed in the central Arctic Ocean (Krumpen et al., 2019). As a consequence, less sediment and, we suggest, less benthic-derived ice biota from shallow Siberian shelf areas may reached our research area. Satellite-backtracking data, which showed the origin of the specific ice floes sampled during this study, support that hypothesis (Krumpen, pers. communication). Finally, Rotifera only made up 1% of the sea-ice meiofauna abundance compared to a pan-Arctic average share of 22% (Bluhm et al., 2018) and even 33% to the pack-ice meiofauna north of Svalbard (Schünemann and Werner, 2004). According to Bluhm et al. (2018), Rotifera tend to get more abundant the later the season. Correspondingly, the early sampling season could explain the low abundance of Rotifera during this study. The abundance of sea-ice meiofauna is known to vary at least as much among seasons than regions typically reaching its peak by late spring/early summer (Schünemann and Werner, 2004; Bluhm et al., 2018). Thus, differences in abundances between studies are in part due to different seasons of sampling. A small fraction of the difference may also be explained by the fact that this study reports data from the bottom 10 cm while on average one-third of the abundance may be found outside this layer (Bluhm et al., 2018). However, inspection of the melted top 10 cm of our ice cores showed sea-ice meiofauna was absent from this layer.

Sea-ice chl *a* concentration can be used as an indicator for the prevalent food conditions in the pack ice for the dominant sympagic grazers in this study, Harpacticoida and copepod nauplii, who are known to feed on ice algae (Grainger and Hsiao, 1990; Gradinger and Bluhm, 2020). With a mean of 420 μg chl *a* m^{-2}, the chl *a* concentration was markedly lower than in a summer pack-ice study from the same region almost two decades earlier when it reached a mean of 1,200 μg chl *a* m^{-2} (Gradinger et al., 1999). It is possible that some of the ice algae were already flushed out of the ice, given the low bulk salinities (<5 PSU) and moderate temperatures of the sea ice, which indicated the onset of ice melting during this late spring expedition. Another explanation for the low chl *a* concentration could be the snow thickness, which resulted in extreme low irradiance under the ice as could be shown during this study for most of the ice stations (Massicotte et al., 2019). Sea-ice chl *a* concentration did not correlate with sea-ice meiofauna abundance, although in other studies this was the case (Gradinger, 1999; Nozais et al., 2001).

Both chl *a* concentration and sea-ice meiofauna abundance can vary by orders of magnitude on small spatial scales and representative sampling should encompass large sample sizes or sensor profiles (Lange et al., 2017). It is, therefore, possible that the sample size of this study was too small to disentangle patchiness effects from the potential relationship between ice algae and sea-ice meiofauna. Although ice coring can cause inherent biases, because of the potential to lose part of the bottom section and/or brine, it is the current standard method for assessing the community

TABLE 6 | List of under-ice fauna with mean abundance and frequency of occurrence across the sample area.

Under-ice fauna taxon	Mean abundance [ind.m^{-2}]	*SD*	Range	Freq. of occurrence [%]	Relative abundance [%]
ARTHROPODA von Siebold, 1848					
Crustacea Brünnich, 1772					
Copepoda Milne Edwards, 1840					
Harpacticoida G.O. Sars 1903	< 0.01	0.01	0–0.02	0.07	< 0.01
Tisbe Lilljeborg, 1853 spp.	0.01	0.03	0–0.12	0.21	< 0.01
Oithona Baird, 1843 sp.	0.17	0.62	0–2.34	0.21	0.03
Calanus hyperboreus Krøyer, 1838	11.52	13.39	0.20–49.21	1.00	1.90
Calanus glacialis Jaschnov, 1955	35.94	59.76	0.40–231.30	1.00	5.92
Calanus finmarchicus (Gunnerus, 1765)	51.60	69.94	2.05–260.83	1.00	8.51
Nauplii (Copepoda)	140.63	462.95	0–1746.59	0.79	23.18
Paraeuchaeta Scott, 1909 spp.	< 0.01	< 0.01	0–0.01	0.07	< 0.01
Metridia longa (Lubbock, 1854)	0.05	0.19	0–0.70	0.07	0.01
Clausocalanidae Giesbrecht, 1893	0.51	1.33	0–5.08	0.50	0.08
Malacostraca Latreille, 1802					
Amphipoda Latreille, 1806					
Themisto Guerin, 1825 spp.	0.12	0.47	0–1.75	0.14	0.02
Themisto libellula (Lichtenstein in Mandt, 1822)	0.11	0.31	0–1.17	0.43	0.02
Themisto abyssorum (Boeck, 1871)	0.02	0.07	0–0.25	0.14	< 0.01
Apherusa glacialis (Hansen, 1888)	1.90	2.37	0.06–7.52	1.00	0.31
Onisimus glacialis (G.O. Sars, 1900)	< 0.01	< 0.01	0–0.01	0.07	< 0.01
Eusirus Krøyer, 1845 spp.	< 0.01	0.01	0–0.05	0.07	< 0.01
Euphausiacea Dana, 1852					
Thysanoessa longicaudata Krøyer, 1846	0.06	0.13	0–0.46	0.36	0.01
Isopoda Latreille, 1817	0.01	0.03	0–0.12	0.21	< 0.01
Decapoda Latreille, 1802					
Zoaea larvae	0.01	0.04	0–0.16	0.14	< 0.01
Hexanauplia Oakley et al., 2013					
Cirripedia Burmeister, 1834	8.83	15.04	0–55.85	0.93	1.46
CHAETOGNATHA not documented	0.52	1.29	0–4.79	0.29	0.09
Sagittoidea not documented					
Eukrohnia hamata (Moebius, 1875)	1.07	1.24	0–2.90	0.71	0.18
Parasagitta elegans (Verrill,1873)	0.09	0.16	0–0.60	0.57	< 0.01
CHORDATA Haeckel, 1874					
Appendicularia Fol, 1874	351.57	1313.40	0–4914.82	0.29	57.96
Oikopleura Mertens, 1830 spp.	0.33	1.25	0–4.68	0.07	0.06
Osteichthyes larvae	0.01	0.05	0–0.19	0.07	< 0.01
MOLLUSCA not documented					
Gastropoda Cuvier, 1795					
Limacina helicina (Phipps, 1774)	< 0.01	< 0.01	0–0.01	0.14	< 0.01
Clione limacina (Phipps, 1774)	0.01	0.02	0–0,08	0.14	< 0.01
ANNELIDA incertae sedis					
Polychaeta Grube, 1850	0.15	0.33	0–1.12	0.36	0.02
Trochophora larvae	0.85	2.70	0–10.15	0.21	0.14
CNIDARIA Hatschek, 1888					
Hydrozoa Owen, 1843	< 0.01	< 0.01	0–0.01	0.07	< 0.01
XENACOELOMORPHA Philippe et al., 2011	0.51	1.26	0–4.22	0.29	0.08

"Chaetognatha" refers to individuals which could not be identified to species level. SD, standard deviation; Freq. of occurrence, frequency of occurrence.

structure of sea-ice meiofauna (Gradinger and Bluhm, 2009; Eicken et al., 2014). We recommend morphological studies such as this one to be combined with molecular approaches that are increasingly used for enhanced taxonomic resolution (Hardge et al., 2017; Marquardt et al., 2018; Pitusi, 2019).

Under-Ice Fauna

The overall mean abundance of under-ice fauna was 607 ind.m^{-2} during this study, which is one order of magnitude higher than in the only other SUIT study from the central Arctic Ocean from summer 2012 (David et al., 2015). The diversity of the under-ice fauna, however, was

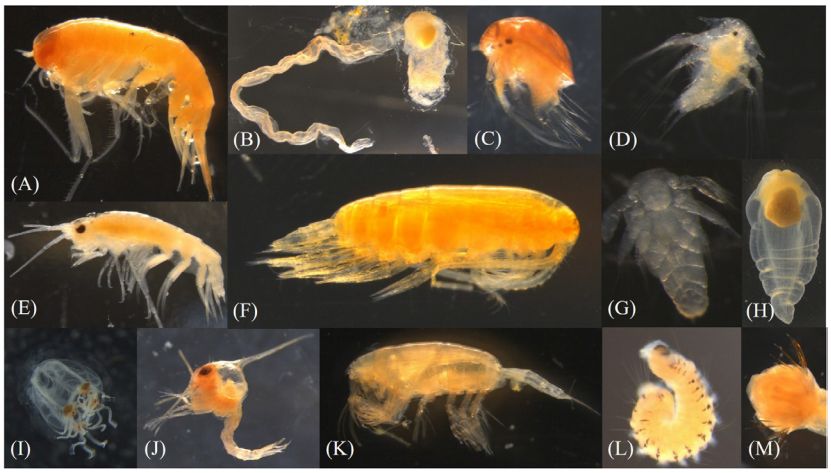

FIGURE 7 | Pictures of under-ice fauna **(A)** *Themisto* sp., **(B)** Appendicularia, **(C,D)** Cirripedia, **(E)** *Apherusa glacialis*, **(F)** *Calanus* sp., **(G)** Nauplius, **(H)** *Clione limacina*, **(I)** Hydrozoa, **(J)** Zoaea larvae, **(K)** *Paraeuchaeta* sp., **(L)** Polychaeta, **(M)** Chaetognatha (head). Photographs by Julia Ehrlich.

very much in accordance with studies from the Laptev Sea (Werner and Arbizu, 1999) and the central Arctic Ocean (David et al., 2015). Highest taxa richness and abundance of the under-ice fauna were found at stations with highest surface chl *a* values, though overall phytoplankton concentrations of the surface waters were relatively low compared to other studies (David et al., 2015; Castellani et al., in press).

It is well known that Crustacea such as Copepoda and Amphipoda can live associated with Arctic sea ice (Arndt and Swadling, 2006; Søreide et al., 2010; Hop et al., 2011). Apart from one occurrence of remarkably high abundance of Appendicularia (station 32), copepod nauplii and *Calanus* species were the most abundant and most frequent taxa across the sampled area. *C. finmarchicus*, the dominant *Calanus* species found in this study (**Figure 3**), is a boreal Atlantic species and is characteristic of the zooplankton community in Arctic areas with a strong inflow of Atlantic Water (Auel and Hagen, 2002; Rudels et al., 2013; Ehrlich, 2015). It shows a drastic decrease in abundance to <1 ind.m^{-2} toward the central deep basins (Kosobokova and Hirche, 2009; Kosobokova et al., 2011; David et al., 2015). *C. glacialis* and *C. hyperboreus* in turn are rather characteristic of Arctic conditions and dominated the under-ice fauna community in the central Arctic Ocean in other studies (Kosobokova and Hirche, 2000; David et al., 2015). As a well-known inhabitant of Arctic waters and an abundant species in first-year ice dominated environments (Werner and Auel, 2005) the high occurrence of *C. glacialis* in the present study is no surprise. In contrast to *C. finmarchicus*, this species reproduces in Arctic waters. Some studies predict a replacement of *C. glacialis* by the smaller and less energy-rich *C. finmarchicus* with increasing atlantification (Bonnet et al., 2005; Richardson, 2008; Polyakov et al., 2017). Potential consequences of that replacement for the Arctic ecosystem are not sufficiently assessed yet, but a recent study suggests it might not be as severe as previously assumed given the authors found copepod lipid content to be more related to habitat conditions than species identity (Renaud et al., 2018). The relatively low abundance of *C. hyperboreus* in this study can be explained by the fact that it is a high Arctic and deep water species, which occurs less in the meltwater layer underneath the ice (Hop et al., 2011). Both *C. glacialis* and *C. hyperboreus*, however, do use the under-ice environment as a nursing ground and time nauplii development with the springtime peak of primary production (Falk-Petersen et al., 2008; Kosobokova and Hirche, 2009; Søreide et al., 2010). High abundances of copepod nauplii under the ice, especially at the earlier sampled stations during this expedition, may have been related to spawning below the sea ice earlier in spring and to the release of nauplii from the sea ice.

Appendicularia are common in the Arctic Ocean (Kosobokova and Hirche, 2000; Auel and Hagen, 2002; Ershova and Kosobokova, 2019), but were not reported in such high abundance in the study region before. Mumm (1993) reported a relative abundance of 3% in the Nansen Basin in summer and similar ranges for Appendicularia were also reported from Kosobokova and Hirche (2000), and Ehrlich (2015) from the central Arctic Ocean. Similar to our study, David et al. (2015) reported a single station with a high abundance of Appendicularia in the ice-water interface layer from the central Arctic Ocean (52.6 ind.m^{-2}). Such isolated high abundances indicate a high patchiness under the sea ice. Maybe Appendicularia can make use of the increased primary production in the Arctic measured by Arrigo et al. (2008) and others, including under-ice blooms, which occur beneath annual sea ice (Assmy et al., 2017; Wollenburg et al., 2018). As Appendicularia are soft-bodied filter feeders and capable of responding faster to shifts in primary production than crustaceans

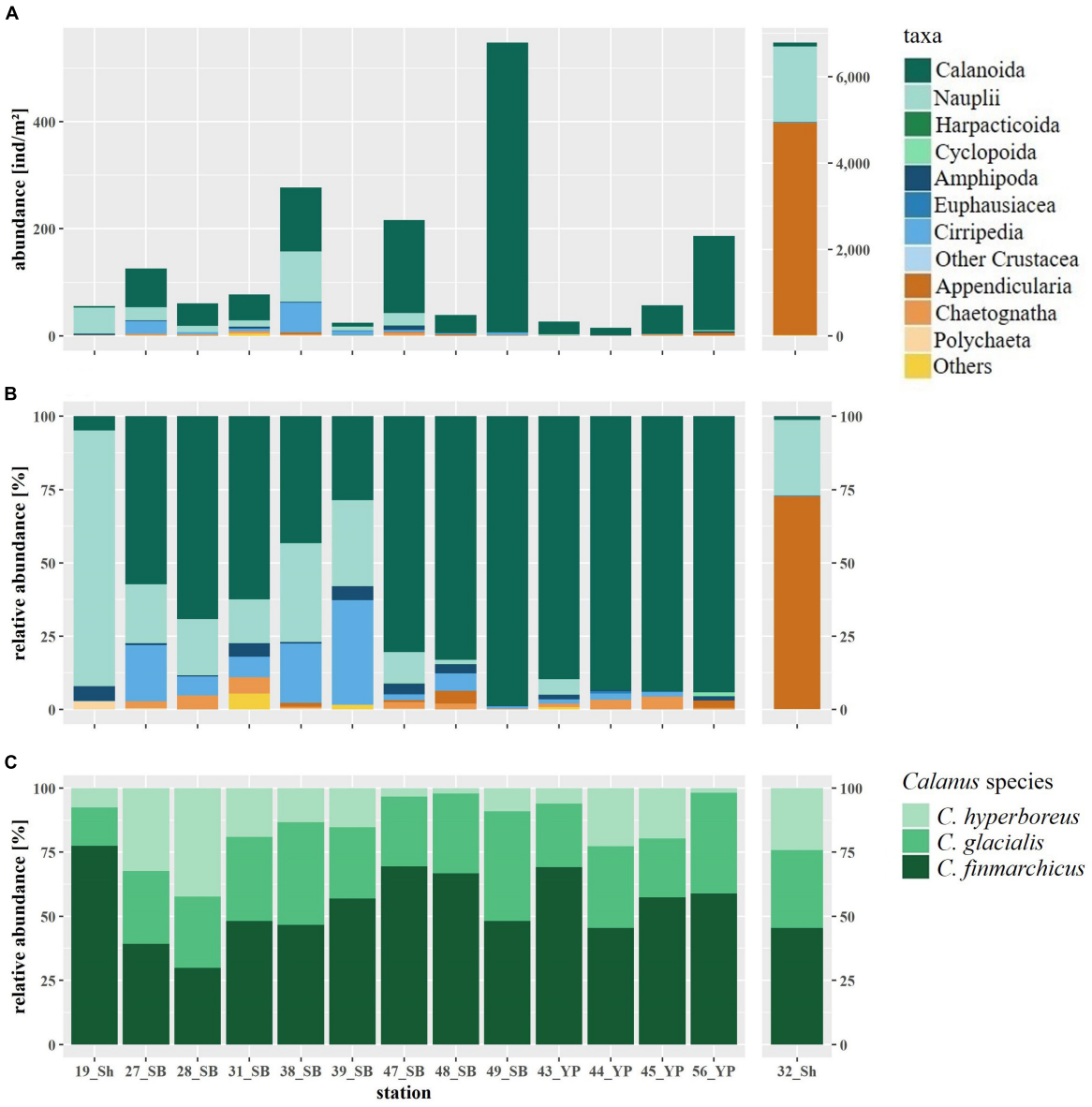

FIGURE 8 | (A) Abundance and **(B)** relative abundance of the under-ice fauna and **(C)** relative abundance of the three *Calanus* species at SUIT stations arranged by geographical region (Sh, shelf; SB, Sophia Basin; YP, Yermak Plateau). SUIT Station 32 has a different *y*-axis, because of high Appendicularia abundance. "Others" includes the rare taxa Hydrozoa, Osteichthyes larvae, Xenacoelomorpha, *Clione limacina*, *Limacina helicina*. "Other Crustacea" includes Isopoda and Zoaea larvae.

would (Hopcroft et al., 2005), their high abundance at one station might be a consequence of following a highly productive patch of water.

Amphipoda were rare in this study in comparison with their abundances in the under-ice fauna north of Svalbard almost three decades earlier (Lønne and Gulliksen, 1991). A more recent study from 2012 from the central Arctic Ocean, however, showed a similar range of sympagic Amphipoda abundance as the present study (David et al., 2015). An explanation for the decline of Amphipoda abundance could be that it seems to be positively related to the complexity of ice structures and the age of the ice (Bluhm et al., 2010; Hop et al., 2011; Bluhm et al., 2017). In the area north of Svalbard, multi-year ice has been declining dramatically since the mid-2000s

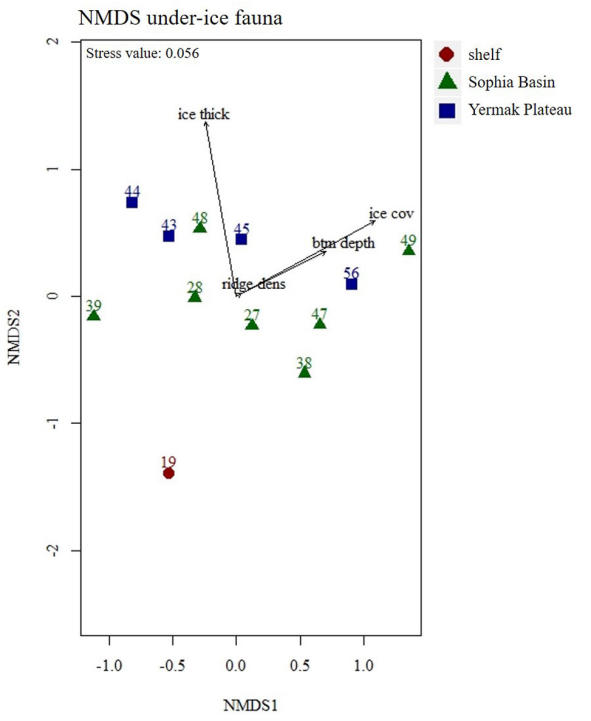

FIGURE 9 | Non-metric Multidimensional Scaling (NMDS) plot of under-ice fauna abundances with four fitted environmental variables. Stations were color coded according to geographical regions (shelf, Sophia Basin, and Yermak Plateau). Ice thick, ice thickness; ice cov, ice coverage; btm depth, bottom depth; ridge dens, ridge density.

(Polyakov et al., 2012; Perovich and Richter-Menge, 2015) and with it the abundance of sympagic Amphipoda (Bluhm et al., 2017). In our study, mainly ∼1.5 year-old sea ice (Peeken, 2016) covered the sampling area and might have been the reason for the low abundance of sympagic Amphipoda. *Apherusa glacialis* was the most abundant among the amphipod species and occurred at every station. This is in accordance with other studies (Werner and Auel, 2005; Hop et al., 2011; David et al., 2015). The species occurs under any ice type through the Arctic Ocean, though it is also found occasionally in the water column (Kunisch et al., 2020). As surface chl *a* concentration was very low during this study, the low abundance of *A. glacialis* might be related to food limitation. The larger amphipod species *Gammarus wilkitzkii* and *Eusirus* sp. were absent or very rare in the analyzed samples, but were actually found regularly, albeit in very low abundances in the larger (7 mm mesh) shrimp net of the SUIT (Schaafsma, pers. communication).

CONCLUSION

Although the results of this study show that the present taxa in the sea-ice and the under-ice water were in accordance with previous studies from this region, some relevant deviations in community composition have occurred. Some of the previously found sympagic taxa were conspicuously absent (e.g., Acoela, Platyhelminthes, and Nematoda) or rare (Rotifera, and ice Amphipoda) in our study area. This finding might reflect the changes in connectivity between the ice-producing shelf and the pack-ice areas in the last decades (Krumpen et al., 2019). The change from a multi-year to an annual sea-ice system means also a change from an ecosystem where a relatively constant community of sympagic fauna can establish over years to one where the community needs to reestablish annually and thus comprises more organisms from the pelagic habitat. This would apply especially to the sea-ice meiofauna, which is more tightly reflecting sea-ice processes, while the under-ice fauna is more influenced by water-mass processes. The under-ice community in part reflected the inflow of the Atlantic Water in this area. While Atlantic Water has in the past been below our sampled stratum, recent evidence documents decreased freshwater content from ice melt, because of less sea ice in the area, increased salinity, and enhanced mixing of Atlantic Water upward (Lind et al., 2018; Renner et al., 2018). Increased water temperatures might result in a further northward shift of Atlantic species, such as *C. finmarchicus* and will cause changes in the sympagic ecosystem by increasing competition for resources and space. Potential changes in sympagic community composition should be monitored to evaluate if occurrences of certain taxa such as Appendicularia are actually increasing and the trend of decreasing benthic-origin taxa continues. Consistent and increased taxonomic resolution (through molecular analysis, Hardge et al., 2017; Marquardt et al., 2018; Pitusi, 2019) is also recommended. Bio-physically coupled datasets should be prioritized to unequivocally link the reduction in the sea ice to change of sympagic fauna.

DATA AVAILABILITY STATEMENT

The datasets generated for this study are available on PANGAEA (Ehrlich et al., 2020a,b).

AUTHOR CONTRIBUTIONS

JE wrote the manuscript. AB, HF, and JE designed the sampling of this study. FS, GC, IP, and HF collected the samples of sea-ice meiofauna and under-ice fauna. JE and BB analyzed the sea-ice meiofauna samples. JE and FS analyzed the under-ice fauna samples. FS and IP contributed to the biological dataset. GC and FS contributed to the environmental dataset. AB contributed to the taxonomical accuracy of the manuscript. JE analyzed the data and prepared all figures and tables. BB, FS, and HF contributed to data interpretation. All authors contributed to the discussion of various versions of the manuscript.

FUNDING

JE was funded by the national scholarships "Promotionsstipendium nach dem Hamburger Nachwuchsfördergesetz (HmbNFG)" and "Gleichstellungsfond 2017 (4-GLF-2017)", both granted by the University of Hamburg. The German Academic Exchange Service (DAAD) and the graduate school "POLMAR" at Alfred Wegener Institute Bremerhaven supported JE's visit at The Arctic University of Norway's Institute of Arctic and Marine Biology. FS received support by Wageningen Marine Research, which is commissioned by the Netherlands Ministry of Agriculture, Nature and Food Quality (LNV) under its Statutory Research Task Nature & Environment WOT-04-009-047.04. The Netherlands Polar Programme (NPP), managed by the Dutch Research Council (NWO) funded this research under project nr. ALW 866.13.009. BB's contribution was under the framework of the Arctic Seasonal Ice Zone Ecology project, co-funded by UiT – The Arctic University of Norway and the Tromsø Research Foundation (Project Number 01vm/h15) and the Arctic ABC Project (Project Number #244319), funded by the Norwegian Research Council. IP, JE, GC, and HF were funded by the PACES (Polar Regions and Coasts in a Changing Earth System) programme of the Helmholtz Association and the expedition Grant No. AWI_PS92_00. HF, JE, and GC were part of the Helmholtz Association Young Investigators Groups *Iceflux*: Ice-ecosystem carbon flux in polar oceans (VH-NG-800).

ACKNOWLEDGMENTS

We thank the Captain and crew of Polarstern for their excellent support during the PS92 expedition. We are greatful for the technical help and great support during the work at sea and on the ice by team members Michiel van Dorssen and André Meijboom. We thank Ulrike Dietrich and Mischa Ungermann for their help with the sea-ice sampling. We thank Rolf Gradinger (UiT) for his support during the lab analysis of sea-ice meiofauna. The SUIT for this study was kindly provided by Jan Andries van Franeker (Wageningen Marine Research).

SUPPLEMENTARY MATERIAL

The Supplementary Material for this article can be found online at: https://www.frontiersin.org/articles/10.3389/fmars.2020.00452/full#supplementary-material

REFERENCES

Arctic Council Secretariat (2016). *Memo on the State of the Arctic Marine Biodiversity Report (SAMBR)*. Tromsø: Arctic Council Secretariat.

Ardyna, M., Babin, M., Gosselin, M., Devred, E., Rainville, L., and Tremblay, J. É (2014). Recent Arctic Ocean sea ice loss triggers novel fall phytoplankton blooms. *Geophys. Res. Lett.* 41, 6207–6212. doi: 10.1002/2014gl061047

Arndt, C. E., and Pavlova, O. (2005). Origin and fate of ice fauna in the Fram Strait and Svalbard area. *Mar. Ecol. Progr. Ser.* 301, 55–66. doi: 10.3354/meps301055

Arndt, C. E., and Swadling, K. M. (2006). Crustacea in arctic and antarctic sea ice: distribution, diet and life history strategies. *Adv. Mar. Biol.* 51, 197–315. doi: 10.1016/s0065-2881(06)51004-1

Arrigo, K. R., van Dijken, G., and Pabi, S. (2008). Impact of a shrinking Arctic ice cover on marine primary production. *Geophys. Res. Lett.* 35:L19603. doi: 10.1029/2008gl035028

Arrigo, K. R., and van Dijken, G. L. (2015). Continued increases in Arctic Ocean primary production. *Progr. Oceanogr.* 136, 60–70. doi: 10.1016/j.pocean.2015.05.002

Assmy, P., Fernández-Méndez, M., Duarte, P., Meyer, A., Randelhoff, A., Mundy, C. J., et al. (2017). Leads in Arctic pack ice enable early phytoplankton blooms below snow-covered sea ice. *Sci. Rep.* 7:40850.

Auel, H., and Hagen, W. (2002). Mesozooplankton community structure, abundance and biomass in the central Arctic Ocean. *Mar. Biol.* 140, 1013–1021. doi: 10.1007/s00227-001-0775-4

Beszczynska-Möller, A., Fahrbach, E., Schauer, U., and Hansen, E. (2012). Variability in Atlantic water temperature and transport at the entrance to the Arctic Ocean, 1997–2010. *ICES J. Mar. Sci.* 69, 852–863. doi: 10.1093/icesjms/fss056

Beuchel, F., and Lønne, O. (2002). Population dynamics of the sympagic amphipods *Gammarus wilkitzkii* and *Apherusa glacialis* in sea ice north of Svalbard. *Polar Biol.* 25, 241–250. doi: 10.1007/s00300-001-0329-8

Bluhm, B. A., and Gradinger, R. (2008). Regional variability in food availability for Arctic marine mammals. *Ecol. Appl.* 18, S77–S96.

Bluhm, B. A., Gradinger, R. R., and Schnack-Schiel, S. B. (2010). Sea ice meio-and macrofauna. *Sea Ice* 2, 357–393. doi: 10.1002/9781444317145.ch10

Bluhm, B. A., Hop, H., Vihtakari, M., Gradinger, R., Iken, K., Melnikov, I. A., et al. (2018). Sea ice meiofauna distribution on local to pan-Arctic scales. *Ecol. Evol.* 8, 2350–2364. doi: 10.1002/ece3.3797

Bluhm, B. A., Swadling, K. M., and Gradinger, R. (2017). "Sea ice as a habitat for macrograzers," in *Sea Ice*, Ed. D. N Thomas (Hoboken, NJ: Wiley), 394–414. doi: 10.1002/9781118778371.ch16

Bonnet, D., Richardson, A., Harris, R., Hirst, A., Beaugrand, G., Edwards, M., et al. (2005). An overview of *Calanus helgolandicus* ecology in European waters. *Progr. Oceanogr.* 65, 1–53. doi: 10.1016/j.pocean.2005.02.002

Bray, J. R., and Curtis, J. T. (1957). An ordination of the upland forest communities of southern Wisconsin. *Ecol. Monogr.* 27, 325–349. doi: 10.2307/1942268

Budge, S., Wooller, M., Springer, A., Iverson, S. J., McRoy, C., and Divoky, G. (2008). Tracing carbon flow in an arctic marine food web using fatty acid-stable isotope analysis. *Oecologia* 157, 117–129. doi: 10.1007/s00442-008-1053-7

Carey, A. Jr. (1985). *Sea Ice Biota*. Boca Raton, FL: CRC Press.

Carey, A. G. Jr. (1992). The ice fauna in the shallow southwestern Beaufort Sea. Arctic Ocean. *J. Mar. Syst.* 3, 225–236. doi: 10.1016/0924-7963(92)90002-p

Carey, A. G. Jr., and Montagna, P. A. (1982). Arctic Sea Ice Fauna1 Assemblage: First approach to description and source of the underice meiofauna. *Mar. Ecol. Progr. Ser.* 8, 1–8. doi: 10.3354/meps008001

Carmack, E., Polyakov, I., Padman, L., Fer, I., Hunke, E., Hutchings, J., et al. (2015). Toward quantifying the increasing role of oceanic heat in sea ice loss in the new Arctic. *Bull. Am. Meteorol. Soc.* 96, 2079–2105. doi: 10.1175/bams-d-13-00177.1

Castellani, G., Lüpkes, C., Hendricks, S., and Gerdes, R. (2014). Variability of A rctic sea-ice topography and its impact on the atmospheric surface drag. *J. Geophys. Res.* 119, 6743–6762. doi: 10.1002/2013jc009712

Castellani, G., Schaafsma, F., Arndt, S., Lange, B. A., Peeken, I., Ehrlich, J., et al. (in press). Large-scale variability of physical and biological sea-ice properties in polar oceans. *Front. Mar. Sci.*

Clarke, K., and Ainsworth, M. (1993). A method of linking multivariate community structure to environmental variables. *Mar. Ecol. Progr. Ser.* 92, 205–205.

Clarke, K. R., and Warwick, R. (2001). *Change in Marine Communities: An Approach to Statistical Analysis and Interpretation*. Plymouth: Primer-E Ltd.

Comiso, J. C. (2012). Large decadal decline of the Arctic multiyear ice cover. *J. Clim.* 25, 1176–1193. doi: 10.1175/jcli-d-11-00113.1

Conover, R. (1988). Comparative life histories in the genera *Calanus* and *Neocalanus* in high latitudes of the northern hemisphere. *Hydrobiologia* 167, 127–142. doi: 10.1007/978-94-009-3103-9_11

Damgaard, R., and Davenport, J. (1994). Salinity tolerance, salinity preference and temperature tolerance in the high-shore harpacticoid copepod *Tigriopus brevicornis*. *Mar. Biol.* 118, 443–449. doi: 10.1007/bf00350301

Darnis, G., Robert, D., Pomerleau, C., Link, H., Archambault, P., Nelson, R. J., et al. (2012). Current state and trends in Canadian Arctic marine ecosystems: II. Heterotrophic food web, pelagic-benthic coupling, and biodiversity. *Clim. Change* 115, 179–205. doi: 10.1007/s10584-012-0483-8

David, C., Lange, B., Rabe, B., and Flores, H. (2015). Community structure of under-ice fauna in the Eurasian central Arctic Ocean in relation to environmental properties of sea-ice habitats. *Mar. Ecol. Progr. Ser.* 522, 15–32. doi: 10.3354/meps11156

Ehrlich, J. (2015). *Diversity and Distribution Of High-Arctic Zooplankton in the Eurasian Basin in Late Summer 2012*. Hamburg: University of Hamburg/Alfred-Wegener-Institut.

Ehrlich, J., Schaafsma, F. L., Bluhm, B. A., Peeken, I., Castellani, G., Brandt, A., et al. (2020a). Sea-ice meiofauna (>10 μm) abundance in Arctic pack ice north of Svalbard during the Polarstern expedition PS92 in 2015. *PANGAEA*. doi: 10.1594/PANGAEA.915960

Ehrlich, J., Schaafsma, F. L., Bluhm, B. A., Peeken, I., Castellani, G., Brandt, A., et al. (2020b). Under-ice fauna abundance of Arctic pack ice north of Svalbard during the Polarstern expedition PS92 in 2015. *PANGAEA*. doi: 10.1594/PANGAEA.915961

Eicken, H., Bluhm, B. A., Collins, R. E., Haas, C., Ingham, M., Gradinger, R., et al. (2014). "Field techniques in sea-ice research," in *Cold Regions Science and Marine Technology*, Ed. H. H. Shen (Paris: EOLSS Publishers), 1–20.

Ershova, E. A., and Kosobokova, K. N. (2019). Cross-shelf structure and distribution of mesozooplankton communities in the East-Siberian Sea and the adjacent Arctic Ocean. *Polar Biol.* 42, 1353–1367. doi: 10.1007/s00300-019-02523-2522

Falk-Petersen, S., Leu, E., Berge, J., Kwasniewski, S., Nygård, H., Røstad, A., et al. (2008). Vertical migration in high Arctic waters during autumn 2004. *Deep Sea Res. Part II Top. Stud. Oceanogr.* 55, 2275–2284. doi: 10.1016/j.dsr2.2008.05.010

Falk-Petersen, S., Mayzaud, P., Kattner, G., and Sargent, J. R. (2009). Lipids and life strategy of Arctic Calanus. *Mar. Biol. Res.* 5, 18–39.

Fernández-Méndez, M., Katlein, C., Rabe, B., Nicolaus, M., Peeken, I., Bakker, K., et al. (2015). Photosynthetic production in the central Arctic Ocean during the record sea-ice minimum in 2012. *Biogeosciences* 12, 3525–3549. doi: 10.5194/bg-12-3525-2015

Flores, H., David, C., Ehrlich, J., Hardge, K., Kohlbach, D., Lange, B. A., et al. (2019). Sea-ice properties and nutrient concentration as drivers of the taxonomic and trophic structure of high-Arctic protist and metazoan communities. *Polar Biol.* 42, 1377–1395. doi: 10.1007/s00300-019-02526-z

Flores, H., Van Franeker, J. A., Siegel, V., Haraldsson, M., Strass, V., Meesters, E. H., et al. (2012). The association of Antarctic krill *Euphausia superba* with the under-ice habitat. *PLoS One* 7:e31775. doi: 10.1371/journal.pone.0031775

Friedrich, C. (1997). Ökologische Untersuchungen zur Fauna des arktischen Meereises. *Ber. zur Polarforschung* 246:211.

Garrison, D. L., and Buck, K. R. (1986). Organism losses during ice melting: a serious bias in sea ice community studies. *Polar Biol.* 6, 237–239. doi: 10.1007/bf00443401

Gosselin, M., Levasseur, M., Wheeler, P. A., Horner, R. A., and Booth, B. C. (1997). New measurements of phytoplankton and ice algal production in the Arctic Ocean. *Deep Sea Res. Part II Top. Stud. Oceanogr.* 44, 1623–1644. doi: 10.1016/s0967-0645(97)00054-4

Gradinger, R. (1999). Integrated abundance and biomass of sympagic meiofauna in Arctic and Antarctic pack ice. *Polar Biol.* 22, 169–177. doi: 10.1007/s003000050407

Gradinger, R., and Bluhm, B. (2009). "Assessment of the abundance and diversity of sea ice biota," in *Field Techniques for Sea-Ice Research*, eds H. Eicken, and M. Salganek (Fairbanks, AK: University of Alaska Press), 283.

Gradinger, R., and Bluhm, B. A. (2020). First analysis of an Arctic sea ice meiofauna food web based on abundance, biomass and stable isotope ratios. *Mar. Ecol. Progr. Ser.* 634, 29–43. doi: 10.3354/meps13170

Gradinger, R., Friedrich, C., and Spindler, M. (1999). Abundance, biomass and composition of the sea ice biota of the Greenland Sea pack ice. *Deep Sea Res. Part II Top. Stud. Oceanogr.* 46, 1457–1472. doi: 10.1016/s0967-0645(99)00030-2

Gradinger, R., Spindler, M., and Weissenberger, J. (1992). On the structure and development of Arctic pack ice communities in Fram Strait: a multivariate approach. *Polar Biol.* 12, 727–733.

Gradinger, R. R., and Bluhm, B. A. (2004). In-situ observations on the distribution and behavior of amphipods and Arctic cod (*Boreogadus saida*) under the sea ice of the High Arctic Canada Basin. *Polar Biol.* 27, 595–603.

Gradinger, R. R., Meiners, K., Plumley, G., Zhang, Q., and Bluhm, B. A. (2005). Abundance and composition of the sea-ice meiofauna in off-shore pack ice of the Beaufort Gyre in summer 2002 and 2003. *Polar Biol.* 28, 171–181. doi: 10.1007/s00300-004-0674-5

Grainger, E., and Hsiao, S. I. (1990). Trophic relationships of the sea ice meiofauna in Frobisher Bay. Arctic Canada. *Polar Biol.* 10, 283–292.

Granskog, M. A., Assmy, P., and Koç, N. (2020). "Emerging Traits of Sea Ice in the Atlantic Sector of the Arctic" in *Climate Change and the White World*, eds P. S. Goel, R. Ravindra, and S. Chattopadhyay (Berlin: Springer), 3–10. doi: 10.1007/978-3-030-21679-5_1

Granskog, M. A., Fer, I., Rinke, A., and Steen, H. (2018). Atmosphere-Ice-Ocean-Ecosystem processes in a thinner arctic sea ice regime: the norwegian young sea ICE (N-ICE2015) expedition. *J. Geophys. Res.* 123, 1586–1594. doi: 10.1002/2017jc013328

Gulliksen, B., and Lønne, O. J. (1989). Distribution, abundance, and ecological importance of marine sympagic fauna in the Arctic. *Rapp. PV Reun. Cons. Int. Explor. Mer.* 188, 133–138.

Haas, C. (2003). Dynamics versus thermodynamics: The sea ice thickness distribution. *Sea Ice* 1, 82–111. doi: 10.1002/9780470757161.ch3

Hardge, K., Peeken, I., Neuhaus, S., Lange, B. A., Stock, A., Stoeck, T., et al. (2017). The importance of sea ice for exchange of habitat-specific protist communities in the Central Arctic Ocean. *J. Mar. Syst.* 165, 124–138. doi: 10.1016/j.jmarsys.2016.10.004

Hirche, H.-J., and Kosobokova, K. (2007). Distribution of *Calanus finmarchicus* in the northern North Atlantic and Arctic Ocean—expatriation and potential colonization. *Deep Sea Res. Part II Top. Stud. Oceanogr.* 54, 2729–2747. doi: 10.1016/j.dsr2.2007.08.006

Hop, H., Mundy, C. J., Gosselin, M., Rossnagel, A. L., and Barber, D. G. (2011). Zooplankton boom and ice amphipod bust below melting sea ice in the Amundsen Gulf, Arctic Canada. *Polar Biol.* 34, 1947–1958. doi: 10.1007/s00300-011-0991-994

Hop, H., and Pavlova, O. (2008). Distribution and biomass transport of ice amphipods in drifting sea ice around Svalbard. *Deep Sea Res. Part II Top. Stud. Oceanogr.* 55, 2292–2307. doi: 10.1016/j.dsr2.2008.05.023

Hop, H., Poltermann, M., Lønne, O. J., Falk-Petersen, S., Korsnes, R., and Budgell, W. P. (2000). Ice amphipod distribution relative to ice density and under-ice topography in the northern Barents Sea. *Polar Biol.* 23, 357–367. doi: 10.1007/s003000050456

Hopcroft, R., Clarke, C., Nelson, R., and Raskoff, K. (2005). Zooplankton communities of the Arctic's Canada Basin: the contribution by smaller taxa. *Polar Biol.* 28, 198–206. doi: 10.1007/s00300-004-0680-7

Hughes, T., Bellwood, D., Baird, A., Brodie, J., Bruno, J., and Pandolfi, J. (2011). Shifting base-lines, declining coral cover, and the erosion of reef resilience: comment on Sweatman et al.(2011). *Coral Reefs* 30, 653–660. doi: 10.1007/s00338-011-0787-6

Jeffries, M. O., Overland, J. E., and Perovich, D. K. (2013). The arctic. *Phys. Today* 66:35.

Kiko, R., Kern, S., Kramer, M., and Mütze, H. (2017). Colonization of newly forming Arctic sea ice by meiofauna: a case study for the future Arctic? *Polar Biol.* 40, 1277–1288. doi: 10.1007/s00300-016-2052-5

Kohlbach, D., Graeve, M., Lange, B. A., David, C., Peeken, I., and Flores, H. (2016). The importance of ice algae-produced carbon in the central Arctic Ocean ecosystem: Food web relationships revealed by lipid and stable isotope analyses. *Limnol. Oceanogr.* 61, 2027–2044. doi: 10.1002/lno.10351

Kosobokova, K., and Hirche, H.-J. (2000). Zooplankton distribution across the Lomonosov Ridge, Arctic Ocean: species inventory, biomass and vertical structure. *Deep Sea Res. Part I Oceanogr. Res. Papers* 47, 2029–2060. doi: 10.1016/s0967-0637(00)00015-7

Kosobokova, K., and Hirche, H.-J. (2009). Biomass of zooplankton in the eastern Arctic Ocean–a base line study. *Progr. Oceanogr.* 82, 265–280. doi: 10.1016/j.pocean.2009.07.006

Kosobokova, K. N., Hopcroft, R. R., and Hirche, H.-J. (2011). Patterns of zooplankton diversity through the depths of the Arctic's central basins. *Mar. Biodivers.* 41, 29–50. doi: 10.1007/s12526-010-0057-9

Krumpen, T., Belter, H. J., Boetius, A., Damm, E., Haas, C., Hendricks, S., et al. (2019). Arctic warming interrupts the Transpolar Drift and affects long-range transport of sea ice and ice-rafted matter. *Sci. Rep*. 9:5459.

Kruskal, J. B. (1964). Nonmetric multidimensional scaling: a numerical method. *Psychometrika* 29, 115–129. doi: 10.1007/bf02289694

Kunisch, E. H., Bluhm, B. A., Daase, M., Gradinger, R., Hop, H., Melnikov, I. A., et al. (2020). Pelagic occurrences of the ice amphipod *Apherusa glacialis* throughout the Arctic. *J. Plankton Res.* 42, 73–86. doi: 10.1093/plankt/fbz072

Kwok, R., and Cunningham, G. (2015). Variability of Arctic sea ice thickness and volume from CryoSat-2. *Philos. Trans. R. Soc. A* 373:20140157.

Lange, B. A., Katlein, C., Castellani, G., Fernández-Méndez, M., Nicolaus, M., Peeken, I., et al. (2017). Characterizing spatial variability of ice algal chlorophyll a and net primary production between sea ice habitats using horizontal profiling platforms. *Front. Mar. Sci.* 4:349. doi: 10.3389/fmars.2017.00349

Lange, B. A., Katlein, C., Nicolaus, M., Peeken, I., and Flores, H. (2016). Sea ice algae chlorophyll *a* concentrations derived from under-ice spectral radiation profiling platforms. *J. Geophys. Res.* 121, 8511–8534. doi: 10.1002/2016jc011991

Legendre, P., and Legendre, L. F. (2012). *Numerical Ecology*. Amsterdam: Elsevier.

Lind, S., Ingvaldsen, R. B., and Furevik, T. (2018). Arctic warming hotspot in the northern Barents Sea linked to declining sea-ice import. *Nat. Clim. Change* 8, 634–639. doi: 10.1038/s41558-018-0205-y

Lønne, O., and Gulliksen, B. (1991). Sympagic macro-fauna from multiyear sea-ice near Svalbard. *Polar Biol.* 11, 471–477.

Madsen, S., Nielsen, T., and Hansen, B. (2001). Annual population development and production by *Calanus finmarchicus*, *C. glacialis* and *C. hyperboreus* in Disko Bay, western Greenland. *Mar. Biol.* 139, 75–83.

Mardia, K., Kent, J. T., and Bibby, J. M. (1979). *Multivariate Analysis*. San Francisco, CA: WordPress.

Marquardt, M., Kramer, M., Carnat, G., and Werner, I. (2011). Vertical distribution of sympagic meiofauna in sea ice in the Canadian Beaufort Sea. *Polar Biol.* 34, 1887–1900. doi: 10.1007/s00300-011-1078-y

Marquardt, M., Majaneva, S., Pitusi, V., and Søreide, J. E. (2018). Pan-Arctic distribution of the hydrozoan Sympagohydra tuuli? First record in sea ice from Svalbard (European Arctic). *Polar Biol.* 41, 583–588. doi: 10.1007/s00300-017-2219-8

Massicotte, P., Peeken, I., Katlein, C., Flores, H., Huot, Y., Castellani, G., et al. (2019). Sensitivity of phytoplankton primary production estimates to available irradiance under heterogeneous sea ice conditions. *J. Geophys. Res.* 124, 5436–5450. doi: 10.1029/2019jc015007

Melnikov, I. (2018). "Characterization of the Biodiversity of Modern Sea Ice in the North Pole Region," in *Doklady Earth Sciences*, Ed. N. S. Bortnikov (Berlin: Springer), 792–795. doi: 10.1134/s1028334x18060132

Melnikov, I., and Kulikov, A. (1980). "The cryopelagic fauna of the central Arctic basin," in *Biology of the central Arctic Basin*, eds M. E. Vinogradov, and I. A. Mel'nikov, (Moscow: Nauka), 97–111.

Melnikov, I. A., Zhitina, L. S., and Kolosova, H. G. (2001). The Arctic sea ice biological communities in recent environmental changes (scientific note). *Mem. Natl. Inst. Polar Rev. Spl. Issue* 54:409416.

Michel, C., Nielsen, T. G., Nozais, C., and Gosselin, M. (2002). Significance of sedimentation and grazing by ice micro-and meiofauna for carbon cycling in annual sea ice (northern Baffin Bay). *Aquatic Microb. Ecol.* 30, 57–68. doi: 10.3354/ame030057

Mumm, N. (1993). Composition and distribution of mesozooplankton in the Nansen Basin, Arctic Ocean, during summer. *Polar Biol.* 13, 451–461.

Nicolaus, M., Katlein, C., Maslanik, J., and Hendricks, S. (2012). Changes in Arctic sea ice result in increasing light transmittance and absorption. *Geophys. Res. Lett.* 39:L24501.

Nozais, C., Gosselin, M., Michel, C., and Tita, G. (2001). Abundance, biomass, composition and grazing impact of the sea-ice meiofauna in the North Water, northern Baffin Bay. *Mar. Ecol. Progr. Ser.* 217, 235–250. doi: 10.3354/meps217235

Oksanen, J., Blanchet, F., Friendly, M., Kindt, R., Legendre, P., McGlinn, D., et al. (2018). *vegan: Community Ecology Package. R package version 2.5-2*.

Peeken, I. (2016). The Expedition PS92 of the Research Vessel POLARSTERN to the Arctic Ocean in 2015. *Rep. Polar Mar. Res.* 694:153. doi: 10.2312/BzPM_0694_2016

Perovich, D. K., and Richter-Menge, J. A. (2015). Regional variability in sea ice melt in a changing Arctic. *Philos. Trans. R. Soc. A* 373:20140165.

Pielou, E. C. (1969). *An Introduction to Mathematical Ecology*. Hoboken, NJ: Wiley-Interscience.

Pitusi, V. (2019). *Seasonal Abundance and Activity of Sympagic Meiofauna in Van Mijenfjorden, Svalbard*. Tromsø: UiT Norges arktiske universitet.

Poltermann, M., Hop, H., and Falk-Petersen, S. (2000). Life under Arctic sea ice–reproduction strategies of two sympagic (ice-associated) amphipod species, Gammarus wilkitzkii and *Apherusa glacialis*. *Mar. Biol.* 136, 913–920. doi: 10.1007/s002270000307

Polyakov, I. V., Pnyushkov, A. V., Alkire, M. B., Ashik, I. M., Baumann, T. M., Carmack, E. C., et al. (2017). Greater role for Atlantic inflows on sea-ice loss in the Eurasian Basin of the Arctic Ocean. *Science* 356, 285–291. doi: 10.1126/science.aai8204

Polyakov, I. V., Walsh, J. E., and Kwok, R. (2012). Recent changes of Arctic multiyear sea ice coverage and the likely causes. *Bull. Am. Meteorol. Soc.* 93, 145–151. doi: 10.1175/bams-d-11-00070.1

R Core Team (2018). R: A Language and Environment for Statistical Computing. Vienna: R Foundation for Statistical Computing. Available online at: https://www.R-project.org/

Rabenstein, L., Hendricks, S., Martin, T., Pfaffhuber, A., and Haas, C. (2010). Thickness and surface-properties of different sea-ice regimes within the Arctic Trans Polar Drift: Data from summers 2001, 2004 and 2007. *J. Geophys. Res.* 115:C12.

Renaud, P. E., Daase, M., Banas, N. S., Gabrielsen, T. M., Søreide, J. E., Varpe, Ø, et al. (2018). Pelagic food-webs in a changing Arctic: a trait-based perspective suggests a mode of resilience. *ICES J. Mar. Sci.* 75, 1871–1881. doi: 10.1093/icesjms/fsy063

Renner, A., Sundfjord, A., Janout, M., Ingvaldsen, R., Beszczynska-Möller, A., Pickart, R., et al. (2018). Variability and redistribution of heat in the Atlantic Water boundary current north of Svalbard. *J. Geophys. Res.* 123, 6373–6391. doi: 10.1029/2018jc013814

Richardson, A. J. (2008). In hot water: zooplankton and climate change. *ICES J. Mar. Sci.* 65, 279–295. doi: 10.1093/icesjms/fsn028

Riemann, F., and Sime-Ngando, T. (1997). Note on sea-ice nematodes (Monhysteroidea) from Resolute Passage. Canadian high Arctic. *Pol. Biol.* 18, 70–75. doi: 10.1007/s003000050160

Rudels, B. (1987). *On the Mass Balance of the Polar Ocean, with Special Emphasis on the Fram Strait*. Tromsø: Norsk Polarinstitutt.

Rudels, B., Jones, E. P., Schauer, U., and Eriksson, P. (2004). Atlantic sources of the Arctic Ocean surface and halocline waters. *Polar Res.* 23, 181–208. doi: 10.3402/polar.v23i2.6278

Rudels, B., Schauer, U., Björk, G., Korhonen, M., Pisarev, S., Rabe, B., et al. (2013). Observations of water masses and circulation in the Eurasian Basin of the Arctic Ocean from the 1990s to the late 2000s. *OS Special Issue* 9, 147–169. doi: 10.5194/os-9-147-2013

Schlitzer, R., Anderson, R. F., Dodas, E. M., Lohan, M., Geibert, W., Tagliabue, A., et al. (2018). The GEOTRACES intermediate data product 2017. *Chem. Geol.* 493, 210–223.

Schünemann, H., and Werner, I. (2004). Seasonal variations in distribution patterns of sympagic meiofauna in Arctic pack ice. *Mar. Biol.* 146, 1091–1102. doi: 10.1007/s00227-004-1511-1517

Serreze, M. C., Holland, M. M., and Stroeve, J. (2007). Perspectives on the Arctic's shrinking sea-ice cover. *Science* 315, 1533–1536. doi: 10.1126/science.1139426

Shannon, C., and Weaver, W. (1963). The measurement theory of communication.

Shepard, R. N. (1962). The analysis of proximities: multidimensional scaling with an unknown distance function. I. *Psychometrika* 27, 125–140. doi: 10.1007/bf02289630

Søreide, J. E., Carroll, M. L., Hop, H., Ambrose, W. G. Jr., Hegseth, E. N., and Falk-Petersen, S. (2013). Sympagic-pelagic-benthic coupling in Arctic and Atlantic waters around Svalbard revealed by stable isotopic and fatty acid tracers. *Mar. Biol. Res.* 9, 831–850. doi: 10.1080/17451000.2013.775457

Søreide, J. E., Hop, H., Carroll, M. L., Falk-Petersen, S., and Hegseth, E. N. (2006). Seasonal food web structures and sympagic–pelagic coupling in the European

Arctic revealed by stable isotopes and a two-source food web model. *Progr. Oceanogr.* 71, 59–87. doi: 10.1016/j.pocean.2006.06.001

Søreide, J. E., Leu, E., Berge, J., Graeve, M., and Falk-Petersen, S. (2010). Timing of blooms, algal food quality and *Calanus glacialis* reproduction and growth in a changing Arctic. *Glob. Change Biol.* 16, 3154–3163.

Tran, S., Bonsang, B., Gros, V., Peeken, I., Sarda-Esteve, R., Bernhardt, A., et al. (2013). A survey of carbon monoxide and non-methane hydrocarbons in the Arctic Ocean during summer 2010. *Biogeosciences* 10, 1909–1935. doi: 10.5194/bg-10-1909-2013

Tremblay, J. -É, Anderson, L. G., Matrai, P., Coupel, P., Bélanger, S., Michel, C., et al. (2015). Global and regional drivers of nutrient supply, primary production and CO2 drawdown in the changing Arctic Ocean. *Progr. Oceanogr.* 139, 171–196. doi: 10.1016/j.pocean.2015.08.009

Tremblay, J. -É, and Gagnon, J. (2009). "The effects of irradiance and nutrient supply on the productivity of Arctic waters: a perspective on climate change," in *Influence of Climate Change on the Changing Arctic And Sub-Arctic Conditions*, Ed. J. Nihoul (Berlin: Springer), 73–93. doi: 10.1007/978-1-4020-9460-6_7

van Franeker, J. A., Flores, H., and Van Dorssen, M. (2009). *The Surface and Under Ice Trawl (SUIT). Frozen Desert Alive-The role of sea ice for Pelagic Macrofauna and Its Predators*. PhD thesis, University of Groningen, Groningen, 181–188.

Werner, I., and Arbizu, P. M. (1999). The sub-ice fauna of the Laptev Sea and the adjacent Arctic Ocean in summer 1995. *Polar Biol.* 21, 71–79. doi: 10.1007/s003000050336

Werner, I., and Auel, H. (2005). Seasonal variability in abundance, respiration and lipid composition of Arctic under-ice amphipods. *Mar. Ecol. Progr. Ser.* 292, 251–262. doi: 10.3354/meps292251

Wickham, H. (2016). *ggplot2: Elegant Graphics for Data Analysis*. Berlin: Springer.

Wickham, H. (2018). *Scales: Scale Functions for Visualization [WWW Document]*. Available online at: https://cran.r-project.org/package=scales (accessed May 5, 2019).

Wickham, H., and Ruiz, E. (2018). *dbplyr: A'dplyr'Back End for Databases. R package version 1*.

Wollenburg, J., Katlein, C., Nehrke, G., Nöthig, E.-M., Matthiessen, J., Wolf-Gladrow, D. A., et al. (2018). Ballasting by cryogenic gypsum enhances carbon export in a Phaeocystis under-ice bloom. *Sci. Rep.* 8, 1–9.

Zar, J. (1984). *Biostatistical Analysis*, 2nd Edn. Englewood Cliffs, NJ: Prentice-Hall.

Zuur, A., Ieno, E. N., and Smith, G. M. (2007). *Analyzing Ecological Data*. Berlin: Springer Science & Business Media.

Conflict of Interest: The authors declare that the research was conducted in the absence of any commercial or financial relationships that could be construed as a potential conflict of interest.

frontiers

Supplementary Material

1 Supplementary tables

Supplementary Table 1: Correlation coefficients after Spearman's rank correlation of environmental parameters at ice stations. Temp: temperature, Sal: salinity, Chl *a*: chlorophyll *a* ice; Ice thick: ice thickness; Snow thick: snow thickness; Btm depth: bottom depth; light blue: correlation coefficient > 0.8; light grey: excluded parameters for PCA analysis; black: included parameters in PCA

Environmental parameter	*Temp*	*Sal*	*Chl a*	*Ice thick*	*Snow thick*	*Btm depth*
Temp		-0,50	0,09	0,40	-0,92	0,69
Sal			-0,57	-0,08	0,21	-0,14
Chl a				0,59	-0,28	0,46
Ice thic					-0,63	0,94
Snow thick						-0,82
Btm depth						

Supplementary Table 2: Correlation coefficients after Spearman's rank correlation of environmental parameters at SUIT stations. Temp: temperature; Sal: salinity, Chl *a*: chlorophyll *a* surface water; Ice thick: ice thickness; Ice cover: ice coverage; Btm depth: bottom depth; Ridge dens: ridge density; light blue: correlation coefficient > 0.8; light grey: excluded parameters for PCA analysis; black: included parameters in PCA

Environmental parameter	*Temp*	*Sal*	*Chl a*	*Ice thick*	*Ice cover*	*Btm depth*	*Ridge dens*
Temp		0,72	-0,97	0,92	-0,79	-0,59	-0,1
Sal			-0,93	0,74	-0,73	-0,91	-0,7
Chl a				-0,89	0,86	0,85	0,4
Ice thick					-0,72	-0,61	-0,2
Ice cover						0,82	0,3
Btm depth							0,7
Ridge dens							

Chapter II

Large-Scale Variability of Physical and Biological Sea-Ice Properties in Polar Oceans

G. Castellani[1], F. L. Schaafsma[2], S. Arndt[1], B. A. Lange[1,3], I. Peeken[1], **J. Ehrlich**[1,4], C. David[1,5], R. Ricker[1], T. Krumpen[1], S. Hendricks[1], S. Schwegmann[6], P. Massicotte[7], H. Flores[1,4]
(2020)

[1] Alfred Wegener Institute Helmholtz-Zentrum für Polar- und Meeresforschung, Bremerhaven, Germany
[2] Wageningen Marine Research, Den Helder, Netherlands
[3] Norwegian Polar Institute, Fram Centre, Tromsø, Norway
[4] Center of Natural History (CeNak), University of Hamburg, Hamburg, Germany
[5] Department of Biology, Dalhousie University, Halifax, NS, Canada
[6] Bundesamt für Seeschifffahrt und Hydrographie, Rostock, Germany
[7] Takuvik Joint International Laboratory (UMI 3376) Université Laval (Canada) Centre National de le Recherche Scientifique (France) Québec-Océan/Pavillon Alexandre-Vachon Université Laval, Quebec City, QC, Canada

Frontiers in Marine Science 7:536. doi: 10.3389/fmars.2020.00536

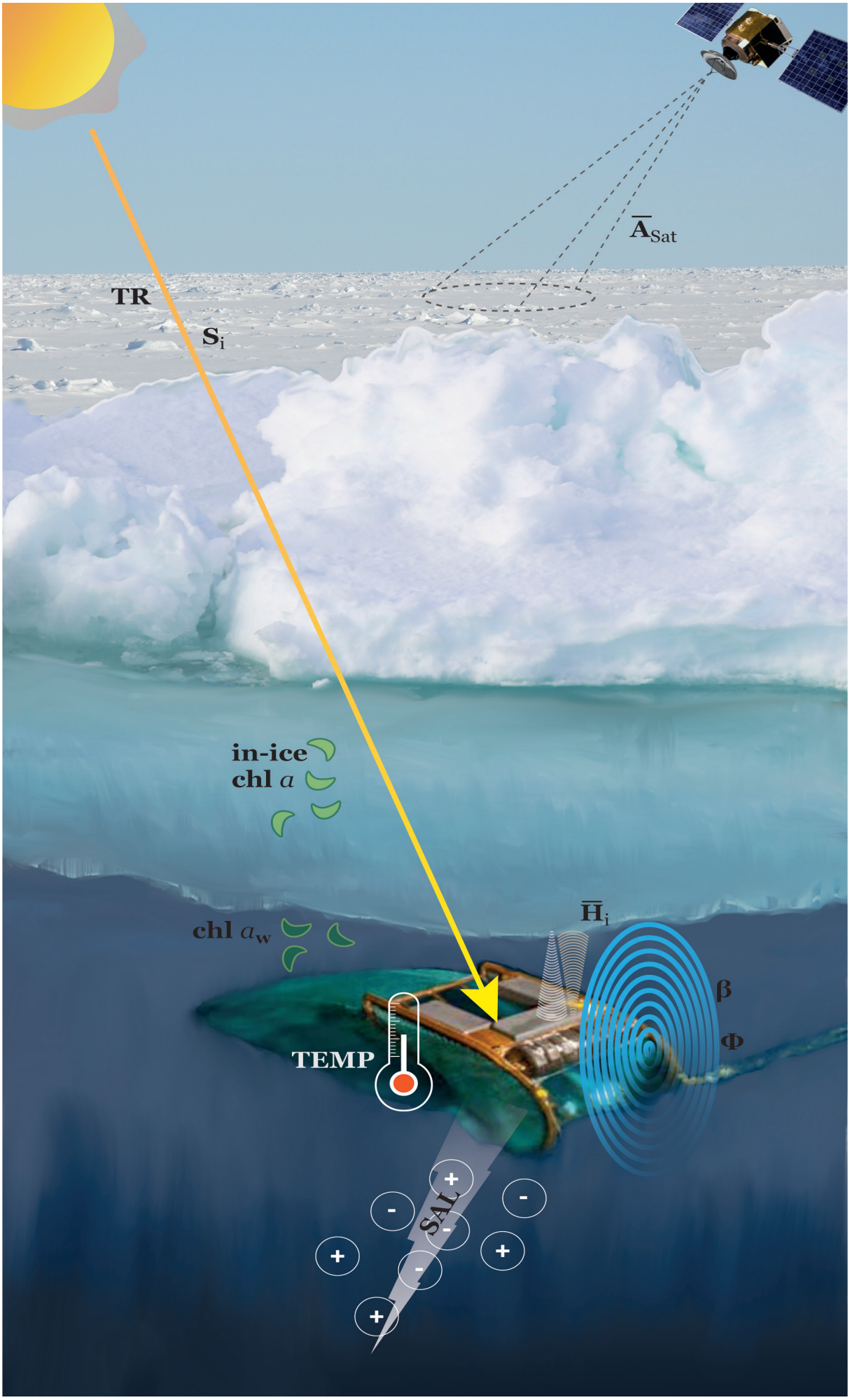
$\overline{A}_{Sat}$
TR
S_i
in-ice
chl *a*
chl a_w
$\overline{H}_i$
β
Φ
TEMP
SAL
+
-

frontiers in Marine Science

ORIGINAL RESEARCH
published: 12 August 2020
doi: 10.3389/fmars.2020.00536

Large-Scale Variability of Physical and Biological Sea-Ice Properties in Polar Oceans

Giulia Castellani[1], Fokje L. Schaafsma[2], Stefanie Arndt[1], Benjamin A. Lange[1,3], Ilka Peeken[1], Julia Ehrlich[1,4], Carmen David[1,5], Robert Ricker[1], Thomas Krumpen[1], Stefan Hendricks[1], Sandra Schwegmann[6], Philippe Massicotte[7] and Hauke Flores[1,4]*

[1] Alfred Wegener Institute Helmholtz-Zentrum für Polar- und Meeresforschung, Bremerhaven, Germany, [2] Wageningen Marine Research, Den Helder, Netherlands, [3] Norwegian Polar Institute, Fram Centre, Tromsø, Norway, [4] Center of Natural History (CeNak), University of Hamburg, Hamburg, Germany, [5] Department of Biology, Dalhousie University, Halifax, NS, Canada, [6] Bundesamt für Seeschifffahrt und Hydrographie, Rostock, Germany, [7] Takuvik Joint International Laboratory (UMI 3376) Université Laval (Canada) Centre National de le Recherche Scientifique (France) Québec-Océan/Pavillon Alexandre-Vachon Université Laval, Quebec City, QC, Canada

OPEN ACCESS

Edited by:
Laura Lorenzoni, National Aeronautics and Space Administration (NASA), United States

Reviewed by:
Kevin Arrigo, Stanford University, United States
Lee W. Cooper, University of Maryland Center for Environmental Science (UMCES), United States
Samuel Laney, Woods Hole Oceanographic Institution, United States

***Correspondence:**
Giulia Castellani
giulia.castellani@awi.de

Specialty section:
This article was submitted to Ocean Observation, a section of the journal Frontiers in Marine Science

Received: *15 November 2019*
Accepted: *12 June 2020*
Published: *12 August 2020*

Citation:
Castellani G, Schaafsma FL, Arndt S, Lange BA, Peeken I, Ehrlich J, David C, Ricker R, Krumpen T, Hendricks S, Schwegmann S, Massicotte P and Flores H (2020) Large-Scale Variability of Physical and Biological Sea-Ice Properties in Polar Oceans. Front. Mar. Sci. 7:536. doi: 10.3389/fmars.2020.00536

In this study, we present unique data collected with a Surface and Under-Ice Trawl (SUIT) during five campaigns between 2012 and 2017, covering the spring to summer and autumn transition in the Arctic Ocean, and the seasons of winter and summer in the Southern Ocean. The SUIT was equipped with a sensor array from which we retrieved: sea-ice thickness, the light field at the underside of sea ice, chlorophyll *a* concentration in the ice (in-ice chl *a*), and the salinity, temperature, and chl *a* concentration of the under-ice water. With an average trawl distance of about 2 km, and a global transect length of more than 117 km in both polar regions, the present work represents the first multi-seasonal habitat characterization based on kilometer-scale profiles. The present data highlight regional and seasonal patterns in sea-ice properties in the Polar Ocean. Light transmittance through Arctic sea ice reached almost 100% in summer, when the ice was thinner and melt ponds spread over the ice surface. However, the daily integrated amount of light under sea ice was maximum in spring. Compared to the Arctic, Antarctic sea-ice was thinner, snow depth was thicker, and sea-ice properties were more uniform between seasons. Light transmittance was low in winter with maximum transmittance of 73%. Despite thicker snow depth, the overall under-ice light was considerably higher during Antarctic summer than during Arctic summer. Spatial autocorrelation analysis shows that Arctic sea ice was characterized by larger floes compared to the Antarctic. In both Polar regions, the patch size of the transmittance followed the spatial variability of sea-ice thickness. In-ice chl *a* in the Arctic Ocean remained below 0.39 mg chl *a* m^{-2}, whereas it exceeded 7 mg chl *a* m^{-2} during Antarctic winter, when water chl *a* concentrations remained below 1.5 mg chl *a* m^{-2}, thus highlighting its potential as an important carbon source for overwintering organisms. The data analyzed in this study can improve large-scale physical and ecosystem models, habitat mapping studies and time series analyzed in the context of climate change effects and marine management.

Keywords: sea ice, Arctic, Antarctic, under-ice light, spatial variability, ice algae, ice thickness

1. INTRODUCTION

Sea ice is one of the Earth system components most sensitive to climate change. Besides playing an essential role in global ocean circulation (e.g., Schmitz, 1995; Ferrari et al., 2014) and in regulating Earth's climate and weather (e.g., Liu, 2012; Dethloff et al., 2019), sea ice is crucial for the Arctic and Antarctic polar food webs (e.g., Eicken, 1992; McMinn et al., 2010; Meyer and Auerswald, 2014). Arctic and Antarctic pack ice serve as unique habitats for microalgae (Arrigo, 2014), which contribute to primary production and carbon transfer to higher trophic levels (Gradinger, 1999; Søreide et al., 2006; Budge et al., 2008; Fernández-Méndez et al., 2015; Wang et al., 2015, 2016; Kohlbach et al., 2016, 2017a,b, 2018; Schaafsma et al., 2017). Since light is the energy source of algae, the quantity and spectral composition of the light that penetrates the ice and reaches the surface ocean impacts primary productivity and biological activity at the bottom of the sea ice and below in the water column. Due to changes from complete darkness to 24 h daylight, and extreme natural variations in water temperature in high latitudes, the concentration of primary production in both the sea ice and the water column undergoes a seasonal cycle, which has a major impact on food availability and life cycle of animals living in polar regions (Swadling et al., 1997; Brierley and Thomas, 2002). Small organisms living inside or under the sea ice, and feeding on residing algae in (ice algae) or below (phytoplankton) it, transfer both ice-algae-produced and phytoplankton-produced carbon to the pelagic food web (Budge et al., 2008; Wang et al., 2015, 2016; Kohlbach et al., 2016, 2017a,b, 2018). Thus, knowledge of sea ice and under-ice environmental properties as drivers of large-scale patterns in the abundance and distribution of sea-ice algae and phytoplankton, and, consequently, of zooplankton and nekton, is essential for understanding ecosystem functioning and predicting possible consequences of climate change for the ecosystems (Flores et al., 2011, 2019; David et al., 2015, 2016; Ehrlich et al., 2020).

Sampling in polar regions is limited in space and time because of the harsh weather during most of the year and because of the remote and hard to access locations. Particularly for sea-ice algae, for which chlorophyll *a* (in the following abbreviated as chl *a*) is usually used as a proxy for their biomass, estimates are often based on a small number of ice core observations, which do not fully capture the patchiness and the spatial and temporal variability in their distribution (Miller et al., 2015; Lange et al., 2016, 2017b). Satellite remote sensing during the past decades has vastly improved, enabling large-scale monitoring of certain sea-ice parameters, such as sea-ice concentration and thickness. However, uncertainties of global satellite sea-ice concentration and thickness retrievals on smaller scales, e.g., in the range of a few kilometers, can reach the magnitude of the measurement itself (Ivanova et al., 2014; Ricker et al., 2015). Moreover, despite new satellite advancements (i.e., ALOS—Advanced Land Observation Satellite), resolving small scale features such as ridges is still a challenge due to the relatively large footprint. Satellite snow depth retrievals are under development, but further evaluation and validation are needed (Guerreiro et al., 2016). Furthermore, satellite measurements do not provide enough information for the study of in-ice and under-ice environmental characteristics. This is particularly true for ice algae and phytoplankton in ice-covered regions that cannot be observed by satellite so that a comprehensive picture of their distribution on large scales remains difficult to obtain. Therefore, non-disruptive time series of sea-ice algae are non-existent. Only recently, technological developments allowed the estimation of under-ice properties, including light and in-ice chl *a*, on the scale of hundreds of meters in the Arctic region (Nicolaus et al., 2012; Nicolaus and Katlein, 2013; Katlein et al., 2015, 2019; Lange et al., 2017b) and in the Antarctic (Arndt et al., 2017).

The effects of ice algae on the spectral distribution of light under the ice were first observed by Maykut and Grenfell (1975), followed by studies focused on investigating the wavelengths that are affected by the presence of algae (Legendre and Gosselin, 1991), and on distinguishing between effects of algae and snow on the spectral distribution of under-ice light (Perovich, 1990). Mundy et al. (2007) used, for the first time, normalized difference indices (NDI) for studying the effects of ice algae and snow on the under-ice hyperspectral measurements conducted under landfast first-year ice in the Canadian Arctic Archipelago. After comparing different methods for in-ice chl *a* retrieval, the NDI method was employed by Melbourne-Thomas et al. (2015) to estimate ice-algae biomass in two Antarctic regions, the Weddell Sea and off East Antarctica, and to retrieve in-ice chl *a* in the Weddell Sea in winter (Meiners et al., 2017). Lange et al. (2016) developed and compared different algorithms for the retrieval of ice algae in the Arctic pack ice during summer 2012, and applied such algorithms to under-ice hyperspectral measurements collected with under-ice profiling platforms (Lange et al., 2017b). For the first time, in this work these methods are applied to multi-annual data sets of under-ice hyperspectral measurements conducted over hundreds to thousands of meters, providing a unique large-scale study of the spatial variability of Arctic and Antarctic sea-ice algae biomass estimates.

In the present study, we present data collected with a Surface and Under Ice Trawl (SUIT) and used these data to characterize ice-associated environments in the Arctic Ocean and the Southern Ocean. We aim to provide a regional, and seasonal comparison of sea-ice properties on large scales in both Polar regions with a focus on: (1) under-ice water properties, (2) ice thickness, (3) light transmittance through sea ice and under-ice light, and (4) in-ice chl *a* estimates. Moreover, the spatial scale covered by the present data sets also allow for an (5) unprecedented investigation of the scales of variability for all the variables measured. Our account of the meter- to kilometer variability of structural and optical sea-ice properties should contribute to the validation and parameterizations of sea-ice models as well as habitat mapping in the polar oceans.

2. DATA AND METHODS

2.1. Data

Data were collected during five campaigns in the Arctic Ocean and in the Southern Ocean, on board *RV Polarstern* (**Figures 1**, **2**

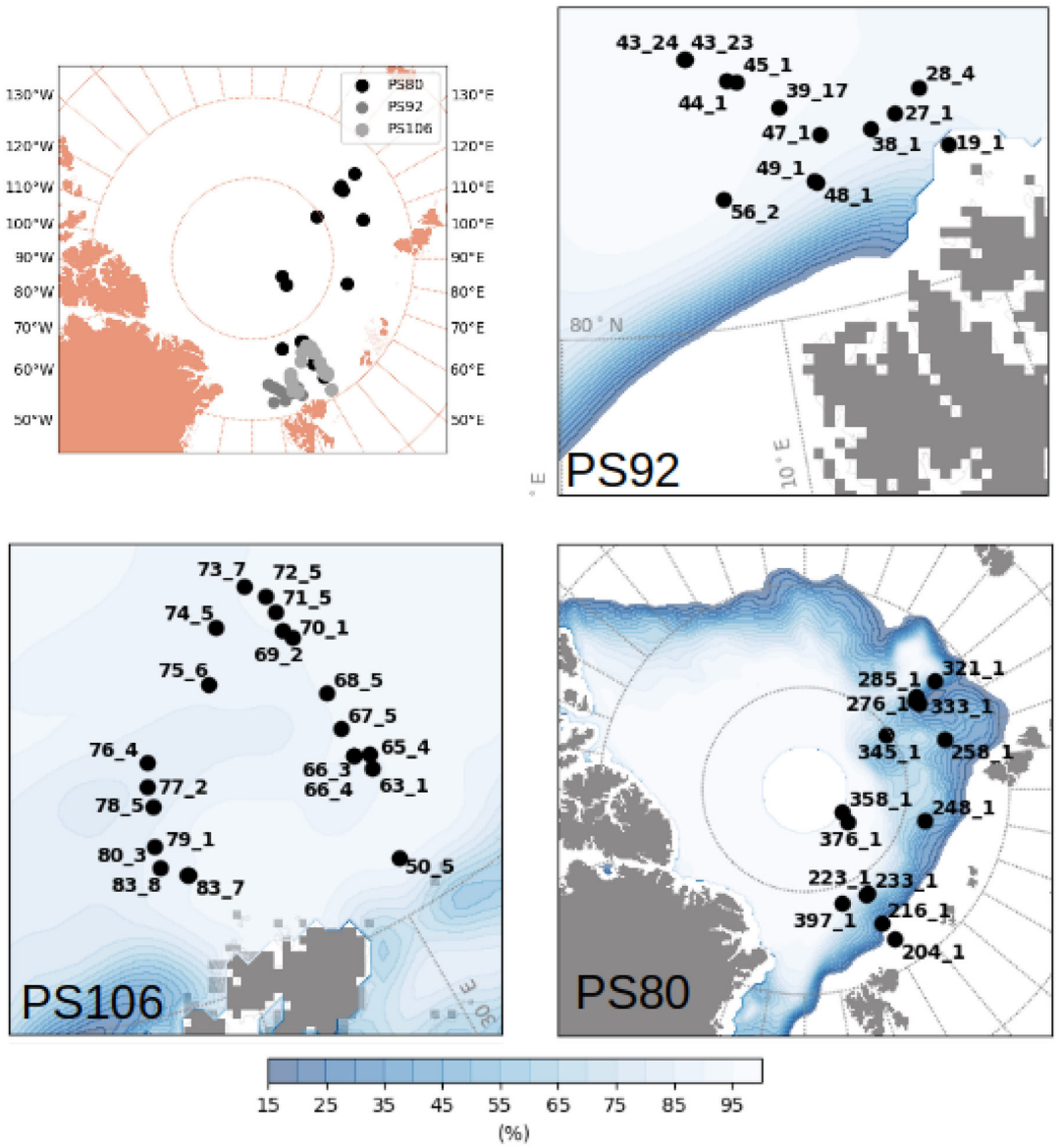

FIGURE 1 | Map of the Arctic with the stations carried out during PS80 (summer-autumn 2012), PS92 (early spring 2015) and PS106 (late spring 2017). Ice concentration averaged over the period of sampling of each expedition was taken from OSISAF (EUMETSAT, 2011).

and **Table 1**). In the Arctic Ocean, data were collected during early springtime (PS92, May-June 2015, Peeken, 2016), late springtime (PS106, June-July 2017, Macke and Flores, 2018), and during summer-autumn (PS80, August-September 2012, Boetius, 2013). In the Southern Ocean, the campaigns cover wintertime (PS81, August-October 2013, Meyer and Auerswald, 2014), and summertime (PS89, December 2014-January 2015, Boebel, 2015).

Sampling was performed with Surface and Under Ice Trawls (SUIT, van Franeker et al., 2009; Flores et al., 2012). The SUIT consists of a steel frame with a 2 × 2 m opening and two 15 m long nets: a 7 mm half-mesh commercial shrimp net, and a zooplankton net with a 0.15 mm (PS106) or 0.30 mm (PS80, PS81, PS89, PS92) mesh. Floats attached to the frame keep the net at the surface or right at the sea-ice underside. An asymmetric brindle forces the net to tow off at an angle of approximately 60° so that it samples undisturbed sea ice away from the ship's wake. Previous studies using the SUIT nets have described in detail the ecological and biological aspects of the catch and distribution of organisms in both polar regions (Flores et al.,

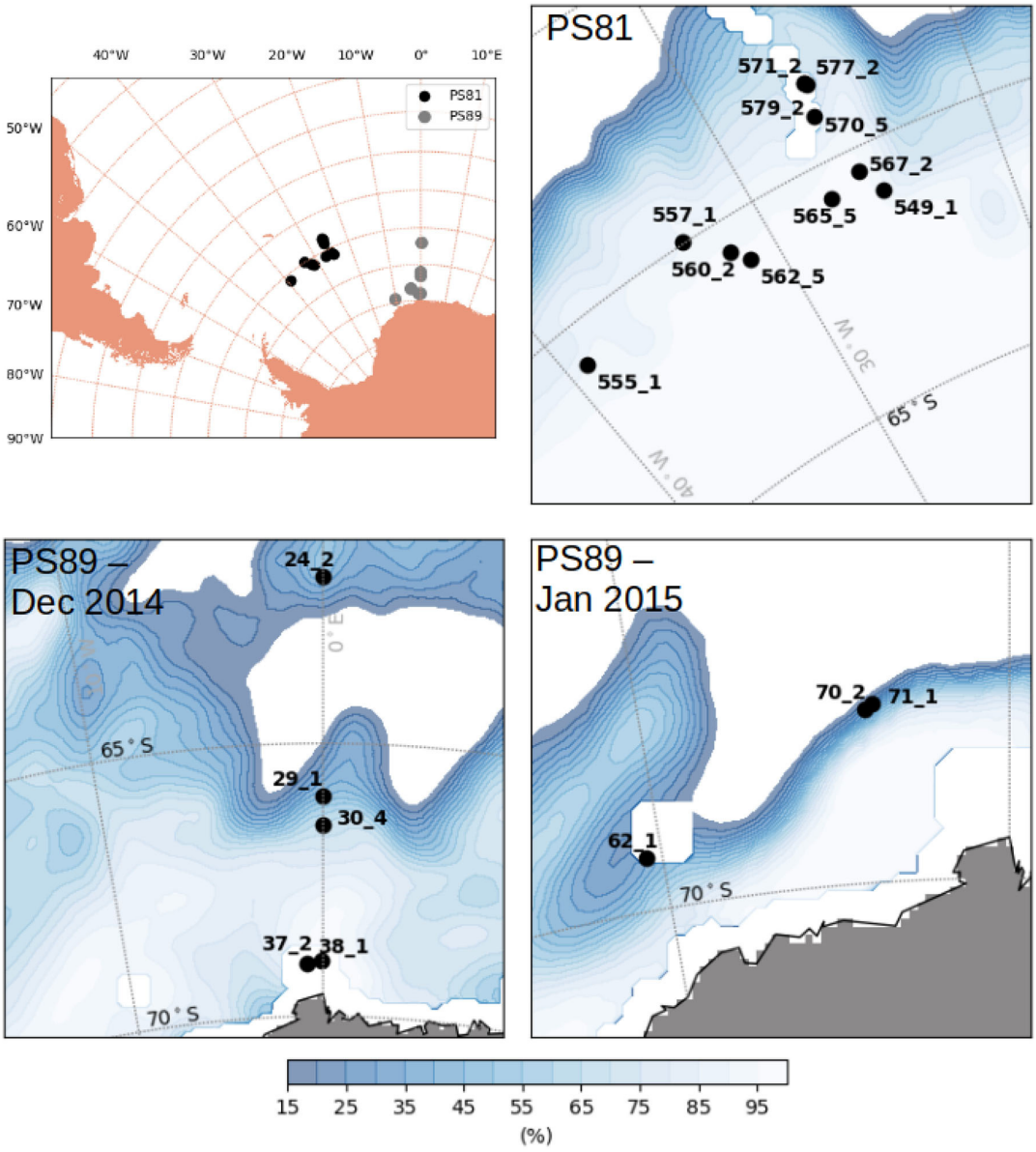

FIGURE 2 | Map of the Antarctic with stations carried out during PS81 (winter 2013) and PS89 (summer 2014/2015). Ice concentration averaged over the period of sampling of each expedition was taken from OSISAF (EUMETSAT, 2011).

2011, 2012, 2019; David et al., 2015, 2016, 2017; Schaafsma et al., 2016, 2017). Since 2012 the SUIT is equipped with a sensors array (Lange et al., 2016, 2017b; Lange, 2017) developed in order to conduct coincident quantitative observations of the sea-ice and under-ice water environments. The sensors allow the direct observations of: (1) water inflow speed and direction, pitch and roll angles, and pressure (i.e., depth) using an Acoustic Doppler Current Profiler (ADCP; Nortek Aquadopp® Profiler) with three acoustic beams, which allows 3-dimensional measurements of current velocities, at a frequency of 2 MHZ, and a sampling interval of 1 s; (2) water temperature, water salinity (practical salinity scale PSS-78; Fofonoff, 1985), and water depth by using a Conductivity Temperature Depth (CTD) probe (Sea and Sun Technology CTD75M memory probe) with a sampling interval of 0.1 s; (3) under-ice water chl *a* concentrations using a fluorometer (Cyclops, Turner Designs, USA) incorporated into the CTD; (4) distance from the ice surface by using an altimeter (Tritech PA500/6-E) incorporated into the CTD; (5) under-ice

TABLE 1 | Table with listed, for each expedition, the number of profiles considered in the analysis (N_{hauls}), the total profile length, the mean ice concentration ($\bar{A}$), mean total ice thickness ($\bar{H}_i$) and mean snow depth ($\bar{H}_s$), under-ice water chl *a* (chl a_w) multiplied by the vertical section of the SUIT (2 m) to obtain integrated values, temperature and salinity.

Expedition	Sampling dates	N_{hauls}	Profile length (m)	$\bar{A}$ (%)	$\bar{H}_i$ (m)	$\bar{H}_s$ (cm)	chl a_w (mg m^{-2})	T (°C)	S
PS80	05.08–29.09.2012	14	27,347	64.1	1.09	0–2	1.32	-1.20	31.36
PS81	22.08–22.10.2013	11	17,743	94.8	0.85	5–60	2.02	-1.85	33.95
PS89	14.12.2014–20.01.2015	8	14,661	83.7	1.07	5–100	0.80	-1.65	33.69
PS92	27.05–23.06.2015	13	21,256	72.2	1.77	5–40	6.90	-1.60	33.85
PS106	29.06–13.07.2017	21	36,188	94.2	1.91	5–20	2.74	-1.66	33.17

Expeditions in the Southern Ocean are highlighted in gray.

light levels using Ramses spectral radiometers (Trios GmbH, Rastede, Germany) with a wavelength range from 350 to 920 nm and a resolution of 3.3 nm. Incident solar radiation and under-ice irradiance were measured using an irradiance sensor (RAMSES-ACC) containing a cosine receptor with a 180° field-of-view. Under-ice radiance measurements were acquired using a radiance sensor (RAMSES-ARC) with a 9° field of view. As explained in detail in Lange (2017), the combined information from these different sensors allow also the retrieval of: (1) sea-ice draft derived by combining the CTD depth measurements with the distance from the ice (altimeter), and then corrected with pitch and roll measurements from the ADCP, as described in section 2.2; (2) ice-algal chl *a* derived from the Ramses spectral radiometers as described in section 2.4 (see also **Table S1**). Snow depth was recorded by visual observation of the ice under which the SUIT was traveling: A marked stick extending from the starboard side of the ship helps in quantifying the thickness of snow on top of the ice floes that are tilted during the ship passage. Part of these data have been used in previous works to study the relationship of environmental properties of sea-ice habitats with the community structure of sympagic fauna in the Arctic Ocean (PS80 and PS92, David et al., 2015, 2016; Schaafsma, 2018; Flores et al., 2019; Ehrlich et al., 2020), and in the Southern Ocean (PS81, Schaafsma et al., 2016, 2017; David et al., 2017), to develop and test algorithms for estimating in-ice chl *a* (PS80, Lange et al., 2016; Lange, 2017), to retrieve Arctic primary production on large scales in the Arctic summer (PS80 Lange, 2017; Lange et al., 2017b), and to estimate Arctic under-ice primary production based on under-ice irradiance measurements (PS92, Massicotte et al., 2019). All data collected during PS89 and PS106 are so far unpublished. Although data were collected during different years, this data set allows the investigation of differences between seasons in both the Arctic and the Antarctic, assuming that the sampling is representative of the season.

The profile lengths used for calculation of mean quantities (e.g., ice and snow thickness, water temperature and salinity, chl *a* in water and sea ice) correspond to the distance between the start and end trawl points, excluding parts of the profiles where the sensors data were unreliable due, for example, to sensors failure or damage. Thus, the profile length does not always correspond to the trawled distance, i.e., the total distance during which the net was towed in water by the ship, used to calculate the density of animals (e.g., David et al., 2017).

The sampled regions were different between expeditions: during Arctic spring (PS92 and PS106) data were collected north of Svalbard (**Figure 1**), in the latitudinal band between 80° N and 85° N. PS92 stations were located on the Yermak Plateau (lon < 10° E, later referred to as Yermak stations), in the Sophia Basin and along the Svalbard shelf/slope (lon > 10° E, later referred to as basin & shelf stations). Some PS106 stations were also located in the Basin & shelf area (10° E < lon < 20° E), the others were located between 20° E and 30° E. During Arctic summer (PS80), the sampling region extended toward the North Pole and to 130° E, thus covering the Nansen Basin and the Amundsen Basin. The two Southern Ocean expeditions (**Figure 2**) took place in the Weddell Sea, but at different latitudinal locations. During winter (PS81), data were collected between 52° S and 61.5° S. During summer (PS89), the Marginal Ice Zone (MIZ) had already retreated, forming a belt relatively close to the continent, and facilitating the sampling of southern areas (between 66° S and 69° S). During the southward trip in December 2014, the MIZ extended to ∼66° S, during the return trip northward in January the MIZ had retreated to ∼68° S. We will refer to the two different MIZs as Dec-MIZ and Jan-MIZ. In the period in-between the sampling of the two MIZs, the ship traveled through the inner pack-ice area that we will refer to as the pack-ice area.

2.2. Draft Calculation

Retrieval of the sea-ice draft makes use of the combination of depth h_w given by the pressure sensor of the CTD, distance from the ice h_a computed from the altimeter, and pitch β and roll ϕ movement of the SUIT:

$$d = h_w - \left(h_a \times \cos\beta \times \cos\phi\right) - h_{CTD} \times \sin\left(\alpha + \beta\right). \quad (1)$$

The CTD and the altimeter are connected but mounted in different parts of the SUIT, thus they are located at different depths. h_{CTD} is the distance between CTD and altimeter, α is the angle formed between the CTD probe, the CTD sensor, and the altimeter (see Figure 3 in Lange, 2017). In some cases, due to the failure of one instrument, the entire set of information was not available. In this case, we used the simplified version of equation (1) that does not include the pitch and roll correction:

$$d = h_w - \left(h_a - h_{CTD}\right). \quad (2)$$

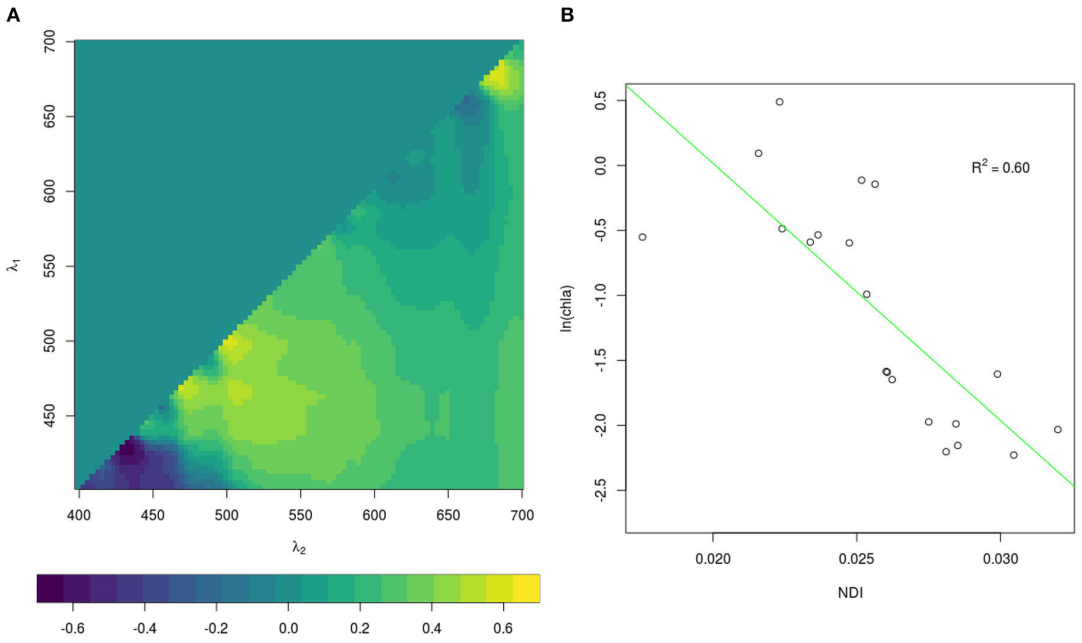

FIGURE 3 | Correlation surfaces **(A)** of normalized difference indices for integrated chl *a* for PS92 and PS106. λ_1 and λ_2 are wavelengths pairs. Relationship **(B)** between observed normalized difference indices and integrated chl *a* (dots). The green line represents the fitted relationship given by the algorithm^C in **Table 2**.

This is equivalent of assuming that the SUIT is towed perfectly parallel to the ice and, even if only an approximation, it has been proven reliable ($R^2 = 0.78$) in determining draft when the entire set of information was not available (Lange, 2017; Lange et al., 2017b). Handling of data gaps due to sensors malfunctioning or failure is explained in the **Supplementary Material**. Ice concentration for each profile was computed as the percentage of data points where ice thickness H_i was larger than zero. Ice thickness was computed by using a fixed density value ($\rho = 0.917\,\mathrm{g\,cm^{-3}}$) for the sea ice. By doing this, final ice thickness values include both sea ice and snow, and we will refer to it as total thickness in the following (Lange et al., 2019). Mean and median thicknesses were computed for $H_i > 0$ and they include ridges. Keels of ridges were detected along each profile by using the Rayleigh criterion (Rabenstein et al., 2010; Castellani et al., 2014, 2015). A detailed analysis of the distribution and properties of ridges detected along each SUIT profile will be provided in a separate study.

During all expeditions, a helicopter-borne frequency-domain electromagnetic induction sounding system (EM-Bird) was used to measure the total sea-ice thickness (sea-ice thickness plus snow depth, Haas et al., 2009). The 4-m long EM-Bird was towed at a height of 10–15 m above the surface under a helicopter along mainly triangular flight tracks. With this method, the larger scale sea-ice thickness distribution can be observed also away from the ship track, which usually follows the easier sea-ice conditions in a region. Each triangle leg covered 15–30 nautical miles.

2.3. Under-Ice Light

Irradiance and radiance values were integrated over the Photosynthetically Active Radiation wavelength range (PAR; 400–700 nm). Since the SUIT does not always travel parallel to the ice but can encounter obstacles that make it swing, we included in the analysis only data with an inclination angle lower than 15° (Lange et al., 2017b). In order to reduce the effect of under-ice water between the actual position of the sensors mounted in the SUIT frame and the underneath side of the ice, we excluded all measurements associated with an altimeter value larger than 1.5 m following works by Katlein et al. (2015, 2016, 2017), Lange et al. (2016, 2017b).

Transmittance was calculated as the ratio between under-ice and incoming radiation, the latter measured with a Ramses sensor mounted on the ship's crows nest. Due to a sensor failure during summer 2012 (PS80) we used incoming global radiation data, which are obtained with a pyanometer, also placed in the same region as the above described sensor. For comparison, a regression between the two sensors was calculated for the simultaneous measuring period and gave excellent agreement. Thus, data from this were used to calculate transmittance values in September 2012. A detailed method used to obtain radiation values to cover this period can be found in the **Supplementary Material**.

The quantity of light reaching the underside of the ice layer is important for sea-ice algae and phytoplankton, as well as for sympagic fauna. In order to compare the amount of light between expeditions and sampling stations independently from

the time of the day when we sampled, we calculated the insolation parameter as:

$$S_i = \int_0^{24} I_h TR_i dh\,, \tag{3}$$

where S_i is the insolation value (mol photons m^{-2} d^{-1}) at position i along each profile, TR_i is the transmittance value at position i, and I_h is the modeled hourly incoming solar radiation (μmol photons m^{-2} s^{-1}) above the surface (1°x1°spatial resolution, daily temporal resolution, interpolated hourly) based on the radiative transfer model SBDART (Ricchiazzi et al., 1998) as described in Laliberté et al. (2016). These data do not consider atmospheric parameters, such as cloudiness, which can affect the amount of radiation reaching the ship, where the incoming irradiance sensor is usually mounted. So defined, the insolation S_i is the amount of light passing through the bottom of the sea ice (i.e., PAR available for ice algae), at a specific position along the profile over an entire day. It is important to notice that the absence of information on cloud cover, or any other atmospheric parameter that could dampen the amount of light reaching the ice surface, potentially lead to overestimating the actual insolation values.

2.4. Retrieval of In-Ice Chlorophyll *a*

Since the retrieval of extensive spatial and temporal observations of sea-ice algae is limited in large part due to destructive techniques (i.e., based on the collection of sea ice from the field and subsequent melting and filtering of the ice), many studies in the past decades focused on estimating sea-ice algae based on under-ice hyperspectral measurements (Perovich, 1996; Mundy et al., 2007; Melbourne-Thomas et al., 2015; Lange et al., 2016; Meiners et al., 2017; Wongpan et al., 2018). In the present study, we employed normalized difference indices (NDIs) and Empirical Orthogonal Functions (EOFs) of under-ice spectra to estimate the concentration of chl *a* present in the ice. The heterogeneity of the environment covered by the present data set required the development of a specific algorithm for each expedition. The algorithms applied to the different data sets are listed in **Table 2**. For Arctic summer (PS80) data we used the EOF algorithm developed by Lange et al. (2016) based, amongst others, on the PS80 data set. Lange et al. (2016) recommended the EOF algorithm, instead of NDI, because it proved to be most reliable in catching the variability of in-ice chl *a* in the PS80 data set. For the Southern Ocean (PS81 and PS89) we used the NDI algorithm derived by Melbourne-Thomas et al. (2015) for the Weddell Sea. This algorithm was found to provide the most robust predictions of integrated chl *a* in comparison to others tested by Melbourne-Thomas et al. (2015). The NDI algorithm was developed based on summer data, and it is thus applicable to Antarctic summer (PS89). Meiners et al. (2017) applied the same algorithm to under-ice hyperspectral data collected with an ROV deployed during the Antarctic winter (PS81). Results showed that the algorithm provides a good fit with ice-core data collected during ice stations, we thus applied the same algorithm to the SUIT winter data (PS81). The NDI algorithm for Arctic spring (PS92 and PS106) was developed by comparison between coincident under-ice hyperspectral and in-ice chl *a* measurements of in total 8 ice stations carried out during the same campaigns. The accordance in sampling time (May-June-July), sampling region (**Figure 1**), and similarity of sea-ice properties (see section 3.2.1) justifies merging the data from these two spring expeditions. We used a total of 19 coincident measurements of under-ice irradiance and integrated chl *a* retrieved by measuring autotrophic pigments with High-Performance Liquid Chromatography (HPLC, for more details, see Tran et al., 2013). The NDIs for each wavelength pair were correlated with the integrated chl *a* values. Values lower than 0.1 mg m^{-2} were excluded from the analysis. Correlation surfaces of normalized difference indices are shown in **Figure 3A**. We then used a linear model to explore the relationship between predicted chl *a* from the NDI algorithm and integrated chl *a* from the ice cores (**Figure 3B**). The NDI algorithm developed explains 60% of the variability ($R^2 = 0.60$).

TABLE 2 | Normalized Difference Indices and Empirical Orthogonal Functions algorithms used to retrieve in-ice chl *a* for the different expeditions.

Expedition	NDI algorithm
PS80	0.7–3.0 s_2 + 1.1 s_4 + 2.4 s_6 − 6.5 s_7^2 + 3.9 s_9^2[a]
PS81	0.39 + 31.7 NDI(479:468)[b]
PS89	0.39 + 31.7 NDI(479:468)[b]
PS92	3.98–197.93 NDI(427:434)[c]
PS106	3.98–197.93 NDI(427:434)[c]

[a]*From Lange et al. (2016) where s_i are the EOF modes.* [b]*From Melbourne-Thomas et al. (2015).* [c]*Retrieved as explained in section 2.4.*

An example of a SUIT profile including CTD data, retrieved ice draft, and retrieved in-ice chl *a* is shown in **Figure 4**. The sampling frequency of the RAMSES radiometers was lower than the one of the CTD and ADCP. In order to match ice thickness/draft with under-ice hyperspectral measurements, we computed averages of thickness and draft values falling between the beginning and the end of each light measurement.

2.5. Statistical Analysis

We applied Principal Component Analysis (PCA) to assess spatial and seasonal patterns in the variability of physical properties of the sea ice and the underlying water sampled by the SUIT separately for each hemisphere. We included in this analysis the parameters water temperature, salinity, total ice thickness from the present study, and ridge depth and ridge density (Rabenstein et al., 2010; Castellani et al., 2014, 2015, G. Castellani, unpublished data). Near-normal distribution of data, as assumed by PCA, was checked by visual inspection of histograms. In order to achieve near-normal distribution of the data, total ice thickness and ridge density were square-root transformed.

To test for significant differences between the frequency distributions of total ice thickness data from the EM-bird and the SUIT, we applied the Kolmogorov–Smirnov test. Before applying the test, the SUIT data were resampled to the footprint of the EM-bird (40 m) by averaging the data for each 40 m segment

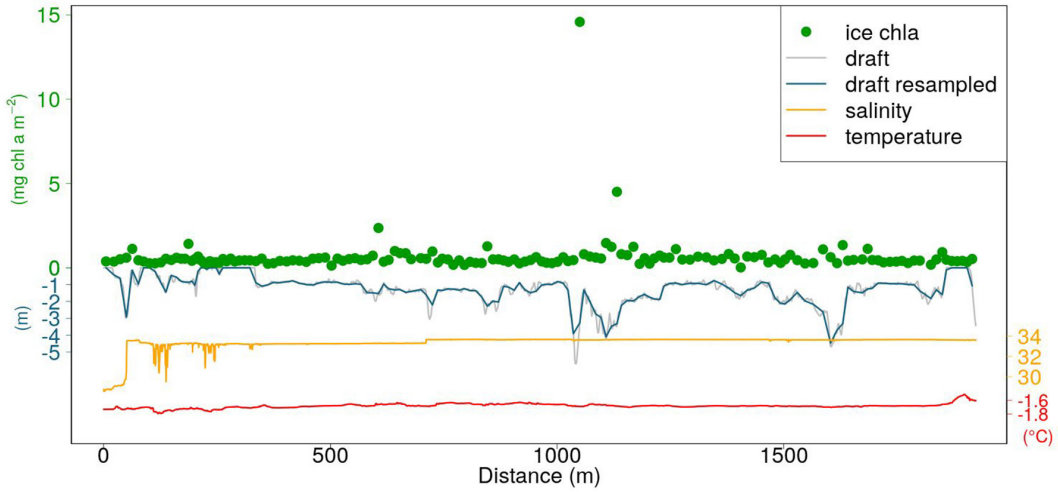

FIGURE 4 | Example of a SUIT profile (station PS92-47_1). Orange and red lines represent surface salinity and temperature, respectively. The gray line is the draft obtained with Equation (1). The blue line is the draft resampled at the frequency of the RAMSES radiometers sampling (section 2.4). The green circles represent in-ice chl *a* retrieved by applying the NDI algorithm^{c} in **Table 2**.

of each thickness profile. All statistical analyses were performed with the software R version 3.5.2 (R-Development-Core-Team, 2018), applying the package *vegan* (Oksanen et al., 2013).

2.6. Spatial Autocorrelation Analysis

Spatial autocorrelation was used to investigate the horizontal patchiness of sea-ice draft for 55 stations. Spatial autocorrelation analyses were also conducted for transmittance and in-ice chl *a* biomass. However, the transect nature of the surveys, the large interval spacing and small sample sizes, in comparison to draft, limited the spatial analyses of in-ice chl *a* to only 7 stations and of transmittance to only 10 stations. Autocorrelation was estimated using Moran's I (Moran, 1950; Legendre and Fortin, 1989; Legendre and Legendre, 1998), which was calculated for each SUIT survey at equally spaced (25 m) distance classes. Individual autocorrelation coefficients (e.g., Moran's I estimates) were plotted for each distance class as a spatial correlogram (Legendre and Fortin, 1989; Legendre and Legendre, 1998) using the R software function *correlog* from the *pgirmess* package (Giraudoux, 2018). Autocorrelation coefficients for each distance class were assigned a two-sided *p*-value according to Legendre and Fortin (1989) and Legendre and Legendre (1998). The presence of spatial autocorrelation (i.e., patchiness) was determined if the correlogram was considered globally significant at $p < 0.05$. We used the first x-intercept of globally significant correlogram lines as an indicator of the patch size for sea ice draft, *Pd* (Legendre and Fortin, 1989; Legendre and Legendre, 1998). This methodology is consistent with spatial autocorrelation analyses conducted on ROV gridded data from one of the same cruises (PS80, Lange et al., 2017b) and in other snow and sea ice studies (e.g., Gosselin et al., 1986; Rysgaard et al., 2001; Granskog et al., 2005; Søgaard et al., 2010).

3. RESULTS

3.1. Arctic Ocean

3.1.1. Sea Ice and Under-Ice Water Properties

Under-ice water properties for the three Arctic expeditions are presented in detail in **Tables 3–5**. In spring (PS92 and PS106), under-ice water temperatures were lower and salinities were higher compared to summer (PS80). The mean under-ice water chl *a* was highest in spring (6.34 ± 5.94 mg m^{-2} in May 2015, PS92) and lowest in autumn (1.60 ± 0.64 mg m^{-2} in September 2012, PS80). Besides seasonal differences, the data also show a regional pattern. During spring 2015 (PS92) there was a distinct difference between Yermak stations and the stations on the Sophia Basin & shelf (**Table 3**). The latter had higher under-ice water chl *a* (with a mean of 12.52 ± 9.14 mg m^{-2} compared to 1.80 ± 2.2 mg m^{-2} for the Yermak stations), higher mean under-ice water temperature (-1.54 ± 0.13 °C compared to -1.77 ± 0.05 °C) and lower mean salinity (33.70 ± 0.43 compared to 34.13 ± 0.23). We could not confirm if this pattern was repeated on PS106 because the Yermak Plateau was not reached. However, during this expedition higher temperatures, lower salinities and very high chl *a* values (up to 20 mg m^{-2}) in the surface layer were associated with the shelf-slope area toward the end of the expedition, and were probably related to the beginning of ice breakup (**Table 4**). During spring 2017 (PS106), time progression corresponded to a decrease in temperature and salinity and an increase in under-ice water chl *a* (PS106, **Table 4**). During summer 2012 (PS80), the stations situated in the Nansen Basin were characterized by higher salinities (mean 31.85 ± 0.94) and lower surface chl *a* (mean 0.66 ± 0.28 mg m^{-2}), whereas stations in the Amundsen Basin had lower mean salinities (31.02 ± 1.71) and higher mean chl *a* concentrations (1.46 ± 0.60 mg m^{-2}, **Table 5**, David et al., 2015).

TABLE 3 | Table for PS92 with, for each station (stn), the total profile length, the mean ice concentration ($\bar{A}$) along profile, mean snow depth ($\bar{H}_s$) and mean total ice thickness ($\bar{H}_i$), under-ice water chl *a* (chl a_w) multiplied by the vertical section of the SUIT (2 m) to obtain integrated values, under-ice water temperature and salinity, ice concentration retrieved from satellite ($\bar{A}_{Sat}$), median in-ice chl *a* (interquartile range), mean transmittance TR (± one standard deviation), mean Insolation S_i (± one standard deviation), and the draft patch size (P_d).

stn	Profile length (m)	$\bar{A}$ (%)	$\bar{H}_s$ (cm)	$\bar{H}_i$ (m)	chl a_w (mg m^{-2})	T (°C)	S	$\bar{A}_{Sat}$	In-ice chl *a* (mg m^{-2})	TR	S_i mol photons m^{-2} d^{-1}	P_d (m)
19_1	2876.5	24.94	5–20	1.05	7.04	−1.26	33.89	80.34	0.26 (0.16–0.40)	0.18 (0.27)	9.23 (14.07)	250
27_1	1912.5	90.80	10–40	1.07	8.86	−1.44	33.39	90.20	-	0.24 (0.26)	12.92 (14.12)	150
28_4	1143	97.07	30–40	1.27	4.60	−1.42	34.08	89.24	0.30 (0.15–0.46)	0.02 (0.10)	1.14 (5.63)	-
38_1	1449	94.93	5–40	1.20	17.56	−1.66	33.72	84.82	0.59 (0.37–0.82)	-	-	50
39_17	1053	70.19	10–40	1.59	0.9	−1.83	33.85	100	0.22 (0.16–0.31)	0.27 (0.24)	15.74 (13.84)	75
43_23	1281	32.93	20–30	1.77	0.54	−1.80	34.05	100	0.12 (0.05–0.19)	0.04 (0.08)	2.48 (4.60)	100
43_24	576	63.83	20–30	1.19	0.5	−1.80	34.24	100	0.14 (0.13–0.28)	0.32 (0.31)	19.08 (18.21)	-
44_1	1938	71.65	10–20	3.84	0.78	−1.76	34.16	94.01	0.12 (0.08–0.19)	0.20 (0.22)	12.04 (13.24)	275
45_1	1468	82.12	10–30	1.83	1.04	−1.74	34.32	96.44	0.21 (0.13–0.35)	0.04 (0.10)	2.26 (6.07)	175
47_1	1923.5	89.27	10	1.46	21.16	−1.68	33.38	92.79	0.47 (0.36–0.58)	0.09 (0.16)	5.12 (9.22)	250
48_1	2254.5	69.20	10–20	1.72	5.66	−1.48	33.51	100	0.23 (0.17–0.29)	0.18 (0.20)	10.98 (11.59)	225
49_1	1846.5	94.67	15–25	1.85	11.16	−1.61	33.43	100	0.30 (0.19–0.41)	0.08 (0.14)	5.05 (8.47)	50
56_2	1534.5	81.73	5	2.33	3.94	−1.72	34.02	88.96	0.26 (0.19–0.34)	0.12 (0.22)	7.23 (12.73)	125

In white are the stations located west of 10°E on the Yermak Plateau, in light gray are the stations located east of 10°E in the Basin & shelf area.

TABLE 4 | Table for PS106 with, for each station (stn), the total profile length, the mean ice concentration ($\bar{A}$) along profile, mean snow depth ($\bar{H}_s$) and mean total ice thickness ($\bar{H}_i$), under-ice water chl *a* (chl a_w) multiplied by the vertical section of the SUIT (2 m) to obtain integrated values, under-ice water temperature and salinity, ice concentration retrieved from satellite ($\bar{A}_{Sat}$), and median in-ice chl *a* (interquartile range), mean transmittance TR (± one standard deviation), mean Insolation S_i (± one standard deviation), and the draft patch size (P_d).

stn	Profile length (m)	$\bar{A}$ (%)	$\bar{H}_s$ (cm)	$\bar{H}_i$ (m)	chl a_w (mg m^{-2})	T (°C)	S	$\bar{A}_{Sat}$	In-ice chl *a* (mg m^{-2})	TR	S_i mol photons m^{-2} d^{-1}	P_d (m)
50_5	1691	93.11	10–20	1.19	1.76	−1.81	34.07	87.39	0.25 (0.18–0.31)	0.21 (0.23)	12.42 (13.71)	575
63_1	1309	88.70	-	0.97	1.00	−1.63	33.52	92.61	0.19 (0.15–0.23)	0.25 (0.26)	14.55 (15.11)	150
65_4	2213	95.75	5	2.29	-	-	-	96.61	-	0.12 (0.22)	6.99 (12.68)	150
66_3	97.5	65.82	10–20	0.50	0.40	−1.68	33.66	97.52	-	-	-	-
66_4	1005	97.46	20	1.77	1.64	−1.72	33.59	97.52	0.22 (0.13–0.30)	-	-	50
67_5	1466.5	94.04	5–10	1.29	2.62	−1.72	33.29	95.41	0.22 (0.15–0.31)	0.20 (0.25)	11.76 (14.23)	75
68_5	1320.5	93.60	15	2.38	1.96	−1.78	33.14	92.19	0.21 (0.16–0.36)	0.09 (0.18)	5.02 (10.27)	150
69_2	1158.5	97.50	-	1.58	1.82	−1.76	33.34	90.57	0.19 (0.16–0.23)	0.11 (0.13)	6.23 (7.66)	100
70_1	2627	98.08	Y	1.97	1.50	−1.74	33.81	90.10	0.14 (0.11–0.18)	0.10 (0.20)	5.94 (11.56)	225
71_5	3304	98.34	20	2.44	1.621	−1.78	32.44	91.10	0.11 (0.07–0.14)	0.10 (0.19)	5.68 (11.02)	225
72_5	2217.5	91.55	5–20	1.01	2.28	−1.77	33.26	91.53	0.23 (0.16–0.29)	0.25 (0.30)	14.43 (17.01)	450
73_7	2947.5	95.59	15–20	2.56	1.02	−1.72	34.10	92.34	0.17 (0.09–0.21)	0.14 (0.24)	7.82 (13.72)	225
74_5	2493.5	99.00	10–20	1.77	0.96	−1.72	34.07	84.10	0.12 (0.07–0.16)	0.15 (0.17)	8.46 (9.81)	225
75_6	2274	95.25	5–20	1.77	0.48	−1.63	33.84	85.02	0.15 (0.10–0.22)	0.24 (0.30)	13.22 (16.91)	550
76_4	2400	98.44	10–15	1.94	1.18	−1.68	33.87	77.68	0.11 (0.06–0.15)	0.19 (0.30)	10.82 (16.48)	325
77_2	2013.5	64.08	20	2.44	0.71	−1.64	33.19	77.21	0.18 (0.14–0.21)	0.33 (0.33)	18.50 (18.48)	725
78_5	1422.5	98.63	-	2.04	1.10	−1.66	33.51	77.06	0.11 (0.08–0.15)	0.08 (0.09)	4.46 (5.02)	100
79_1	1580.5	93.86	5–10	2.94	2.40	−1.68	33.33	77.60	0.19 (0.16–0.26)	0.16 (0.20)	8.80 (11.01)	300
80_3	2020.5	92.38	-	1.82	20.16	−1.06	32.99	77.79	0.39 (0.29–0.47)	0.16 (0.15)	8.50 (8.15)	125
83_7	626	98.56	-	1.90	3.38	−1.40	32.25	90.09	0.26 (0.20–0.28)	0.27 (0.20)	14.74 (11.12)	125
83_8	2103.5	99.33	-	1.75	4.96	−1.39	28.33	88.72	0.25 (0.23–0.28)	0.38 (0.23)	20.71 (12.45)	225

In light gray are the stations located west of 20°E in the Basin & shelf area.

TABLE 5 | Table for PS80 with, for each station (stn), the total profile length, the mean ice concentration ($\bar{A}$) along profile, mean snow depth ($\bar{H}_s$) and mean total ice thickness ($\bar{H}_i$), under-ice water chl *a* (chl a_w) multiplied by the vertical section of the SUIT (2 m) to obtain integrated values, under-ice water temperature and salinity, ice concentration retrieved from satellite ($\bar{A}_{Sat}$), and median in-ice chl *a* (interquartile range), mean transmittance TR (± one standard deviation), mean Insolation S_i (± one standard deviation), and the draft patch size (P_d).

stn	Profile length (m)	$\bar{A}$ (%)	$\bar{H}_s$ (cm)	$\bar{H}_i$ (m)	chl a_w (mg m^{-2})	T (°C)	S	$\bar{A}_{Sat}$	In-ice chl *a* (mg m^{-2})	TR	S_i mol photons m^{-2} d^{-1}	P_d (m)
204_1	2567	31.1	-	0.07	-	0.87	31.81	0	-	-	-	
216_1	2754.5	67.7	-	0.55	-	−1.06	30.89	26.88	0.0 (0.0–0.2)	0.38 (0.31)	13.91 (11.21)	-
223_1	1118.5	69.6	-	1.35	-	−1.53	32.04	72.26	0.2 (0.0–0.7)	0.24 (0.25)	8.40 (8.66)	-
233_1	2227	68.9	-	2.62	0.60	−1.60	32.83	100	0.1 (0.0–0.4)	0.36 (0.31)	11.90 (7.61)	-
248_1	3590	66.3	-	1.20	-	-	-	68.83	-	-	-	-
258_1	1679.5	91.2	-	0.65	0.72	−1.61	32.60	86.17	-	-	-	-
276_1	748	100.0	-	0.26	1.29	−1.42	30.21	52.02	-	-	-	-
285_1	1538	91.9	-	0.82	1.64	−1.56	30.65	54.16	0.1 (0.0–0.9)	-	-	-
321_1	1586.5	50.5	-	1.02	1.62	−1.60	29.19	51.46	0.9 (0.0–1.7)	0.16 (0.22)	1.96 (2.83)	-
333_1	1833	5.4	-	0.84	0.94	−1.22	30.08	11.05	-	0.56 (0.1)	5.83 (1.85)	-
345_1	2143	67.2	-	0.94	1.10	−1.60	30.14	36.55	1.9 (0.0–4.4)	0.28 (0.26)	2.02 (1.85)	-
358_1	2203	91.7	2.0	1.39	1.60	−1.81	33.12	100	0.9 (0.4–1.7)	0.10 (0.16)	0.12 (0.18)	-
376_1	189.5	87.6	-	2.46	1.38	−1.82	33.07	100	-	-	-	-
397_1	1460	89.8	Y	0.37	1.32	−1.80	32.18	99.90	-	0.02 (0.02)	0.008 (0.008)	-

In gray shades are the stations located in the Nansen Basin whereas the white ones are located in the Amundsen Basin.

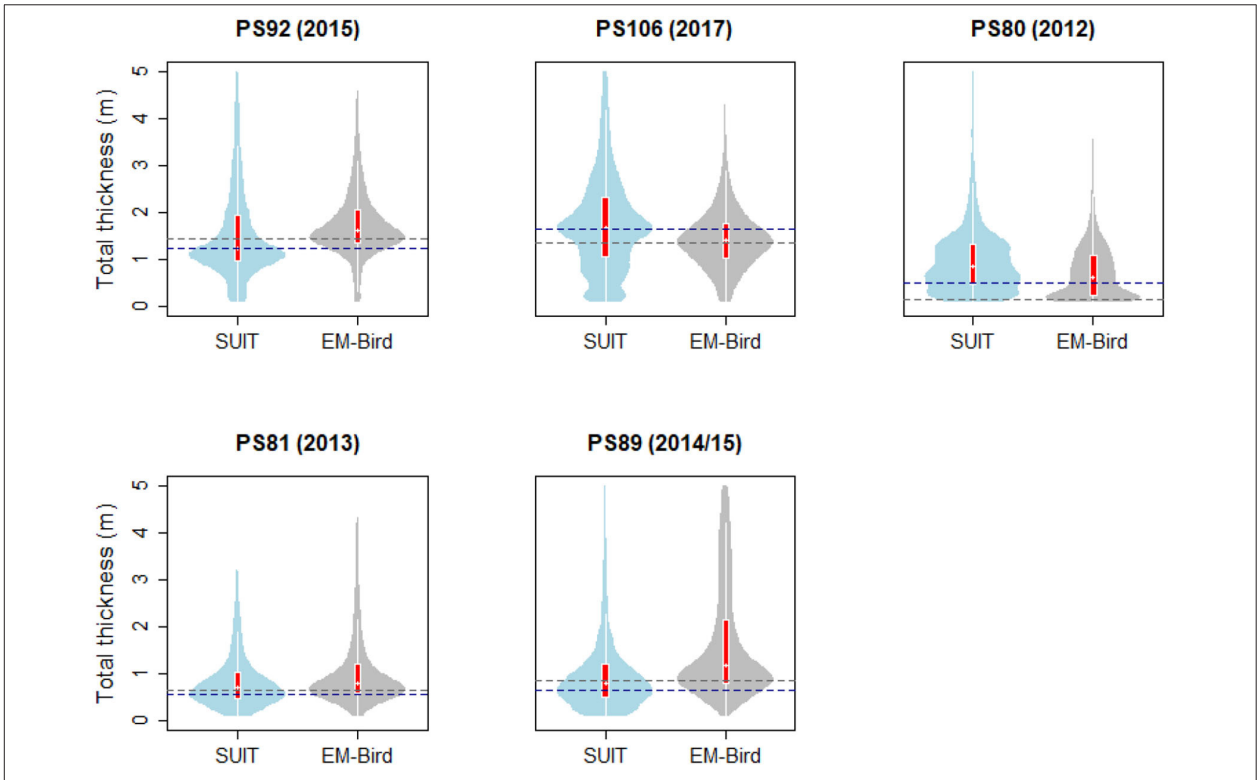

FIGURE 5 | Violin plots of total thickness (sea ice and snow) computed from the SUIT stations and from the EM-bird measurements in the vicinity of SUIT stations. The "violins" show density functions of the relative frequency distribution of the data. Superimposed on the violin plots are box plots showing the median (white dot), the 1st to 3rd quartile range (red boxes), and the lowest and highest data points within approximate 1.5 times the interquartile range (white lines extending from the boxes). Dashed lines indicate the modes of SUIT (blue) and EM-Bird (gray) data. Data were restricted to the interval 0.1–5.0 m total thickness.

During the springtime campaigns in 2015 (PS92) and 2017 (PS106), Arctic sea ice was covered with snow, whereas during summer 2012 (PS80) the ice surface was covered by melt ponds. Despite the difference in timing, snow depth decreased during both PS92 and PS106 and melt ponds started to form at the end of both expeditions (**Tables 3**, **4**). Toward the end of summer 2012 (PS80), refreeze started and snow accumulated over the ice (**Table 5**). Modal sea-ice thickness (**Figure 5**) was the highest in the Arctic spring, with modes of 1.25 m and 1.65 m in 2015 (PS92) and 2017 (PS106), respectively, and lowest during the summer campaign in 2012 (PS80), with a primary mode for very thin ice (<10 cm). With an explained variability of 81.9% for the first two principal components, the outcome of the PCA (**Figure 6A**) confirms a high similarity of the two springtime data sets (PS92, PS106), and a distinctly different combination of physical sea-ice and under-ice properties in most stations sampled during summertime (PS80). Salinity and ridge properties were the main drivers of the variability in sea-ice and under-ice properties (**Figure 6A**). The analysis of regional patterns shows that total ice thickness decreased eastwards with a decrease of modal thickness from the Yermak stations (1.25 m) to the Sophia Basin & shelf stations (1.05 m) in May-June 2015 (PS92), and in July 2017 (PS106) from the Sophia Basin & shelf stations (1.75 m) to the stations east of 20°E (1.55 m).

EM-bird data (**Figure 5**) show a similar pattern as the SUIT data, with a decrease in mean total ice thickness between spring and summer from 1.8 and 1.44 m during spring 2015 (PS92) and 2017 (PS106), respectively, to 0.71 m in summer 2012 (PS80). The shape of the ice-thickness distributions in spring was broadly similar between EM-bird data and SUIT data. However, a statistical comparison of the two data sets indicated significant differences between the two methods in all three sampling seasons (Kolmogorov–Smirnov test, $p \ll 0.001$), probably due to differences of several decimeters in the modes of the thickness distributions. Histograms of total thickness for both the SUIT and the EM-bird data are presented in the **Supplementary Material**.

3.1.2. Under-Ice Light and Light-Derived In-Ice Chlorophyll *a* Concentration

Values of transmittance show a mode for $TR < 0.05$ in both spring and summer. However, the summer mean value is larger (0.203 compared to 0.136 and 0.184 in 2015 and 2017, respectively). During summer 2012, high transmittance values were more frequent compared to spring 2015 and 2017. The similarity in the distribution of transmittance data during spring 2015 and 2017, shows that the two campaigns sampled the same variability in sea-ice and snow conditions (**Figure 7**). A monthly comparison shows that there was a change in mean transmittance from 0.22 ± 0.03 in May 2015 to 0.33 ± 0.3 in August 2012, then a decrease to 0.12 ± 0.19 in September 2012. The extinction coefficient k_b calculated by non-linear regression from the May subset of the data showed the largest value with $k_b = 8.678\ m^{-1}$. In June and July the extinction coefficients were lower, with values of 2.209 and $1.679\ m^{-1}$, respectively, reaching the minimum at $1.576\ m^{-1}$ in August (PS80). The extinction coefficient increased again in September to $6.552\ m^{-1}$. Insolation values in the Arctic (**Figure 7**) ranged from 0.00 to 57.17 mol photons m^{-2} d^{-1} during spring 2017 (PS106). In the comparison of May 2015 (PS92) and July (PS106), mean values ranged from 11.71 ± 14.17 mol photons m^{-2} d^{-1} to 10.24 ± 13.77 mol photons m^{-2} d^{-1}, and maximum values from 45.12 to 57.17 mol photons m^{-2} d^{-1}. During summer 2012, the shape of the distribution changed with respect to spring 2015 and 2017 and showed a smaller spread of values with maximum insolation at $S_i = 36.35$ mol photons m^{-2} d^{-1} compared to 51.77 mol photons m^{-2} d^{-1} and 57.17 mol photons m^{-2} d^{-1} during 2015 (PS92) and 2017 (PS106), respectively. Histograms of transmittance and insolation are presented in the **Supplementary Material**.

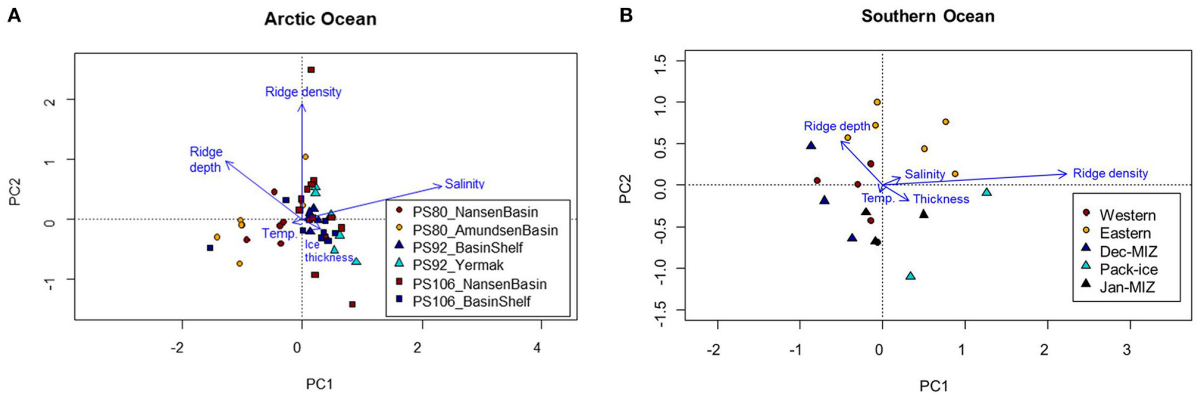

FIGURE 6 | Principal component analysis for the Arctic Ocean and the Southern Ocean. In the Arctic Ocean **(A)**, stations are divided within each expedition between Nansen and Amundsen basin (PS80), Yermak and Basin & shelf stations (PS92), and Basin & shelf stations vs. Western stations in the Nansen Basin (PS106). In the Southern Ocean **(B)**, stations are divided between westernmost and easternmost stations (PS81), and between January MIZ, December MIZ, and pack-ice stations (PS89).

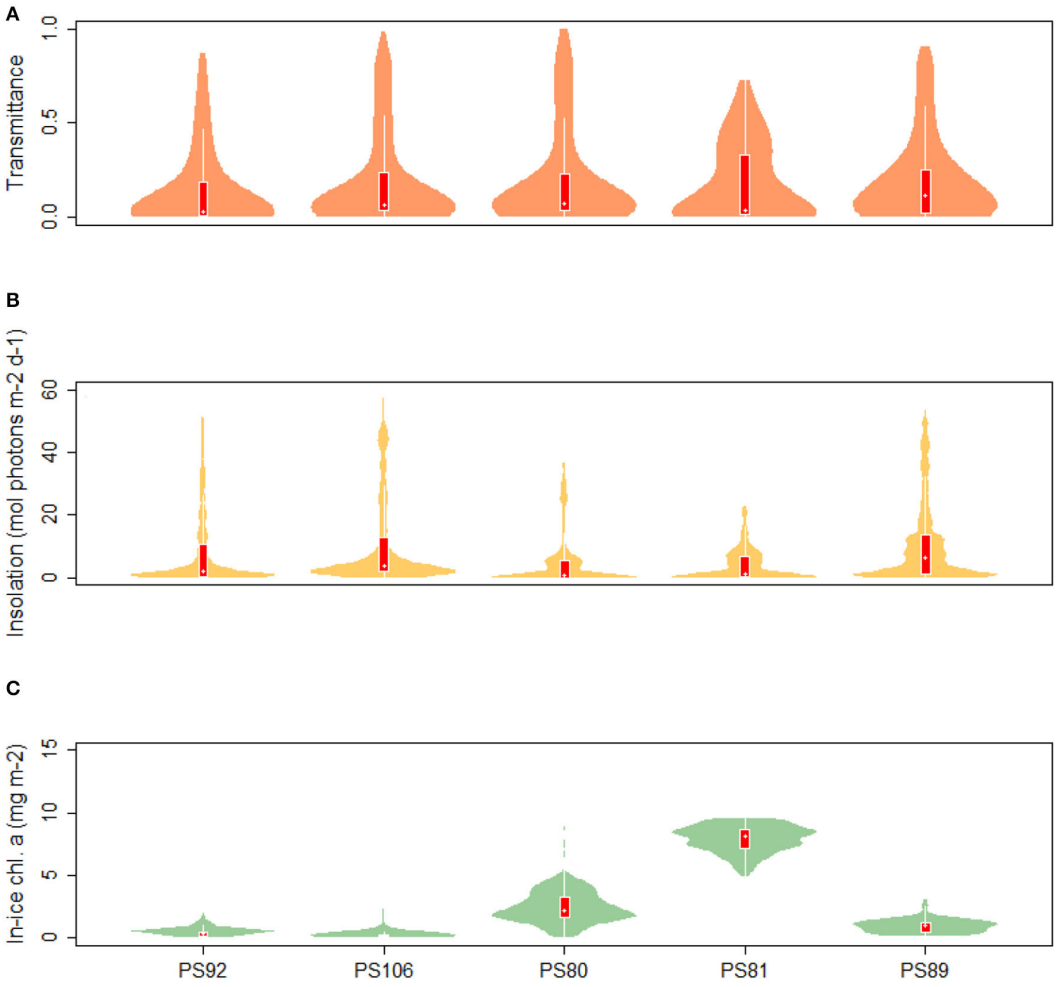

FIGURE 7 | Violin plots of **(A)** transmittance, **(B)** insolation, and **(C)** chl *a* concentration in sea ice. The "violins" show density functions of the relative frequency distribution of the data. Superimposed on the violin plots are box plots showing the median (white dot), the 1st to 3rd quartile range (red boxes), and the lowest and highest data points within approximate 1.5 times the interquartile range (white lines extending from the boxes).

During PS92 the stations on the Yermak Plateau had the lowest in-ice chl *a* values, whereas the Basin & shelf stations had the highest (**Table 3**). High chl *a* concentrations were also found in the Basin & shelf area during PS106, but in this case the spatial variability was less pronounced (**Table 4**). During summer 2012 (PS80), the Nansen Basin presented lower values of in-ice chl *a* compared to the Amundsen Basin. In the area of overlap between PS80 and PS106 stations, chl *a* values from the two campaigns were very similar, varying around 0.2 mg chl $a\,m^{-2}$. Distributions of in-ice chl *a* are similar for the two spring campaigns, whereas the distribution of values from the summer campaign shows significantly higher values (**Figure 7C**). Histograms of in-ice chl *a* are presented in the **Supplementary Material**.

3.2. Antarctic

3.2.1. Sea Ice and Under-Ice Water Properties

During the Antarctic winter in 2013 (PS81), under-ice water temperatures were always close to the freezing point (**Tables 1**, **6**) and uniform between sampling stations with a mean temperature of -1.85 ± 0.01°C. During summertime 2014/15 (PS89, **Table 7**), mean surface temperatures ranged between -1.67 ± 0.12 °C in the Dec-MIZ and -1.58 ± 0.12 °C in the Jan-MIZ. Lowest under-ice water temperatures characterized the pack-ice area sampled in December, with a mean of -1.86 ± 0.01°C. Likewise, the mean chl *a* concentration in the under-ice water was lower in winter 2013 (PS81, mean 0.42 ± 0.12 mg m^{-2}) than in summer 2014/15 (PS89, mean 0.88 ± 0.62 mg m^{-2}), and mean salinity was higher (34.22 ± 0.12 psu) in winter 2013

TABLE 6 | Table for PS81 with, for each station (stn), the total profile length, the mean ice concentration ($\bar{A}$) along profile, mean snow depth ($\bar{H_s}$) and mean total ice thickness ($\bar{H_i}$), under-ice water chl *a* (chl a_w) multiplied by the vertical section of the SUIT (2 m) to obtain integrated values, under-ice water temperature and salinity, ice concentration retrieved from satellite ($\bar{A}_{Sat}$), and median in-ice chl *a* (interquartile range), mean transmittance TR (± one standard deviation), mean Insolation S_i (± one standard deviation), and the draft patch size (P_d).

stn	Profile length (m)	$\bar{A}$ (%)	$\bar{H_s}$ (cm)	$\bar{H_i}$ (m)	chl a_w (mg m^{-2})	T (°C)	S	$\bar{A}_{Sat}$	In-ice chl *a* (mg m^{-2})	TR	S_i mol photons m^{-2} d^{-1}	P_d (m)
549_1	763.5	96.60	20–50	0.71	0.42	−1.86	34.22	92.36	7.80 (7.47–8.42)	0.01 (0.007)	0.13 (0.08)	50
555_1	298	52.60	20–50	0.30	0.32	−1.85	34.33	87.40	8.71*	0.07 (0.09)	1.14 (1.56)	-
557_1	2186	95.86	5–10	0.81	0.50	−1.86	33.86	95.28	-	-	-	100
560_2	1840	92.12	10	1.11	0.44	−1.68	33.83	98.91	-	0.38 (0.12)	6.66 (2.12)	75
562_5	1502.5	96.61	20–30	0.80	0.52	−1.86	33.77	96.88	-	-	-	125
565_5	1623	99.17	20–30	1.55	0.36	−1.87	34.22	100	8.13 (6.79–9.35)	-	-	-
567_2	800.5	92.07	60	0.32	0.82	−1.88	33.62	95.53	-	-	-	75
570_5	2114	95.93	15	0.64	0.92	−1.86	33.86	86.83	-	-	-	-
571_2	2291	94.68	15	0.54	0.62	−1.84	34.14	86.99	-	-	-	-
577_2	3184	95.68	20–50	0.85	0.62	−1.84	33.75	81.54	8.23 (7.50-8.51)	0.17 (0.21)	5.44 (6.65)	-
579_2	1140.5	95.70	Y	1.11	1.18	−1.83	34.10	81.54	-	-	-	100

*In gray shades are the westernmost stations, in white are the easternmost stations. *For station 555_1 there is only one value for in-ice chl a and we report it here only to help data interpretation.*

TABLE 7 | Table for PS89 with, for each station (stn), the total profile length, the mean ice concentration ($\bar{A}$) along profile, mean snow depth ($\bar{H_s}$) and mean total ice thickness ($\bar{H_i}$), under-ice water chl *a* (chl a_w) multiplied by the vertical section of the SUIT (2 m) to obtain integrated values, under-ice water temperature and salinity, ice concentration retrieved from satellite ($\bar{A}_{Sat}$), and median in-ice chl *a* (interquartile range), mean transmittance TR (± one standard deviation), mean Insolation S_i (± one standard deviation), and the draft patch size (P_d).

stn	Profile length (m)	$\bar{A}$ (%)	$\bar{H_s}$ (cm)	$\bar{H_i}$ (m)	chl a_w (mg m^{-2})	T (°C)	S	$\bar{A}_{Sat}$	In-ice chl *a* (mg m^{-2})	TR	S_i mol photons m^{-2} d^{-1}	P_d (m)
24_2	1835	81.45	25	0.75	0.90	−1.79	33.42	64.80	0.68 (0.35–1.20)	0.18 (0.23)	10.73 (13.59)	-
29_1	2291.5	75.68	5	0.45	1.24	−1.74	33.62	45.23	-	0.18 (0.23)	10.87 (13.74)	400
30_4	3004	54.55	10	0.53	0.60	−1.54	33.76	69.80	0.86 (0.34–1.30)	0.24 (0.29)	14.23 (17.06)	125
37_2	389	71.37	30–40	1.49	0.68	−1.85	33.80	100	1.03 (1.00–1.23)	0.30 (0.22)	17.60 (12.92)	50
38_1	944	97.83	30–80	1.89	1.34	−1.86	34.28	99.90	-	0.01 (0.02)	0.46 (0.89)	150
62_1	2718	83.58	20	1.06	0.54	−1.70	33.65	42.69	1.13 (0.70–1.42)	0.28 (0.30)	15.22 (15.79)	200
70_2	1120.5	100	10–100	1.65	0.68	−1.39	33.70	39.75	0.86 (0.62–1.00)*	0.15 (0.12)	8.07 (6.18)	75
71_1	2359	94.58	20	1.46	0.66	−1.53	33.63	33.46	0.89 (0.67–1.02)*	0.20 (0.20)	10.28 (10.48)	150

*In light gray shades are the stations located in the Marginal Ice Zone in December (referred to as Dec-MIZ), in white are the stations in the pack-ice area, whereas in dark gray are the stations located in the Marginal Ice Zone in January (referred to as Jan-MIZ). *Values for in-ice chl a at stations 70_2 and 71_1 were retrieved even if the altimeter values were missing (so it was not possible to filter the data) and are given to help the data interpretation in section 4.*

(PS81) than in summer 2014/15 (33.63 ± 0.24 psu). Between December (PS89, Dec-MIZ) and January (PS89, Jan-MIZ), both under-ice water temperature and chl *a* decreased, whereas salinity did not show any pattern (**Table 7**). The pack-ice area had different water properties compared to the MIZs, and it was characterized by significantly colder temperatures, more saline waters, and higher surface chl *a* concentrations (**Table 7**).

Sea ice in the Southern Ocean was covered with snow during both winter 2013 (PS81, **Table 6**) and summer 2014/15 (PS89, **Table 7**). The snow depth ranged from 5 to 60 cm in winter 2013 (PS89) and from 5 and 100 cm in summer 2014/15 (PS89). Modal ice thickness was lowest in winter 2013 (PS81, 0.45 m) and highest in summer 2014/15 (PS89, 0.75 m) in the Jan-MIZ (**Figure 5**). During both expeditions, the differences in total ice thickness varied from thinner ice in the northern latitudes to thicker ice in southern parts of the sampling areas. In PS89, the shape of the thickness frequency distribution in the pack-ice zone was different from the ones of the MIZs with a longer tail toward larger thickness values (data not shown). Ice thickness distribution from the EM-bird data (**Figure 5**) was similar in shape to those of the SUIT for both expeditions. In EM-bird data, however, modal ice thicknesses were somewhat higher compared to SUIT data (**Figure 5**), with a mode of 0.65 m in winter (PS81), and a mode of 0.85 m in summer (PS89). As in the Arctic Ocean, a statistical comparison of the two data sets indicated significant differences between the two methods in both sampling seasons (Kolmogorov–Smirnov test, $p < 0.001$). Besides the differences in modal thickness, this difference was also related to greater variations in the sampling of very thin ice between the two methods, with a larger proportion of thinner ice in the SUIT data compared to EM-bird data.

The PCA biplot of the physical sea-ice and under-ice properties during the two Southern Ocean expeditions showed a gradual separation of the two sampling seasons, indicating that most stations sampled in winter (PS81) were associated with lower under-ice water temperatures and higher salinities than most stations sampled in summer (PS89) (**Figure 6B**). The cumulative explained variability of the two first principal components was 95.4%. Within each expedition, the PCA ordination reflected the differences between sampling regions (**Figure 6B**).

3.2.2. Under-Ice Light and Derived Chlorophyll *a* Concentration

In the Southern Ocean, distributions for transmittance show a principal mode at 0.05 during both winter 2013 (PS81) and summer 2014/15 (PS89) (**Figure 7A**). The spread of values was larger during summer, with a maximum transmittance of 0.91 in summer 2014 (PS89) compared to 0.73 in winter 2013 (PS81). A comparison between data from August (PS81) and January (PS89) did not show a significant difference in mean transmittance values, but a difference in maximum transmittance of 0.03 in August (PS81) and 0.9 in January (PS89). Extinction coefficients showed a large variability, with values ranging from k_b = 1.439 m^{-1} in September 2013 (PS81) to k_b = 20.72 m^{-1} in December 2014 (PS89). During both campaigns, insolation values showed a mode at S_i = 0.5 mol photons m^{-2} d^{-1}, but mean values differed considerably with 3.86 ± 5.07 mol photons m^{-2} d^{-1} in winter 2013 (PS81) and 11.09 ± 13.08 in summer 2014/15 (PS89) (**Figure 7B**). The range of variability between winter and summer was very different, with a maximum at S_i = 22.72 mol photons m^{-2} d^{-1} in winter 2013 (PS81, **Table 6**) compared to S_i = 53.51 mol photons m^{-2} d^{-1} in December 2014 (PS89, **Table 7**).

During winter 2013, in-ice chl *a* was significantly higher than during summer, with a mean of 7.91 ± 1.07 mg chl *a* m^{-2} in winter compared 0.88 ± 0.51 mg chl *a* m^{-2} in summer (**Figure 7C**). Principal modes were at 8.5 and 1.3 mg chl *a* m^{-2} during winter and summer, respectively. The variability within expeditions was low in both seasons. During summer 2014/15 higher in-ice chl *a* values were measured in the Jan-MIZ, compared to the Dec-MIZ.

3.3. Spatial Autocorrelation Analysis

The summary of the spatial autocorrelation analysis and the results for the patch size in both the Arctic and the Antarctic are presented in **Table 8**. Spatial autocorrelation analysis resulted in significant sea ice draft patch size estimates for 13 of the 19 SUIT stations in the Southern Ocean and 42 of the 48 SUIT stations in the Arctic Ocean, with significant results for almost all cruises. Patch size, which for ice draft can be interpreted as the size of smooth sea-ice areas, varied from 50 to 750 m with a mean of 221±156 m (**Table 8**) for the Arctic Ocean. In the Southern Ocean, autocorrelation analysis showed a draft patch size varying from 50 to 400 m (with an average of 129±92 m, **Table 8**), with larger values for the summer expedition (PS89). The spatial autocorrelation analysis for transmittance (i.e., patch sizes) showed statistical significant results for SUIT in 3 of the 19 SUIT stations in Antarctica and in 7 of the 48 SUIT stations in the Arctic Ocean, with no statistically significant results during the summer Arctic cruise PS80. Our analysis showed a significant Pearson's correlation between the patch size of draft and transmittance (correlation coefficient = 0.77; N = 9; p = 0.016), indicating that sea-ice draft (i.e., total ice thickness) is the driver of variability in sea-ice transmittance. Correlograms for one SUIT haul for each expedition are shown in **Figure 8** together with a comparison in patch size between the two Polar regions for both ice draft and transmittance.

TABLE 8 | Summary of the patch size for total thickness, transmittance and in-ice chl *a* as result of the spatial autocorrelation analysis (section 2.6).

Patch	Southern ocean	Arctic ocean
Draft *t* = -2.6332 df = 34.687 *p* = 0.01255	129 ± 92 m (13)	221 ± 156 m (42)
In-ice chl *a* *t*-test = *NA*	200 ± 0 m (1)	242 ± 66 m (6)
Transmittance *t* = -2.75 df = 7.8561 *p* = 0.02549	117 ± 29 m (3)	221 ± m 90 (7)

Student's t tests were performed to test for significant differences in patch sizes of draft, in-ice chl a and transmittance between Southern Ocean and Arctic Ocean SUIT surveys.

4. DISCUSSION

4.1. Environmental Properties

This study presents the first characterization of sea ice and under-ice environments from multiple expeditions and seasons on the scale of kilometers in both ice-covered polar oceans. In the Arctic Ocean, ice and snow start to melt with the spring to summer progression and the increase in atmospheric and oceanic temperatures. The results showed this seasonal progression with a decrease of snow cover with subsequent formation of melt ponds, and a decrease of salinity in the under-ice water, an indicator of the presence of melt water under the ice. More light was found to penetrate the ice as time progressed, which can be attributed to a decrease in both ice thickness and snow cover (**Tables 3–5**). Similar patterns were seen in previous studies (e.g., Nicolaus et al., 2010). At some sampling stations, increased light penetration was accompanied by an increase of under-ice water chl *a* concentrations. During the two spring campaigns in 2015 and 2017 (PS92 and PS106), sampled locations were situated closely together with an overlap in the region 10°E < lon < 20°E, defined as the Basin & shelf region. When comparing the two expeditions, the spatial pattern appeared stronger than the inter-annual one. During the PS92 expedition, the Basin & shelf region showed a difference in water masses, characterized by more saline and warmer water, compared to the Yermak Plateau (Meyer A. et al., 2017). The under-ice water chl *a* concentration

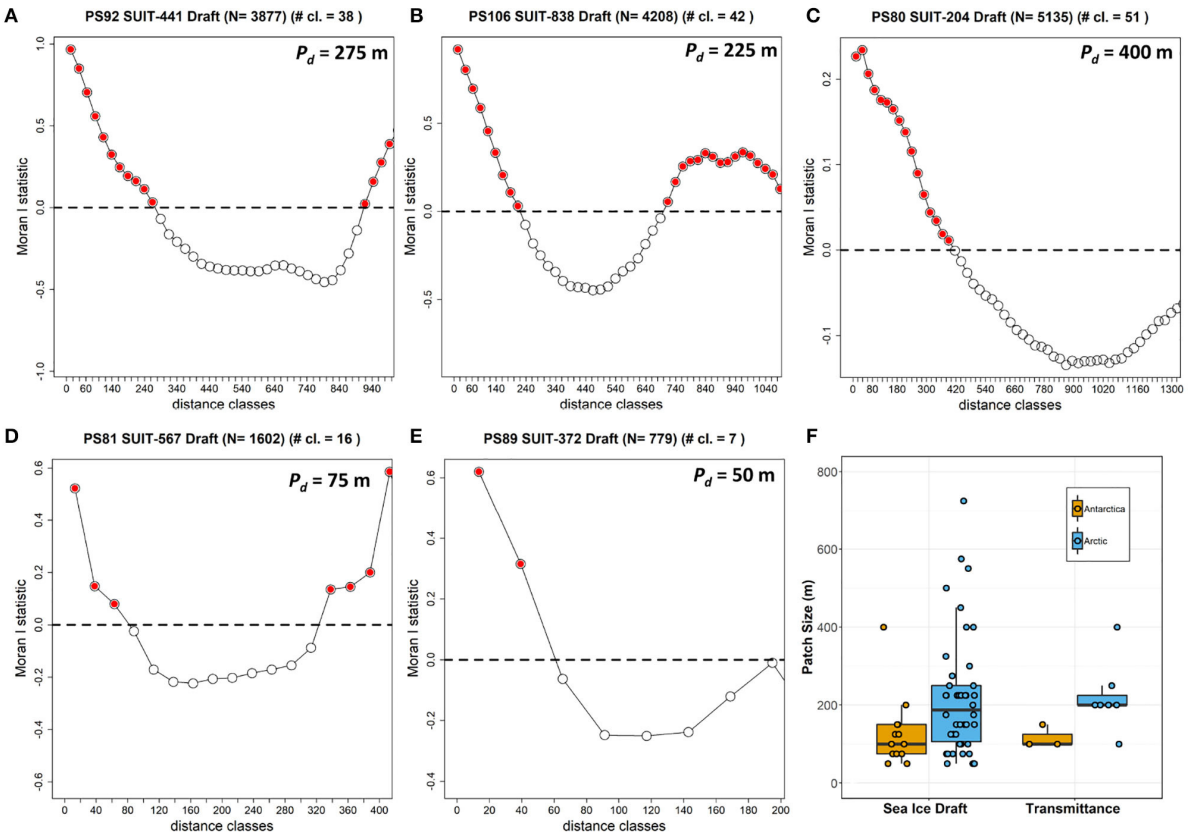

FIGURE 8 | Correlograms showing Moran's I vs. distance classes for selected SUIT surveys as examples in the Arctic (top row): **(A)** PS80 station 204_1; **(B)** PS92 station 44_1; **(C)** PS106 station 83_8; and in Antarctica: **(D)** PS81 station 567_2; **(E)** PS89 station 37_2. Red filled circles represent significant values at $p < 0.05$. **(F)** Boxplot summarizing all sea ice draft patch sizes determined from all SUIT surveys grouped by polar region.

was lower over the Yermak Plateau compared to the Basin & shelf region. In addition to these measurements, Assmy et al. (2017) found that the Basin & shelf area was characterized by large leads allowing light to penetrate through the ice which potentially explains increased chl *a* concentrations and a higher primary production compared to the Yermak region (Massicotte et al., 2019). The two regions also differed in the composition of under-ice fauna, and zooplankton abundances were generally very low in the under-ice water over the Yermak Plateau (Ehrlich et al., 2020). In summer 2012 (PS80), the Nansen vs. Amundsen Basin separation (**Table 5**) emerged clearly from the under-ice water salinity and chl *a* concentration, pointing to two different environmental regimes: an Atlantic influenced and nutrient-rich regime in the Nansen Basin, and a nutrient-poor regime influenced from the Laptev Sea shelf in the Amundsen Basin (David et al., 2015; Flores et al., 2019). Surface temperature, however, showed a seasonal decrease toward winter. Ice thickness differences between the two basins (not shown here) remained very small pointing to similar sea-ice conditions in the two basins (**Figure 6A**). However, the Amundsen Basin, which was sampled later in the season, had a principal mode at a thickness value of 0.65 m (figures not shown) and a secondary mode for very thin ice (values < 0.1), indicating that refreeze started already. Additionally, under-ice water parameters differed between the two basins (**Table 5**), as well as the zooplankton community structure, which showed a dominance of copepods in the Nansen Basin, but a co-dominance of copepods and amphipods in the Amundsen Basin (David et al., 2015).

The shape of the total sea-ice thickness distributions from the SUIT data agreed largely with those from the EM-measurements. In both, the Arctic Ocean and the Southern Ocean, however, median and modal total thicknesses from the EM-bird and the SUIT differed by up to several decimeters, causing significant differences between the two distributions with no systematic bias toward one instrument (**Figure 5**). These differences could be due to differences in the geographical area covered by the two devices, thus one of the instruments might have collected a larger amount of data points in a region with thicker/thinner ice compared to the other instrument. This was particularly the case in PS89, where the EM-measurements included areas covered by landfast ice, which were not sampled with the SUIT (data not shown). Differences between SUIT and EM-measurements

were probably also a result of a balance between systematic biases of the two devices: On the one hand, SUIT-based total thickness estimates could have been negatively biased because the ship tends to travel in areas where navigation is easier (i.e., thinner ice; PS92, PS81, PS89). On the other hand, the lower spatial resolution of the EM-measurements causes an under-representation of deep ridges compared to the SUIT, shifting the distribution of total thicknesses toward the lower end (PS106, PS80). Moreover, the way snow is treated might introduce bias. The EM-bird directly measures snow plus ice thickness, on the other hand, for the SUIT, ice draft is converted into total ice thickness. Therefore, a change in the actual snow depth will have different impacts on SUIT and EM-bird ice thickness retrievals. When comparing with satellite data (column $\bar{A}_{Sat}$ in **Tables 3**–**7**), the SUIT can provide representative ice-concentration values. Only in the marginal ice zone, where the SUIT preferentially sampled only the ice-covered parts of the grid cell detected by satellites, greater differences occurred (David et al., 2015).

Transmittance values largely reflected sea ice and snow conditions. The greater ice thickness during spring 2017 (PS106) compared to 2015 (PS92) was associated with lower mean transmittance values (**Tables 3**, **4**), whereas the absence of snow during summer 2012 (PS80) led to higher transmittance (**Table 5** and **Figure 7**). A larger spread of values during spring 2017 (PS106) compared to spring 2015 (PS92), however, points to higher variability of sea-ice and snow conditions, which was confirmed by Katlein et al. (2019), and which could be explained by the slightly different sampling period extending more toward summer during PS106. We estimated the insolation parameter (i.e., the daily integrated sunlight received) in order to obtain a representative comparison between SUIT hauls even if they were carried out at different times of the day. Mean insolation values in summer were higher than in spring, as a result of the larger transmittance values. However, the spread of values was wider in spring, which was related to incoming solar radiation that is maximum in the months of June-July compared to August-September (Arrigo et al., 2012; Arndt and Nicolaus, 2014). Extinction coefficients calculated from the present data set include the effect of both snow thickness and ice thickness, thus they represent bulk coefficients. Our summer values correspond to the ones generally known for bare ice (Grenfell and Maykut, 1977; Perovich, 1996; Light et al., 2008). The values presented here are in good agreement with those shown recently by Katlein et al. (2019), where bulk coefficients varied from $\sim$5 m^{-1} in May to $\sim$1 m^{-1} in August, and then increased again in September (Katlein et al., 2019, their **Figure 8**).

In the Southern Ocean, variations within winter 2013 (PS81) stations in salinity and temperature were rather small due to a quasi-homogeneous winter layer circulation in the Weddell Sea (David et al., 2017). The north-eastward sampling performed during the winter-spring transition led to a gradual decrease in sea-ice coverage, higher under-ice insolation, and an increase of under-ice water chl *a* by the end of the expedition, indicating that the productive season commenced (David et al., 2017). As for the Arctic expeditions, disentangling spatial and temporal patterns is challenging. Despite this difficulty, we can conclude that larger thickness values in the Jan-MIZ can be explained by the more southern locations. Total ice thickness distribution for winter 2013 (PS81) and summer 2014/15 (PS89) were similar, indicating similar sea-ice conditions. The cyclonic drift pattern of the Weddell Gyre moves sea ice from the eastern Weddell Sea/Lazarev Sea northwestward (Kwok et al., 2017) in a regime of mainly free drift. This decreases the tendency of sea ice to deform (G. Castellani, unpublished data) and it leads to more uniform sea-ice conditions in that area.

The similarity in snow cover and ice thickness between winter 2013 (PS81) and summer 2014/15 (PS89) leads to comparable transmittance values, even though the maximum transmittance values were lower in winter than in summer. Differently from the Arctic, Antarctic sea ice remained covered by relatively thick snow also during summer, explaining why transmittance values never approached 1.

4.2. In-Ice Chl *a*

We applied NDI and EOF algorithms to retrieve in-ice chl *a* from under-ice irradiance and transmittance spectra. We used one algorithm for Arctic summer (Lange et al., 2016), one for the Antarctic regions (Melbourne-Thomas et al., 2015), and one for the Arctic spring. In all the three cases, the retrieved values of in-ice chl *a* were in good agreement with ice-cores data collected during PS80 (Fernández-Méndez et al., 2015), and during PS92 and PS106 (Ehrlich et al., 2020, I. Peeken, unpublished data), and with derived in-ice chl *a* based on ROV measurements during PS81 (Meiners et al., 2017).

In the Arctic, the progression in snowmelt is visible in the increase of in-ice chl *a* with seasonal progression. Spring campaigns were conducted from late May onward, when incoming light levels were already high enough to cause an algal bloom, but snow cover obviously hampered this. Ice-algae growth was limited by the snow cover and the increase of in-ice chl *a* in the last stations during both PS92 and PS106 reflected the better light conditions after the onset of snowmelt. In-ice chl *a* concentrations were higher toward the end of summer 2012 (PS80) than in the two Arctic spring studies. This indicates that the ice-algae bloom only commenced after the onset of snowmelt, as expected from modeling studies (Castellani et al., 2017). During our sampling of PS80, large parts of the ice-algae bloom had already been released to the sea floor due to basal melting (Boetius et al., 2013), indicating that the observed in-ice chl *a* values had probably been considerably higher during the peak of the bloom.

In-ice chl *a* in the Antarctic winter was much higher than on any other expedition in the Arctic Ocean or the Southern Ocean. Our winter values agree well with values obtained from ice cores collected during the same expedition (Meiners et al., 2017). The presence of high biomass despite very low transmittance and insolation values indicate that the algae present in winter are the result of a previous accumulation of high biomass along the entire core length, more than an active growth at the bottom (Meiners et al., 2012). Winter in-ice algal assemblages often consist mainly of diatoms (Garrison and Close, 1993; Ugalde et al., 2016). During PS81 this was confirmed by sea-ice fatty acid compositions (Kohlbach et al., 2017b), and algae found in the stomach of larval krill (Schaafsma et al., 2017). Notably, in-ice chl *a* mean values in

the Antarctic in winter were always higher than phytoplankton chl *a* values from the under-ice water. This was valid also for some stations during summer (i.e., stations 30_4, 37_2, 62_1, 70_1, and 71_1). Several Antarctic species are attracted to the sea ice during both summer and winter, including Antarctic krill *Euphasia superba* (Flores et al., 2011, 2012, 2014), showing the importance of sea ice-derived carbon for the Southern Ocean food web (Jia et al., 2016; Kohlbach et al., 2017b, 2018, 2019). This basal role of sea-ice derived carbon has a major impact on the distribution, abundance, life-cycle and possibly survival of many organisms residing in ice-covered oceans.

4.3. Physical and Biological Comparison

The present data set agrees with the well-known characteristics of the two polar regions, thus proves to be representative of the environment sampled. Variability in sea-ice properties was higher in the Arctic Ocean compared to the Southern Ocean. Furthermore, our spatial autocorrelation analysis of total sea-ice thickness showed smaller patch sizes in the Southern Ocean than in the Arctic Ocean. Interpreting this as bottom roughness, we can say that the Antarctic sea ice was characterized by smaller floes, or smaller patches of level ice compared to the Arctic, pointing to the different sea-ice drift, growth, and deformation regimes (Haas, 2008; Massom and Stammerjohn, 2010). Additionally, the correlation between total thickness and transmittance patch sizes indicates that, at floe-scales of around 120 m for the Southern Ocean and around 220 m for the Arctic Ocean, total ice thickness is a good predictor for transmittance, which is in agreement with previous work from the Arctic (e.g., Katlein et al., 2015). At smaller spatial scales, typically around 10 m, Katlein et al. (2015) found that surface properties such as melt ponds (during Arctic summer) were the best predictor for transmittance, which was not possible to resolve with the present data set due to the large spacing intervals between subsequent under-ice irradiance measurements (>10 m). The snow remains thick in the Antarctic during summer, whereas during Arctic summer snow melts completely and melt ponds form on the sea ice surface (Eicken, 2003; Nicolaus et al., 2012; Webster et al., 2018). Despite higher transmittance, insolation values (i.e., the amount of daily light that an algae receives at the bottom of the sea ice) were higher in the Arctic spring than in summer. The range of transmittance values during PS80 was higher compared to values collected in the same Arctic region and in the same season, but one year earlier, with a Remotely Operated Vehicle (ROV, Nicolaus and Katlein, 2013) diving under the ice (Nicolaus et al., 2012), and compared to those collected in July 2014 with an AUV diving under an ice floe (Katlein et al., 2015). The same holds for the transmittance values for PS81 and PS89: the range of transmittance variability measured with the SUIT was higher, and with higher mean values, than those obtained during the same expeditions with the ROV (PS81 data were published in Arndt et al., 2017, PS89 are unpublished data). Differences arise mainly from sampling methodologies. Whereas, with the ROV data are collected under a single, relatively uniform ice floe, the SUIT travels through a more heterogeneous environment, including also very thin ice or brash ice present in between ice floes. For this reason, the different methods sample differently and transmittance values can be higher when calculated from the SUIT data set compared to the ROV data set (Massicotte et al., 2019). Furthermore, a towed approach such as the SUIT is more robust compared to robotic platforms (e.g., ROVs and AUVs) and is thus able to ride directly along the underside of the sea ice at large distances with minimal concern about damage and losing the platform. However, the towed SUIT is subject to minimum speed requirements in order to maintain momentum while breaking sea ice and to representatively catch under-ice fauna, which is a main objective of SUIT deployments. Thus, ROVs and AUVs can survey the under ice environment at a more controlled and lower speed providing a greater spatial resolution, however, at the cost of spatial coverage.

As expected, insolation values were very low in winter (PS81). Despite the highest snow cover and the low transmittance values, during the Antarctic summer (PS89) the under-ice insolation was greater than in the Arctic summer (PS80). This difference reflected the different latitudinal ranges of the two sampling areas. The difference in maximum latitude (70°S compared to 85°N) and the difference in solar inclination lead to stronger incoming radiation during the Antarctic summer (PS89) than during the Arctic summer (PS80), leading to stronger under-ice insolation. Surface chl *a* values were higher in the Arctic (particularly in spring) than in the Antarctic. In contrast, in-ice chl *a* values were higher in Antarctic sea ice. Moreover, in the Arctic the amount of in-ice chl *a* was always lower than phytoplankton chl *a*, whereas the opposite is true in the Southern Ocean. This highlights the importance of sea ice-derived carbon especially for Antarctic ecosystems, both in summer and in winter.

Sea-ice represents a permanent or seasonal habitat for many species in the polar oceans. The SUIT does not only uniquely cover relatively large areas, but also enables a simultaneous sampling of environmental data and under-ice fauna (collected with the two nets attached to the SUIT frame). Collected data have, therefore, enabled the study of the relationship between the sea-ice environment and the distribution of zooplankton and nekton species at the ice-water interface at a scale of kilometers. The surface zooplankton communities of both the Arctic and Southern Ocean have been found to respond to the presence (or absence) of sea ice in all sampled seasons, and variations in under-ice zooplankton community structure have been related to sea-ice environmental properties (Flores et al., 2011, 2012, 2014, 2019; David et al., 2015, 2016; Schaafsma et al., 2017; Ehrlich et al., 2020). In the Arctic Ocean, for example, abrupt changes were observed from a dominance of ice-associated amphipods (*Apherusa glacialis*) at ice-covered stations to a dominance of pelagic amphipods (*Themisto libellula*) at nearby ice-free stations (David et al., 2015). In addition, high numbers of the copepods *Calanus hyperboreus* and *Calanus glacialis* were found in the ice-water interface layer, in spite of low under-ice water chl *a* within the sampling area (David et al., 2015), which indicated that they were grazing on ice algae (Runge and Ingram, 1991; Kohlbach et al., 2016). Higher abundances of the polar cod (*Boreogadus saida*), which is regarded as a key species in the Arctic Ocean, were related to relatively low under-ice surface salinity, thick sea-ice and high sea-ice coverage (David et al., 2016). In the Southern

Ocean, differences in sea-ice drift pathways were closely related to the condition of krill larvae and the proportion of ice algae in their diet, at the beginning of the productive season (PS81) in the Weddell Sea (Kohlbach et al., 2017b; Schaafsma et al., 2017). The community structure of under-ice fauna was associated to changes in under-ice water parameters (David et al., 2017).

The presented data set and the environmental information from this study allow for further research on the relationship between large scale distributional patterns of under-ice fauna and sea-ice structures, such as the abundance and size of pressure ridges and hummocks, which have been suggested as structures where organisms, including both algae and zooplankton, accumulate (Gradinger et al., 2010; Lange et al., 2017a,b). Studies of Gradinger (1999) and Nozais et al. (2001) analyzed the potential role of sympagic fauna in controlling algal production due to grazing, but both drew contradictory conclusions. Whereas, Nozais et al. (2001) strongly suggest that the grazing impact of sea-ice meiofauna on ice algae was negligible, Gradinger (1999) found significant positive correlations between the integrated ice-algae and sympagic fauna biomass, and potential ingestion rates. Also other studies, often using data collected by divers, found evidence that abundance and distribution of certain species were related to the structure of the sea ice (Gruzov et al., 1967; Carey, 1985; Grainger and Hsiao, 1990; Garrison, 2015; Meyer B. et al., 2017), examples being the amphipods *Gammarus wilkitzkii* (Beuchel and Lønne, 2002) and *Apherusa glaciali* (Poltermann, 1998; Gradinger et al., 2010) in the Arctic Ocean. Gaining knowledge on the relationship between structure and faunal biomass on a larger scale, potentially will allow for prediction of an oceanwide distribution based on sea-ice parameters.

5. CONCLUSIONS

In this study, we presented and analyzed a large data set collected during five expeditions covering different years, seasons, and regions in both the Arctic Ocean and the Southern Ocean. Data were collected with a Surface and Under-Ice Trawl (SUIT), which allows the characterization of the sympagic environment on the kilometer scale. The data proved to be representative in characterizing the physical environment, and highlighted regional and seasonal differences in both hemispheres. Analysis of spatial variability showed a significant difference in the spatial scale of the variability of sea-ice properties between the Arctic and Antarctic, and showed that the total ice thickness was a driver for variability in sea-ice transmittance. The introduction of a new parameter, the insolation (i.e., daily integrated under-ice PAR) showed that more light for photosynthesis is available for biological production in the Antarctic summer compared to the Arctic summer, despite the large snow cover in the Antarctic and the higher transmittance in the Arctic. For the first time, we could provide in-ice chl *a* estimates over large spatial scales derived with the same methodology, for both the Arctic and the Antarctic. Our results showed that ice algae biomass was generally at comparable levels in both hemispheres during summertime, it was low in Arctic spring and particularly high in the Antarctic winter. In a future study, the present data set will be used to compare results and to improve parameters of sea-ice biogeochemical models.

DATA AVAILABILITY STATEMENT

The datasets generated for this study are available at https://doi.pangaea.de/10.1594/PANGAEA.902056.

AUTHOR CONTRIBUTIONS

GC wrote the paper, processed the data to obtain sea-ice draft and in-ice chl *a*, and prepared most of the figures. SA processed the RAMSES data to obtain integrated irradiance and radiance values and also to extract the wavelengths. RR provided the satellite ice concentration data. PM provided modeled downwelling irradiance data. IP supervised the Arctic sea ice biology sampling and processed all HPLC samples. FS, HF, and JE contributed to develop the structure of the manuscript and FS provided information on the snow depth per each SUIT haul. TK, SH, SS, and BL collected the EM-bird data. BL processed and plotted the EM-data, provided in-ice chl *a* estimates for PS80, and carried out the spatial autocorrelation analysis. GC, HF, JE, BL, FS, and CD contributed to SUIT data collection. JE, FS, CD, and HF contributed to data interpretation in connection with biological data. HF supervised the construction of the SUIT and designed the sampling for all the campaigns and conducted statistical analyses. All co-authors contributed to the discussion of results and to the preparation of the manuscript.

FUNDING

This study was primarily funded by the Helmholtz Association through the Young Investigators Group *Iceflux* (VH-NG-800) and the Research Program PACES II. RR was financed by the European Space Agency Climate Change Initiative Sea Ice project SK-ESA-2012-12. Antarctic research by Wageningen Marine Research is commissioned by the Netherlands Ministry of Agriculture, Nature and Food Quality (LNV) under its Statutory Research Task Nature & Environment WOT-04-009-047.04. The Netherlands Polar Programme (NPP), managed by the Netherlands Organisation for Scientific Research (NWO) funded this research under project nr. ALW 866.13.009. SA was financed by the German Research Council (DFG) in the framework of the priority programme *Antarctic Research with comparative investigations in Arctic ice areas* by grant to SPP1158, AR1236/1, and the Alfred-Wegener-Institut Helmholtz-Zentrum für Polar- und Meeresforschung. Part of this work resulted from the *EcoLight* project (grant number 03V01465), part of the Changing Arctic Ocean programme, jointly funded by the UK Natural Environment Research Council (NERC) and the German Federal Ministry of Education and Research (BMBF). JE was funded by the national scholarships "Promotionsstipendium nach dem Hamburger Nachwuchsfördergesetz (HmbNFG)" and

"Gleichstellungsfond 2017 (4-GLF-2017)", both granted by the University of Hamburg.

ACKNOWLEDGMENTS

We thank Captain Uwe Pahl, Captain Stefan Schwarze, Captain Thomas Wunderlich, and the crews of the RV Polarstern. We thank the scientific cruise leaders Antje Boetius (PS80), Bettina Meyer (PS81), Olaf Boebel (PS89), IP (PS92), and Andreas Macke and HF (PS106) for their excellent support and guidance with work at sea. We thank Jan Andries van Franeker (WUR) for kindly providing the Surface and Under-Ice Trawl (SUIT) and Michiel van Dorssen for technical support. The sampling with the SUIT, and on the ice, would have not been possible without the help of many volunteers during each expedition.

SUPPLEMENTARY MATERIAL

The Supplementary Material for this article can be found online at: https://www.frontiersin.org/articles/10.3389/fmars.2020.00536/full#supplementary-material

REFERENCES

Arndt, S., Meiners, K. M., Ricker, R., Krumpen, T., Katlein, C., and Nicolaus, M. (2017). Influence of snow depth and surface flooding on light transmission through Antarctic pack ice. *J. Geophys. Res. Oceans* 122, 2108–2119. doi: 10.1002/2016JC012325

Arndt, S., and Nicolaus, M. (2014). Seasonal cycle and long-term trend of solar energy fluxes through Arctic sea ice. *Cryosphere* 8, 2219–2233. doi: 10.5194/tc-8-2219-2014

Arrigo, K. R. (2014). Sea ice ecosystems. *Annu. Rev. Mar. Sci.* 6, 439–467. doi: 10.1146/annurev-marine-010213-135103

Arrigo, K. R., Perovich, D. K., Pickart, R. S., Brown, Z. W., van Dijken, G. L., Lowry, K. E., et al. (2012). Massive phytoplankton blooms under Arctic sea ice. *Science* 336, 1408–1408. doi: 10.1126/science.1215065

Assmy P., Fernández-Méndez, M., Duarte P., Meyer A., Randelhoff A., Mundy C. J., et al. (2017). Leads in Arctic pack ice enable early phytoplankton blooms below snow-covered sea ice. *Sci. Rep.* 7:40850. doi: 10.1038/srep40850

Beuchel, F., and Lønne, O. (2002). Population dynamics of the sympagic amphipods *Gammarus wilkitzkii* and *Apherusa glacialis* in sea ice north of Svalbard. *Polar Biol.* 25, 241–250. doi: 10.1007/s00300-001-0329-8

Boebel, O. (2015). *The Expedition PS89 of the Research Vessel POLARSTERN to the Weddell Sea in 2014/2015*. Berichte zur Polar- und Meeresforschung. Reports on Polar and Marine Research, 689.

Boetius, A. (2013). *The Expedition of the Research Vessel "Polarstern" to the Arctic in 2012 (ARK-XXVII/3)*. Berichte zur Polar- und Meeresforschung. Reports on Polar and Marine Research, 663.

Boetius, A., Albrecht, S., Bakker, K., Bienhold, C., Felden, J., Fernández-Méndez, M., et al. (2013). Export of algal biomass from the melting Arctic sea ice. *Science* 339, 1430–1432. doi: 10.1126/science.1231346

Brierley, A., and Thomas, D. N. (2002). Ecology of southern ocean pack ice. *Adv. Mar. Biol.* 43, 171–276. doi: 10.1016/S0065-2881(02)43005-2

Budge, S. M., Wooller, M. J., Springer, A. M., Iverson, S. J., McRoy, C. P., and Divoky, G. J. (2008). Tracing carbon flow in an Arctic marine food web using fatty acid-stable isotope analysis. *Oecologia* 157, 117–129. doi: 10.1007/s00442-008-1053-7

Carey, A. (1985). "Marine ice fauna: arctic," in *Sea Ice Biota*, ed. R. A. Horner (Boca Raton, FL: CRC Press), 173–190. doi: 10.1201/9781351076548-8

Castellani, G., Gerdes, R., Losch, M., and Lüpkes, C. (2015). "Impact of sea-ice bottom topography on the Ekman pumping," in *Towards an Interdisciplinary Approach in Earth System Science, Springer Earth System Sciences*, eds G. Lohmann, H. Meggers, V. Unnithan, D. Wolf-Gladrow, J. Notholt, and A. Bracher (Cham: Springer International Publishing), 139–148. doi: 10.1007/978-3-319-13865-7_16

Castellani, G., Losch, M., Lange, B. A., and Flores, H. (2017). Modeling Arctic sea-ice algae: Physical drivers of spatial distribution and algae phenology. *J. Geophys. Res. Oceans* 122, 7466–7487. doi: 10.1002/2017JC012828

Castellani, G., Lüpkes, C., Hendricks, S., and Gerdes, R. (2014). Variability of Arctic sea ice topography and its impact on the atmospheric surface drag. *J. Geophys. Res. Oceans* 119, 6743–6762. doi: 10.1002/2013JC009712

David, C., Lange, B., Rabe, B., and Flores, H. (2015). Community structure of under-ice fauna in the Eurasian central Arctic Ocean in relation to environmental properties of sea-ice habitats. *Mar. Ecol. Prog. Ser.* 522, 15–32. doi: 10.3354/meps11156

David, C., Lange, B. A., Krumpen, T., Schaafsma, F. L., van Franeker, J. A., and Flores, H. (2016). Under-ice distribution of polar cod *Boreogadus saida* in the central Arctic Ocean and their association with sea-ice habitat properties. *Polar Biol.* 39, 981–994. doi: 10.1007/s00300-015-1774-0

David, C., Schaafsma, F. L., van Franeker, J. A., Lange, B. A., Brandt, A., and Flores, H. (2017). Community structure of under-ice fauna in relation to winter sea-ice habitat properties from the Weddell Sea. *Polar Biol.* 40, 247–261. doi: 10.1007/s00300-016-1948-4

Dethloff, K., Handorf, D., Jaiser, R., Rinke, A., and Klinghammer, P. (2019). Dynamical mechanisms of Arctic amplification. *Ann. N. Y. Acad. Sci.* 1436, 184–194. doi: 10.1111/nyas.13698

Ehrlich, J., Schaafsma, F. L., Bluhm, B. A., Peeken, I., Castellani, G., Brandt, A., et al. (2020). Sympagic fauna in- and under arctic pack ice in the annual sea-ice system of the new arctic. *Front. Mar. Sci.* 7:452. doi: 10.3389/fmars.2020.00452

Eicken, H. (1992). The role of sea ice in structuring Antarctic ecosystems. *Polar Biol.* 12, 3–13. doi: 10.1007/BF00239960

Eicken, H. (2003). "Chapter 2: From the microscopic, to the macroscopic, to the regional scale: growth, microstructure and properties of sea ice," in *Sea Ice: An Introduction to its Physics, Chemistry, Biology and Geology*, eds D. N. Thomas and G. S. Dieckmann (Blackwell Science Ltd.), 22–81. doi: 10.1002/9780470757161.ch2

EUMETSAT (Ocean and Sea Ice Satellite Application Facility, 2011). *Ocean and Sea Ice Satellite Application Facility (2011), Global Sea Ice Concentration Reprocessing Dataset 1978-2009 (v1.1)*.

Fernández-Méndez, M., Katlein, C., Rabe, B., Nicolaus, M., Peeken, I., Bakker, K., et al. (2015). Photosynthetic production in the central Arctic Ocean during the record sea-ice minimum in 2012. *Biogeosciences* 12, 3525–3549. doi: 10.5194/bg-12-3525-2015

Ferrari, R., Jansen, M. F., Adkins, J. F., Burke, A., Stewart, A. L., and Thompson, A. F. (2014). Antarctic sea ice control on ocean circulation in present and glacial climates. *Proc. Natl. Acad. Sci. U.S.A.* 111, 8753–8758. doi: 10.1073/pnas.1323922111

Flores, H., David, C., Ehrlich, J., Hardge, K., Kohlbach, D., Lange, B. A., et al. (2019). Sea-ice properties and nutrient concentration as drivers of the taxonomic and trophic structure of high-Arctic protist and metazoan communities. *Polar Biol.* 42, 1377–1395. doi: 10.1007/s00300-019-02526-z

Flores, H., Hunt, B. P., Kruse, S., Pakhomov, E. A., Siegel, V., van Franeker, J. A., et al. (2014). Seasonal changes in the vertical distribution and community structure of Antarctic macrozooplankton and micronekton. *Deep Sea Res. I Oceanogr. Res. Pap.* 84, 127–141. doi: 10.1016/j.dsr.2013.11.001

Flores, H., van Franeker, J. A., Cisewski, B., Leach, H., Van de Putte, A. P., Meesters, E. H., et al. (2011). Macrofauna under sea ice and in the open surface layer of the Lazarev Sea, Southern Ocean. *Deep Sea Res. II Top. Stud. Oceanogr.* 58, 1948–1961. doi: 10.1016/j.dsr2.2011.01.010

Flores, H., van Franeker, J. A., Siegel, V., Haraldsson, M., Strass, V., Meesters, E. H., et al. (2012). The association of Antarctic krill *Euphausia superba*

with the under-ice habitat. *PLoS ONE* 7:e31775. doi: 10.1371/journal.pone.0031775

Fofonoff, N. P. (1985). Physical properties of seawater: a new salinity scale and equation of state for seawater. *J. Geophys. Res. Oceans* 90, 3332–3342. doi: 10.1029/JC090iC02p03332

Garrison, D., and Close, A. (1993). Winter ecology of the sea ice biota in Weddell Sea pack ice. *Mar. Ecol. Prog. Ser*. 96, 17–31. doi: 10.3354/meps096017

Garrison, D. L. (2015). Antarctic sea ice biota. *Integr. Comp. Biol*. 31, 17–34. doi: 10.1093/icb/31.1.17

Giraudoux, P. (2018). *pgirmess: Spatial Analysis and Data Mining for Field Ecologists*. R package version 1.6.9.

Gosselin, M., Legendre, L., Therriault, J.-C., Demers, S., and Rochet, M. (1986). Physical control of the horizontal parchiness of sea-ice microalgae. *Mar. Ecol. Prog. Ser*. 29, 289–298. doi: 10.3354/meps029289

Gradinger, R. (1999). Integrated abundance and biomass of sympagic meiofauna in Arctic and Antarctic pack ice. *Polar Biol*. 22, 169–177. doi: 10.1007/s003000050407

Gradinger, R., Bluhm, B., and Iken, K. (2010). Arctic sea-ice ridges–Safe heavens for sea-ice fauna during periods of extreme ice melt? *Deep Sea Res. II Top. Stud. Oceanogr*. 57, 86–95. doi: 10.1016/j.dsr2.2009.08.008

Grainger, E. H., and Hsiao, S. I. C. (1990). Trophic relationships of the sea ice meiofauna in Frobisher Bay, Arctic Canada. *Polar Biol*. 10, 283–292. doi: 10.1007/BF00238427

Granskog, M., Kaartokallio, H., Kuosa, H., Thomas, D., Ehn, J., and Sonninen, E. (2005). Scales of horizontal patchiness in chlorophyll a, chemical and physical properties of landfast sea ice in the gulf of Finland (Baltic sea). *Polar Biol*. 28, 276–283. doi: 10.1007/s00300-004-0690-5

Grenfell, T. C., and Maykut, G. A. (1977). The optical properties of ice and snow in the Arctic basin. *J. Glaciol*. 18, 445–463. doi: 10.1017/S0022143000021122

Gruzov, Y., Propp, M., and Pushkin, A. (1967). Biological associations of coastal areas of the Davis Sea (based on the observations of divers). *Sov. Antarct. Exped. Inf. Bull*. 6, 523–533.

Guerreiro, K., Fleury, S., Zakharova, E., Rémy, F., and Kouraev, A. (2016). Potential for estimation of snow depth on arctic sea ice from cryosat-2 and Saral/Altika missions. *Remote Sens. Environ*. 186, 339–349. doi: 10.1016/j.rse.2016.07.013

Haas, C. (2008). "Chapter 3: Dynamics versus thermodynamics: the sea ice thickness distribution," in *Sea Ice: An Introduction to its Physics, Chemistry, Biology and Geology*, eds D. N. Thomas and G. S. Dieckmann (John Wiley & Sons, Ltd.), 82–111. doi: 10.1002/9780470757161.ch3

Haas, C., Lobach, J., Hendricks, S., Rabenstein, L., and Pfaffling, A. (2009). Helicopter-borne measurements of sea ice thickness, using a small and lightweight, digital EM system. *J. Appl. Geophys*. 67, 234–241. doi: 10.1016/j.jappgeo.2008.05.005

Ivanova, N., Johannessen, O. M., Pedersen, L. T., IEEE-Members, and Tonboe, R. T. (2014). Retrieval of arctic sea ice parameters by satellite passive microwave sensors: a comparison of eleven sea ice concentration algorithms. *IEEE Trans. Geosci. Remote Sens*. 52, 7233–7246. doi: 10.1109/TGRS.2014.2310136

Jia, Z., Swadling, K. M., Meiners, K. M., Kawaguchi, S., and Virtue, P. (2016). The zooplankton food web under East Antarctic pack ice-A stable isotope study. *Deep Sea Res. II Top. Stud. Oceanogr*. 131, 189–202. doi: 10.1016/j.dsr2.2015.10.010

Katlein, C., Arndt, S., Belter, H. J., Castellani, G., and Nicolaus, M. (2019). Seasonal evolution of light transmission distributions through Arctic sea ice. *J. Geophys. Res. Oceans*. 124, 5418–5435. doi: 10.1029/2018JC014833

Katlein, C., Arndt, S., Nicolaus, M., Perovich, D. K., Jakuba, M. V., Suman, S., et al. (2015). Influence of ice thickness and surface properties on light transmission through Arctic sea ice. *J. Geophys. Res. Oceans* 120, 5932–5944. doi: 10.1002/2015JC010914

Katlein, C., Perovich, D. K., and Nicolaus, M. (2016). Geometric effects of an inhomogeneous sea ice cover on the under ice light field. *Front. Earth Sci*. 4:6. doi: 10.3389/feart.2016.00006

Katlein, C., Schiller, M., Belter, H. J., Coppolaro, V., Wenslandt, D., and Nicolaus, M. (2017). A new remotely operated sensor platform for interdisciplinary observations under sea ice. *Front. Mar. Sci*. 4:281. doi: 10.3389/fmars.2017.00281

Kohlbach, D., Graeve, M., Lange, B. A., David, C., Peeken, I., and Flores, H. (2016). The importance of ice algae-produced carbon in the central Arctic Ocean ecosystem: food web relationships revealed by lipid and stable isotope analyses. *Limnol. Oceanogr*. 61, 2027–2044. doi: 10.1002/lno.10351

Kohlbach, D., Graeve, M., Lange, B. A., David, C., Schaafsma, F. L., van Franeker, J. A., et al. (2018). Dependency of Antarctic zooplankton species on ice algae-produced carbon suggests a sea ice-driven pelagic ecosystem during winter. *Glob. Change Biol*. 24, 4667–4681. doi: 10.1111/gcb.14392

Kohlbach, D., Lange, B. A., Graeve, M., Vortkamp, M., and Flores, H. (2019). Varying dependency of Antarctic euphausiids on ice algae- and phytoplankton-derived carbon sources during summer. *Mar. Biol*. 166:79. doi: 10.1007/s00227-019-3527-z

Kohlbach, D., Lange, B. A., Schaafsma, F. L., David, C., Vortkamp, M., Graeve, M., et al. (2017b). Ice algae-produced carbon is critical for overwintering of antarctic krill *Euphausia superba*. *Front. Mar. Sci*. 4:310. doi: 10.3389/fmars.2017.00310

Kohlbach, D., Schaafsma, F. L., Graeve, M., Lebreton, B., Lange, B. A., David, C., et al. (2017a). Strong linkage of polar cod (Boreogadus saida) to sea ice algae-produced carbon: evidence from stomach content, fatty acid and stable isotope analyses. *Prog. Oceanogr*. 152, 62–74. doi: 10.1016/j.pocean.2017.02.003

Kwok, R., Pang, S. S., and Kacimi, S. (2017). Sea ice drift in the Southern Ocean: regional patterns, variability, and trends. *Elem. Sci. Anth*. 5:32. doi: 10.1525/elementa.226

Laliberté, J., Bélanger, S., and Frouin, R. (2016). Evaluation of satellite-based algorithms to estimate photosynthetically available radiation (PAR) reaching the ocean surface at high northern latitudes. *Remote Sens. Environ*. 184, 199–211. doi: 10.1016/j.rse.2016.06.014

Lange, B. A. (2017). *Spatial variability of Arctic sea ice algae* (Ph.D. thesis). University of Hamburg, Hamburg, Germany. Available online at: http://ediss.sub.uni-hamburg.de/volltexte/2017/8460

Lange, B. A., Beckers, J. F., Casey, J. A., and Haas, C. (2019). Airborne observations of summer thinning of multiyear sea ice originating from the Lincoln sea. *J. Geophys. Res. Oceans* 124, 243–266. doi: 10.1029/2018JC014383

Lange, B. A., Flores, H., Michel, C., Beckers, J. F., Bublitz, A., Casey, J. A., et al. (2017a). Pan-Arctic sea ice-algal chl *a* biomass and suitable habitat are largely underestimated for multiyear ice. *Glob. Change Biol*. 23, 4581–4597. doi: 10.1111/gcb.13742

Lange, B. A., Katlein, C., Castellani, G., Fernández-Méndez, M., Nicolaus, M., Peeken, I., et al. (2017b). Characterizing spatial variability of ice algal chlorophyll a and net primary production between sea ice habitats using horizontal profiling platforms. *Front. Mar. Sci*. 4:349. doi: 10.3389/fmars.2017.00349

Lange, B. A., Katlein, C., Nicolaus, M., Peeken, I., and Flores, H. (2016). Sea ice algae chlorophyll *a* concentrations derived from under-ice spectral radiation profiling platforms. *J. Geophys. Res. Oceans*. 121, 8511–8534. doi: 10.1002/2016JC011991

Legendre, L., and Gosselin, M. (1991). In situ spectroradiometric estimation of microalgal biomass in first-year sea ice. *Polar Biol*. 11, 113–115. doi: 10.1007/BF00234273

Legendre, P., and Fortin, M. J. (1989). Spatial pattern and ecological analysis. *Vegetatio* 80, 107–138. doi: 10.1007/BF00048036

Legendre, P., and Legendre, L. (1998). "Spatial analysis," in *Numerical Ecology*, eds P. Legendre and L. Legendre (Amsterdam, BV: Elsevier Science), 707–786.

Light, B., Grenfell, T. C., and Perovich, D. K. (2008). Transmission and absorption of solar radiation by Arctic sea ice during the melt season. *J. Geophys. Res. Oceans* 113:C03023. doi: 10.1029/2006JC003977

Liu, Z. (2012). Dynamics of interdecadal climate variability: a historical perspective. *J. Clim*. 25, 1963–1995. doi: 10.1175/2011JCLI3980.1

Macke, A., and Flores, H. (2018). *The Expeditions PS106/1 and 2 of the Research Vessel POLARSTERN to the Arctic Ocean in 2017*. Berichte zur Polar- und Meeresforschung. Reports on Polar and Marine Research, 719.

Massicotte, P., Peeken, I., Katlein, C., Flores, H., Huot, Y., Castellani, G., et al. (2019). Sensitivity of phytoplankton primary production estimates to available irradiance under heterogeneous sea-ice conditions. *J. Geophys. Res. Oceans*. 124, 5436–5450. doi: 10.1029/2019JC015007

Massom, R. A., and Stammerjohn, S. E. (2010). Antarctic sea ice change and variability-physical and ecological implications. *Polar Sci.* 4, 149–186. doi: 10.1016/j.polar.2010.05.001

Maykut, G. A., and Grenfell, T. C. (1975). The spectral distribution of light beneath first-year sea ice in the Arctic Ocean. *Limnol. Oceanogr.* 20, 554–563. doi: 10.4319/lo.1975.20.4.0554

McMinn, A., Pankowskii, A., Ashworth, C., Bhagooli, R., Ralph, P., and Ryan, K. (2010). In situ net primary productivity and photosynthesis of Antarctic sea ice algal, phytoplankton and benthic algal communities. *Mar. Biol.* 157, 1345–1356. doi: 10.1007/s00227-010-1414-8

Meiners, K. M., Arndt, S., Bestley, S., Krumpen, T., Ricker, R., Milnes, M., et al. (2017). Antarctic pack ice algal distribution: Floe-scale spatial variability and predictability from physical parameters. *Geophys. Res. Lett.* 44, 7382–7390. 2017GL074346. doi: 10.1002/2017GL074346

Meiners, K. M., Vancoppenolle, M., Thanassekos, S., Dieckmann, G. S., Thomas, D. N., Tison, J.-L., et al. (2012). Chlorophyll *a* in Antarctic sea ice from historical ice core data. *Geophys. Res. Lett.* 39:L21602. doi: 10.1029/2012GL053478

Melbourne-Thomas, J., Meiners, K. M., Mundy, C. J., Schallenberg, C., Tattersall, K. L., and Dieckmann, G. S. (2015). Algorithms to estimate Antarctic sea ice algal biomass from under-ice irradiance spectra at regional scales. *Mar. Ecol. Prog. Ser.* 536, 107–121. 10.3354/meps11396. doi: 10.3354/meps11396

Meyer A., Sundfjord, A., Fer, I., Provost, C., Villacieros Robineau, N., Koenig, Z., et al. (2017). Winter to summer oceanographic observations in the Arctic Ocean north of Svalbard. *J. Geophys. Res. Oceans* 122, 6218–6237. doi: 10.1002/2016JC012391

Meyer B., Freier U., Grimm V., Groeneveld J., Hunt B. P. V., Kerwath S., et al. (2017). The winter pack-ice zone provides a sheltered but food-poor habitat for larval Antarctic krill. *Nat. Ecol. Evol.* 1, 1853–1861. doi: 10.1038/s41559-017-0368-3

Meyer, B., and Auerswald, L. (2014). *The Expedition of the Research Vessel "Polarstern" to the Antarctic in 2013 (ANT-XXIX/7)*. Berichte zur Polar- und Meeresforschung. Reports on Polar and Marine Research, 674.

Miller, L., Fripiat, F., Else, B., Bowman, J., Brown, K., Collins, R., et al. (2015). Methods for biogeochemical studies of sea ice: the state of the art, caveats, and recommendations. *Elem. Sci. Anth.* 3:000038. doi: 10.12952/journal.elementa.000038

Moran, P. A. P. (1950). Notes on continuous stochastic phenomena. *Biometrika* 37, 17–23. doi: 10.1093/biomet/37.1-2.17

Mundy, C. J., Ehn, J. K., Barber, D. G., and Michel, C. (2007). Influence of snow cover and algae on the spectral dependence of transmitted irradiance through Arctic landfast first-year sea ice. *J. Geophys. Res. Oceans* 112:C03007. doi: 10.1029/2006JC003683

Nicolaus, M., Gerland, S., Hudson, S. R., Hanson, S., Haapala, J., and Perovich, D. K. (2010). Seasonality of spectral albedo and transmittance as observed in the Arctic Transpolar Drift in 2007. *J. Geophys. Res. Oceans* 115:C11011. doi: 10.1029/2009JC006074

Nicolaus, M., and Katlein, C. (2013). Mapping radiation transfer through sea ice using a remotely operated vehicle (ROV). *Cryosphere* 7, 763–777. doi: 10.5194/tc-7-763-2013

Nicolaus, M., Katlein, C., Maslanik, J. A., and Hendricks, S. (2012). Changes in Arctic sea ice result in increasing light transmittance and absorption. *Geophys. Res. Lett.* 39, 2699–2700. doi: 10.1029/2012GL053738

Nozais, C., Gosselin, M., Michel, C., and Tita, G. (2001). Abundance, biomass, composition and grazing impact of the sea-ice meiofauna in the North Water, northern Baffin Bay. *Mar. Ecol. Prog. Ser.* 217, 235–250. 10.3354/meps217235. doi: 10.3354/meps217235

Oksanen, J., Blanchett, F., Kindt, R., Legendre, P., Minchin, P., O'Hara, R., et al. (2013). *Vegan: Community Ecology Package Version 2.0-10*.

Peeken, I. (2016). *The Expedition PS92 of the Research Vessel POLARSTERN to the Arctic Ocean in 2015*. Berichte zur Polar- und Meeresforschung. Reports on Polar and Marine Research, 694.

Perovich, D. K. (1990). Theoretical estimates of light reflection and transmission by spatially complex and temporally varying sea ice covers. *J. Geophys. Res. Oceans* 95, 9557–9567. doi: 10.1029/JC095iC06p09557

Perovich, D. K. (1996). *The optical properties of sea ice* (Ph.D. thesis). U.S. Army Cold Regions Research and Engineering Laboratory, Hanover, NH, United States.

Poltermann, M. (1998). Abundance, biomass and small-scale distribution of cryopelagic amphipods in the Franz Josef Land area (Arctic). *Polar Biol.* 20, 134–138. doi: 10.1007/s003000050287

Rabenstein, L., Hendricks, S., Martin, T., Pfaffhuber, A., and Haas, C. (2010). Thickness and surface-properties of different sea-ice regimes within the Arctic Trans Polar Drift: data from summers 2001, 2004 and 2007. *J. Geophys. Res.* 115:C12059. doi: 10.1029/2009JC005846

R-Development-Core-Team (2018). *R: A Language and Environment for Statistical Computing*.

Ricchiazzi, P., Yang, S., Gautier, C., and Sowle, D. (1998). SBDART: a research and teaching software tool for plane-parallel radiative transfer in the Earth's atmosphere. *Bull. Am. Meteorol. Soc.* 79, 2101–2114. doi: 10.1175/1520-0477(1998)079<2101:SARATS>2.0.CO;2

Ricker, R., Hendricks, S., Perovich, D. K., Helm, V., and Gerdes, R. (2015). Impact of snow accumulation on CryoSat-2 range retrievals over Arctic sea ice: an observational approach with buoy data. *Geophys. Res. Lett.* 42, 4447–4455. doi: 10.1002/2015GL064081

Runge, J. A., and Ingram, R. G. (1991). Under-ice feeding and diel migration by the planktonic copepods *Calanus glacialis* and *Pseudocalanus minutus* in relation to the ice algal production cycle in southeastern Hudson Bay, Canada. *Mar. Biol.* 108, 217–225. doi: 10.1007/BF01344336

Rysgaard, S., Kuhl, M., Glud, R., and Hansen, J. (2001). Biomass, production and horizontal patchiness of sea ice algae in a high-arctic fjord (young sound, NE Greenland). *Mar. Ecol. Prog. Ser.* 223, 15–26. doi: 10.3354/meps223015

Schaafsma, F., Kohlbach, D., David, C., Lange, B. A., Graeve, M., Flores, H., and van Franeker, J. A. (2017). Spatio-temporal variability in the winter diet of larval and juvenile Antarctic krill, *Euphausia superba*, in ice-covered waters. *Mar. Ecol. Prog. Ser.* 580, 101–115. doi: 10.3354/meps12309

Schaafsma, F. L. (2018). *Life in the polar oceans: the role of sea ice in the biology and ecology of marine species* (Ph.D. thesis). Wageningen University, Wageningen, Netherlands.

Schaafsma, F. L., David, C., Pakhomov, E. A., Hunt, B. P. V., Lange, B. A., Flores, H., et al. (2016). Size and stage composition of age class 0 Antarctic krill *Euphausia superba* in the ice-water interface layer during winter/early spring. *Polar Biol.* 39, 1515–1526. doi: 10.1007/s00300-015-1877-7

Schmitz, W. J. Jr. (1995). On the interbasin-scale thermohaline circulation. *Rev. Geophys.* 33, 151–173. doi: 10.1029/95RG00879

Søgaard, D., Kristensen, M., Rysgaard, S., Glud, R., Hansen, P., and Hilligsøe, K. (2010). Autotrophic and heterotrophic activity in arctic first-year sea ice: seasonal study from Malene Bight, SW Greenland. *Mar. Ecol. Prog. Ser.* 419, 31–45. doi: 10.3354/meps08845

Søreide, J. E., Hop, H., Carroll, M. L., Falk-Petersen, S., and Hegseth, E. N. (2006). Seasonal food web structures and sympagic-pelagic coupling in the European arctic revealed by stable isotopes and a two-source food web model. *Prog. Oceanogr.* 71, 59–87. doi: 10.1016/j.pocean.2006.06.001

Swadling, K. M., Gibson, J. A. E., Ritz, D. A., Nichols, P. D., and Hughes, D. E. (1997). Grazing of phytoplankton by copepods in eastern Antarctic coastal waters. *Mar. Biol.* 128, 39–48. doi: 10.1007/s002270050066

Tran, S., Bonsang, B., Gros, V., Peeken, I., Sarda-Esteve, R., Bernhardt, A., et al. (2013). A survey of carbon monoxide and non-methane hydrocarbons in the Arctic Ocean during summer 2010. *Biogeosciences* 10, 1909–1935. doi: 10.5194/bg-10-1909-2013

Ugalde, S. C., Westwood, K. J., van den Enden, R., McMinn, A., and Meiners, K. M. (2016). Characteristics and primary productivity of East Antarctic pack ice during the winter-spring transition. *Deep Sea Res. II Top. Stud. Oceanogr.* 131, 123–139. doi: 10.1016/j.dsr2.2015.12.013

van Franeker, J. A., Flores, H., and van Dorssen, M. (2009). *The surface and under ice trawl (SUIT)* (Ph.D. thesis). University of Groningen, Groningen, Netherlands.

Wang, S. W., Budge, S. M., Iken, K., Gradinger, R., Springer, A. M., and Wooller, M. J. (2015). Importance of sympagic production to Bering Sea zooplankton as revealed from fatty acid-carbon stable isotope analyses. *Mar. Ecol. Prog. Ser.* 518, 31–50. doi: 10.3354/meps11076

Wang, S. W., Springer, A. M., Budge, S. M., Horstmann, L., Quakenbush, L. T., and Wooller, M. J. (2016). Carbon sources and trophic relationships of ice seals during recent environmental shifts in the Bering Sea. *Ecol. Appl.* 26, 830–845. doi: 10.1890/14-2421

Webster M., Gerland S., Holland M., Hunke E., Kwok R., Lecomte O., et al. (2018). Snow in the changing sea-ice systems. *Nat. Clim. Change* 8, 946–953. doi: 10.1038/s41558-018-0286-7

Wongpan, P., Meiners, K. M., Langhorne, P. J., Heil, P., Smith, I. J., Leonard, G. H., et al. (2018). Estimation of Antarctic land-fast sea ice algal biomass and snow thickness from under-ice radiance spectra in two contrasting areas. *J. Geophys. Res. Oceans* 123, 1907–1923. doi: 10.1002/2017JC013711

Conflict of Interest: The authors declare that the research was conducted in the absence of any commercial or financial relationships that could be construed as a potential conflict of interest.

Supplement: Large-Scale Variability of Physical and Biological Sea-Ice Properties in Polar Oceans

Giulia Castellani[1,*], Fokje L. Schaafsma[2] , Benjamin A. Lange[1, 3], Stefanie Arndt[1] , Ilka Peeken[1], Julia Ehrlich[1,4], Carmen David[5], Thomas Krumpen[1], Stefan Hendricks[1], Robert Ricker[1], Sandra Schwegmann[6], Philippe Massicotte[7], and Hauke Flores[1]

[1] *Alfred Wegener Institute Helmholtz-Zentrum für Polar- und Meeresforschung, Am Handelshafen 12, 27568 Bremerhaven, Germany*
[2] *Wageningen Marine Research, Ankerpark 27, 1781 AG Den Helder, The Netherlands*
[3] *Norwegian Polar Institute, Fram Centre, Tromsø, Norway*
[4] *University of Hamburg, Hamburg, Germany*
[5] *Department of Biology, Dalhousie University, Halifax, B3H 4R2, Canada*
[6] *Bundesamt für Seeschifffahrt und Hydrographie, Neptunallee 5, 18055 Rostock, Germany*
[7] *Takuvik Joint International Laboratory (UMI 3376) Université Laval (Canada) Centre National de la Recherche Scientifique (France) Québec-Océan / Pavillon Alexandre-Vachon Université Laval, Québec, Canada*

**Correspondence: Giulia Castellani (giulia.castellani@awi.de)*

Handling data gaps

Sensor malfunction

Gaps in the data occurred due to sensor failure or damage during hauls. During PS81 low temperatures caused battery failure of the CTD during some of the hauls. Gaps for salinity and temperature have been filled by linear regression with the sensors mounted on the ship (*David et al., 2017*). This was the case of stations 557_1 and 560_2. During PS89 stations 62_1, 70_2, and 71_1 the altimeter did not work, so draft has been calculated using equation (2) from the main article:

$$d = h_w - (h_a - h_{CTD}),$$

were depth h_w given by the pressure sensor of the CTD, h_{CTD} is the distance between CTD and altimeter and the value of h_a = 0.33 m is given by the altimeter mode retrieved from the other stations. During PS92 station 32_12 (not used in the present analysis) the SUIT ran into a big ridge and the ADCP was damaged. For the following stations, the ADCP was replaced with an older version of the same sensor that has no pitch and roll information. To retrieve the ice draft we used equation (2) from the main article, where h_a is the altimeter mode (h_a = 0.36 m) calculated from the altimeter values of all the PS92 profiles.

Radiation values

During September 2012 (PS80) the sensor mounted on the crow's nest did not measure, so we do not have incoming irradiance data for the calculation of transmittance. To fill this data gap, we used short-wave downward (GLOBAL) radiation measured with the ship sensors (artificially ventilated pyranometer), which is also placed at the level of the crow's nest. To assess the accuracy of the ship sensors we compared the transmittance calculated in August from the crown nest with this new data set and found an excellent agreement between both (r^2 = 0.94). We thus used the ships data for further calculation of transmittance as the ratio between under-ice and incoming radiation.

Supplementary table

Table S1. Summary of the measured and derived variables.

Variable	Units	Description	Sensor	Sampling interval	Final spatial resolution
T	°C	Under-ice temperature	CTD	0.1 s	0.5 m
S		Under-ice salinity	CTD	0.1 s	0.5 m
chl a_w	mg chl *a* m^{-2}	Under-ice chlorophyll *a*	Fluorometer mounted on the CTD	0.1 s	0.5 m
H_i	m	Total thickness (ice + snow)	Combined CTD and ADCP information	1 s (ADCP)	0.5 m
H_s	cm	Snow depth	Visual observation	-	-
TR		Transmittance	RAMSES spectral radiometers	11 s	~20* m
S_i	mol photons m^{-2} d^{-1}	Insolation	Combined transmittance and modelled downwelling radiation	11 s	~20* m
In-ice chl *a*	mg chl *a* m^{-2}	In-ice chlorophyll *a*	Retrieved from under-ice irradiance or radiance	11 s	~20* m

* Depending on the speed of the SUIT

Supplementary Figures

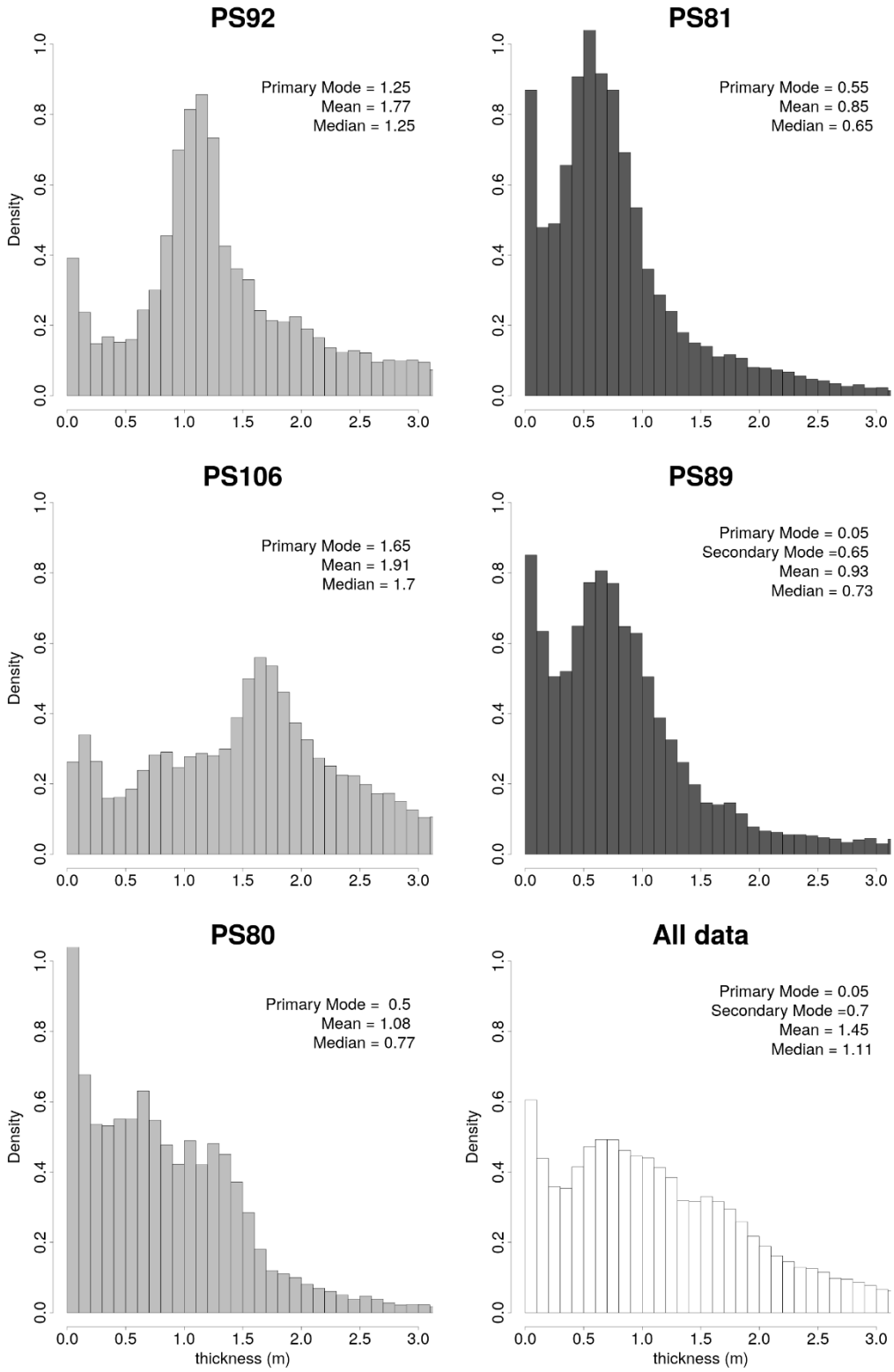

Figure S1. Histograms of ice thickness retrieved from the SUIT sensors array for all the expeditions. Data are filtered for open water. Histogram bins at 0.1 m. Arctic expeditions are highlighted with light grey bars and Antarctic expeditions with dark grey bars.

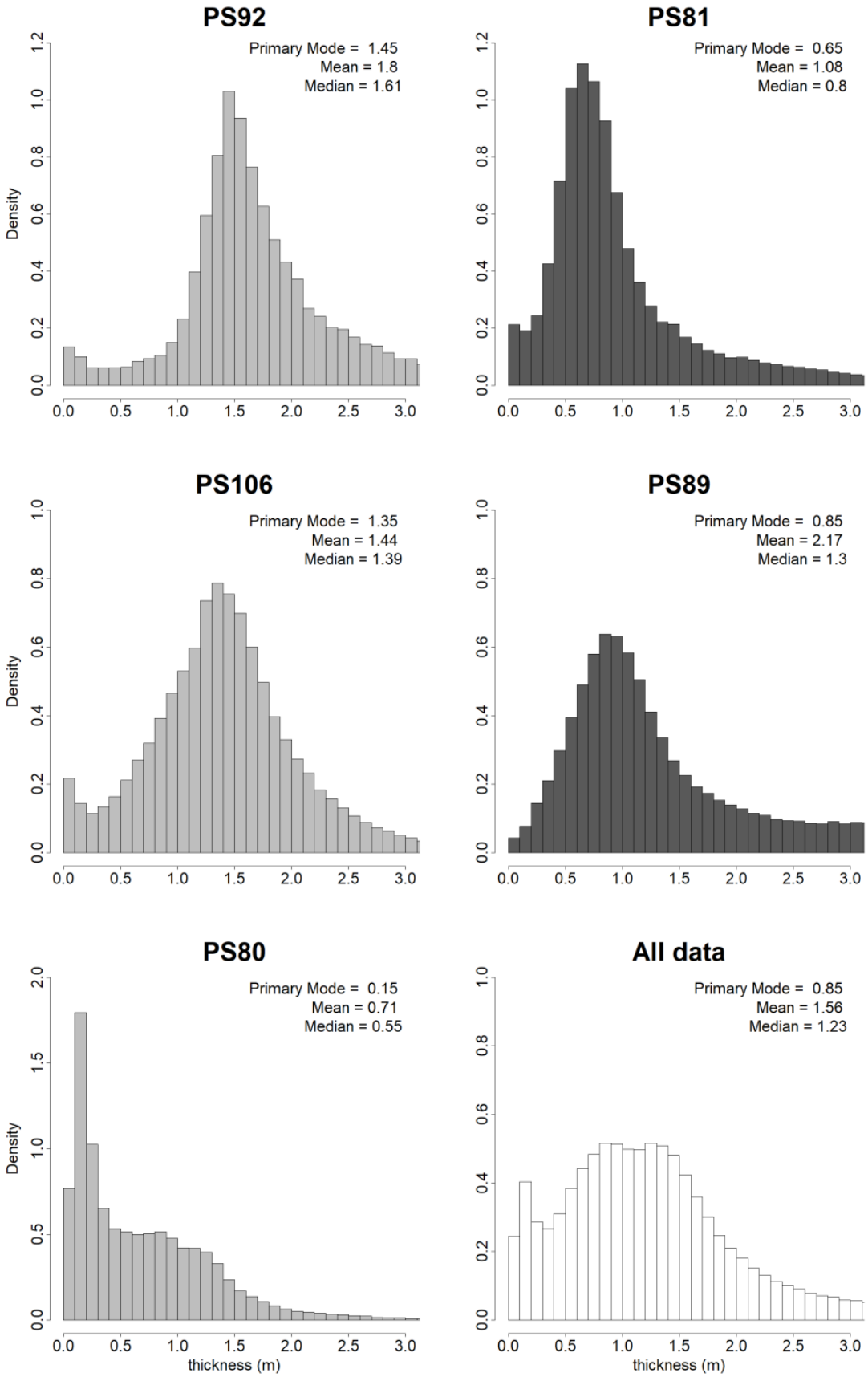

Figure S2. Histograms of ice thickness retrieved from the EM-bird measurements. Histogram bins at 0.1 m. Arctic expeditions are highlighted with light grey bars and Antarctic expeditions with dark grey bars.

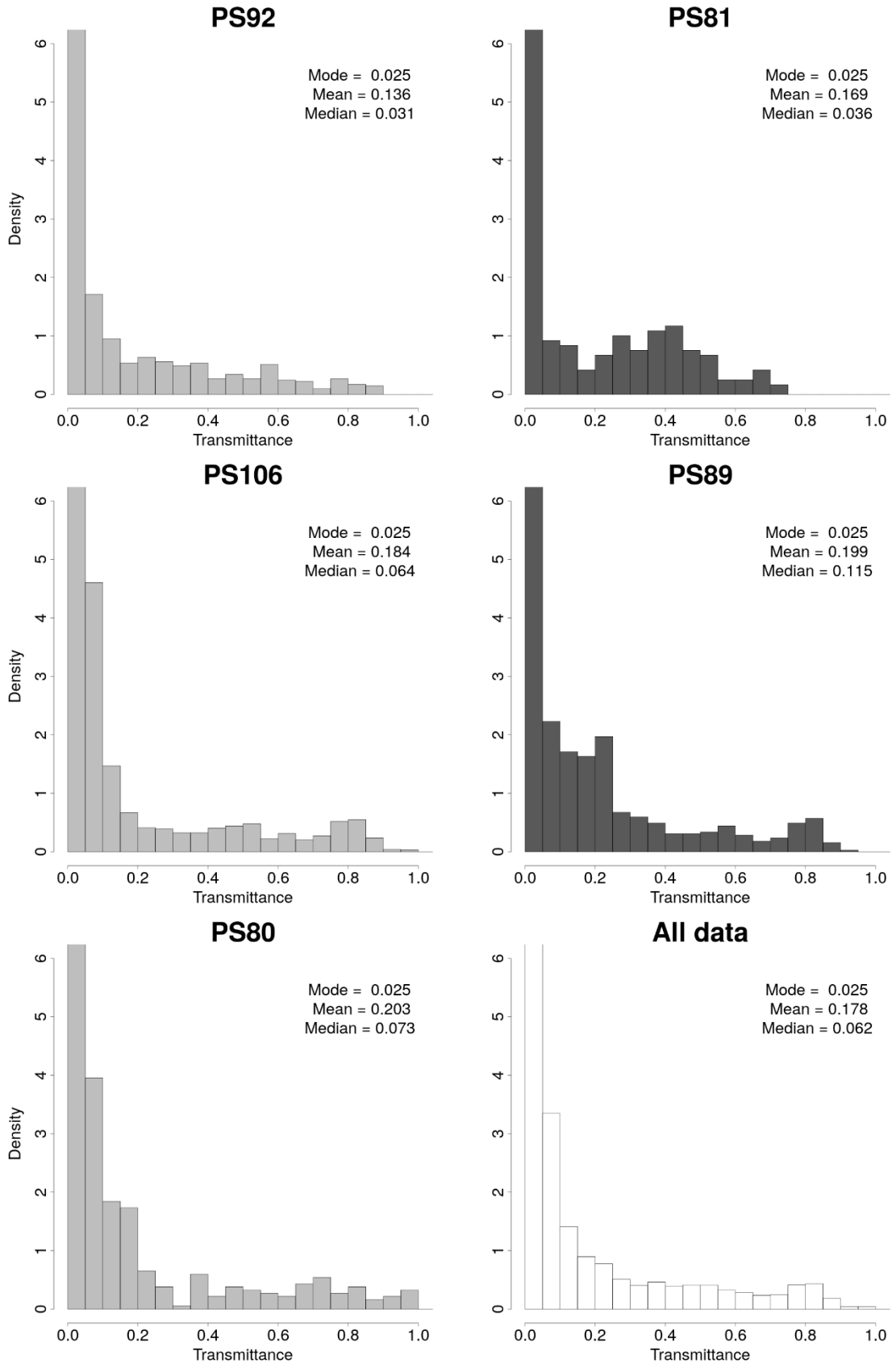

Figure S3. Histograms of ice transmittance. Histogram bins set at 0.05. Arctic expeditions are highlighted with light grey bars and Antarctic expeditions with dark grey bars.

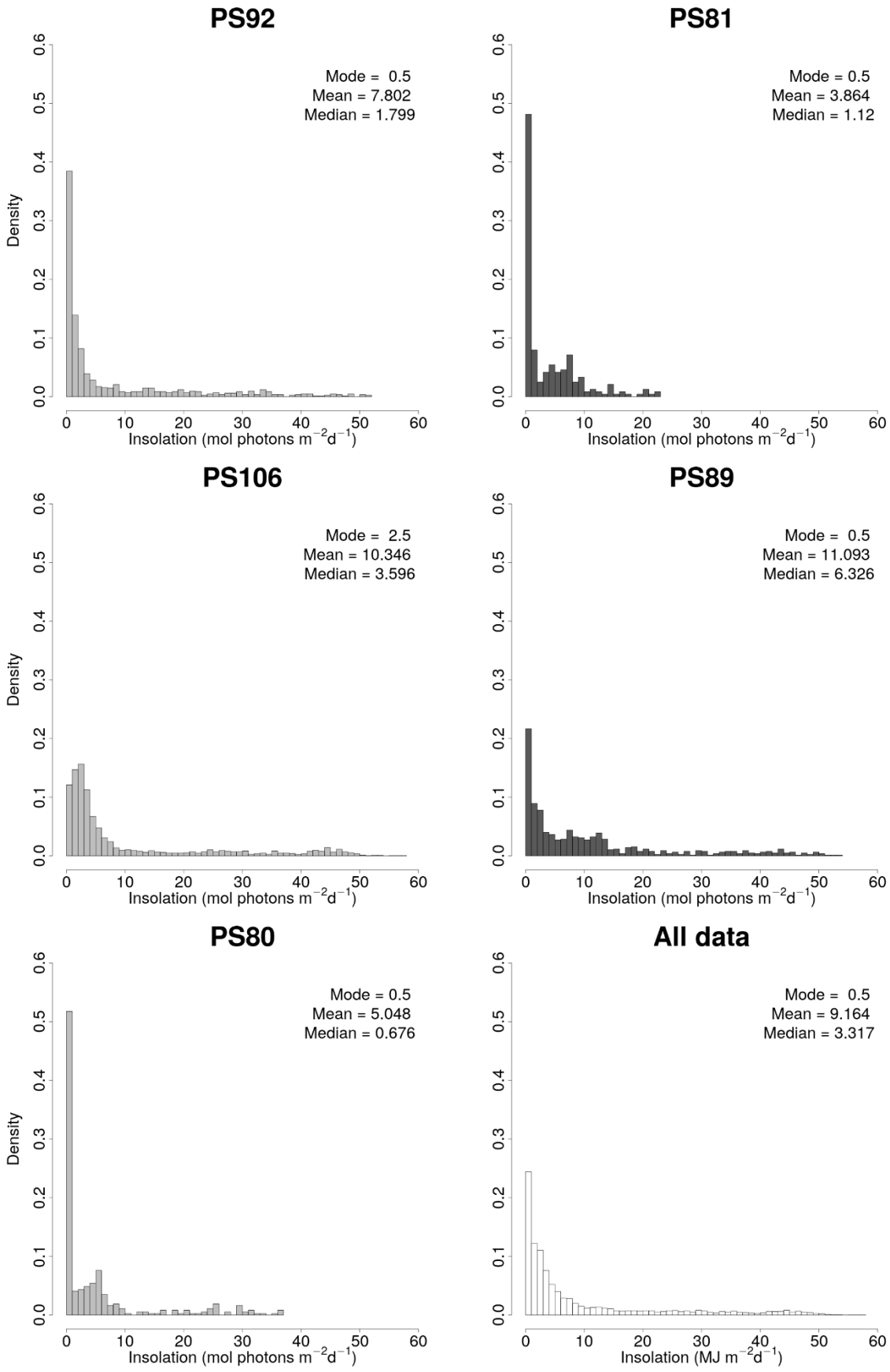

Figure S4. Histograms of under-ice insolation. Histogram bins set at 1. Arctic expeditions are highlighted with light grey bars and Antarctic expeditions with dark grey bars.

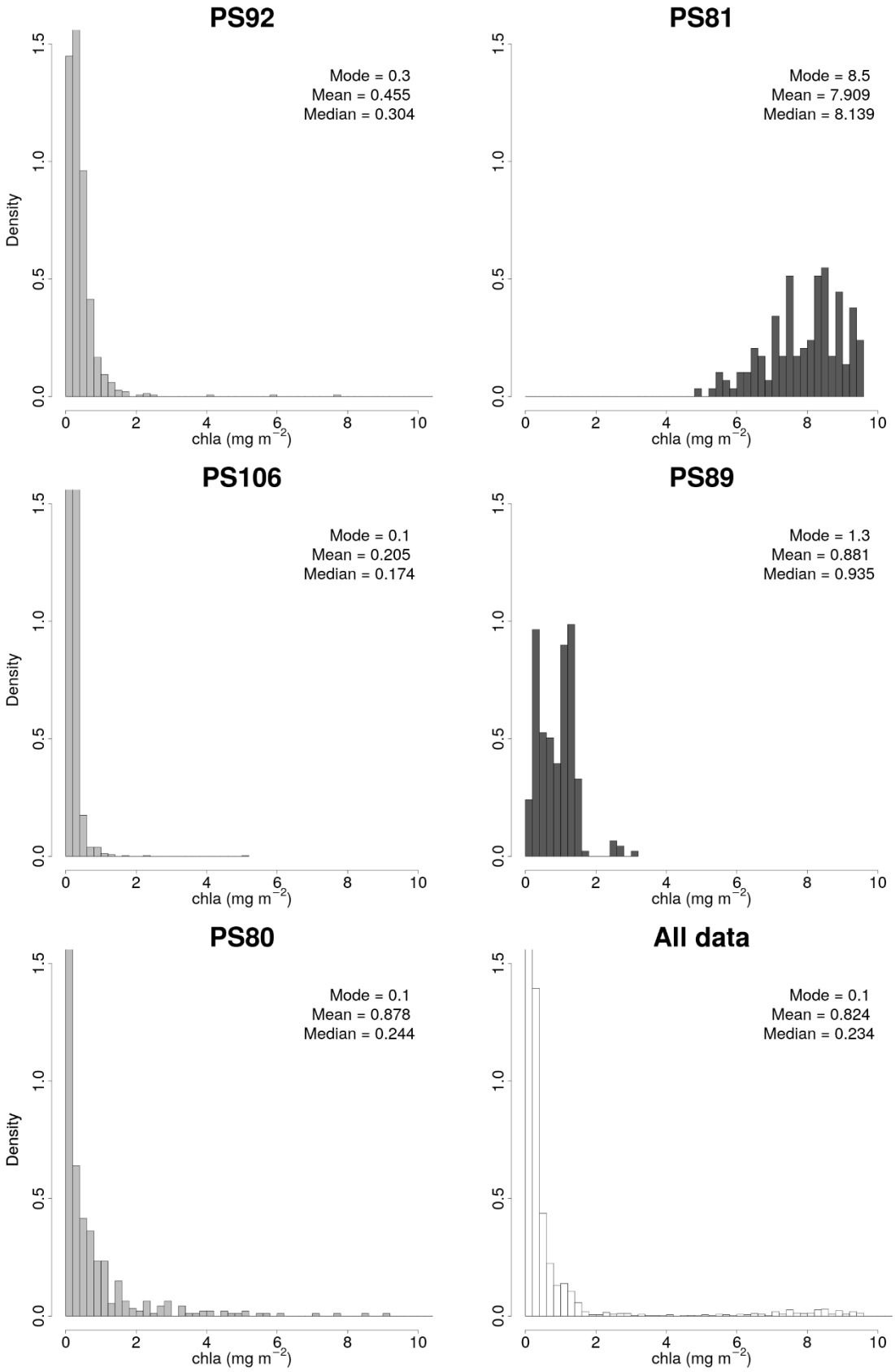

Figure S5. Histograms of in-ice chl *a* for all the expeditions retrieved by applying the algorithms listed in Table 2. Histogram bins set at 0.2 mg chl *a* m^{-2}. Arctic expeditions are highlighted with light grey bars and Antarctic expeditions with dark grey bars.

Chapter III

Sea-ice associated carbon flux in Arctic spring

J. Ehrlich[1,2], B.A. Bluhm[3], I. Peeken[2], P. Massicotte[4], F.L. Schaafsma[5], G. Castellani[2], A. Brandt[6,7], H. Flores[2]

[1] University of Hamburg, Centre for Natural History (CeNak), Hamburg, Germany
[2] Alfred-Wegener-Institute Helmholtz-Centre for Polar- and Marine Research, Bremerhaven, Germany
[3] UiT- The Arctic University of Norway, Institute of Arctic and Marine Biology, Tromsø, Norway
[4] Université Laval, Takuvik Joint International Laboratory, Québec, Canada
[5] Wageningen Marine Research, Den Helder, The Netherlands
[6] Senckenberg Research Institute and Natural History Museum, Frankfurt am Main, Germany
[7] Institute of Ecology, Diversity and Evolution, Goethe University, Frankfurt am Main, Germany

Accepted after 'moderate revisions' in Elementa - Science of the Anthropocene

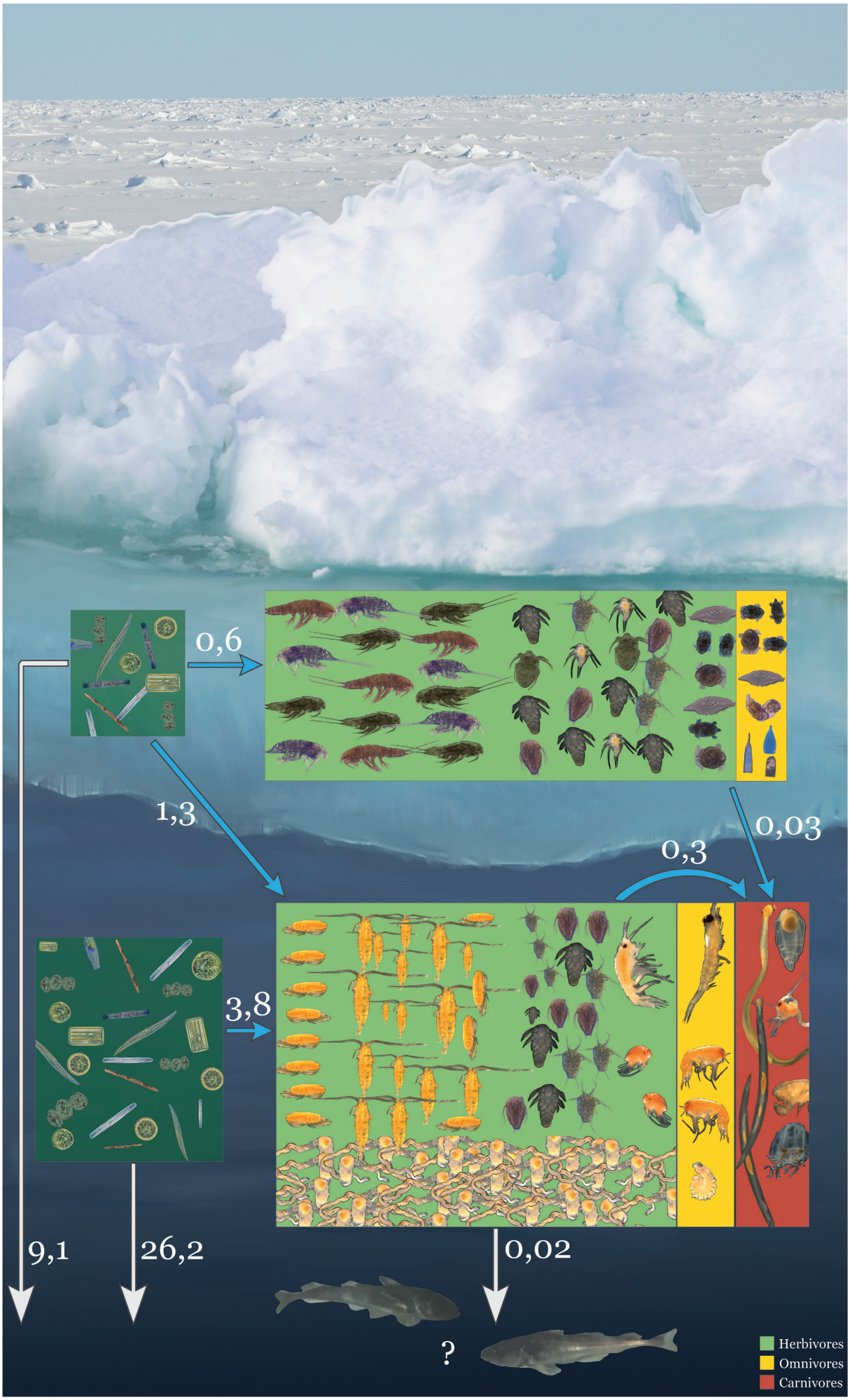
0,6
1,3
0,03
0,3
3,8
9,1
26,2
0,02
?
Herbivores
Omnivores
Carnivores

Sea-ice associated carbon flux in Arctic spring

J. Ehrlich[1,2*], B.A. Bluhm[3], I. Peeken[2], P. Massicotte[4], F.L. Schaafsma[5], G. Castellani[2], A. Brandt[6,7], H. Flores[2]

*** corresponding author:**

[1] University of Hamburg, Centre for Natural History (CeNak), Hamburg, Germany

[2] Alfred-Wegener-Institute Helmholtz-Centre for Polar- and Marine Research, Bremerhaven, Germany

[3] UiT- The Arctic University of Norway, Institute of Arctic and Marine Biology, Tromsø, Norway

[4] Université Laval, Takuvik Joint International Laboratory, Québec, Canada

[5] Wageningen Marine Research, Den Helder, The Netherlands

[6] Senckenberg Research Institute and Natural History Museum, Frankfurt am Main, Germany

[7] Institute of Ecology, Diversity and Evolution, Goethe University, Frankfurt am Main, Germany

Abstract

To evaluate the role of sea-ice associated (sympagic) biota as a source, sink and transmitter of carbon in the Arctic ecosystem, we collected samples from pack ice and under-ice water (0 - 2 m) north of Svalbard from May to June 2015 by sea-ice coring and under-ice trawling. We estimated biomass and primary production of ice algae and under-ice phytoplankton as well as biomass, carbon demand, and secondary production of sea-ice meiofauna (heterotrophs >10 µm) and under-ice fauna (metazoans >300 µm). Sea-ice meiofauna biomass (0.1 - 2.8 mg C m^{-2}) was dominated by harpacticoid copepods (92 %), nauplii (4 %), and Ciliophora (3 %). Under-ice fauna biomass (3.2 - 62.7 mg C m^{-2} per station) was dominated by *Calanus* copepods (54 %) and Appendicularia (23 %), though the latter dominated at only one station. Herbivorous sympagic fauna dominated the carbon demand across the study area and was estimated at 1 mg C m^{-2} day^{-1} for ice algae and 4 mg C m^{-2} day^{-1} for phytoplankton. This demand was covered by the estimated primary production of ice algae (mean 11 mg C m^{-2} day^{-1}) and phytoplankton (mean 30 mg C m^{-2} day^{-1}). Hence, approximately 35 mg C m^{-2} day^{-1} of algal material could potentially sink from the sympagic to the pelagic and benthic realms. The demand of carnivorous under-ice fauna (0.3 mg C m^{-2} day^{-1}) was hardly covered by the sympagic secondary production (0.3 mg C m^{-2} day^{-1}). Our study emphasizes the importance of under-ice fauna for the carbon flux from the sea ice to pelagic and benthic habitats.

Introduction

The Arctic Ocean harbors a unique sympagic ecosystem characterized by organisms that are adapted to an extreme environment comprising polar night, midnight sun, and seasonal or permanent sea-ice cover. The amount of light available for primary production in and under the sea ice is highly variable in space and time and is determined by overall sea-ice cover, sea-ice thickness, snow depth, and sediment in the ice (Gradinger et al., 2009; Massicotte et al., 2019; Castellani et al., 2020). Ice algae tend to be low-light adapted and typically peak in production before the phytoplankton bloom (Leu et al., 2015). Their spring bloom takes place in the bottom centimeters of the sea ice and they are released to the under-ice environment when the ice is melting later in the season (Gradinger, 2009; Leu et al., 2015). Ice algae can also serve as a food source for under-ice grazers, such as ice amphipods or calanoid copepods (Kohlbach et al., 2016). The magnitude of ice-algal production, however, tends to be lower than the phytoplankton production given the much shorter time window for bloom development (Leu et al., 2011). Some studies highlighted the importance of the timing of both blooms for the survival and reproduction of ice-associated (sympagic) fauna, which obtains at least part of its food demand from ice algae when phytoplankton is not yet available (Gradinger, 1999; Søreide et al., 2010; Leu et al., 2011).

The Arctic sea-ice community inside the ice is diverse, comprising bacteria, autotrophic, mixotrophic, and heterotrophic protists (Poulin et al., 2011; Hop et al., 2020), and metazoans (Gradinger, 1999). Although the taxonomic composition of the heterotrophic sea-ice community (sea-ice meiofauna) varies between regions, seasons and ice types, some taxa widely occur in Arctic sea ice (Bluhm et al., 2018). In terms of abundance, heterotrophic protists are often dominated by Ciliophora, whereas the multi-cellular fauna is often dominated by herbivorous Harpacticoida and copepod nauplii (Grainger and Hsiao, 1990; Gradinger, 1999; Bluhm et al., 2018; Ehrlich et al., 2020). These and other sea-ice meiofauna taxa are primarily consumers of ice algae and therefore important links in the transfer of energy from the sea ice to pelagic and benthic food webs (Gradinger, 1999; Nozais et al., 2001; Grebmeier et al., 2010). A recent study of Gradinger and Bluhm (2020) aimed to evaluate the extent of sea-ice meiofauna grazing in landfast ice and the degree to which sea-ice meiofauna, in turn, becomes prey of larger predators beneath the ice. The latter study showed that sea-ice meiofauna has a low grazing impact on the ice-algal spring bloom and leaves the vast majority of organic matter for under-ice, pelagic and benthic communities.

In addition to biota living inside the sea-ice brine channel system, invertebrates dwelling in the under-ice water layer are important for the carbon transfer to deeper water layers, not the least through their diel and seasonal vertical migration. For example, *Calanus* species adapted their life cycles to food availability during ice-algal and phytoplankton blooms (Søreide et al., 2010). *Calanus glacialis* and *C. hyperboreus* comprise the main biomass in the central Arctic Ocean (Auel and

Hagen, 2002; Darnis et al., 2008; Kosobokova and Hirche, 2009). They feed on both ice algae and phytoplankton (Kohlbach et al., 2016) and perform seasonal vertical migration to depths of hundreds of meters whereby they contribute significantly to the carbon cycle of the Arctic Ocean (Fortier et al., 2001; Daase et al., 2016; Darnis et al., 2017). Sympagic amphipods, such as *Apherusa glacialis* also show a high trophic dependency on the ice-algal production, which emphasizes the role of ice algae for the Arctic marine food web (Werner, 1997; Scott et al., 1999; Kohlbach et al., 2016). In addition, the sympagic realm is inhabited by carnivorous taxa, such as large *Paraeuchaeta* copepods, chaetognaths, the amphipod *Themisto libellula* and Polar cod *Boreogadus saida*, which are important for providing carbon to the higher trophic levels in ice-covered seas (Welch et al., 1992; Dalpadado, 2002; David et al., 2016).

Earlier studies investigated the community composition and biomass of sea-ice meiofauna (Friedrich, 1997; Gradinger et al., 1999; Gradinger and Bluhm, 2020) and under-ice fauna (Lønne and Gulliksen, 1991; David et al., 2015; Flores et al., 2019) in the Arctic Ocean. Based on the comparison with earlier studies, the impact of climate warming on the Arctic sea-ice ecosystem has already altered community compositions (Kiko et al., 2017; Ehrlich et al., 2020; Hop et al., 2020). Since sympagic fauna comprises different feeding types accompanied by specific prey preferences, composition and size changes will lead to a decoupling of predator-prey dynamics and to an increase of small-sized species favoring smaller prey (Daufresne et al., 2009; Li et al., 2009). Some studies assessed the dependency of single species on ice algae and phytoplankton (Werner, 1997; Kohlbach et al., 2016) or estimated the vertical flux from ice floes (Moran et al., 2005; Nöthig et al., 2020). A combination of primary production estimates with consumer carbon demand and secondary production for the in-ice and the under-ice realm, however, has not been done before.

To investigate the linkages between sea-ice and under-ice biota and the potential carbon flux from the sympagic realm to the pelagic and benthic systems, our study aimed to:

1) quantify the biomass and production rates of ice algae, under-ice phytoplankton, and sympagic fauna in and under Arctic pack ice;
2) estimate the potential grazing impact of sea-ice meiofauna and under-ice fauna on ice-algal and phytoplankton production, respectively;
3) evaluate the potential predation impact of carnivorous under-ice fauna on the secondary production;
4) estimate the amount of primary production that remains for the pelagic and benthic communities.

Materials and methods

Study area

This study was conducted during the international Transitions in the Arctic Seasonal Sea Ice Zone (TRANSSIZ) expedition aboard RV Polarstern (PS92) between 19 May and 28 June 2015. All samples were taken in the Eurasian sector of the Arctic Ocean near the Atlantic water inflow north of Svalbard between 7.07 - 19.91 °E and 81.01- 82.21 °N. We sampled ice cores at eight ice stations (Figure 1). In close vicinity to those ice stations we also took samples with the Surface and Under-Ice Trawl (SUIT, van Franeker et al., 2009) (Figure 1). Two of the eight ice stations were located on the marginal shelf north of Svalbard (stations 19 and 32), four in the Sophia Basin and on its slope (stations 27, 31, 47, and 39), and two at the Yermak Plateau (stations 43 and 45/46) (Figure 1). During our study ~1.5 year old sea ice covered on average 65 % of the sampling area (Ehrlich et al., 2020). The sampled region is characterized by a strong inflow of Atlantic Water along the West Spitsbergen Current and the Fram Strait branch. This inflow brings the most oceanic heat into the Arctic Ocean and contributes strongly to the observed sea-ice loss in the past decades (Rudels et al., 2004; Rudels et al., 2013; Hughes et al., 2011; Beszczynska-Möller et al., 2012). It is also responsible for the advection of zooplankton from sub-Arctic regions (Bluhm et al., 2011).

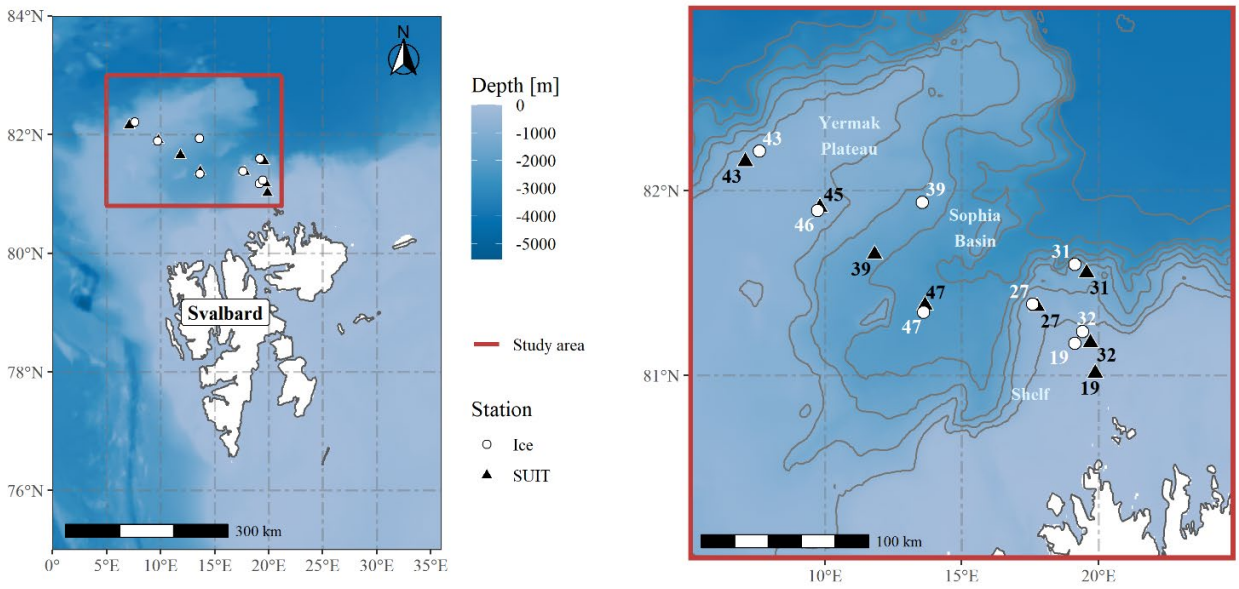

Figure 1: Map of the study area and sampled stations. During the Polarstern expedition PS92 north of Svalbard samples were taken at eight ice stations (white circles) and eight SUIT (Surface and Under-Ice Trawl) stations (black triangles).

Processing and parameter estimation of sea-ice biota

Sampling, biomass, and primary production of ice algae

A main coring site was established at each ice station and several ice cores were taken to determine different biogeochemical variables. The ice cores were drilled with a Kovacs corer (Kovacs Enterprise, Roseburg, USA; inner diameter: 9 cm). For pigment analysis, two ice cores were taken

at each ice station, pooled, and melted in filtered seawater (0.2 µm). The samples were filtered on GF/F filters and immediately frozen in liquid nitrogen and stored at -80 °C until analysis. Chlorophyll *a* (chl *a*) concentrations were measured with high performance liquid chromatography (HPLC) as described in Tran et al. (2013). The carbon biomass of ice algae for the ice stations was estimated from the sea-ice chl *a* concentrations at each station (Ehrlich et al., 2020) and applying an average C:chl ratio of 53 (Vernet et al., 2017), which was reflecting the overall mixed community of diatoms and flagellates found in our study region (Peeken, 2020).

Photosynthesis-irradiance (PE) curves were measured on a second set of two ice cores, which were collected at each ice station. The bottom 1 cm sections of each ice core was transferred in 50 ml of filtered (0.2 µm) surface seawater. Continuous gentle shaking helped to rapidly thaw the sample. All samples were kept in the dark prior to the incubation. PE samples were incubated at different irradiance levels in the presence of ^{14}C-labelled sodium bicarbonate using a method derived from Lewis and Smith (1983). Incubations were carried out in a dimly lit radiation lab under the deck of the vessel to avoid any light stress on the algae. To calculate the primary production using photosynthetic parameters derived from the PE curves, the incoming photosynthetic available radiation at the surface (PAR, $\mathring{E}$(PAR, 0+)) was measured at 10 minutes intervals using a CM 11 global radiation pyranometer (Kipp and Zonen, Delft, Netherlands) installed in the crow's nest of the Polarstern vessel. PE parameter means of the two replicates derived from each ice station (except of station 19) were used to calculate hourly primary production using the following equation:

(1) $pp = ps * (1 - e^{\left(-alpha * \frac{PAR}{ps}\right)})$,

where pp is the photosynthetic rate (mg C m^{-3} h^{-1}) at light saturation, alpha is the photosynthetic efficiency at irradiance close zero (mg C m^{-3} h^{-1} (µmol photon m^{-2} s^{-1})$^{-1}$), and ps (mg C m^{-3} h^{-1}) is an hypothetical maximum photosynthetic rate without photoinhibition. Daily primary production rates were then calculated by integrating hourly primary production over 24 hours (for further details see Massicotte et al., 2019).

Sampling, biomass, carbon demand, and secondary production of sea-ice meiofauna

Sea-ice meiofauna (here heterotrophs >10 µm) was sampled at each of the eight stations. The detailed sampling procedure was as described in Ehrlich et al. (2020). Briefly, the lowermost 10 cm of a set of duplicate ice cores per station were cut off and melted separately with the addition of 200 ml 0.2 µm filtered seawater per 1 cm of ice core to prevent the fauna from osmotic stress during melting (Garrison and Buck, 1986). Melting took place onboard in a dark room at 4 °C. After melting, the samples were concentrated on 10 µm gauze and fixed in 4 % buffered formaldehyde solution until later quantitative analysis. Taxonomic names were verified for correctness and synonymy using the World Register of Marine Species (WoRMS, http://www.marinespecies.org).

The biomass for sea-ice meiofauna taxa was calculated by multiplying abundances (ind. m^{-2}) of each taxon obtained from Ehrlich et al. (2020) by the carbon content per individual of this taxon. Carbon (C) values were taken from the literature (Table S 1). If no value for carbon content of a taxon was found, regression equations from the literature were used to calculate the dry weight, and dry weight-carbon ratios from literature were used to estimate the carbon content of this particular taxon (Table S 1). The mass-specific ingestion rate (% of body C day^{-1}) of each sea-ice meiofauna taxon was calculated according to Gradinger (1999) with the allometric mass specific equation of Moloney and Field (1989):

(2) $I_{max} = 63 * M^{(-0.25)} * 0{,}23326,$

where I_{max} is the daily mass-specific maximum potential ingestion rate (day^{-1}) and M is the biomass of a single organism (pg C). A sea-ice temperature of -1 °C (for details on physical parameters see Ehrlich et al., 2020) and a temperature coefficient (Q10) value of 2 (typical for plankton metazoans, Moloney and Field, 1989) were further assumed. The mass-specific ingestion rate of each taxon was then multiplied by the total carbon biomass of that taxon at every station to determine the carbon demand per day (Table S 1). In order to quantify the fraction of ice-algal carbon demand of key herbivorous sea-ice meiofauna taxa (Harpacticoida, nauplii, Ciliophora), we assumed Harpacticoida and nauplii covering 100 % and Ciliophora 50 % of their carbon demand by feeding on ice algae (Verity, 1991) (Table S 1). Although Harpacticoida and nauplii are also known to feed on Ciliophora (Kramer, 2011), the biomass of Ciliophora in comparison to ice algae was so small (<1 % of ice-algal biomass) that it was considered negligible. For the calculation of sea-ice meiofauna secondary production all production-biomass (P/B) ratios were obtained from Forest et al. (2014). In detail the P/B ratio of 0.062 for Arctic protozooplankton was used for Ciliophora, Tintinnina, Dinophyceae, and Amoebozoa, and the P/B ratio of 0.021 for Arctic nauplii and small zooplankton was used for Harpacticoida, Nauplii, and Rotifera.

Processing and parameter estimation of under-ice biota

Sampling, biomass, and primary production of ice algae and phytoplankton

Prior to arriving or directly after leaving each station, a SUIT was deployed. The SUIT consists of a steel frame with a 2 m x 2 m opening, two parallel, 15 m long nets and a sensor package attached to the opening of the SUIT (for sensor details see Lange et al., 2016). The set of sensors measured environmental variables at each station. Chl *a* concentration of phytoplankton right under the ice was determined by using a fluorometer (Cyclops, Turner Designs, USA), which was incorporated in the CTD (Sea and Sun Technology CTD75M memory probe) and calibrated against chl *a* concentrations measured by high performance liquid chromatography from water column samples. Under-ice irradiance values were measured using Ramses spectral radiometers (Trios GmbH, Rastede, Germany) with a wavelength range from 350 to 920 nm and a resolution of 3.3 nm.

From the under-ice hyperspectral measurements we retrieved ice-algal chl *a* by applying Normalized Difference Indices (NDI) algorithm (for details see Castellani et al., 2020). Due to failure of the sensor package no data could be collected at stations 31 and 32. In addition, missing hyperspectral measurements at station 27 did not allow to retrieve ice-algae chl *a* for this station. The measured chl a concentrations are available in Ehrlich et al. (2020). The carbon biomass of ice algae and phytoplankton at the SUIT stations was calculated as above for sea ice cores.

Primary production for the ice algae and phytoplankton was also calculated similarly as described in the previous section. For calculation of the ice algae primary production an hourly PAR under the ice was calculated by multiplying Ė (PAR, 0+) by the sea-ice transmittance. The sea-ice transmittance was calculated as the ratio between incoming and under-ice light, the latter measured with a RAMSES-ACC irradiance sensor (Trios, GmbH, Rastede, Germany) attached to the SUIT. For the calculation of the phytoplankton primary production we used PE curves determined from additional under-ice water samples, which we collected with Niskin bottles mounted on a Sea-Bird rosette water sampler equipped with a conductivity, temperature and depth (CTD) probe (SBE911+) at each ice station. Available light for phytoplankton photosynthesis was estimated by integrating PAR over the first two meters of the water column under the ice sheet. PAR between 0-2 meters was propagated into the water column using upward attenuation coefficient calculated from radiance profiles measured from the Remotely Operated Vehicle (ROV, for details see Nicolaus and Katlein, 2013). It must be noted that in the marginal ice zone, there were often large leads that increased the amount of light available to phytoplankton. To account for this additional light source available we have applied the method 2 by Massicotte et al. (2019), which aims at averaging production under the ice and in adjacent open waters using a mixing model based on sea-ice concentration (SIC) derived from satellite imagery to upscale the estimates of primary production derived from the SUIT.

Sampling, biomass, carbon demand, and secondary production of under-ice fauna

Under-ice fauna (here metazoans >300 µm) was sampled at each of the eight stations and was caught with the 300 µm zooplankton net of the SUIT with a single sample per station. The catch was concentrated on a 100 µm sieve and a defined fraction was preserved in 4 % buffered formaldehyde solution until later quantitative analysis (for details see Ehrlich et al., 2020). All fauna samples were sorted under stereo- microscopes (Zeiss Discovery.V20 and Leica Model M 205C or a Leica Discovery V8) and identified to the lowest taxonomic level possible. Taxonomic names were verified for correctness and synonymy using the World Register of Marine Species (WoRMS, http://www.marinespecies.org)

The biomass for all under-ice fauna taxa was calculated in the same way as described for sea-ice meiofauna in 2.2.2 (Table S 2). The mass specific ingestion rates [% of body C day^{-1}] for the

biomass-dominant under-ice taxa (*Calanus* spp., Amphipoda, Chaetognatha, Appendicularia), which combined accounted for 99.5 % of the total under-ice fauna biomass, were taken from the literature (Deibel, 1988; Saito and Kiorboe, 2001; Campbell et al., 2016) (Table S 2). For the remaining taxa no mass specific ingestion rates were available and instead the mean value of the above mentioned dominant taxa was used (Table S 2). The mass-specific ingestion rate of each taxon was then multiplied by the total biomass of that taxon at every station to determine the carbon demand per day (Table S 2). To take into account that some of the key herbivores (*C. hyperboreus*, *C. glacialis*, *C. finmarchicus*., *A. glacialis*, and Appendicularia) use both ice algae and phytoplankton as food source in our study area (Kohlbach et al., 2016) we assumed *C. hyperboreus* to cover 25 % and *C. glacialis* to cover 33 % of their carbon demand from ice algae (Kohlbach et al., 2016). For *C. finmarchicus* we took the same value as for *C. glacialis* (33 %) referring to Søreide et al. (2013) who showed that *C. finmarchicus* feed on a mixture of phytoplankton and ice algae. For *A. glacialis* we used an ice-algal share of 86 % of the total carbon demand (Kohlbach et al., 2016). Since Appendicularia are herbivorous filter feeders we assumed no prey selectivity and split their carbon demand corresponding to the ratio of ice-algal and phytoplankton primary production at each station. To get an estimation of the total carbon demand of the sea-ice and the under-ice fauna together, we used their means over all 8 stations as representative of the general study area. The secondary production of under-ice fauna was calculated by using a P/B ratio of 0.012 for all taxa obtained from Forest et al. (2014) for large Arctic mesozooplankton species.

Data visualization

All figures were created with R-Software version 3.6.0 (R Core Team, 2018) and the “ggplot2” package (Wickham, 2016). Additional features of the plots were modified using the packages "scales" (Wickham and Seidel, 2020) and "ggnewscale" (Campitelli, 2019). The plots were combined in grids using the "ggpubr" package (Kassambara, 2020). Map features were handled with functions from the packages "ggspatial" (Dunnington, 2018) and "sf" (Pebesma, 2018). Bathymetry data were taken from the "marmap" package (Pante and Simon-Bouhet, 2013) and spatial information data of countries from "rnaturalearth" and "rnaturalearthhires" (South, 2017; South, 2020).

Results

Biomass, carbon demand, and production of the sea-ice biota

The biomass of ice algae in ice cores ranged between 10.6 and 41.9 mg C m^{-2} per station (mean= 22.3 mg C m^{-2}) (Figure 2a, Table 1). Ice-algal primary production ranged from 0.5 to 13.7 mg C m^{-2} day^{-1} (mean= 4.8 mg C m^{-2} day^{-1}) (Figure 2b, Table 1).

The biomass of sea-ice meiofauna ranged between 0.05 and 2.8 mg C m^{-2} (mean= 1.1 mg C m^{-2}) per station (Figure 2a). Harpacticoida contributed with 92 % by far the most to total biomass (mean= 1.0 mg C m^{-2}) (Figure 3a, Table 1). The remaining biomass was mainly attributed to nauplii (4 %), and Ciliophora (3 %) (Figure 3a, Table 1). The secondary production of sea-ice meiofauna ranged between 0.002 and 0.06 mg m^{-2} day^{-1} (mean= 0.03 mg C m^{-2} day^{-1}) (Figure 2b). Most of the secondary production was attributed to Harpacticoida (84 %) and Ciliophora (9 %) (Table 1). Estimated carbon demand of the sea-ice meiofauna varied from 0.06 to 1.5 mg C m^{-2} day^{-1} (mean= 0.7 mg C m^{-2} day^{-1}) and followed the same pattern as the biomass, with Harpacticoida (81 %), nauplii (9 %), and Ciliophora (8 %) making up the greatest part of the total sea-ice meiofauna carbon demand (Figure 2b, Table 1). Altogether their ice-algal demand was estimated at 0.6 mg C m^{-2} day^{-1} (Table 1). Except for station 27, the ice-algal demand of those taxa was lower than the ice-algal primary production (Figure 3b).

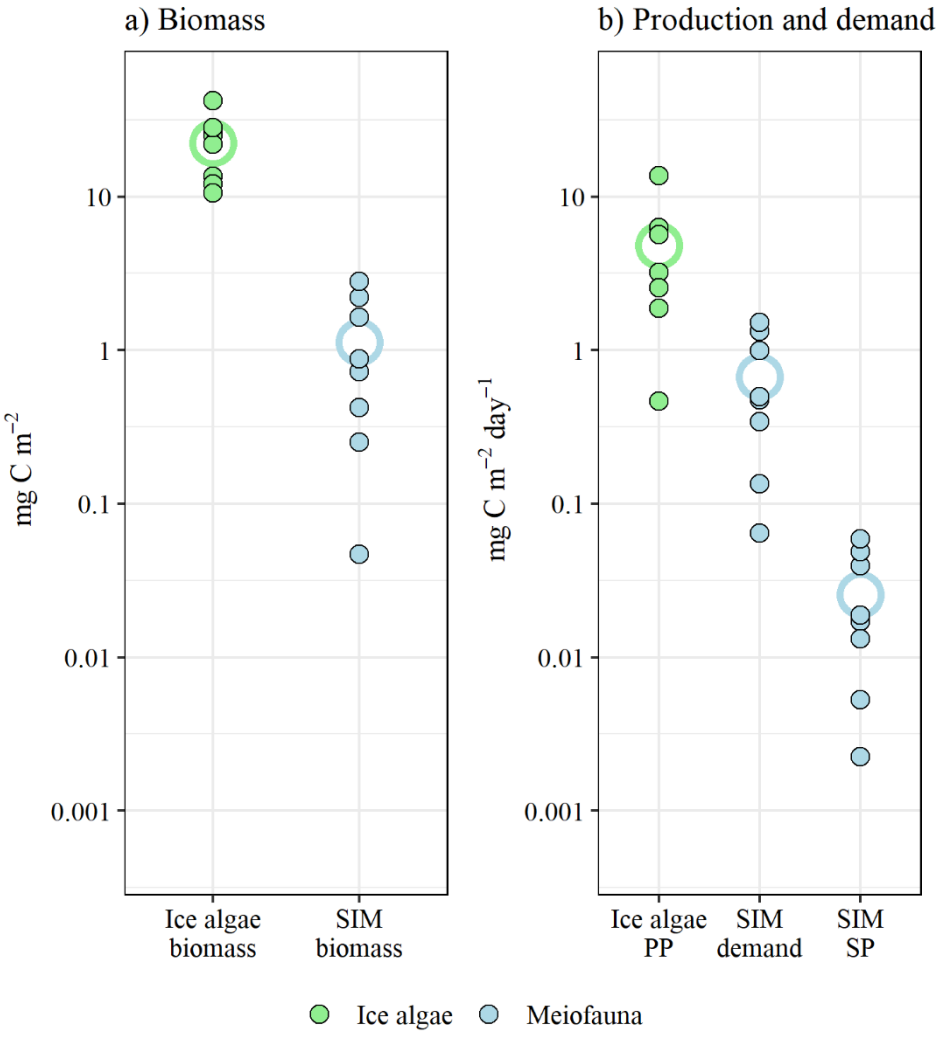

Figure 2: Biomass, carbon demand, and carbon production of ice algae and sea-ice meiofauna. a) Biomass of ice algae and sea-ice meiofauna and b) Carbon production of ice algae and sea-ice meiofauna and carbon demand of sea-ice meiofauna across eight stations north of Svalbard in spring pack ice 2015. Filled circles represent estimates per station. The respective mean value is marked as unfilled circle. Note: y-axis is $\log_{10}$ scaled. PP, primary production; SP, secondary production; SIM, sea-ice meiofauna

Table 1: Mean biomass (B), primary production (PP), secondary production (SP), and carbon demand (CD) for all sea-ice biota including standard deviation (SD) and relative (Rel) shares.

	Mean B (µg C m^{-2})	**SD**	**Range**		**Mean PP (µg C m^{-2} day^{-1})**	**SD**	**Range**					
Ice algae	22,280	10,375	10,548-41,894		4,812	4,405	463-13,664					
Sea-ice meiofauna	**Mean B (µg C m^{-2})**	**SD**	**Range**	**Rel B (%)**	**Mean SP (µg C m^{-2} day^{-1})**	**SD**	**Range**	**Rel SP (%)**	**Mean CD (ice algae) (µg C m^{-2} day^{-1})**	**SD**	**Range**	**Rel CD (%)**
Harpacticoida G.O. Sars, 1903	1,026.3	970.4	0-2,765.6	91.6	21.6	20.4	0-58.1	84.7	541.9 (541.9)	512.4	0-1,460.3	81.1
Nauplii (Copepoda Milne Edwards, 1840)	48.6	46.7	3.3-153.6	4.3	1.0	1.0	0.1-3.2	4.0	60.0 (60.0)	57.7	4.1-189.9	9.0
Rotifera Cuvier, 1817	2.4	5.0	0-13.6	0.2	0.2	0.3	0-0.9	0.6	2.9	5.9	0-16.3	0.4
Ciliophora not documented	37.0	37.6	0-94.2	3.3	2.3	2.3	0-5.8	9.0	53.1 (26.6)	53.9	0-135.2	7.9
Tintinnina Kofoid and Campbell, 1929	5.3	6.3	0-16.8	0.5	0.3	0.4	0-1.0	1.3	7.6	9.1	0-24.1	1.1
Dinophyceae Fritsch, 1927	1.3	2.1	0-4.9	0.1	0.1	0.1	0-0.3	0.3	2.2	3.6	0-8.5	0.3
Amoebozoa Lühe, 1913, emend. Cavalier-Smith, 1998	0.1	0.3	0-0.9	<0.1	<0.1	<0.1	0-0.1	<0.1	0.2	0.5	0-1.3	<0.1
Total	*1,121*	*993*	*47-2,806*	*100*	*25*	*21*	*2-59*	*100*	*668 (628)*	*543*	*64-1,510*	*100*

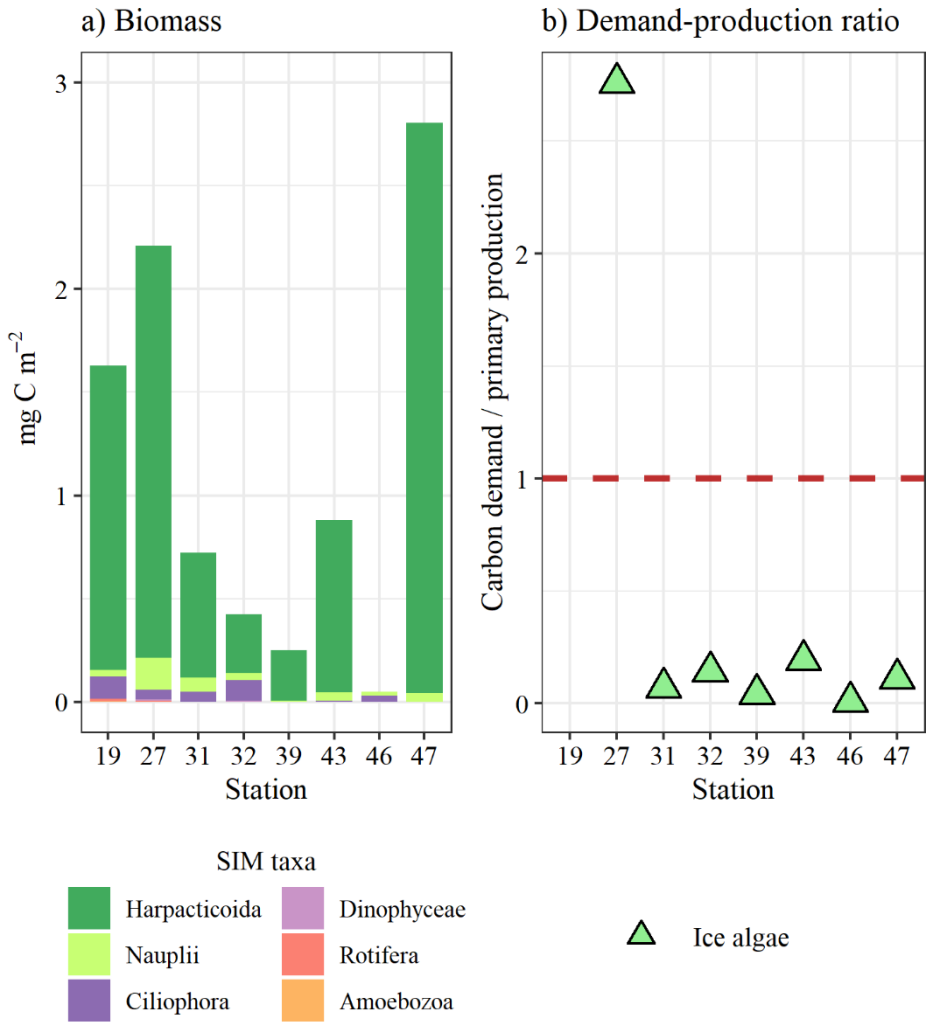

Figure 3: Biomass of sea-ice meiofauna taxa and demand-production ratios at each ice station. a) Biomass of sea-ice meiofauna taxa per station and b) Ratio of carbon demand of herbivorous sea-ice meiofauna (Harpacticoida, nauplii, and Ciliophora combined) versus ice-algal primary production per station. For b) the primary production for station 19 could not be calculated, because no PE curve was established for this station.

Biomass, carbon demand, and production of the under-ice biota

The biomass of ice-algae at SUIT stations ranged between 6.3 and 28.5 mg C m^{-2} (mean= 17.7 mg C m^{-2}) (Figure 4a). The estimated phytoplankton biomass in the 0-2 m under-ice water ranged between 28.6 and 1,121.4 mg C m^{-2} across stations (mean= 352.4 mg C m^{-2}) (Figure 4a). Ice-algal primary production ranged from 3.7 to 34.5 mg C m^{-2} day^{-1} (mean= 16.9 mg C m^{-2} day^{-1}) (Figure 4b, Table 2). The primary production of phytoplankton ranged between 1.2 and 114.3 mg C m^{-2} day^{-1} (mean= 30.4 mg C m^{-2} day^{-1}) (Figure 4b, Table 2).

The biomass of under-ice fauna ranged between 3.2 and 62.7 mg C m^{-2} (mean= 22.2 mg C m^{-2}) (Figure 4a). The majority of the biomass was attributed to the three *Calanus* species, which had similar mean biomasses between 4.5 and 3.1 mg C m^{-2}, and relative contributions to the under-ice fauna between 14 and 20 % (Figure 5a, Table 2). Amphipoda contributed to the total under-ice fauna biomass with a mean of 2.5 mg C m^{-2} and a share of 11 % (Table 2). At station 32, Appendicularia were extremely abundant and thus made up 23 % of the total under-ice fauna biomass (Figure 5a,

Table 2). The combined rest of the under-ice fauna taxa including nauplii, Chaetognatha, and Euphausiacea constituted less than 12 % of the biomass (Table 2). The secondary production of the under-ice fauna ranged between 0.04 and 0.75 mg C m^{-2} day^{-1} across stations (mean= 0.26 mg C m^{-2} day^{-1}) (Figure 4b, Table 2). Similar to the biomass, most of the secondary production was attributed to the three *Calanus* species with means ranging between 0.04 and 0.05 mg C m^{-2} day^{-1}, making up 53 % of the secondary production (Table 2). Appendicularia had a mean share of 23 % and Amphipoda of 11 % to the total secondary production (Table 2). The carbon demand of the under-ice fauna varied from 0.2 to 29.4 mg C m^{-2} day^{-1} across stations (mean= 5.6 mg C m^{-2} day^{-1}) (Figure 4b, Table 2). Taxa which made up most of the total carbon demand of the under-ice fauna were Appendicularia (59 %), *C. finmarchicus* (13 %), *C. hyperboreus* (10 %), *C. glacialis* (8 %), and Amphipoda (1 %) (Table 2). Jointly, the estimated mean carbon demand of these taxa was 1.3 mg C m^{-2} day^{-1} for ice algae and 3.8 mg C m^{-2} day^{-1} for phytoplankton (Table 2). The ice-algal carbon demand of these taxa was always lower than the ice-algal primary production at SUIT stations (Figure 5). This was not the case for the phytoplankton carbon demand, which exceeded the phytoplankton production by a factor of 1.9 at station 45 (Figure 5b). The mass appearance of Appendicularia at station 32 resulted in a local peak (26.4 mg C m^{-2} day^{-1}) of the herbivorous carbon demand.

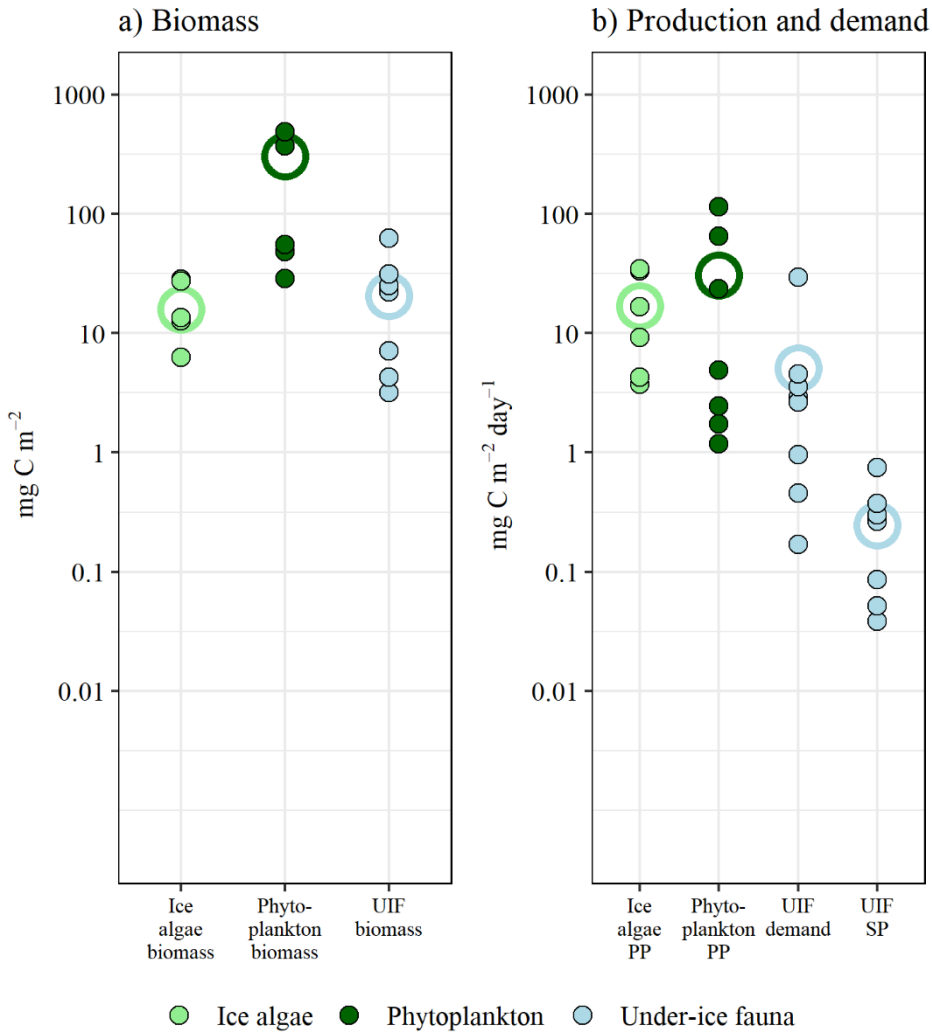

Figure 4: Biomass, carbon demand, and carbon production of ice algae, phytoplankton and under-ice fauna. a) Biomass of ice algae, phytoplankton (0-2 m) and under-ice fauna and b) Carbon production of ice algae, phytoplankton (0-2 m), and under-ice fauna and carbon demand of under-ice fauna across eight stations north of Svalbard in spring pack ice 2015. Filled circles represent estimates per station. The respective mean value is marked as unfilled circle. Note: Y-axis is $\log_{10}$ scaled. PP, primary production; SP, secondary production; UIF, under-ice fauna

Table 2: Mean biomass (B), primary production (PP), secondary production (SP), and carbon demand (CD) for all under-ice biota including standard deviation (SD) and relative (Rel) shares

	Mean B (µg C m^{-2})	**SD**	**Range**		**Mean PP (µg C m^{-2} day^{-1})**	**SD**	**Range**					
Phytoplankton (0-2 m)	352,432	423,321	28,620-1,121,374		30,411	43,527	1,175-114,260					
Ice algae	17,685	9,785	6,295-28,499		16,934	13,922	3,721-34,480					
Under-ice fauna	**Mean B (µg C m^{-2})**	**SD**	**Range**	**Rel B (%)**	**Mean SP (µg C m^{-2} day^{-1})**	**SD**	**Range**	**Rel SP (%)**	**Mean CD (ice algae) (µg C m^{-2} day^{-1})**	**SD**	**Range**	**Rel CD (%)**
Tisbe Lilljeborg, 1853 spp.	<0.1	<0.1	0-0.1	<0.1	<0.1	<0.1	0-0.0	<0.1	<0.1	<0.1	0-0.0	<0.1
Oithona Baird, 1843 sp.	<0.1	<0.1	0-0.0	<0.1	<0.1	<0.1	0-0.0	<0.1	0.0	0.0	0-0.0	<0.1
Calanus hyperboreus Krøyer, 1838	4,386.3	5066.7	5.1-15,758.3	19.8	52.6	60.8	0.1-189.1	19.8	560.0 (140.0)	634.4	1.3-1,988.3	10.0
Calanus glacialis Jaschnov, 1955	3,116.4	2210.7	126.7-5,954.7	14.0	37.4	26.5	1.5-71.5	14.0	448.3 (147.9)	299.0	15.7-757.5	8.0
Calanus finmarchicus (Gunnerus, 1765)	4,542.7	3765.7	492.0-12,415.5	20.5	54.5	45.2	5.9-149.0	20.5	734.1 (242.3)	728.4	59.9-2,382.6	13.2
nauplii (Copepoda)	575.3	1511.2	0-4,314.1	2.6	6.9	18.1	0-51.8	2.6	143.8	377.8	0-1,078.5	2.6
Paraeuchaeta Scott, 1909 spp.	5.6	15.7	0-44.5	<0.1	0.1	0.2	0-0.5	<0.1	1.1	3.1	0-8.9	<0.1
Metridia longa (Lubbock, 1854)	15.9	44.9	0-127.1	0.1	0.2	0.5	0-1.5	0.1	3.2	9.0	0-25.4	0.1
Clausocalanidae Giesbrecht, 1893	8.7	18.1	0-52.8	<0.1	0.1	0.2	0-0.6	0.0	1.7	3.6	0-10.6	<0.1
Themisto Guerin, 1825 spp.	39.2	110.9	0-313.6	0.2	0.5	1.3	0-3.8	0.2	1.0	2.8	0-7.8	<0.1
Themisto libellula (Lichtenstein in Mandt, 1822)	2.6	4.0	0-10.8	<0.1	<0.1	<0.1	0-0.1	<0.1	0.1	0.1	0-0.3	<0.1
Apherusa glacialis (Hansen, 1888)	2,478.9	2,459.7	77.4-6,576.7	11.2	29.7	29.5	0.9-78.9	11.2	62.0 (53.3)	61.5	1.9-164.4	1.1
Onisimus glacialis (G.O. Sars, 1900)	2.9	8.2	0-23.3	<0.1	<0.1	0.1	0-0.3	<0.1	0.1	0.2	0-0.6	<0.1
Thysanoessa longicaudata Krøyer, 1846	38.6	94.1	0-269.1	0.2	0.5	1.1	0-3.2	0.2	7.7	18.8	0-53.8	0.1
Isopoda Latreille, 1817	1.6	4.1	0-11.6	<0.1	<0.1	<0.1	0-0.1	0.0	0.3	0.8	0-2.3	<0.1
Zoaea larvae	<0.1	0.1	0-0.4	<0.1	<0.1	<0.1	0-0.0	<0.1	<0.1	<0.1	0-0.1	<0.1

Cirripedia Burmeister, 1834	17.4	20.2	0.1-59.6	0.1	0.2	0.2	0-0.7	0.1	3.5	4.0	0-11.9	0.1
Chaetognatha not documented	459.2	1298.7	0-3,673.2	2.1	5.5	15.6	0-44.1	2.1	78.1	220.8	0-624.5	1.4
Eukrohnia hamata (Moebius, 1875)	1,274.8	1,486.7	0-3,636.2	5.7	15.3	17.8	0-43.6	5.7	216.7	252.7	0-618.2	3.9
Parasagitta elegans (Verrill,1873)	64.8	107.2	0-319.3	0.3	0.8	1.3	0-3.8	0.3	11.0	18.2	0-54.3	0.2
Appendicularia Fol, 1874	5,151.4	14,565.5	0-41,199.1	23.2	61.8	174.8	0-494.4	23.2	3,296.9 (725.3)	9,321.9	0-26,367.4	59.2
Osteichthyes larvae	0.4	1.2	0-3.3	<0.1	<0.1	<0.1	0-0.0	<0.1	0.1	0.2	0-0.7	<0.1
Limacina helicina (Phipps, 1774)	0.1	0.2	0-0.6	<0.1	<0.1	<0.1	0-0.0	<0.1	<0.1	<0.1	0-0.1	<0.1
Clione limacina (Phipps, 1774)	10.9	30.9	0-87.3	<0.1	0.1	0.4	0-1.1	0.0	2.2	6.2	0-17.4	<0.1
Polychaeta Grube, 1850	<0.1	<0.1	0-0.0	<0.1	<0.1	<0.1	0-0.0	<0.1	<0.1	<0.1	0-0.0	<0.1
Trochophora larvae	3.11	7.41	0-21.3	<0.1	<0.1	0.1	0-0.3	<0.1	0.6	1.5	0-4.3	<0.1
Hydrozoa Owen, 1843	<0.1	<0.1	0-0.0	<0.1	<0.1	<0.1	0-0.0	<0.1	<0.1	<0.1	0-0.0	<0.1
Xenacoelomorpha Philippe, Brinkmann, Copley, Moroz, Nakano, Poustka, Wallberg, Peterson & Telford, 2011	0.36	0.64	0-1.7	<0.1	<0.1	<0.1	0-0.0	<0.1	0.1	0.1	0-0.3	<0.1
Total	*22,197*	*19,396*	*3,184-62,654*	*100*	*266*	*233*	*38-752*	*100*	*5,572 (1,309)*	*9,751*	*170-29,403*	*100*

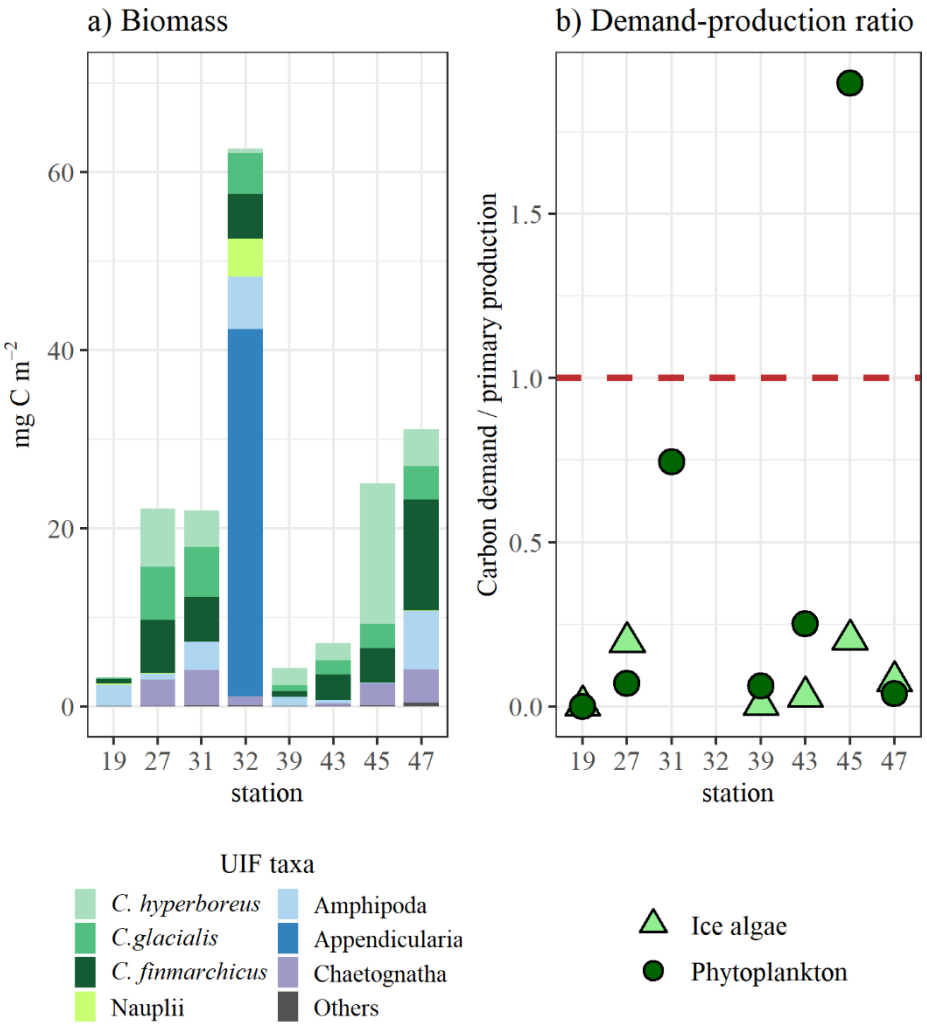

Figure 5: Biomass of under-ice fauna taxa and demand-production ratios at each SUIT station. a) Biomass of under-ice fauna taxa per station and b) Ratio of carbon demand of herbivorous under-ice fauna versus ice-algal primary production and versus phytoplankton primary production per station. Ice-algal primary production estimates were not available for stations 31 and 32. Phytoplankton primary production estimates were not available for station 32. UIF, under-ice fauna; PP, primary production.

Total biomass, carbon demand and production of sympagic biota

Mean algal biomass (phytoplankton and ice algae combined) was estimated at 372 mg C m^{-2} with a primary production of 41 mg C m^{-2} day^{-1}. Ice algae accounted for 27 % of this production (Table 3). Mean biomass of the sympagic fauna (sea-ice meiofauna and under-ice fauna combined) was estimated at 23 mg C m^{-2}, of which sea-ice meiofauna accounted for 5 %. The carbon demand of the sympagic fauna was estimated at a mean of 6 mg C m^{-2} day^{-1}, of which sea-ice meiofauna accounted for 12 % (Table 3). The mean secondary production of all sympagic taxa combined was 0.3 mg C m^{-2} day^{-1}, of which sea-ice meiofauna produced 9 % (Table 3).

Table 3: Total biomass, production, and carbon demand of sympagic biota.

Community	Parameter	Carbon (mg C m^{-2})	In-ice (%)	Under-ice (%)
Primary Producers	Biomass	372	6	94
	Primary production	41 day^{-1}	27	73
Consumers	Biomass	23	5	95
	Carbon demand	6 day^{-1}	12	88
	Secondary production	0.3 day^{-1}	9	91

Discussion

Primary production of sympagic algae

Since the late 1990's phytoplankton primary production over the entire Arctic Ocean has increased by 30 % mainly due to a decrease in sea-ice extent and thickness, but also due to an increased nutrient supply (Arrigo et al., 2015; Ardyna and Arrigo, 2020). In general, annual phytoplankton production tends to exceed ice-algal production in the basins of the Arctic Ocean and on the shelves (Wiedmann et al., 2020). To which degree ice algae contribute to the primary production depends on the season, region, and also on the prevailing ice type (Gosselin et al., 1997; Fernández-Méndez et al., 2015). In an earlier study from the central Arctic Ocean, ice algae contributed up to 57 % to the primary production in summer (Gosselin et al., 1997). In contrast, in a more recent study conducted during the historical sea-ice minimum in summer 2012, ice algae contributed only up to 30 % to total primary production in first year sea ice (Fernández-Méndez et al., 2015). In our spring study (with ~1.5 year old pack ice and a mean ice coverage of 65 %, Ehrlich et al., 2020), we estimated that 27 % of the total sympagic primary production were attributed to ice algae. Our estimated ice-algal production rate (11 mg C m^{-2} day^{-1}) and under-ice phytoplankton production rate (30 mg C m^{-2} day^{-1}) were also well within the range of estimates from the previous summer study of Fernández-Méndez et al. (2015) (ice algae 1-13 mg C m^{-2} day^{-1}, phytoplankton: 0.1-60 mg C m^{-2} day^{-1}). These findings indicate that carbon contributions from the sea ice might not yet be as negligible as some other studies previously assumed (Dupont, 2012; Matrai et al., 2013; Assmy et al., 2017). This result is even more important when we consider future model projections, which indicate further increase of ice-algal production in those areas where sea ice persists (Tedesco et al., 2019). However, estimates on primary production by ice algae should be viewed with caution, since their patchy distribution might bias estimations and show rather a snapshot in time and space. Our spatially integrated SUIT-based estimates were about four times higher than local ice core-based

measurements, confirming that large-scale variability of ice-algal primary production can significantly exceed the variability covered by local measurements (Lange et al., 2017). In our study, we could not separate effects of the sampling scale from those attributed to the different ways used to estimate primary production. However, our findings will be useful for the calibration and validation of biogeochemical models (Tedesco et al., 2019) that upscale the results to the pan Arctic, and for the comparison with satellite measurements (Ardyna et al., 2014).

Biomass, carbon demand and secondary production of sympagic fauna

The estimated mean biomass of sea-ice meiofauna in our study area (1 mg C m^{-2}) is within the range of earlier estimations from the central Arctic Ocean of <0.1-7.4 mg C m^{-2} (Gradinger, 1999). However, in Gradinger (1999) Acoela (then called Turbellaria) (27 %), Crustacea (22 %), Nematoda (20 %), and Ciliophora (15 %) dominated the biomass, whereas in our study Harpacticoida (92 %) was the most dominant taxon, followed by copepod nauplii (4 %), and Ciliophora (3 %). Nematoda and Acoela were neither present in the pack ice of our study nor during the 6-month long N-ICE study in the same year. This absence is assumed to be a consequence of the ongoing change from a multiyear to an annual sea-ice system in this part of the Arctic Ocean (Kiko et al., 2017; Ehrlich et al., 2020). The transition to a taxon-depleted system may have happened in the early 2000s when Kramer (2011) found Ciliophora and Harpacticoida dominating the biomass of the sea-ice meiofauna, but also still found some Acoela and Nematoda in the ice of the central Arctic Ocean in summer.

The mean carbon demand of the sea-ice meiofauna in our study (0.7 mg C m^{-2} day^{-1}) was also within the range of earlier estimates from Gradinger (1999) (<0.1-7.9 mg C m^{-2} day^{-1}), though in Gradinger (1999) protists (36 %) made up the main grazing impact, whereas Harpacticoida (81 %) were the main grazers in our study. This difference indicates that strong changes in taxonomic composition do not necessarily affect the overall grazing pressure of sea-ice meiofauna. In the Arctic spring season, increasing daylight allows the development of a strong ice-algal bloom (Leu et al., 2015; Castellani et al., 2017), which enhances the food availability for herbivorous sea-ice meiofauna, such as Harpacticoida. Earlier studies (excluding Ciliophora) suggested a negligible grazing impact of sea-ice meiofauna on the spring bloom (Nozais et al., 2001; Gradinger, 2009; Gradinger and Bluhm, 2020). While we did include Ciliophora grazing, which accounted for 8 % of the mean sea-ice meiofauna carbon demand, sea-ice meiofauna still grazed only 14 % of the mean ice-algal primary production. We had a single station, however, where the estimated carbon demand of sea-ice meiofauna was 2.8 times higher than the ice-algal primary production (station 27). This suggests that on a local scale, sea-ice meiofauna might have a decisive grazing impact on ice algae, which then in turn cannot provide sufficient carbon for the local under-ice communities.

A recent study, using the same method to sample under-ice fauna as ours, reported a mean under-ice fauna biomass of 7 mg C m^{-2} in the central Arctic Ocean in autumn, dominated by the ice-associated amphipod *A. glacialis* and the copepod species *C. glacialis* and *C. hyperboreus* (Flores et al., 2019). In our spring study, the mean under-ice fauna biomass was three-fold higher (22 mg C m^{-2}) and dominated by the three *Calanus* species (*C. hyperboreus*, *C. glacialis* and *C. finmarchicus*). The extremely high abundance of Appendicularia at one station elevated the biomass in our study by 5 mg C m^{-2}. *Calanus* species are well known to be among the main contributors to the biomass of under-ice fauna in the Arctic Ocean (Werner, 2006). Appendicularia, however, have never been reported in such high biomass directly under the sea ice in this area, though they were observed frequently in surface waters of the ice-covered Canada Basin (Raskoff et al., 2010) and locally in the Nansen Basin (David et al., 2015). In contrast to other studies from the Arctic Ocean (Werner, 2006; Flores et al., 2019), the ice amphipod *A. glacialis* did not dominate the sympagic biomass in this study. *Apherusa glacialis* represents an important food source for other ice-associated fauna such as polar cod, seabirds and seals (Bradstreet and Cross, 1982; Werner, 1997; Kohlbach et al., 2017) and is therefore considered as an important link for the carbon transfer from lower to higher trophic levels in the Arctic marine food web. The low biomass of ice amphipods in our study is consistent with the observed decline of sympagic amphipod biomass in the European Arctic sector over the past decades (Arctic Council Secretariat, 2017). The low abundances of *A. glacialis* may be related to a recent interruption of the Transpolar Drift (Krumpen et al., 2019). Assuming that *A. glacialis* colonizes the sea ice in waters off Siberia to drift across the central Arctic Ocean before potentially returning to the source area with deep currents (Berge et al., 2012), the increasing decay of sea ice along the Transpolar Drift may have released ice amphipods in the central Arctic Basins. Thus, only low abundances were left to recolonize the newly formed ice during its drift towards our study area.

Most of the total carbon demand of the under-ice fauna (6 mg C m^{-2} day^{-1}) was attributed to Appendicularia (at a single location), and the copepods *C. finmarchicus*, *C. hyperboreus*, and *C. glacialis*, all of which are considered to be mainly herbivorous feeders (Stevens et al., 2004). Previous studies focused in particular on the grazing impact of sympagic amphipods on ice algae (Werner and Auel, 2005; Hop and Pavlova, 2008; Kohlbach et al., 2016). However, our study estimated that the three *Calanus* species together had up to a nine times higher ice-algal carbon demand than the amphipod *A. glacialis*. In addition, the patch of high Appendicularia biomass resulted in an estimated grazing impact similar to that of all *Calanus* spp. together. Those results show how patchiness can result in a local boost of carbon demand and therefore lower algae carbon export to other trophic levels. The results also show that determination of grazing pressure on ice algae should consider all dominant taxa when attempting to estimate carbon fluxes in a holistic

assessment. By comparison, the mean carbon demand of the under-ice fauna in our study was one order of magnitude higher than that estimated for the central Arctic Ocean in autumn (0.3 mg C m^{-2} day^{-1}, Flores et al., 2019).

As a key feeder on ice algae, *C. glacialis* is timing its seasonal migration and reproduction to the ice-algal bloom (Søreide et al., 2010; Leu et al., 2011). Thus, ongoing sea-ice melt may cause a mismatch between the bloom and developmental stages of *C. glacialis*, or may cause decreasing ice-algal production in the long run as ice cover declines. Both aspects are considered to entail negative consequences for the entire Arctic marine food web. However, some studies predict a replacement of *C. glacialis* by the smaller (and less energy-rich) *C. finmarchicus* with increasing Atlantification (Bonnet et al., 2005; Richardson, 2008; Polyakov et al., 2017). The higher carbon demand and biomass of *C. finmarchicus* compared to *C. glacialis* in this study could be seen as an indication for the hypothesized replacement. As for biomass and carbon demand also the estimated secondary production of the under-ice fauna was one order of magnitude higher in our study (0.3 mg C m^{-2} day^{-1}) compared to the study of Flores et al. (2019) in the central Arctic Ocean in autumn (0.1 mg C m^{-2} day^{-1}). The seasonal population growth of copepods in our study compared to post-bloom collapse and beginning seasonal migration at the end of summer (David et al., 2015) is probably a major reason for this difference.

Cryopelagic coupling

Our study is the first with a comprehensive approach to determine the trophic dependencies between the sympagic fauna and flora assemblages of the Arctic pack-ice in spring (Figure 6). By identifying the dominating biomass and demand of herbivorous key taxa, we aimed to disentangle the roles of ice-algal and phytoplankton in our study area (Figure 6). Our results show that the potential demand for ice-algal carbon was 30 % of that for phytoplankton, which highlights the current importance of ice algae for the survival of sympagic communities. In general, growth and successful reproduction of higher trophic levels are equally dependent on the quantity and quality of algae. Ice algae are not only known to constitute a high quality food source (Leu et al., 2011; Kohlbach et al., 2016), they also provide *Calanus* spp. and other key taxa of the sympagic realm with carbon weeks before the phytoplankton bloom develops and, thus, ensure successive reproduction (Søreide et al., 2010).

Our study shows that sympagic herbivores do not have the potential to control ice-algal production or phytoplankton production in the Arctic spring (Figure 6). Thus, a surplus of approximately 9.1 mg C m^{-2} day^{-1} of ice-algal carbon and 26.2 mg C m^{-2} day^{-1} of (under-ice) phytoplankton carbon could potentially sink to the pelagic and benthic habitats to provide carbon for the deeper living communities and for sedimentation. It should be considered, though, that the pelagic grazers sampled in the under-ice habitat (especially *Calanus* spp.) constituted only a fraction of their total

population in the upper 100 m, which is in constant exchange with the under-ice environment. This implies that a large proportion of the remaining algal production is probably consumed in the epipelagic layer, before sinking into even deeper layers.

A different pattern was apparent for the carnivorous sympagic fauna whose estimated carbon demand was hardly covered by the sympagic secondary production. This could indicate that the sea-ice habitat is characterized by high competition for prey, and secondary production in the under-ice water layer may be controlled by predators. It is also possible that under-ice predators fed on microzooplankton (Verity et al., 2002), which was not efficiently caught with the 300µm net of the SUIT and is therefore under-estimated in our secondary production calculations. Furthermore, we assume that most carnivores (Chaetognatha, *Themisto* spp.) are vertically mobile and cover a part of their carbon demand from deeper-dwelling prey. Polar cod (*Boreogadus saida*) is an important predator (David et al., 2016), which is not considered in this study. Young polar cod inhabit the under-ice water layer and feed on *A. glacialis*, *Calanus* spp. and the harpacticoid *Tisbe* spp. (Kohlbach et al., 2017). During the sampling for the present study, polar cod were caught in low numbers with the larger 7mm (half-mesh) SUIT net (data not shown), but appear to be underestimated in the catches (David et al., 2016). Therefore, an unknown but likely significant additional carbon demand of this species would need to be added to the carbon budget.

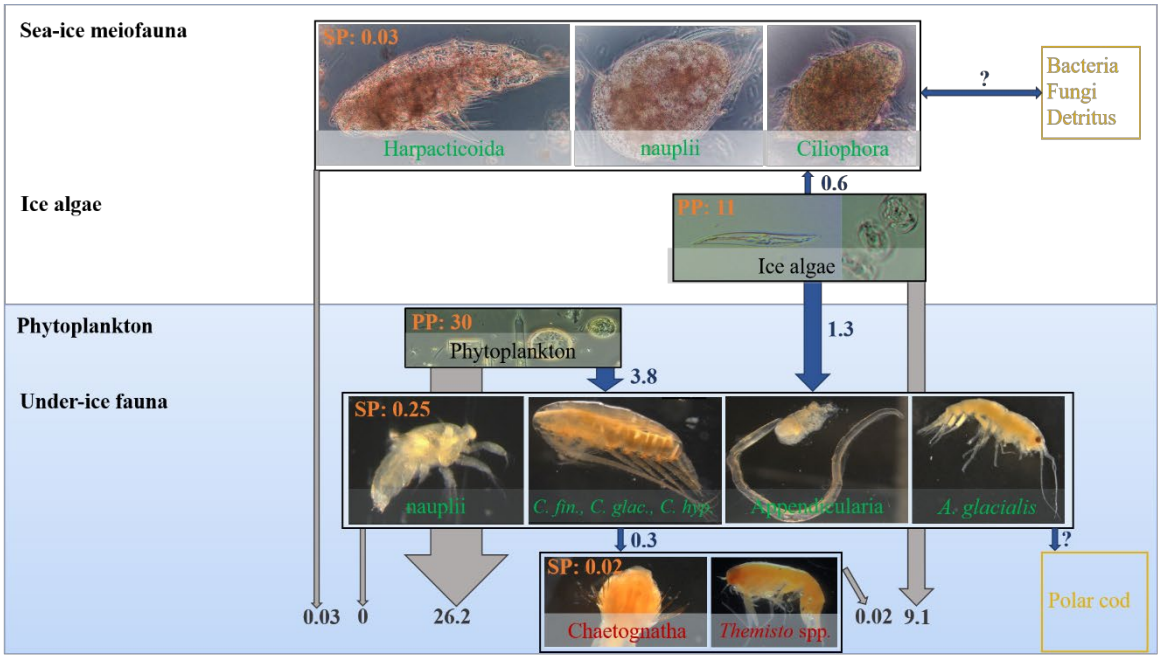

Figure 6: Carbon flux of sympagic biota. Estimated trophic relationships regarding carbon production, consumption, and carbon export (all values are means in mg C m^{-2} day^{-1}) for the sympagic biota of the Atlantic inflow area north of Svalbard in spring. Font colors: green= key taxa of this study which are considered to be mainly herbivorous; red= key taxa of this study which are considered to be carnivorous, yellow= other taxa, which are not included in this study, orange= mean production rate for the respective compartment of the sympagic biota, blue= mean ingestion of the respective consumer, grey= estimated carbon surplus from the respective sympagic compartment which is potentially released to the water column (arrows point in the direction of possible carbon flux; thickness of arrows corresponds to the amount of carbon flux). PP=primary production, SP= secondary production. Photographs by Julia Ehrlich.

Conclusions

Putting together a carbon budget that compiles the biomass, carbon demand, and production of sympagic biota shows that our estimates essentially match the ten percent law of transfer of energy from one trophic level to another (Lindeman, 1942). The level of sympagic primary production in Arctic spring was more than sufficient to cover the carbon demand of the herbivorous sympagic fauna both in and under Arctic pack ice. Under-ice fauna was the main contributor to the cryo-pelagic carbon flux, whereas the contribution of sea-ice meiofauna was low. The three *Calanus* species (*C. finmarchicus, C. glacialis, and C. hyperboreus*) dominated the grazing impact under the ice both on ice algae and phytoplankton. Our quantitative assessment supports the notion that the three *Calanus* species are key drivers of the Arctic marine ecosystem, transferring energy-rich lipid compounds and essential fatty acids to higher trophic levels. Since those species rely on ice algae as food source besides phytoplankton (Kohlbach et al., 2016), the predicted sea-ice loss and with it the decrease of ice algae will lead to a shift in carbon sources for those herbivorous taxa. Phytoplankton production may help to offset potential decreases of ice-algal production to a certain extent. However, a restriction of the ice-algal bloom would also increase the probability of a potential mismatch in particular for the ontogenetic development of *C. glacialis*. The secondary production of the sympagic fauna was hardly sufficient to support the carbon demand of carnivorous under-ice taxa. Subsequently, predators might evade into deeper realms to fulfil their carbon demands. Our results show how important the under-ice fauna is in particular for the maintenance of the carbon flux from the sea ice to deeper living communities.

Contributions

JE, HF, AB, and BB designed the study. HF, FS, GC, and IP conducted the field work and sample collection. JE and BB analyzed the meiofauna samples. JE and FS analyzed the under-ice fauna samples. IP determined the chlorophyll *a* concentration in the sea-ice samples. GC modeled chl *a* concentration in the ice and the 0-2 water column for all SUIT stations. JE calculated the biomass of ice-algae and phytoplankton for all stations. PM calculated the primary production of ice algae and phytoplankton for all stations. JE calculated the biomass, carbon demand, and secondary production of sea-ice meiofauna and under-ice fauna for all stations. JE analyzed the data, wrote the manuscript and prepared all figures and tables. JE, BB, HF, and IP contributed to data interpretation. All authors contributed to different versions of the manuscript.

Competing interests

The authors declare that the research was conducted in the absence of any commercial or financial relationships that could be construed as a potential conflict of interest.

Acknowledgments

We thank the Captain and crew of the Polarstern expedition PS92 for their support and guidance with work at sea. We thank Michiel van Dorssen and André Meijboom for their great help during the fieldwork. The SUIT for this study was kindly provided by Jan Andries van Franeker. We acknowledge support by the Open Access Publication Funds of Alfred-Wegener-Institut Helmholtz-Zentrum für Polar- und Meeresforschung.

Funding

JE was funded by the national scholarships "Promotionsstipendium nach dem Hamburger Nachwuchsfördergesetz (HmbNFG)" and "Gleichstellungsfond 2017 (4-GLF-2017)", both granted by the University of Hamburg. The German Academic Exchange Service (DAAD) and the graduate school "POLMAR" at Alfred Wegener Institute Bremerhaven supported JE's visit at The Arctic University of Norway's Institute of Arctic and Marine Biology. BB's contribution was under the framework of the Arctic Seasonal Ice Zone Ecology project, co-funded by UiT - The Arctic University of Norway and the Tromsø Research Foundation (project number 01vm/h15). IP, JE, GC, and HF were funded by the PACES (Polar Regions and Coasts in a Changing Earth System) programme of the Helmholtz Association and the expedition Grant No AWI_PS92_00 and the programme-oriented research period 4 (POF4) Earth and Environment fund of the Helmholtz association. HF, JE, and GC were part of the Helmholtz Association Young Investigators Groups *Iceflux*: Ice-ecosystem carbon flux in polar oceans (VH-NG-800). FS received support from The Netherlands Ministry of Agriculture, Nature and Food Quality (LNV) under its Statutory Research Task Nature and Environment WOT-04-009-047.04. The Netherlands Polar Programme (NPP), managed by the Dutch Research Council (NWO) funded this research under project nr. ALW 866.13.009. AB work is funded by the Leibnitz Association.

Supplemental material

Table S 1: Carbon content, mass-specific ingestion rate, and trophic type for all taxa of sea-ice meiofauna (docx)

Table S 2: Carbon content, mass specific ingestion rate, and trophic type for all taxa of under-ice fauna (docx)

Data accessibility statement

All data will be available from the PANGAEA database and doi will be provided upon publication.

References

Arctic Council Secretariat. 2017. State of the Arctic Marine Biodiversity Report. Conservation of Arctic Flora and Fauna. *Arctic Council Secretariat.*

Ardyna M, Arrigo KR. 2020. Phytoplankton dynamics in a changing Arctic Ocean. *Nature Climate Change*. doi:10.1038/s41558-020-0905-y.

Ardyna M, Babin M, Gosselin M, Devred E, Rainville L, et al. 2014. Recent Arctic Ocean sea ice loss triggers novel fall phytoplankton blooms. *Geophysical Research Letters* **41**(17): 6207-6212.

Arrigo KR, van Dijken GL. 2015. Continued increases in Arctic Ocean primary production. *Progress in Oceanography* **136**: 60-70.

Assmy P, Fernández-Méndez M, Duarte P, Meyer A, Randelhoff A, et al. 2017. Leads in Arctic pack ice enable early phytoplankton blooms below snow-covered sea ice. *Scientific reports* **7**: 40850.

Auel H, Hagen W. 2002. Mesozooplankton community structure, abundance and biomass in the central Arctic Ocean. *Marine Biology* **140**(5): 1013-1021.

Berge J, Varpe Ø, Moline M, Wold A, Renaud P, et al. 2012. Retention of ice-associated amphipods: possible consequences for an ice-free Arctic Ocean. *Biology Letters* **8**(6): 1012-1015.

Beszczynska-Möller A, Fahrbach E, Schauer U, Hansen E. 2012. Variability in Atlantic water temperature and transport at the entrance to the Arctic Ocean, 1997–2010. *ICES Journal of Marine Science* **69**(5): 852-863.

Bluhm BA, Gebruk AV, Gradinger R, Hopcroft RR, Huettmann F, et al. 2011. Arctic Marine Biodiversity: An Update of Species Richness and Examples of Biodiversity Change. *Oceanography* **24**(3): 232-248.

Bluhm BA, Hop H, Vihtakari M, Gradinger R, Iken K, et al. 2018. Sea ice meiofauna distribution on local to pan-Arctic scales. *Ecol Evol* **8**(4): 2350-2364. doi:10.1002/ece3.3797.

Bonnet D, Richardson A, Harris R, Hirst A, Beaugrand G, et al. 2005. An overview of Calanus helgolandicus ecology in European waters. *Progress in Oceanography* **65**(1): 1-53.

Bradstreet MS, Cross WE. 1982. Trophic relationships at high Arctic ice edges. *Arctic*: 1-12.

Campbell RG, Ashjian CJ, Sherr EB, Sherr BF, Lomas MW, et al. 2016. Mesozooplankton grazing during spring sea-ice conditions in the eastern Bering Sea. *Deep Sea Research Part II: Topical Studies in Oceanography* **134**: 157-172.

Campitelli E. 2019. ggnewscale: Multiple Fill and Color Scales in 'ggplot2 '. *R package version 02 0 URL: https://CRAN R-project org/package= ggnewscale*.

Castellani G, Losch M, Lange BA, Flores H. 2017. Modeling Arctic sea-ice algae: Physical drivers of spatial distribution and algae phenology. *Journal of Geophysical Research: Oceans* **122**(9): 7466-7487.

Castellani G, Schaafsma FL, Arndt S, Lange BA, Peeken I, et al. 2020. Large-Scale Variability of Physical and Biological Sea-Ice Properties in Polar Oceans. *Frontiers in Marine Science* **7**: 536.

Daase M, Hop H, Falk-Petersen S. 2016. Small-scale diel vertical migration of zooplankton in the High Arctic. *Polar Biology* **39**(7): 1213-1223.

Dalpadado P. 2002. Inter-specific variations in distribution, abundance and possible life-cycle patterns of Themisto spp.(Amphipoda) in the Barents Sea. *Polar Biology* **25**(9): 656-666.

Darnis G, Barber DG, Fortier L. 2008. Sea ice and the onshore–offshore gradient in pre-winter zooplankton assemblages in southeastern Beaufort Sea. *Journal of Marine Systems* **74**(3-4): 994-1011.

Darnis G, Hobbs L, Geoffroy M, Grenvald JC, Renaud P, et al. 2017. From polar night to midnight sun: Diel vertical migration, metabolism and biogeochemical role of zooplankton in a high Arctic fjord (Kongsfjorden, Svalbard). *Limnology and Oceanography* **62**(4): 1586-1605.

Daufresne M, Lengfellner K, Sommer U. 2009. Global warming benefits the small in aquatic ecosystems. *Proceedings of the National Academy of Sciences* **106**(31): 12788-12793.

David C, Lange B, Krumpen T, Schaafsma F, van Franeker JA, et al. 2016. Under-ice distribution of polar cod Boreogadus saida in the central Arctic Ocean and their association with sea-ice habitat properties. *Polar Biology* **39**(6): 981-994.

David C, Lange B, Rabe B, Flores H. 2015. Community structure of under-ice fauna in the Eurasian central Arctic Ocean in relation to environmental properties of sea-ice habitats. *Marine Ecology Progress Series* **522**: 15-32. doi:10.3354/meps11156.

Deibel D. 1988. Filter feeding by Oikopleura vanhoeffeni: grazing impact on suspended particles in cold ocean waters. *Marine Biology* **99**(2): 177-186.

Dunnington D. 2018. ggspatial: Spatial Data Framework for ggplot2. *URL: https://cran r-project org/package= ggspatial*.

Dupont F. 2012. Impact of sea-ice biology on overall primary production in a biophysical model of the pan-Arctic Ocean. *Journal of Geophysical Research: Oceans* **117**(C8). doi:10.1029/2011jc006983.

Ehrlich J, Schaafsma FL, Bluhm BA, Peeken I, Castellani G, et al. 2020. Sympagic Fauna in and Under Arctic Pack Ice in the Annual Sea-Ice System of the New Arctic. *Frontiers in Marine Science* **7**(452). doi:10.3389/fmars.2020.00452.

Fernández-Méndez M, Katlein C, Rabe B, Nicolaus M, Peeken I, et al. 2015. Photosynthetic production in the central Arctic Ocean during the record sea-ice minimum in 2012. *Biogeosciences* **12**(11): 3525-3549.

Flores H, David C, Ehrlich J, Hardge K, Kohlbach D, et al. 2019. Sea-ice properties and nutrient concentration as drivers of the taxonomic and trophic structure of high-Arctic protist and metazoan communities. *Polar Biology* **42**(7): 1377-1395.

Forest A, Coupel P, Else B, Nahavandian S, Lansard B, et al. 2014. Synoptic evaluation of carbon cycling in the Beaufort Sea during summer: contrasting river inputs, ecosystem metabolism and air–sea CO2 fluxes. *Biogeosciences* **11**(10): 2827-2856.

Fortier M, Fortier L, Hattori H, Saito H, Legendre L. 2001. Visual predators and the diel vertical migration of copepods under Arctic sea ice during the midnight sun. *Journal of Plankton Research* **23**(11): 1263-1278.

Friedrich C. 1997. Ökologische Untersuchungen zur Fauna des arktischen Meereises. *Ber zur Polarforschung*.

Garrison DL, Buck KR. 1986. Organism losses during ice melting: a serious bias in sea ice community studies. *Polar Biology* **6**(4): 237-239.

Gosselin M, Levasseur M, Wheeler PA, Horner RA, Booth BC. 1997. New measurements of phytoplankton and ice algal production in the Arctic Ocean. *Deep Sea Research Part II: Topical Studies in Oceanography* **44**(8): 1623-1644.

Gradinger R. 1999a. Integrated abundance and biomass of sympagic meiofauna in Arctic and Antarctic pack ice. *Polar Biology* **22**(3): 169-177.

Gradinger R. 1999b. Vertical fine structure of the biomass and composition of algal communities in Arctic pack ice. *Marine Biology* **133**(4): 745-754.

Gradinger R. 2009. Sea-ice algae: Major contributors to primary production and algal biomass in the Chukchi and Beaufort Seas during May/June 2002. *Deep Sea Research Part II: Topical Studies in Oceanography* **56**(17): 1201-1212.

Gradinger R, Bluhm BA. 2020. First analysis of an Arctic sea ice meiofauna food web based on abundance, biomass and stable isotope ratios. *Marine Ecology Progress Series* **634**: 29-43.

Gradinger R, Friedrich C, Spindler M. 1999. Abundance, biomass and composition of the sea ice biota of the Greenland Sea pack ice. *Deep Sea Research Part II: Topical Studies in Oceanography* **46**(6-7): 1457-1472.

Gradinger RR, Kaufman MR, Bluhm BA. 2009. Pivotal role of sea ice sediments in the seasonal development of near-shore Arctic fast ice biota. *Marine Ecology Progress Series* **394**: 49-63.

Grainger E, Hsiao SI. 1990. Trophic relationships of the sea ice meiofauna in Frobisher Bay, Arctic Canada. *Polar Biology* **10**(4): 283-292.

Grebmeier JM, Moore SE, Overland JE, Frey KE, Gradinger R. 2010. Biological response to recent Pacific Arctic sea ice retreats. *Eos, Transactions American Geophysical Union* **91**(18): 161-162.

Hop H, Pavlova O. 2008. Distribution and biomass transport of ice amphipods in drifting sea ice around Svalbard. *Deep Sea Research Part II: Topical Studies in Oceanography* **55**(20-21): 2292-2307.

Hop H, Vihtakari M, Bluhm BA, Assmy P, Poulin M, et al. 2020. Changes in Sea-Ice Protist Diversity With Declining Sea Ice in the Arctic Ocean From the 1980s to 2010s. *Frontiers in Marine Science* **7**(243). doi:10.3389/fmars.2020.00243.

Hughes T, Bellwood D, Baird A, Brodie J, Bruno J, et al. 2011. Shifting base-lines, declining coral cover, and the erosion of reef resilience: comment on Sweatman et al.(2011). *Coral Reefs* **30**(3): 653-660.

Kassambara A. 2020. Package 'ggpubr'.

Kiko R, Kern S, Kramer M, Mütze H. 2017. Colonization of newly forming Arctic sea ice by meiofauna: a case study for the future Arctic? *Polar Biology* **40**(6): 1277-1288.

Kohlbach D, Graeve M, A. Lange B, David C, Peeken I, et al. 2016. The importance of ice algae-produced carbon in the central Arctic Ocean ecosystem: Food web relationships revealed by lipid and stable isotope analyses. *Limnology and Oceanography* **61**(6): 2027-2044.

Kohlbach D, Schaafsma FL, Graeve M, Lebreton B, Lange BA, et al. 2017. Strong linkage of polar cod (Boreogadus saida) to sea ice algae-produced carbon: evidence from stomach content, fatty acid and stable isotope analyses. *Progress in Oceanography* **152**: 62-74.

Kosobokova K, Hirche H-J. 2009. Biomass of zooplankton in the eastern Arctic Ocean–a base line study. *Progress in Oceanography* **82**(4): 265-280.

Kramer M. 2011. The role of sympagic meiofauna in Arctic and Antarctic sea-ice food webs.

Krumpen T, Belter HJ, Boetius A, Damm E, Haas C, et al. 2019. Arctic warming interrupts the Transpolar Drift and affects long-range transport of sea ice and ice-rafted matter. *Scientific reports* **9**(1): 5459.

Lange BA, Katlein C, Castellani G, Fernández-Méndez M, Nicolaus M, et al. 2017. Characterizing spatial variability of ice algal chlorophyll a and net primary production between sea ice habitats using horizontal profiling platforms. *Frontiers in Marine Science* **4**: 349.

Lange BA, Katlein C, Nicolaus M, Peeken I, Flores H. 2016. Sea ice algae chlorophyll a concentrations derived from under-ice spectral radiation profiling platforms. *Journal of Geophysical Research: Oceans* **121**(12): 8511-8534.

Leu E, Mundy C, Assmy P, Campbell K, Gabrielsen T, et al. 2015. Arctic spring awakening–Steering principles behind the phenology of vernal ice algal blooms. *Progress in Oceanography* **139**: 151-170.

Leu E, Søreide J, Hessen D, Falk-Petersen S, Berge J. 2011. Consequences of changing sea-ice cover for primary and secondary producers in the European Arctic shelf seas: timing, quantity, and quality. *Progress in Oceanography* **90**(1-4): 18-32.

Lewis MR, Smith JC. 1983. A small volume, short-incubation-time method for measurement of photosynthesis as a function of incident irradiance. *Marine ecology progress series Oldendorf* **13**(1): 99-102.

Li WK, McLaughlin FA, Lovejoy C, Carmack EC. 2009. Smallest algae thrive as the Arctic Ocean freshens. *Science* **326**(5952): 539-539.

Lindeman RL. 1942. The trophic-dynamic aspect of ecology. *Ecology* **23**(4): 399-417.

Lønne O, Gulliksen B. 1991. Sympagic macro-fauna from multiyear sea-ice near Svalbard. *Polar Biology* **11**(7): 471-477.

Massicotte P, Peeken I, Katlein C, Flores H, Huot Y, et al. 2019. Sensitivity of phytoplankton primary production estimates to available irradiance under heterogeneous sea ice conditions. *Journal of Geophysical Research: Oceans* **124**(8): 5436-5450.

Matrai P, Olson E, Suttles S, Hill V, Codispoti L, et al. 2013. Synthesis of primary production in the Arctic Ocean: I. Surface waters, 1954–2007. *Progress in Oceanography* **110**: 93-106.

Moloney CL, Field JG. 1989. General allometric equations for rates of nutrient uptake, ingestion, and respiration in plankton organisms. *Limnology and Oceanography* **34**(7): 1290-1299.

Moran S, Kelly R, Hagstrom K, Smith J, Grebmeier J, et al. 2005. Seasonal changes in POC export flux in the Chukchi Sea and implications for water column-benthic coupling in Arctic shelves. *Deep Sea Research Part II: Topical Studies in Oceanography* **52**(24-26): 3427-3451.

Nicolaus M, Katlein C. 2013. Mapping radiation transfer through sea ice using a remotely operated vehicle (ROV). *The Cryosphere* **7**: 763-777.

Nöthig E-M, Lalande C, Fahl K, Metfies K, Salter I, et al. 2020. Annual cycle of downward particle fluxes on each side of the Gakkel Ridge in the central Arctic Ocean. *Philosophical Transactions of the Royal Society A* **378**(2181): 20190368.

Nozais C, Gosselin M, Michel C, Tita G. 2001. Abundance, biomass, composition and grazing impact of the sea-ice meiofauna in the North Water, northern Baffin Bay. *Marine Ecology Progress Series* **217**: 235-250. doi:10.3354/meps217235.

Pante E, Simon-Bouhet B. 2013. marmap: a package for importing, plotting and analyzing bathymetric and topographic data in R. *PLoS One* **8**(9): e73051.

Pebesma EJ. 2018. Simple features for R: Standardized support for spatial vector data. *R J* **10**(1): 439.

Peeken I. 2020. Chemtax based phytoplankton group composition during POLARSTERN cruise PS92 [dataset]. Available at https://doi.org/10.1594/PANGAEA.917802.

Polyakov IV, Pnyushkov AV, Alkire MB, Ashik IM, Baumann TM, et al. 2017. Greater role for Atlantic inflows on sea-ice loss in the Eurasian Basin of the Arctic Ocean. *Science* **356**(6335): 285-291. doi:10.1126/science.aai8204.

Poulin M, Daugbjerg N, Gradinger R, Ilyash L, Ratkova T, et al. 2011. The pan-Arctic biodiversity of marine pelagic and sea-ice unicellular eukaryotes: a first-attempt assessment. *Marine Biodiversity* **41**(1): 13-28.

Raskoff K, Hopcroft R, Kosobokova K, Purcell J, Youngbluth M. 2010. Jellies under ice: ROV observations from the Arctic 2005 hidden ocean expedition. *Deep Sea Research Part II: Topical Studies in Oceanography* **57**(1-2): 111-126.

Richardson AJ. 2008. In hot water: zooplankton and climate change. *ICES Journal of Marine Science* **65**(3): 279-295.

Rudels B, Jones EP, Schauer U, Eriksson P. 2004. Atlantic sources of the Arctic Ocean surface and halocline waters. *Polar Research* **23**(2): 181-208.

Rudels B, Schauer U, Björk G, Korhonen M, Pisarev S, et al. 2013. Observations of water masses and circulation in the Eurasian Basin of the Arctic Ocean from the 1990s to the late 2000s. *OS Special Issue: Ice-Atmosphere-Ocean interactions in the Arctic Ocean during IPY: the Damocles project* **9**(1): 147-169.

Saito H, Kiørboe T. 2001. Feeding rates in the chaetognath Sagitta elegans: effects of prey size, prey swimming behaviour and small-scale turbulence. *Journal of Plankton Research* **23**(12): 1385-1398.

Scott CL, Falk-Petersen S, Sargent JR, Hop H, Lønne OJ, et al. 1999. Lipids and trophic interactions of ice fauna and pelagic zooplankton in the marginal ice zone of the Barents Sea. *Polar Biology* **21**(2): 65-70.

Søreide JE, Carroll ML, Hop H, Ambrose Jr WG, Hegseth EN, et al. 2013. Sympagic-pelagic-benthic coupling in Arctic and Atlantic waters around Svalbard revealed by stable isotopic and fatty acid tracers. *Marine Biology Research* **9**(9): 831-850.

Søreide JE, Leu E, Berge J, Graeve M, Falk-Petersen S. 2010. Timing of blooms, algal food quality and Calanus glacialis reproduction and growth in a changing Arctic. *Global change biology* **16**(11): 3154-3163.

South A. 2017. rnaturalearth: World map data from natural earth. *R package version 01 0*.

South A. 2020. rnaturalearthhires: High Resolution World Vector Map Data from Natural Earth used in rnaturalearth.

Stevens C, Deibel D, Parrish C. 2004. Species-specific differences in lipid composition and omnivory indices in Arctic copepods collected in deep water during autumn (North Water Polynya). *Marine Biology* **144**(5): 905-915.

Team RC. 2018. R: A Language and Environment for Statistical Computing: A Graduate Course in Probability. R Foundation for Statistical Computing, Vienna, Austria.

Tedesco L, Vichi M, Scoccimarro E. 2019. Sea-ice algal phenology in a warmer Arctic. *Science Advances* **5**(5): eaav4830.

Tran S, Bonsang B, Gros V, Peeken I, Sarda-Esteve R, et al. 2013. A survey of carbon monoxide and non-methane hydrocarbons in the Arctic Ocean during summer 2010. *Biogeosciences* **10**: 1909-1935.

Van Franeker JA, Flores H, Van Dorssen M. 2009. The surface and under ice trawl (SUIT). *Frozen Desert Alive-The role of sea ice for pelagic macrofauna and its predators PhD thesis University of Groningen*: 181-188.

Verity PG. 1991. Measurement and simulation of prey uptake by marine planktonic ciliates fed plastidic and aplastidic nanoplankton. *Limnology and Oceanography* **36**(4): 729-750.

Verity PG, Wassmann P, Frischer M, Howard-Jones M, Allen A. 2002. Grazing of phytoplankton by microzooplankton in the Barents Sea during early summer. *Journal of marine systems* **38**(1-2): 109-123.

Vernet M, Richardson TL, Metfies K, Nöthig E-M, Peeken I. 2017. Models of plankton community changes during a warm water anomaly in arctic waters show altered trophic pathways with minimal changes in carbon export. *Frontiers in Marine Science* **4**: 160.

Welch HE, Bergmann MA, Siferd TD, Martin KA, Curtis MF, et al. 1992. Energy flow through the marine ecosystem of the Lancaster Sound region, arctic Canada. *Arctic*: 343-357.

Werner I. 1997. Grazing of Arctic under-ice amphipods on sea-ice algae. *Marine Ecology Progress Series* **160**: 93-99.

Werner I. 2006. Seasonal dynamics of sub-ice fauna below pack ice in the Arctic (Fram Strait). *Deep Sea Research Part I: Oceanographic Research Papers* **53**(2): 294-309.

Werner I, Auel H. 2005. Seasonal variability in abundance, respiration and lipid composition of Arctic under-ice amphipods. *Marine Ecology Progress Series* **292**: 251-262.

Wickham H. 2016. *ggplot2: elegant graphics for data analysis*. Springer.

Wickham H, Seidel D. 2020. Scales: Scale functions for visualization. R package version 1.1. 1.

Wiedmann I, Ershova E, Bluhm BA, Nöthig E-M, Gradinger RR, et al. 2020. What Feeds the Benthos in the Arctic Basins? Assembling a Carbon Budget for the Deep Arctic Ocean. *Frontiers in Marine Science* **7**: 224.

Supplementary Material

Table S 1: Carbon content, mass-specific ingestion rate, and trophic type for all taxa of sea-ice meiofauna

Sea-ice meiofauna	Carbon content (µg C ind.$^{-1}$)	Reference	MSI Rate[a] (of body C day^{-1})	Reference	Trophic type[b]	Reference
Harpacticoida sp.	0.600	Friedrich (1997)	0.53	Gradinger (1999)	H	Kramer (2011)
Nauplii (Copepoda)	0.020	Friedrich (1997)	1.24	Gradinger (1999)	H-O	Kramer (2011)
Ciliophora	0.011	Friedrich (1997)	1.43	Gradinger (1999)	Het	Kramer (2011)
Tintinnina	0.011	Friedrich (1997)	1.43	Gradinger (1999)	Het	Kramer (2011)
Dinophyceae	0.005	Menden-Deuer & Lessard (2000)	1.73	Gradinger (1999)	Mix	Kramer (2011)
Rotifera	0.023	Friedrich (1997)	1.19	Gradinger (1999)	Het	Kramer (2011)
Amoebozoa	0.011	Friedrich (1997)	1.43	Gradinger (1999)	Het	Kramer (2011)

[a] Equation, which was used for calculation of mass specific ingestion rate after Gradinger 1999 (from Moloney and Field, 1989): $I_{max} = 63*M^{(-0.25)}*0.23326$.

[b] H, herbivorous; O, omnivorous; C, carnivorous

Table S 2: Carbon content, mass specific ingestion rate, and trophic type for all taxa of under-ice fauna

Under-ice fauna	Carbon content (µg C ind^{-1})	Reference	MSI Rate[a] (of body C day^{-1})	Reference	Trophic type[b]	Reference
Tisbe spp.	0.6	Friedrich (1997)	0.20	*	H - O	Grainger et al. (1985)
Oithona sp.	1.3	Ashijan et al. (2003)	0.20	*	O - C	Grainger et al. (1985)
C. hyperboreus					H - O	Stevens et al. (2004)
CI	4.6	Ashijan et al. (2003)	0.25	Campbell et al. (2016)		
CII	16.6	Ashijan et al. (2003)	0.25	Campbell et al. (2016)		
CIII	58.4	Ashijan et al. (2003)	0.25	Campbell et al. (2016)		
CIV	214.9	Ashijan et al. (2003)	0.25	Campbell et al. (2016)		
CV	713.0	Ashijan et al. (2003)	0.12	Campbell et al. (2016)		
AF	2635.7	Ashijan et al. (2003)	0.12	Campbell et al. (2016)		
C. glacialis					H - O	Stevens et al. (2004)

CI	5.0	Eilertsen et al.(1989)	0.25	Campbell et al. (2016)		
CII	17.0	Eilertsen et al.(1989)	0.25	Campbell et al. (2016)		
CIII	46.5	Eilertsen et al.(1989)	0.25	Campbell et al. (2016)		
CIV	100.0	Ashijan et al. (2003)	0.25	Campbell et al. (2016)		
CV	382.7	Ashijan et al. (2003)	0.12	Campbell et al. (2016)		
AF	577.2	Ashijan et al. (2003)	0.12	Campbell et al. (2016)		
C. finmarchicus					H - O	Stevens et al. (2004)
CF I	72.0	Campbell et al. (2016)	0.25	Campbell et al. (2016)		
CF II	72.0	Campbell et al. (2016)	0.25	Campbell et al. (2016)		
CF III	72.0	Campbell et al. (2016)	0.25	Campbell et al. (2016)		
CF IV	72.0	Campbell et al. (2016)	0.25	Campbell et al. (2016)		
CF V	252.0	Campbell et al. (2016)	0.12	Campbell et al. (2016)		
AF	252.0	Campbell et al. (2016)	0.12	Campbell et al. (2016)		
Nauplii	2.5	Ashijan et al. (2003)	0.25	Irigoien et al. (2003)	H	Hopcroft (2005)
Paraeuchaeta spp.	3269.6	Mumm (1991), AFDW[mg]=0.0075* PL[mm]^3.274, PL=6.4	0.20	*	C	Hopcroft (2005)
Metridia longa	182.4	Ashijan et al. (2003)	0.20	*	O - C	Falk-Petersen et al. (1987)
Clausocalanidae	10.4	Campbell et al. (2016), for Pseudocalanus	0.20	*	H - O	Norrbin et al. (1990)
Themisto spp.	1836.4	DW=0.0005*L[mm]^ 3.4189, L=15 (F.L. Schaafsma pers. comm.), C=0.35 DW (N. Zakharova pers. comm.)	0.025	Auel & Werner (2003), based on their allometric approach body dry mass vs ingestion for *T. libellula*	O - C	Falk-Petersen et al. (1987)
Themisto libellula	1836.4	DW=0.0005*L[mm]^3.4189, L=15 (F.L. Schaafsma pers. comm.), C=0.35 DW (N. Zakharova, pers. comm.)	0.025	Auel & Werner (2003), based on their allometric approach body dry mass vs ingestion for *T. libellula*	O	Scott et al. (1999)

Apherusa glacialis	875.0	DW=5.247 mg (Werner, 1997), C=0.35 DW (N. Zakharova pers. comm.)	0.025	same as for *T. libellula*	H	Kohlbach et al. (2016)
Onisimus glacialis	4235.0	DW=12.1 mg (Werner, 1997), C=0.35 DW (N. Zakharova pers. comm.)	0.025	same as for *T. libellula*	O	Bradstreet & Cross (1982)
Thysanoessa longicaudata	579.5	DW=0.000291*L[mm]^ 3.5451962, L=10.7 (F.L. Schaafsma pers. comm.), C=0.45 DW (N. Zakharova pers. comm.)	0.20	*	O	Hopcroft (2005)
Isopoda	100.0	Ashijan et al. (2003)	0.20	*	O	Hopcroft (2005)
Zoaea larvae	2.5	Ashijan et al. (2003)	0.20	*	O - C	Arndt & Swadling (2006)
Cirripedia nauplii	2.5	Ashijan et al. (2003)	0.20	*	H	Arndt & Swadling (2006)
Limacina helicina	113.1	Mizdalski (1988)	0.20	*	H	Hopcroft (2005)
Clione limacina	9264.0	Mizdalski (1988)	0.20	*	C	Hopcroft (2005)
Polychaeta	0.1	Donnelly et al. (1994)	0.20	*	O	Hopcroft (2005)
Trochophora larvae	2.1	Anger et al. (1986)	0.20	*	O	Hopcroft (2005)
Chaetognatha	767.1	MW of *Eukrohnia hamata* and *Parasagitta elegans*	0.17	Saito & Kiorboe (2001)	C	Hopcroft (2005)
Eukrohnia hamata	1004.9	Log10DM[µg] = 3.32Log10TL[mm]-1.14 (Imao 2005), TL= 21.3 (measured), C= 54.2% DW (Donnelly et al. 1994)	0.17	Saito &, Kiorboe (2001)	C	Hopcroft (2005)
Parasagitta elegans	529.4	Log10DM[µg] = 2.91Log10TL[mm]-0.79 (Imao 2005), TL= 21.2 (measured), C= 45.3% DW (Donnelly et al. 1994)	0.17	Saito & Kiorboe (2001)	C	Hopcroft (2005)
Appendicularia	8.4	LogC[µg]=3.2*LogTL[µm]-8.93 (Deibel 1988), TL=12mm (measured)	0.64	Deibel (1988)	H	Hopcroft (2005)

Hydrozoa	3.3	DW[mg]=0.00194*TL[mm]^3.05 (Matthews & Hestad (1977) for Aglantha digitale, TL=2mm (measured), C=20.4% DW (Runge et al. 1987)	0.20	*	C	Hopcroft (2005)
Osteichthyes larvae	17.2	Harris et al. (1986)	0.20	*	C	Hopcroft (2005)
Xenacoelomorpha	0.4	Friedrich (1997)	0.20	*	O	Kramer (2011)

[a] Where ingestion rate is * the rate was calculated from the mean ingestion rate of taxa who made up 99.5 % of the biomass

[b] H, herbivorous; O, omnivorous; C, carnivorous

References supplementary material

Anger K, Anger V, Hagmeier E. 1986. Laboratory studies on larval growth ofPolydora ligni, Polydora ciliata, andPygospio elegans (Polychaeta, Spionidae). *Helgoländer Meeresuntersuchungen* **40**(4): 377-395.

Arndt CE, Swadling KM. 2006. Crustacea in Arctic and Antarctic Sea Ice: Distribution, Diet and Life History Strategies. *Advances in Marine Biology Volume 51*. 197-315.

Ashjian CJ, Campbell RG, Welch HE, Butler M, Van Keuren D. 2003. Annual cycle in abundance, distribution, and size in relation to hydrography of important copepod species in the western Arctic Ocean. *Deep Sea Research Part I: Oceanographic Research Papers* **50**(10-11): 1235-1261.

Auel H, Werner I. 2003. Feeding, respiration and life history of the hyperiid amphipod Themisto libellula in the Arctic marginal ice zone of the Greenland Sea. *Journal of Experimental Marine Biology and Ecology* **296**(2): 183-197.

Bradstreet MS, Cross WE. 1982. Trophic relationships at high Arctic ice edges. *Arctic*: 1-12.

Campbell RG, Ashjian CJ, Sherr EB, Sherr BF, Lomas MW, et al. 2016. Mesozooplankton grazing during spring sea-ice conditions in the eastern Bering Sea. *Deep Sea Research Part II: Topical Studies in Oceanography* **134**: 157-172.

Deibel D. 1988. Filter feeding by Oikopleura vanhoeffeni: grazing impact on suspended particles in cold ocean waters. *Marine Biology* **99**(2): 177-186.

Donnelly J, Torres J, Hopkins T, Lancraft T. 1994. Chemical composition of Antarctic zooplankton during austral fall and winter. *Polar Biology* **14**(3): 171-183.

Eilertsen HC, Tande K, Taasen J. 1989. Vertical distributions of primary production and grazing by Calanus glacialis Jaschnov and C. hyperboreus Krøyer in Arctic waters (Barents Sea). *Polar Biology* **9**(4): 253-260.

Falk-Petersen S, Sargent JR, Tande KS. 1987. Lipid composition of zooplankton in relation to the sub-Arctic food web. *Polar Biology* **8**(2): 115-120.

Friedrich C. 1997. Ökologische Untersuchungen zur Fauna des arktischen Meereises. *Ber zur Polarforschung*.

Gradinger R. 1999. Integrated abundance and biomass of sympagic meiofauna in Arctic and Antarctic pack ice. *Polar Biology* **22**(3): 169-177.

Grainger EH, Hsiao SI, Pinkewycz N, Mohammed A, Neuhof V. 1985. *The food of ice fauna and zooplankton in Frobisher Bay*. Arctic Biological Station, Department of Fisheries and oceans.

Harris R, Nishiyama T, Paul A. 1986. Carbon, nitrogen and caloric content of eggs, larvae, and juveniles of the walleye pollock, Theragra chalcogramma. *Journal of Fish Biology* **29**(1): 87-98.

Hopcroft R, Clarke C, Nelson R, Raskoff K. 2005. Zooplankton communities of the Arctic's Canada Basin: the contribution by smaller taxa. *Polar Biology* **28**(3): 198-206.

Imao F. 2005. Zooplankton community structure and functional role in carbon cycle in the Oyashio region, western North Pacific. Master's Thesis, Hokkaido University.

Irigoien X, Titelman J, Harris RP, Harbour D, Castellani C. 2003. Feeding of Calanus finmarchicus nauplii in the Irminger Sea. *Marine Ecology Progress Series* **262**: 193-200.

Kohlbach D, Graeve M, A. Lange B, David C, Peeken I, et al. 2016. The importance of ice algae-produced carbon in the central Arctic Ocean ecosystem: Food web relationships revealed by lipid and stable isotope analyses. *Limnology and Oceanography* **61**(6): 2027-2044.

Kramer M. 2011. The role of sympagic meiofauna in Arctic and Antarctic sea-ice food webs.

Matthews J, Hestad L. 1977. Ecological studies on the deep-water pelagic community of Korsfjorden, Western Norway: length/weight relationships for some macroplanktonic organisms. *Sarsia* **63**(1): 57-63.

Menden-Deuer S, Lessard EJ. 2000. Carbon to volume relationships for dinoflagellates, diatoms, and other protist plankton. *Limnology and oceanography* **45**(3): 569-579.

Mizdalski E. 1988. Weight and length data of zooplankton in the Weddell Sea in austral spring 1986 (ANT V/3). *Berichte zur Polarforschung (Reports on Polar Research)* **55**.

Moloney CL, Field JG. 1989. General allometric equations for rates of nutrient uptake, ingestion, and respiration in plankton organisms. *Limnology and Oceanography* **34**(7): 1290-1299.

Mumm N. 1991. Zur sommerlichen Verteilung des Mesozooplanktons im Nansen-Becken, Nordpolarmeer= On the summerly distribution of mesozooplankton in the Nansen Basin, Arctic Ocean. *Berichte zur Polarforschung (Reports on Polar Research)* **92**.

Norrbin M, Olsen R-E, Tande K. 1990. Seasonal variation in lipid class and fatty acid composition of two small copepods in Balsfjorden, northern Norway. *Marine Biology* **105**(2): 205-211.

Runge J, Pepin P, Silvert W. 1987. Feeding behavior of the Atlantic mackerel Scomber scombrus on the hydromedusa Aglantha digitale. *Marine Biology* **94**(3): 329-333.

Saito H, Kiørboe T. 2001. Feeding rates in the chaetognath Sagitta elegans: effects of prey size, prey swimming behaviour and small-scale turbulence. *Journal of Plankton Research* **23**(12): 1385-1398.

Scott CL, Falk-Petersen S, Sargent JR, Hop H, Lønne OJ, et al. 1999. Lipids and trophic interactions of ice fauna and pelagic zooplankton in the marginal ice zone of the Barents Sea. *Polar Biology* **21**(2): 65-70.

Stevens C, Deibel D, Parrish C. 2004. Species-specific differences in lipid composition and omnivory indices in Arctic copepods collected in deep water during autumn (North Water Polynya). *Marine Biology* **144**(5): 905-915.

Werner I. 1997. Grazing of Arctic under-ice amphipods on sea-ice algae. *Marine Ecology Progress Series* **160**: 93-99.

Chapter IV

Sea-ice properties and nutrient concentration as drivers of the taxonomic and trophic structure of high-Arctic protist and metazoan communities

H. Flores[1,2], C. David[1,2,3], **J. Ehrlich**[1,2], K. Hardge[1], D. Kohlbach[1,2], B.A. Lange[1,2], B. Niehoff[1], E.-M. Nöthig[1], I. Peeken[1], K. Metfies[1,5]

(2019)

[1] Section Polar Biological Oceanography, Alfred Wegener Institut Helmholtz-Zentrum für Polar- und Meeresforschung, Bremerhaven, Germany
[2] Centre for Natural History (CeNak), University of Hamburg, Zoological Museum, Hamburg, Germany
[3] Institut Français de Recherche Pour l'Exploitation de la Mer (Ifremer), Plouzané, France
[4] Fisheries and Oceans Canada, Freshwater Institute, Winnipeg, MB, Canada
[5] Helmholtz Institute for Functional Marine Biodiversity (HIFMB), Oldenburg, Germany

Polar Biology 42:1377. doi: 10.1007/s00300-019-02526-z

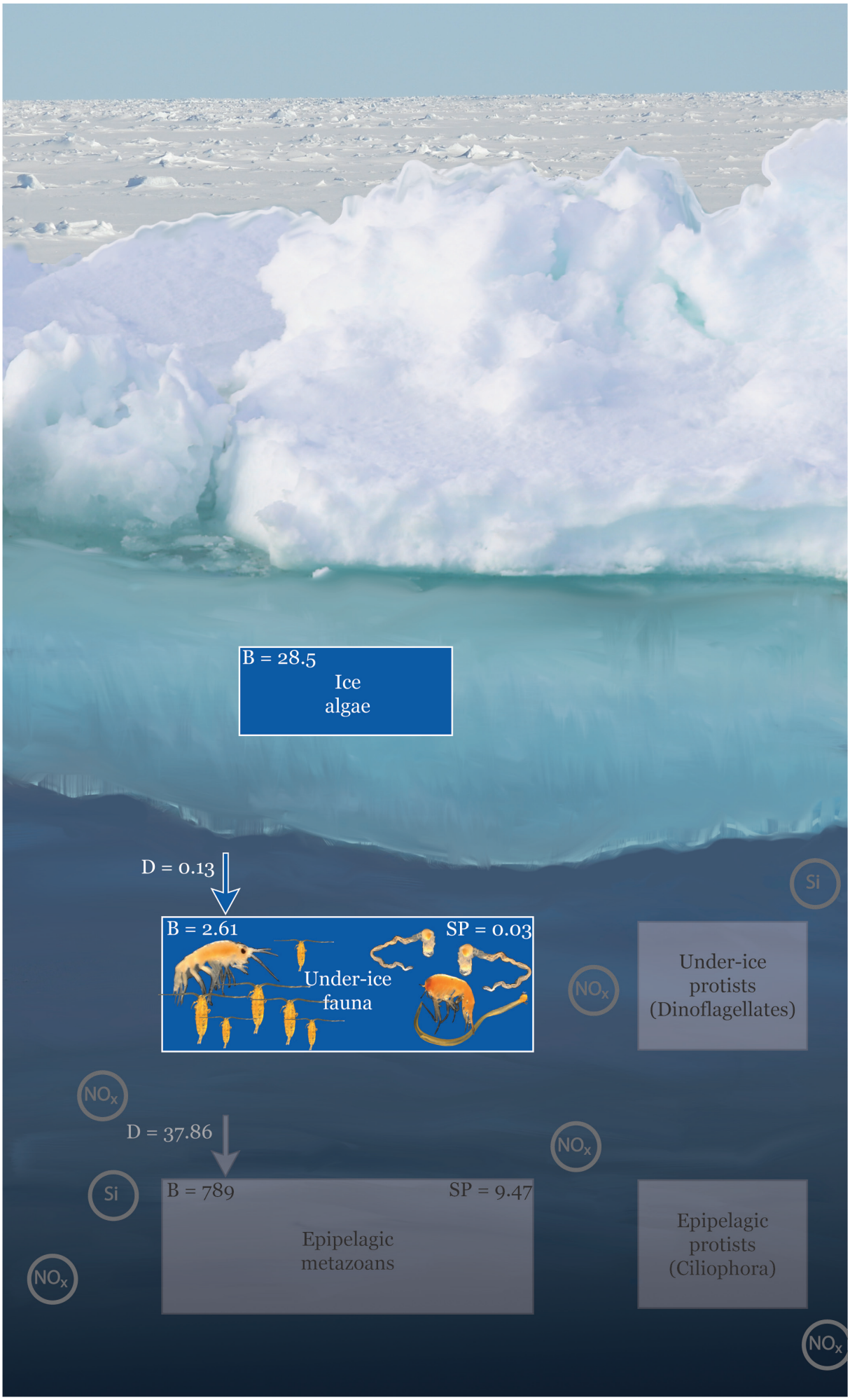
B = 28.5
Ice
algae
D = 0.13
B = 2.61
SP = 0.03
Under-ice
fauna
Si
Under-ice
protists
(Dinoflagellates)
NOx
NOx
D = 37.86
NOx
Si
B = 789
SP = 9.47
Epipelagic
metazoans
Epipelagic
protists
(Ciliophora)
NOx
NOx

Polar Biology
https://doi.org/10.1007/s00300-019-02526-z

ORIGINAL PAPER

Sea-ice properties and nutrient concentration as drivers of the taxonomic and trophic structure of high-Arctic protist and metazoan communities

Hauke Flores[1,2] · Carmen David[1,2,3] · Julia Ehrlich[1,2] · Kristin Hardge[1] · Doreen Kohlbach[1,2] · Benjamin A. Lange[1,2,4] · Barbara Niehoff[1] · Eva-Maria Nöthig[1] · Ilka Peeken[1] · Katja Metfies[1,5]

Received: 10 January 2019 / Revised: 14 June 2019 / Accepted: 18 June 2019

Abstract

In the Arctic Ocean, sea-ice decline will significantly change the structure of biological communities. At the same time, changing nutrient dynamics can have similarly strong and potentially interacting effects. To investigate the response of the taxonomic and trophic structure of planktonic and ice-associated communities to varying sea-ice properties and nutrient concentrations, we analysed four different communities sampled in the Eurasian Basin in summer 2012: (1) protists and (2) metazoans from the under-ice habitat, and (3) protists and (4) metazoans from the epipelagic habitat. The taxonomic composition of protist communities was characterised with 18S meta-barcoding. The taxonomic composition of metazoan communities was determined based on morphology. The analysis of environmental parameters identified (i) a 'shelf-influenced' regime with melting sea ice, high-silicate concentrations and low NO_x (nitrate + nitrite) concentrations; (ii) a 'Polar' regime with low silicate concentrations and low NO_x concentrations; and (iii) an 'Atlantic' regime with low silicate concentrations and high NO_x concentrations. Multivariate analyses of combined bio-environmental datasets showed that taxonomic community structure primarily responded to the variability of sea-ice properties and hydrography across all four communities. Trophic community structure, however, responded significantly to NO_x concentrations. In three of the four communities, the most heterotrophic trophic group significantly dominated in the NO_x-poor shelf-influenced and Polar regimes compared to the NO_x-rich Atlantic regime. The more heterotrophic, NO_x-poor regimes were associated with lower productivity and carbon export than the NO_x-rich Atlantic regime. For modelling future Arctic ecosystems, it is important to consider that taxonomic diversity can respond to different drivers than trophic diversity.

Keywords Arctic Ocean · Sea ice · Community structure · Protists · Zooplankton · Under-ice fauna · Nutrients · Trophic ecology

Introduction

The Arctic Ocean has been experiencing a rapid decline in sea-ice volume (Kwok and Rothrock 2009; Laxon et al. 2013) and sea-ice extent over the past two decades (Serreze et al. 2007; Stroeve et al. 2012; Simmonds 2015). Model

Electronic supplementary material The online version of this article (https://doi.org/10.1007/s00300-019-02526-z) contains supplementary material, which is available to authorized users.

✉ Hauke Flores
hauke.flores@awi.de

[1] Section Polar Biological Oceanography, Alfred Wegener Institut Helmholtz-Zentrum für Polar- und Meeresforschung, Bremerhaven, Germany

[2] Centre for Natural History (CeNak), University of Hamburg, Zoological Museum, Hamburg, Germany

[3] Institut Français de Recherche Pour l'Exploitation de la Mer (Ifremer), Plouzané, France

[4] Fisheries and Oceans Canada, Freshwater Institute, Winnipeg, MB, Canada

[5] Helmholtz Institute for Functional Marine Biodiversity (HIFMB), Oldenburg, Germany

Published online: 28 June 2019

simulations have indicated that an ice-free Arctic Ocean during summer is likely to occur by the mid of the twenty-first century (Wang and Overland 2009; Stroeve et al. 2012). In the water column, significant environmental changes are expected to occur, such as an increase in surface water temperatures, changing circulation patterns, increased ocean acidification, enhanced stratification, and nutrient limitation (IPCC 2014). These changes will profoundly impact on ecosystem structure and function, such as carbon and nutrient cycling, carbon export, and availability of marine-living resources. Studies on Arctic plankton communities have demonstrated ongoing change in community composition and in the distribution of ecological key species related to ocean warming and sea ice decline (e.g. Bluhm et al. 2011; Wassmann 2011; Wassmann et al. 2011; Kraft et al. 2013; Nöthig et al. 2015; Hardge et al. 2017a, b). Sea-ice decline has been linked to enhanced pelagic primary production (Arrigo and van Dijken 2011, 2015), mainly due to increased light availability (Nicolaus et al. 2012). In contrast, increased freshwater input due to river runoff may result in decreased primary production, because of lower nutrient availability (Yun et al. 2016). Besides nutrient supply, other factors are also likely to affect Arctic ecosystem structure, such as oceanic CO_2 uptake and increased temperatures (Tremblay et al. 2015).

In the central Arctic Ocean, the bulk of the total primary production is often generated by sea-ice algae rather than phytoplankton (Gosselin et al. 1997; Fernández-Méndez et al. 2015). Reduced sea-ice algae production due to habitat/substrate loss can influence fundamental patterns of carbon flux in the food web. Recently, it was shown that abundant ecological key species, such as *Calanus* spp. and juvenile polar cod *Boreogadus saida*, significantly depend on carbon produced by ice algae (Budge et al. 2008; Søreide et al. 2010; Wang et al. 2015; Kohlbach et al. 2016, 2017). Kohlbach et al. (2016) demonstrated that the cumulative carbon demand by metazoan grazers far exceeded primary production rates by phytoplankton and sea-ice algae during summer. This suggests that intermediate trophic levels of the food web depend on heterotrophic carbon sources to a much greater extent than previously suggested (David et al. 2015; Kohlbach et al. 2016). While the transformation of Arctic sea-ice habitats continues, increased dependency on heterotrophic carbon transmitters may be a significant factor changing the trophic functioning of biological communities in the future Arctic Ocean.

In summer 2012, the lowest sea-ice extent since the beginning of satellite-based observations was recorded in the Arctic Ocean (Parkinson and Comiso 2013). In the Eurasian Basin of the Arctic Ocean, a vast area of rapidly degrading sea ice opened up in regions that are normally ice-covered year-round (Fig. 1; Stroeve et al. 2012; Boetius et al. 2013). Interacting with the anomalous 2012 sea ice situation was a contrast between nutrient-rich Atlantic Water entering through the Fram Strait, nutrient-depleted Polar Water advected from the central Arctic Ocean, and shelf-influenced

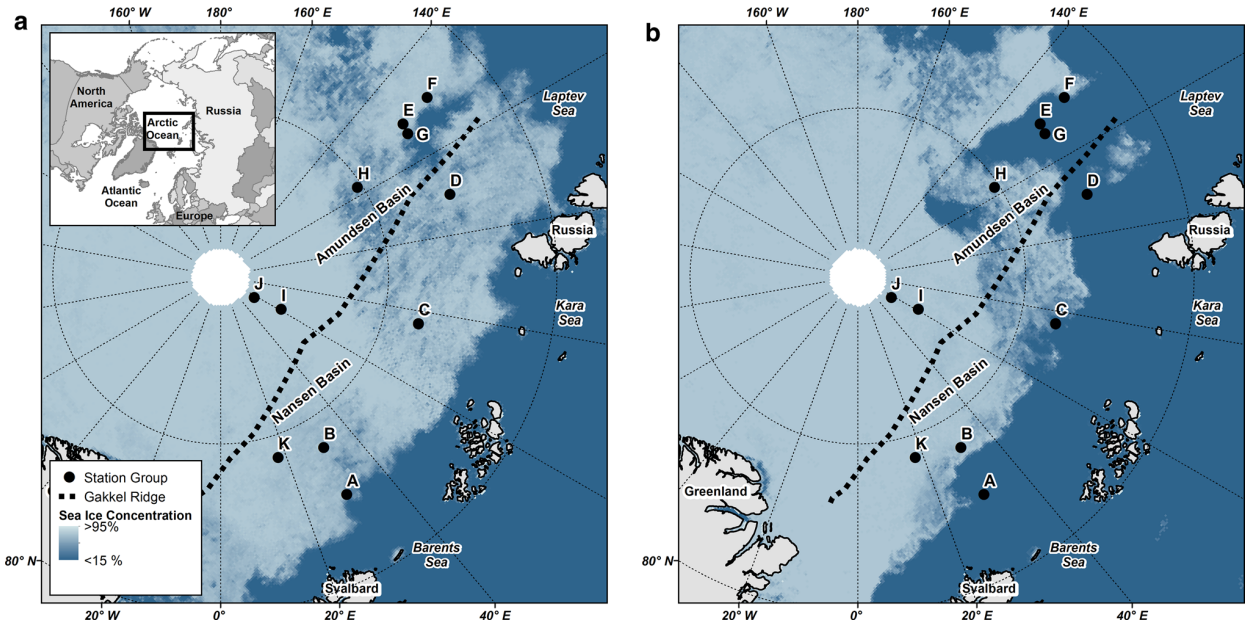

Fig. 1 Overview of the research area with sampling locations and major topographic features. Sea-ice concentration derived from SSMIS satellite data (www.meereisportal.de) is shown on 14th of August (**a**) and 13th of September 2012 (**b**). Capital letters indicate sampling locations from Table 1

water from the Laptev Sea (Lalande et al. 2014; David et al. 2015; Fernández-Méndez et al. 2015; Metfies et al. 2016). Sampling this unprecedented situation of extreme reduction of sea ice during *Polarstern* expedition PS80 gave the unique opportunity to sample both protist and metazoan communities simultaneously with hydrographical conditions, nutrient concentrations and sea-ice properties.

Changes in the taxonomic and trophic structure of these communities can have a strong impact on key ecosystem functions, such as primary and secondary production, carbon-, and nutrient cycling. The rapid environmental changes in the Arctic Ocean likely act differently on sea ice-associated communities compared to planktonic communities. In high-Arctic ecosystems, however, the response of biological communities to different drivers interacting with each other is poorly understood, especially in the under-ice habitat (Wassmann et al. 2011). In this study, we use a range of morphological, molecular, and statistical tools to analyse the structure of protist and metazoan communities both in the under-ice habitat and in the epipelagic habitat in the Eurasian Basin of the Arctic Ocean. We hypothesize that (1) the structure of both protist and metazoan communities responds to similar environmental drivers in each habitat; and (2) that changes in taxonomic composition in relation to environmental variability will be resembled in the trophic structure of these communities. To test these hypotheses, we:

(a) identified physical–chemical drivers structuring environmental regimes, such as sea-ice properties, hydrography and nutrient concentrations;
(b) analysed the relationship of the taxonomic composition of Arctic protist and metazoan communities with these environmental drivers;
(c) investigated if environmental drivers were associated with both the taxonomic and the trophic community structure.

Material and methods

Research area

The samples were collected from 7 August to 29 September 2012 during the RV *Polarstern* expedition PS80 (ARK-XXVII/3, "IceArc") in the central Arctic Ocean (Fig. 1). The area sampled extended over the Eurasian Basin, ranging from 82° to 89°N, and from 30° to 130°E, and was entirely situated in deep-sea waters (depth range 3409–4384 m; Table 1). Samples and data were collected with various sampling gear at altogether 46 stations. For the purpose of this study, we grouped these stations into 11 locations identified by the letters A to K, based on spatio-temporal proximity. Most sampling locations were associated with drifting sea-ice stations. The sampling around these locations, therefore, extended over a period of up to 3 days, and covered a latitudinal drift distance of up to 14.5 nm (28 km). A complete account of all stations sampled for this study was provided in Table 1.

Sampling of environmental parameters

Water column

A conductivity temperature depth probe (CTD) with a carousel water sampler was used to collect environmental parameters from the water column. The CTD (Seabird SBE9+) was equipped with a fluorometer (Wetlabs FLRTD), a dissolved oxygen sensor (SBE 43) and a transmissiometer (Wetlabs C-Star). Details of the CTD sampling procedure were provided by Boetius et al. (2013). Data are available online in the PANGAEA database (Rabe et al. 2012). Nutrient samples were collected at multiple depths, and analysed in an air-conditioned lab container with a continuous flow auto analyser (Technicon TRAACS 800) following the procedure described by Boetius et al. (2013). Measurements were made simultaneously on four channels: PO_4, Si, $NO_2 + NO_3$ together and NO_2 separately. Nutrient values for the purpose of this study were taken from the depth of the chlorophyll *a* maximum. The depth of the upper mixed layer (MLD) was calculated from the ship CTD profiles after Shaw et al. (2009). Integrated values for water temperature and salinity within the MLD were derived by averaging continuous CTD profile data between the surface and the MLD. A stratification index was estimated as the density gradient between the density of the mixed layer and the density of the water 5 m below the MLD.

Under-ice habitat

Under-ice metazoans and environmental parameters of the ice–water interface layer (0–2 m) were sampled with a Surface and Under-Ice Trawl (SUIT) (van Franeker et al. 2009). The SUIT consisted of a steel frame with a 2 m × 2 m opening and two parallel 15 m-long nets attached: (1) a 7 mm half-mesh commercial shrimp net, which covered 1.5 m of the opening width; and (2) a 0.3 mm mesh zooplankton net, which covered 0.5 m of the opening width. SUIT haul durations varied between 17 and 42 min (mean = 29 min) over an average distance of 1.5 km. Water inflow speed and direction were calculated using a Nortek Aquadopp® Acoustic Doppler Current Profiler (ADCP). The trawled area was calculated by multiplying the distance trawled in water, estimated from ADCP data, with the net width. The SUIT sampling technique and performance has been described in detail by David et al. (2015) and Flores et al. (2012). A sensor array was mounted on the SUIT frame, comprising among

Table 1 Stations sampled during the expedition PS80. Nearby stations were grouped together as 'locations' represented by letters A to K

Location	Station	Date	Latitude (°N)	Longitude (°E)	Depth (m)	Parameters
A	PS80/215–1	08/07/2012	82.488	30.001	3618	CTD
	PS80/216–1	08/07/2012	82.483	30.027	3610	ui-metazoans
B	PS80/223–1	08/09/2012	84.070	30.434	4016	ui-metazoans
	PS80/224–1	08/09/2012	84.051	31.112	4014	ice/ui-protists
	PS80/226–1	08/09/2012	84.028	31.236	4013	ep-metazoans
	PS80/227–1	08/09/2012	84.026	31.225	4011	CTD
	PS80/230–1	08/11/2012	84.022	31.221	4011	CTD/ep-protists
	PS80/233–1	08/11/2012	84.045	31.298	4011	ui-metazoans
C	PS80/237–1	08/14/2012	83.987	78.103	3585	ice
	PS80/242–1	08/16/2012	83.902	76.067	3409	CTD
	PS80/243–1	08/16/2012	83.911	75.971	3418	ep-metazoans
	PS80/248–1	08/16/2012	83.934	75.500	3424	ui-metazoans
D	PS80/254–1	08/19/2012	82.696	109.119	3571	CTD
	PS80/255–1	08/20/2012	82.671	109.590	3569	ice/ui-protists
	PS80/256–1	08/20/2012	82.674	109.590	3571	CTD/ep-protists
	PS80/258–1	08/20/2012	82.743	109.627	3575	ui-metazoans
	PS80/261–1	08/21/2012	82.939	109.864	3599	ep-metazoans
E	PS80/276–1	08/25/2012	83.076	129.125	4188	ui-metazoans
	PS80/277–1	08/25/2012	82.883	130.130	4161	ice
	PS80/279–1	08/25/2012	82.887	129.969	4166	ep-metazoans
	PS80/281–1	08/26/2012	82.893	129.826	4186	CTD
	PS80/285–1	08/26/2012	82.896	129.782	4174	ui-metazoans
F	PS80/321–1	09/04/2012	81.717	130.033	4011	ui-metazoans
	PS80/323–1	09/04/2012	81.926	131.129	4031	ice/ep-protists
	PS80/324–1	09/04/2012	81.925	131.120	4040	CTD
	PS80/328–1	09/05/2012	81.889	130.792	4036	ep-metazoans
	PS80/329–1	09/05/2012	81.876	130.878	4032	CTD/ep-protists/ui-protists
	PS80/331–1	09/05/2012	81.905	130.863	4011	ui-metazoans
G	PS80/333–1	09/06/2012	82.989	127.103	4036	ui-metazoans
	PS80/333–2	09/06/2012	83.003	127.177	4188	CTD
H	PS80/335–1	09/07/2012	85.102	122.245	4355	ice/ep-protists/ui-protists
	PS80/336–1	09/07/2012	85.100	122.255	4357	CTD/ep-protists
	PS80/337–1	09/07/2012	85.092	122.262	4356	ep-metazoans
	PS80/342–1	09/09/2012	85.158	123.349	4353	CTD
	PS80/345–1	09/09/2012	85.254	123.842	4354	ui-metazoans
I	PS80/349–1	09/18/2012	87.934	61.217	4380	CTD/ep-protists/ui-protists
	PS80/351–1	09/18/2012	87.933	60.991	4384	ep-metazoans
	PS80/354–1	09/19/2012	87.925	60.954	4384	CTD
	PS80/357–1	09/19/2012	87.925	61.125	4381	CTD/ep-protists
J	PS80/360–1	09/22/2012	88.828	58.864	4374	ice/ep-protists/ui-protists
	PS80/364–1	09/22/2012	88.811	57.411	4375	CTD
	PS80/367–1	09/23/2012	88.792	56.674	4375	ep-metazoans
	PS80/370–1	09/23/2012	88.771	55.936	4377	CTD/ep-protists
K	PS80/384–1	09/28/2012	84.375	17.454	3513	ice/ep-protists/ui-protists
	PS80/387–1	09/28/2012	84.368	17.525	3897	CTD
	PS80/386–1	09/28/2012	84.371	17.503	3774	ep-metazoans
	PS80/396–1	09/29/2012	84.346	17.815	4015	CTD/ep-protists
	PS80/397–1	09/29/2012	84.172	17.922	4028	ui-metazoans

CTD water column parameters sampled with the ship's CTD (temperature, salinity, nutrients), *ice* sea-ice parameters, *ui* under ice, *ep* epipelagic

other devices a CTD probe with built-in fluorometer and an altimeter used to derive ice thickness profiles and under-ice chlorophyll *a* concentrations (David et al. 2015). Gridded daily sea-ice concentrations for the Arctic Ocean derived from SSMIS satellite data using the algorithm specified by Spreen et al. (2008), were downloaded from the sea-ice portal hosted at the University of Bremen (www.meereisportal.de). For each sea-ice station, sea-ice concentration was averaged from nine adjacent grid cells, with the grid cell in which the station was situated as the centre. A detailed description of environmental sampling and parameter estimations was provided by David et al. (2015). An overview of the environmental parameters and their ranges was provided in Table 2.

Chlorophyll *a* concentration

Particulate organic matter (POM) from water samples was collected on Whatman GF/F glass fibre glass fibre filters (0.7 µm), extracted in 90% acetone and analyzed with a Turner-Design fluorometer according to standard procedure (Edler 1979; Evans et al. 1987). Calibration of the fluorometer was carried out with standard solutions of Chlorophyll *a* (Sigma, Germany). To estimate chlorophyll *a* content of sea ice, ice cores were collected at each ice stations using a 9 cm-diameter ice corer (Kovacs). Ice cores were cut in segments, which were each melted in 4 °C with 0.2 µm filtered sea water in the dark. For details of sea-ice sampling see Boetius et al. (2013) and Lange et al. (2016). For pigment analysis of filtered ice core samples to each filter 50 µl internal standard (canthaxanthi), 1.5 ml acetone and small glass beads were added and the samples kept frozen at – 20 °C for 15 min. Cell were disrupted for 20 s with a Precellys® tissue homogenizer. The centrifugation of the extract was performed in a cooled centrifuge (0°) and the supernatant liquid was kept and filtered through a 17 mm HPLC 0.2 µm PTFE filter (LABSOLUTE). Pigment measurement was carried out with a Waters HPLC-system equipped with an auto sampler (717 plus), a pump (600), a Photodiode array detector (2996), a fluorescence detector (2475) and the EMPOWER software. The analysis of the pigments was conducted by reverse-phase HPLC, with a VARIAN Microsorb-MV3 C8 column (4.6 × 100 mm) and HPLC-grade solvent (Merck). For details see Kilias et al. (2013).

Sampling of organisms from the under-ice and the pelagic habitats

Protists

Sampling of epipelagic protists was carried out with a rosette sampler equipped with 24 Niskin bottles attached to the ship CTD. Samples were taken during the up-cast at the vertical maximum of chlorophyll *a* fluorescence determined during the downcast. The sampling depth varied between 10 and 50 m. Two-litre subsamples were transferred into PVC bottles. Under-ice protist samples were collected with a Kemmerer bottle (6.3 l) lowered through an ice hole directly below the ice. Protists were collected for molecular analyses by sequential filtration of one water sample through three different mesh sizes (10 µm, 3 µm, 0.4 µm) at a vacuum pressure of − 200 mbar using Isopore Membrane Filters (Millipore, USA). Filters were stored in Eppendorf tubes (Eppendorf, Germany) at − 80 °C until further processing in the laboratory.

In this study, we used a subset of an 18S meta-barcoding-data set comprising a total of 56 samples collected in different ice-influenced habitats (Hardge et al. 2017a). DNA samples were processed as described in Hardge et al. (2017a). DNA extraction was carried out with the NucleoSpin® Plant II kit (Macherey–Nagel) following the manufacturer's protocol. The V4 region was amplified in triplicates using the

Table 2 Environmental parameters used in analyses

Parameter	Code	Unit	Device	Min	Max
Mean sea ice concentration	SIC	%	Satellite	4	100
Modal ice thickness	SIT	m	SUIT CTD	0	1.4
Mean temperature in the mixed layer	T.ML	°C	Ship CTD	− 1.79	− 0.96
Mean salinity in the mixed layer	S.ML	PSU	Ship CTD	30.06	33.36
Mean turbidity in the mixed layer	Tb.ML	%	Ship CTD	93.22	95.56
Mixed layer depth	MLD	m	Ship CTD	9	34
Stratification index	Strat		Ship CTD	0.02	1.19
SiO_4^{2-} conc. at the chl *a* maximum	Si	µmol l^{-1}	Ship CTD	1.17	4.80
$NO_3^{2-} + NO_2^{3-}$ conc. at the chl *a* maximum	NO_x	µmol l^{-1}	Ship CTD	0.12	6.84
Mean chlorophyll *a* conc. in sea ice	Chl.ice	mg m^{-3}	Ice cores	0.19	6.25
Mean chl *a* conc. in the under-ice habitat	Chl.ui	mg m^{-3}	SUIT CTD	0.19	1.13
Mean chl *a* conc. in the mixed layer	Chl.ML	mg m^{-3}	Ship CTD	0.06	0.30

Chl a chlorophyll *a*, *Min* minimum value, *Max* maximum value

universal primer set TAReuk454FWD1 and TAReukREV3 (Stoeck et al. 2010). The DNA amplification was carried out in two rounds using a Mastercycler (Eppendorf, Germany). Resulting PCR products were purified with NucleoSpin® Gel & PCR Clean up kit (Macherey–Nagel) according to the manufacturer's protocol. Pooled triplicates were sequenced on the MiSeq 18S meta-barcoding platform (2×300 paired-end reads). The library preparation was done with the TruSeq RNA Library Preparation Kit v2 according to the manufacturer's protocol. We used QIIME version 1.8.0 (Caporaso et al. 2010) for sequence analysis. Operational taxonomic units (OTUs) were determined de novo at a minimum similarity threshold of 98%. According to Bokulich et al. (2013), OTUs consisting of less than 0.005% of processed sequences were removed. Representative sequences of each OTU were aligned with the bioinformatics pipeline called PhyloAssigner (Vergin et al. 2013). The compiled reference database is available on request in ARB-format.

164 of the 210 protist taxa identified with sequence analysis were assigned to the trophic groups "autotrophs", "mixotrophs" and "heterotrophs" based on published knowledge on their trophic function (Online Resource ESM1). Based on the relative sequence abundance of combined OTUs with identical taxonomic labels, the proportional contribution of autotrophs, mixotrophs and heterotrophs was calculated for each sampling location.

Metazoans

Under-ice metazoans were sampled with the SUIT. After retrieval of the catch from the SUIT, the material was preserved in 4% formaldehyde/seawater solution for quantitative analysis. The samples were analysed for species composition and abundance at the Alfred Wegener Institute following the procedure described by David et al. (2015). In all macrofauna species, total body length was measured to the nearest 1 mm using a stereo microscope coupled to a digital image analysis system (Leica Model M 205C and image analysis software LAR 4.2). Copepods were classified by developmental stage and sex. Epipelagic metazoans were sampled with a Multinet (Hydrobios, Kiel). The Multinet had a mouth opening area of 0.25 m^2 and was equipped with five nets (150 µm), which were sequentially opened and closed to five sample discrete depth intervals (1500–1000–500–200–50–0 m). In the present study, only samples from the uppermost depth stratum (0–50 m) were considered. The samples were preserved in 4% formaldehyde/seawater solution buffered with borax. In the laboratory, the samples were subdivided with a plankton splitter (Hydrobios) usually to 1/8 and at maximum to 1/64. Abundant species ($n > 50$ in an aliquot) were sorted only from one subsample, while less abundant species were sorted from at least two subsamples. Areal abundances (ind. m^{-2}) were calculated by dividing the total number of animals in each net by the water volume filtered, and multiplying the resulting volumetric density by the vertical depth range sampled.

We estimated the individual dry mass of freeze-dried SUIT samples of the five most abundant amphipod species. To account for the high variability in size distribution between sampling sites of the amphipod *Themisto libellula*, a size-dry weight relationships was established. This relationship was then used to estimate the dry mass of *Themisto* spp. at each station based on their total biovolume and mean size, respectively. Dry mass of *Calanus* copepods was estimated based on size- and stage composition data (Ehrlich 2015) and published individual dry mass values (Ashjian et al. 2003). Dry mass of all other taxa was calculated using published mean individual dry mass values (e.g. Falk-Petersen et al. 1981; Ashjian et al. 2003). An account of individual dry weights, both measured and estimated from the literature, was provided in the Online Resource (ESM2).

Metazoan taxa were assigned to the trophic groups "herbivores", "omnivores" and "carnivores" based on published knowledge of their feeding ecology (Online Resource ESM2). Based on the relative dry mass of each taxon, the proportional contribution by mass of herbivores, omnivores and carnivores was calculated for each sampling location.

Statistical analysis

Environmental data

We used principal component analysis (PCA) to analyse spatial patterns in the environmental properties of sampling locations. In the PCA ordination, sampling locations having a similar structure in their environmental properties are grouped closer together than locations that show greater differences in environmental properties. The environmental gradients are shown relative to the ordination axes. Near-normal distribution of data, as assumed by PCA, was confirmed by visual inspection of histograms. To achieve near-normal distribution of the data, sea-ice concentration (SIC) was double-square transformed, mixed layer depth (MLD) and nitrate + nitrite concentration (NO_x) were square-root transformed, and the Stratification Index (Strat) was log-transformed (for all parameter codes see Table 2). To obtain an optimal representation of the structure of environmental data, we first performed a PCA with the full set of environmental parameters (Table 2), and then performed a stepwise backward selection, until the combination of parameters was found in which the cumulative proportion of variance of the first four components reached a maximum. From the PCA biplot, groups of locations with similar environmental properties ('regimes') were identified visually. Statistically significant differences in single environmental parameters between these regimes were assessed with an analysis of

variance (ANOVA), followed by the Tukey Honest Significance test (Tukey HSD).

Community analysis

To analyse the relationship of the community structure with environmental parameters, we performed canonical correspondence analyses (CCA). The CCA ordination groups sampling locations that have a similar taxonomic structure closer together than locations that show greater differences in taxonomic structure. In addition, it projects this ordination in relation to environmental gradients for assessing the association of taxonomic structure with environmental parameters. CCAs were conducted for each of the four communities: under-ice protists, epipelagic protists, under-ice metazoans, and epipelagic metazoans. Square-root transformation and Wisconsin standardization were applied to under-ice and epipelagic metazoan data. In each CCA, combinations of up to four environmental parameters were sequentially selected based on the maximum contribution of eigenvalues to the mean-squared contingency coefficient (cumulative proportion). In the final CCA of each community, the cumulative proportion reached at least 50%, and the joint effect of constraints was significant. The significance of the joint effect of constraints was tested with an ANOVA-like permutation test for CCA using 1000 permutations (in R termed 'anova.cca', Oksanen et al. 2013).

Trophic structure

We used Student's *t* test to test for significant differences in the proportional contribution of single trophic groups between NO*x*-poor and NO*x*-rich regimes. To analyse the relationship of trophic groups with environmental parameters in more detail, we used generalized linear models (GLM, McCullagh and Nelder 1989). GLMs are used to fit relationships of single response variables (e.g. 'percentage of herbivores') with combinations of one or more explanatory variables (here: environmental parameters), thereby allowing to choose appropriate assumptions about the error distribution of the model. In this study, we modelled the proportion of each trophic group in each community (response variable) in relation to up to two environmental parameters (explanatory variables). Because the response variables were proportional data, we assumed a binomial error distribution with a flexible dispersion parameter (in R termed 'quasibinomial'). The same transformations as in the PCA were applied to SIC, MLD, Strat and NO_x to achieve near-normal distribution of the data. To find the most parsimonious model, we sequentially added up to two environmental parameters to each model and retained those parameters which had significant model terms and the lowest residual deviance.

For all analyses, we used Rs software version 3.5.2 (R Core Team 2017).

Results

Environmental properties

The research area was characterised by mixed layer depths (MLD) between 9 and 34 m, and chlorophyll *a* concentrations in the mixed layer (Chl.ML) ranged from 0.06 to 0.30 mg m^{-3} (Table 2). Location A was situated at the ice edge and was the only location where water temperatures in the mixed layer (T.ML) were > − 1 °C (Fig. 2a). All other stations were situated within the pack-ice during the early (locations B–D; Fig. 1a), or during the late phase of the sampling period (locations I–K; Fig. 1b). Locations A and E–H were positioned close to large open water areas (Fig. 1b). They shared low values of salinity in the mixed layer (S.ML) and relatively low values of sea-ice concentration (SIC) and thickness (SIT), indicating an advanced state of sea-ice melt (Fig. 2b, g, h). Locations D–J were characterised by lower nitrate + nitrite concentrations at the depth of the chlorophyll *a* maximum (NO_x; < 2.5 µmol l^{-1}) than the other locations. In this group, locations E–H showed elevated silicate concentrations at the depth of the chlorophyll *a* maximum (Si; Fig. 2e). At locations A–C and K, NO_x values exceeded 3.5 µmol l^{-1} (Fig. 2f).

A principle component analysis (PCA) including the environmental parameters NO_x, S.ML, SIC, Si and T.ML could explain 99.85% of the first four principle components. The biplot of the first two components (explaining altogether 92.64% of the variance) showed that the most pronounced environmental gradient in the research area followed the variability of S.ML and Si along component axis 1 (Fig. 3). This 'shelf-ocean' gradient reflected the transition from locations E–H off the Laptev Sea, characterised by the fresh, silicate-rich waters and decaying sea ice ('shelf-influenced regime') to the silicate-poor, more oceanic locations A–D and I–K. (Figs. 2b, e, 3). Crossing this shelf-ocean gradient, an 'NO_x' gradient reflected the transition from NO_x-poor waters at the shelf-influenced regime (E–H) and a 'Polar regime' with low Si values (D, I, J) to NO_x-rich waters entering from the Fram Straight at locations A–C and K ('Atlantic regime'; Figs. 2f, 3). Mean values of Si and NO_x were significantly different between the regimes separated by these two interacting gradients (Si: ANOVA, $F_2 = 23.18$, $p < 0.001$, Tukey HSD: Shelf-influenced versus Atlantic regime $p = 0.001$/Shelf-influenced versus Polar regime $p < 0.001$; NO_x: ANOVA, $F_2 = 14.01$, $p = 0.002$, Tukey HSD: Polar versus Atlantic regime $p = 0.009$/Shelf/influenced versus Atlantic regime $p = 0.003$).

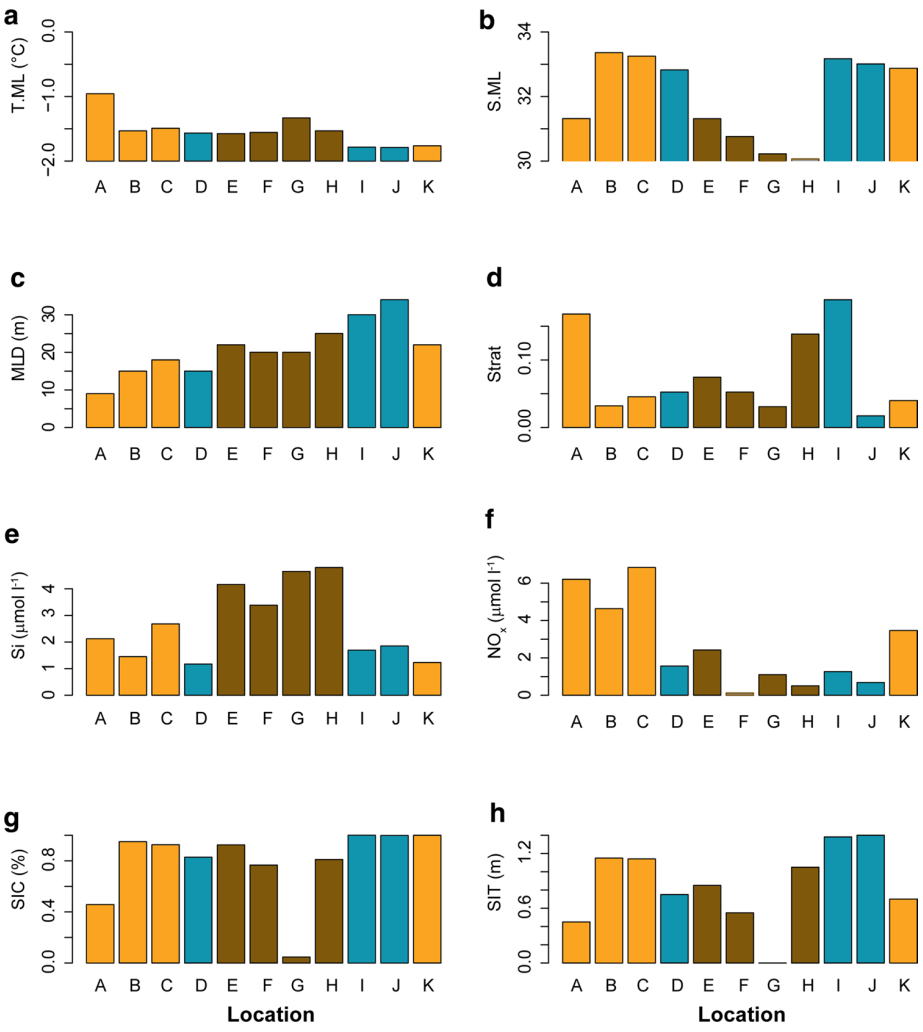

Fig. 2 Environmental properties at the sampling locations. Environmental parameters have the same codes as shown in Table 2: *T.ML* water temperature in the mixed layer (**a**), *S.ML* salinity in the mixed layer (**b**), *MLD* mixed layer depth (**c**), *Strat* stratification index (**d**), *Si* Silicate concentration at the depth of the chlorophyll *a* maximum (**e**), NO_x Nitrate + Nitrite concentration at the depth of the chlorophyll a maximum (**f**), *SIC* sea ice concentration (**g**), *SIT* ice thickness (**h**). Capital letters indicate sampling locations from Table 1. The bars are coloured according to environmental regimes identified with the PCA (Fig. 3): *brown* shelf-influenced regime (Locations E-H); *orange* Atlantic regime (Locations A-C, K), *turquoise* = Polar regime (Locations D, I, J). (Color figure online)

Community structure

General community composition

From the 11 locations considered in this study, we sampled 7 locations for under-ice and epipelagic protists, 9 locations for under-ice metazoans, and 9 locations for epipelagic metazoans (Table 1). In each community, the sampling included locations from all three environmental regimes. In the protist community from under-ice water, OTUs from dinoflagellates (~40% of total sequences) dominated, with the highest sequence abundances in the Gymnodiniaceae (*Gymnodinium* spp., *Karlodinium* spp. and *Gyrodinim* spp.). In the epipelagic layer, the share of OTUs from non-dinoflagellate heterotrophic protists was often higher than the share of dinoflagellate OTUs, with the highest sequence abuncances in Ciliophora (Oligotrichea). The under-ice metazoan community comprised both ice-associated and pelagic species. It was numerically dominated by the ice-associated amphipod *Apherusa glacialis,* and the pelagic copepods *Calanus glacialis* and *C. hyperboreus.* The epipelagic metazoan community was dominated by copepods in numbers and biomass. By far the most abundant species were *C. hyperboreus* and *Calanus* spp. (predominantly *C. finmarchicus*). Detailed analyses of the taxonomic composition of protist and metazoan communities were provided in David et al. (2015), Ehrlich (2015) and Hardge et al. (2017a).

Community structure in relation to environmental parameters

In all four communities, the ordination followed gradients of sea-ice influence (SIC, SIT), stratification (MLD, Strat) and shelf influence (S.ML, Si; Table 3). With two exceptions (under-ice metazoans: location A in Fig. 4c; epipelagic metazoans: location C in Fig. 4d), locations with high sea-ice influence (B–C, I–K) were separated along the SIC/SIT gradient from those with lower sea-ice influence (D–H;

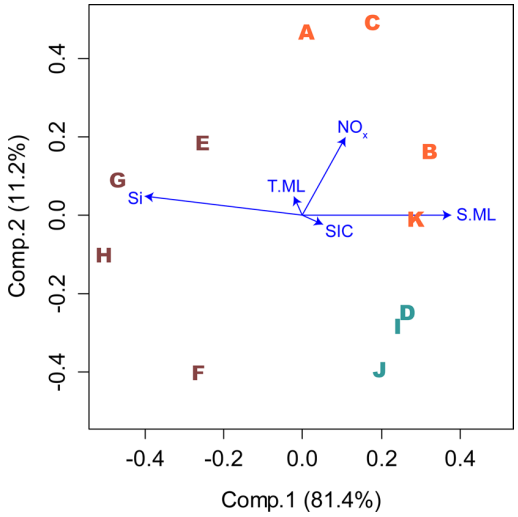

Fig. 3 Biplot of a principle component analysis (PCA) of environmental properties in the research area. Capital letters represent sampling locations from Table 1. Letters were colour-coded according to visually identified oceanographic regimes: *brown* = shelf-influenced regime (Locations E-H); *orange* = Atlantic regime (Locations A-C, K), *turquoise* = Polar regime (Locations D, I, J). Blue arrows point into the direction of increasing values of environmental parameters in the ordination. Percentage values in axis annotations indicate proportion of explained variance of the PCA. Environmental parameters (Table 2): *NO_x* Nitrate + Nitrite concentration at the depth of the chlorophyll *a* maximum, *S.ML* salinity in the mixed layer, *Si* Silicate concentration at the depth of the chlorophyll *a* maximum, *SIC* sea ice concentration, *T.ML* temperature in the mixed layer. (Color figure online)

Figs. 2, 4). NO_x was only important in protist communities (Table 3, Fig. 4a, b).

Trophic structure

Whereas the taxonomic structure of all four communities predominantly reflected the variability of sea-ice influence, stratification and shelf influence (Table 3, Fig. 4), the trophic structure differed predominantly between locations in the NO_x-rich Atlantic regime and locations in the NO_x-poor Polar and shelf-influenced regimes.

The protist community of the under-ice water was dominated by OTUs of mixotrophic taxa, reflecting the high share of OTUs from dinoflagellates (Hardge et al. 2017a). Locations in NO_x-poor waters of the polar and shelf-influenced regimes (D, F and H–J) had a significantly higher share of heterotrophy-associated OTUs than locations of the Atlantic regime (B, K; *t* test: $t_{2.24} = 6.32$, $p < 0.05$; Fig. 5a). Within the NO_x-poor regimes, locations associated with thicker ice (H–J) had proportionally higher shares of OTUs indicative of autotrophic taxa compared to locations with thinner, decaying sea ice (D, F; Figs. 2h, 5a).

In the epipelagic protist community, OTUs of heterotrophs were generally more abundant compared to the protist community sampled in the under-ice layer, reflecting the high share of protozoan sequences in this community (Hardge et al. 2017a). Similar to the under-ice protist community, the proportion of heterotrophic OTUs was higher at the NO_x-poor locations in the Shelf-influenced and Polar regimes (D, F, H–J) than at locations in the Atlantic regime (B, K), but this pattern was not statistically significant (*t* test: $p > 0.05$). Rather, the share of OTUs from mixotrophs was significantly lower, and the share of OTUs from autotrophs was significantly higher at NO_x-poor locations compared to locations in the Atlantic regime (*t* test; mixotrophs: $t_{4.42} = -4.58$, $p < 0.01$; autotrophs: $t_{4.63} = 4.98$, $p < 0.01$; Fig. 5b).

The under-ice metazoan community was characterized by a high variability in the biomass share of herbivores, ranging from < 30 to > 90% (Fig. 5c). The biomass share of herbivores decreased along the more open and fresher surface water at stations D–G with relatively thin ice (Figs. 1, 2h, 5c). At NO_x-poor locations in the shelf-influenced and Polar regimes (D–H), the proportional biomass of herbivores was significantly lower, and proportional biomasses of carnivores was significantly higher compared to locations in the Atlantic regime (A–C, K) (*t* test: herbivores: $t_{9.75} = 2.91$, $p < 0.05$; carnivores: $t_{6.93} = -2.56$, $p < 0.05$).

Table 3 Significant (CCA-ANOVA; $p < 0.05$) combinations of environmental parameters explaining > 50% of the variability in the CCA ordination of protist and metazoan communities at the ice–water interface and in the epipelagic habitat. In each CCA, the selected significant environmental parameters were indicated by the letter "x"

Community	Prop	MLD	Strat	NO_x	S.ML	Si	SIC	SIT
uiw-protists	0.81	x		x		x	x	
uiw-metazoans	0.55	x			x	x		x
ep-protists	0.75	x		x	x		x	
ep-metazoans	0.58		x		x	x	x	

Habitats: *uiw* under-ice water, *ep* pipelagic; *Env.* parameters: *MLD* mixed layer depth, NO_x = Nitrate + Nitrite concentration at the depth of the chlorophyll *a* maximum, *S.ML* salinity in the mixed layer, *Si* silicate concentration at the depth of the chlorophyll *a* maximum, *SIC* sea ice concentration, *Strat* stratification index, *SIT* ice thickness. Statistics: prop. = proportional contribution of eigenvalues to constraints

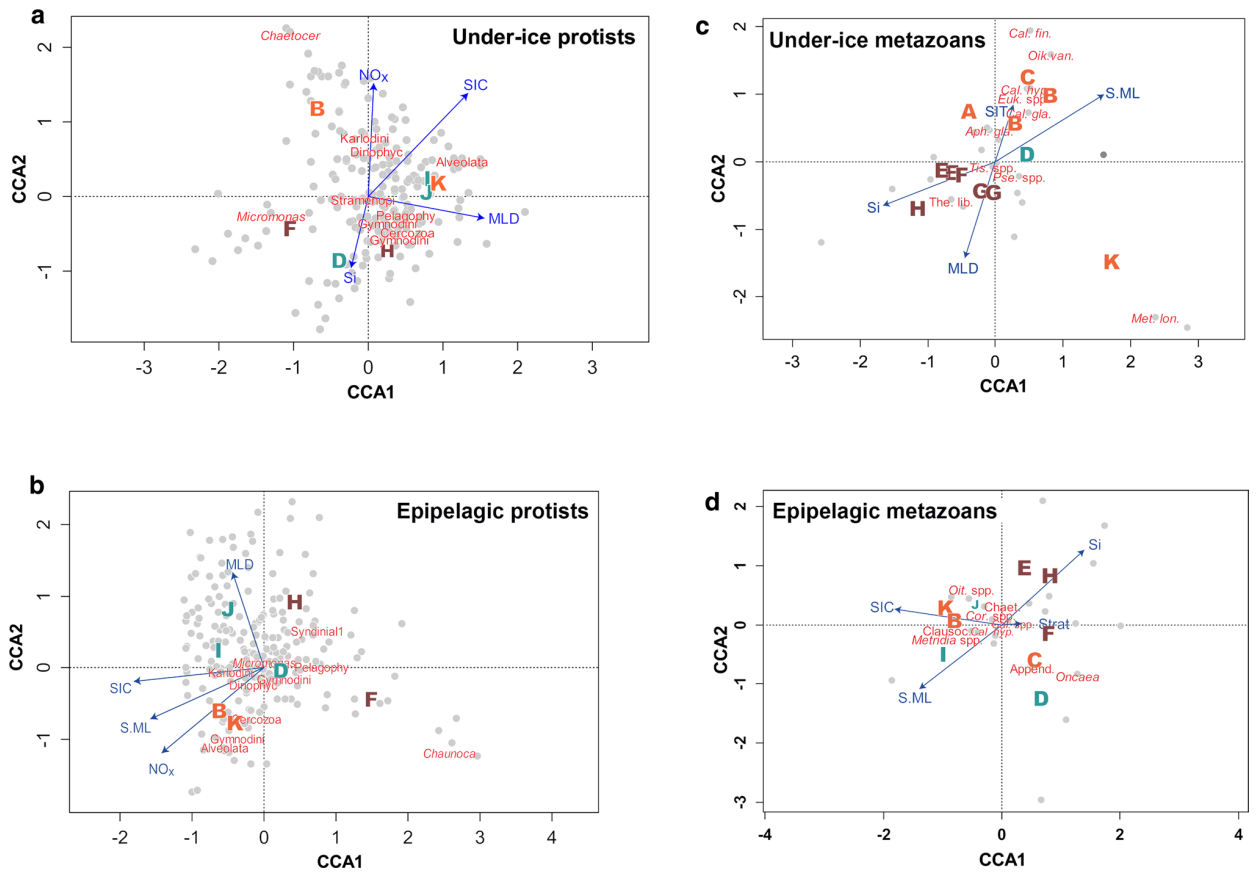

Fig. 4 Biplots from a canonical correspondence analysis (CCA) of under-ice protist (**a**), epipelagic protist (**b**), under-ice metazoan (**c**) and epipelagic metazoan (**d**) communities in relation to environmental gradients. Capital letters in biplots indicate sampling locations (Table 1). Letters were colour-coded according to oceanographic regimes (Fig. 3): *brown* = shelf-influenced regime (Locations E-H); *orange* = Atlantic regime (Locations A-C, K), turquoise = Polar regime (Locations D, I, J). Blue arrows point into the direction of increasing values of environmental parameters in the ordination. Grey dots indicate the position of individual protist OTUs and metazoan taxa in the ordination. The corresponding taxonomic information is provided in the Online Resource (ESM1, ESM2). Environmental parameters (Table 2): *MLD* mixed layer depth, NO_x Nitrate + Nitrite concentration at the depth of the chlorophyll *a* maximum, *S.ML* salinity in the mixed layer, *Si* Silicate concentration at the depth of the chlorophyll *a* maximum, *SIC* sea ice concentration, Strat = stratification index, SIT = ice thickness. (Color figure online)

In the epipelagic metazoan community, the variability of the biomass share of herbivores versus carnivores showed a similar pattern compared to the under-ice protist and under-ice metazoan communities (Fig. 5 a, b, d). Accordingly, at NO_x-poor locations in the shelf-influenced and Polar regimes (D–F, H–J), the proportional biomass of herbivores was significantly lower, and the proportional biomass of omnivores and carnivores was significantly higher compared to locations in the Atlantic regime (B, C, K) (*t* test; herbivores: $t_{3.06} = 4.10$, $p < 0.05$; omnivores: $t_{3.19} = -3.45$, $p < 0.05$; carnivores: $t_{3.06} = -3.85$, $p < 0.05$).

To more accurately investigate the relationship of trophic structure with the variability of environmental parameters interacting with each other, we used GLMs to analyse the combined effect of up to two environmental parameters on the relative share of each trophic group from each community in each habitat. In 10 of the 12 models, the selection procedure resulted in 'best' models with significant effects ($p < 0.05$) (Table 4). In under-ice communities, the proportional contribution of each trophic group was associated with different environmental parameters. For the under-ice protist community, the selected GLMs indicated that temperature and turbidity of the mixed layer had a positive effect on the share of autotrophs, while heterotrophs were negatively related to NO_x values and positively related to chlorophyll *a* concentrations in sea ice. The share of mixotrophs was negatively related to ice thickness (Table 4). In under-ice metazoan models, S.ML was the only environmental parameter related to the two trophic groups to which a GLM could be fitted. S.ML had a positive effect on the share of herbivores, and a negative effect on the share of carnivores (Table 4). Because this

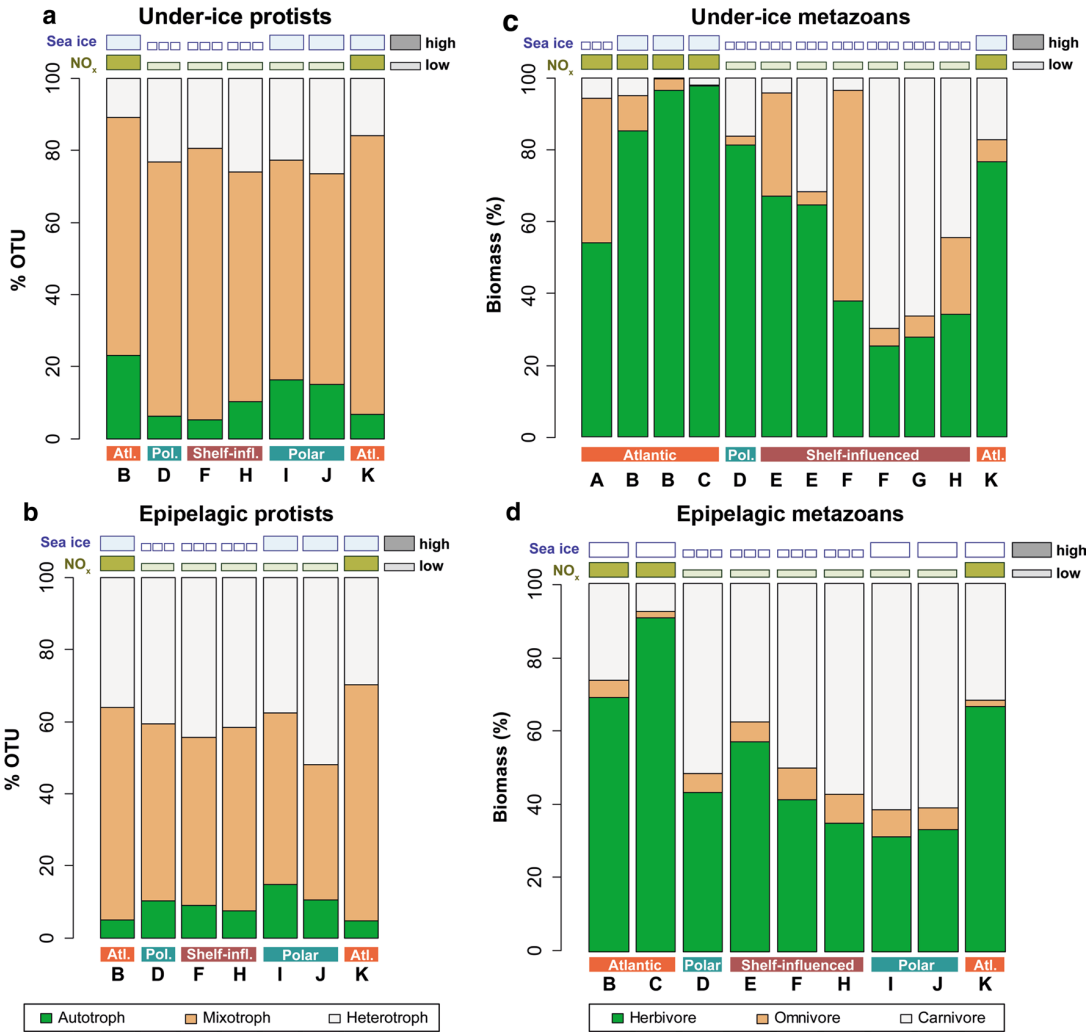

Fig. 5 Trophic structure of under-ice protist (**a**), epipelagic protist (**b**), under-ice metazoan (**c**) and epipelagic metazoan (**d**) communities. The heights of the coloured sections in the bars indicate the proportional abundances of operational taxonomic units (OTU) in protist communities and biomass shares in metazoan communities. Capital letters indicate sampling locations from Table 1. Duplicate letters indicate repeated sampling at the same location (Table 1). Symbols above the bars indicate either 'high' or 'low' conditions of sea ice and NO*x*, respectively, based on the data shown in Fig. 2. The coloured horizontal blocks below the bars indicate the 3 hydrographical regimes of the research area: Atlantic regime (orange), shelf-influenced regime (brown), and Polar regime (turquoise). (Color figure online)

community was not sampled at locations I and J, however, the variability of S.ML largely coincided with the variability of NO_x in this dataset.

In the epipelagic layer, NO_x had a significant effect in all five GLMs fitted (Table 4). The two trophic groups of protist communities to which a GLM could be fitted were both associated with the chlorophyll *a* concentration in the mixed layer (Chl.ML) and NO_x, with a positive effect in the model of mixotrophs, and a negative effect of these parameters in the model of heterotrophs (Table 4). In epipelagic metazoan models, NO_x was the only environmental parameter significantly related to all three trophic groups, with a positive effect in the model of herbivores and negative effects in the models of omnivores and carnivores (Table 4).

Discussion

Structure of the environment

In summer 2012, the Eurasian Basin was characterised by extremely low sea-ice coverage, super-imposed on environmental gradients determined by the large-scale hydrography of the Arctic Ocean. Sea-ice-conditions changed from a

Table 4 Summary of 'best' Generalized Linear Models (GLM) of the relationship between the proportional contribution of trophic groups and environmental parameters in protist and metazoan communities in the under-ice layer and the epipelagic layer

Community	Trophic group	*RD*	T.ML	S.ML	Tb.ML	Chl.ML	NO_x	SIT	Chl.ice
uiw-protists	Autotrophs	0.04	+		+				
uiw-protists	Mixotrophs	0.02						-	
uiw-protists	Heterotrophs	0.02					-		+
uiw-metazoans	Herbivores	0.50		+					
uiw-metazoans	Omnivores	-	*no model fitted*						
uiw-metazoans	Carnivores	2.16		-					
ep-protists	Autotrophs	-	*no model fitted*						
ep-vprotists	Mixotrophs	0.02				+	+		
ep-protists	Heterotrophs	0.01				-	-		
ep-metazoans	Herbivores	0.29					+		
ep-metazoans	Omnivores	0.03					-		
ep-metazoans	Carnivores	0.30					-		

The directional effect of each parameter on the response variable is indicated by "+" signs (dark shading) and "−" signs (light shading)

Habitats: *ep* epipelagic, *uiw* under-ice water; Environmental parameters: *Chl.ice* chlorophyll *a* concentration in sea ice, *Chl.ML* chlorophyll *a* concentration in the mixed layer, *NO_x* nitrate + nitrite concentration at the depth of the chlorophyll *a* maximum, *S.ML* salinity in the mixed layer, *SIT* ice thickness, *Tb.ML* turbidity in the mixed layer, *T.ML* temperature in the mixed layer; statistics: *RD* residual deviance of GLM

Significance of model terms: $*p < 0.05$, $**0.05 < p < 0.001$; $***p < 0.001$

nearly closed sea-ice cover at the beginning of our sampling in the Nansen Basin (Fig. 1a), through an opening area of rapid sea-ice melt in the Laptev Sea sector south of 86°N, and back into freezing conditions at higher latitudes and towards the end of the survey in late September (Fig. 1b). Sea-ice concentration (SIC) was a significant, but not very pronounced contributor to our PCA (Fig. 3). However, the vast ice-free zone in the Laptev Sea sector may have been under-represented by our satellite-derived sea-ice concentration values from the relatively small areas around our ice-covered sampling stations (Fig. 1b). In the epipelagic layer, the most pronounced environmental gradient was created by the silicate concentration in the chlorophyll *a* maximum (Si). The high-silicate concentrations at locations E–H in the shelf-influenced regime reflected the influence of Laptev Sea water carrying high amounts of silicate originating from the Lena delta inflow, as compared to the low Si values at all other locations (Fig. 2; Bauch et al. 2014; Bluhm et al. 2015). The salinity in the mixed layer (S.ML) varied largely in the opposite direction of the silicate gradient (Figs. 2, 3). Crossing this silicate/salinity gradient, Nitrate + Nitrite concentrations in the chlorophyll *a* maximum (NO_x) changed from high values in the Atlantic regime (locations A–C, K) to low values in the shelf-influenced and Polar regime (locations D–J). This large-scale NO_x-gradient was consistent with the known pattern of NO_x distribution in the Arctic Ocean during summer (Codispoti et al. 2013; Bluhm et al. 2015): In the Eurasian Basin, nitrate is predominantly advected by the Atlantic water inflow through the Fram Strait and across the Barents Sea, and transported along the Eurasian shelf break, where our sampling locations A–C and K were situated. After reaching the Laptev Sea sector, surface waters are depleted of NO_x and recirculated across the Eurasian Basin towards the Fram Strait, passing the positions of our NO_x-poor sampling locations D–J (Kattner et al. 1999; Rudels et al. 2013; Bluhm et al. 2015).

Taxonomic community structure

Gradients of sea-ice influence (SIC, SIT), stratification of the water column (MLD, Strat) and shelf influence (S.ML, Si) were common drivers of the community structure in all four communities (Table 3). The effects of these drivers on community composition cannot be entirely disentangled from each other, because the directions of their gradients often overlapped in the CCA ordination (Fig. 4). However, the general pattern in the four CCA ordinations showed that locations associated with low sea-ice influence were separated from stations with high sea-ice influence along gradients of sea-ice properties (SIC, SIT; Fig. 4). Sea ice

influences protist communities in the water column primarily by limiting light intrusion, affecting photo-autotrophic growth (Sakshaug 2004). Other important factors influencing protist community composition are limitation of nutrient supply from deeper water layers due to enhanced stratification under melting sea ice (Fujiwara et al. 2014), and exchange between the water column and in-ice communities through physical processes and active migration (Hardge et al. 2017a). The observed relationship between protist community structure and sea-ice properties contrasts an extensive analysis by Ardyna et al. (2011) in the Canadian Arctic, which found that sea ice-conditions played only a minor role. The work of Ardyna et al. (2011) was conducted on the Pacific-influenced shelf of the Canadian Archipelago, whereas our study was conducted in the deep Eurasian Basin. Apart from these biogeographical differences, it is possible that the range of mean sea-ice concentrations (2–23%) observed by Ardyna et al. (2011) in late summer was too limited to significantly affect protist communities through shading, stratification, or organism exchange. In agreement with Ardyna et al. (2011), the structure of protist communities in our study was also significantly related to NO_x gradients. In metazoan communities, however, a significant influence of NO_x was not observed in our dataset (Table 3).

In the under-ice metazoan community, a strong response to sea-ice influence was expected due to the high proportional abundance of sea ice-associated (sympagic) amphipods, e.g. *Apherusa glacialis* and *Onisimus glacialis* (Hop et al. 2000; Poltermann et al. 2000; Gradinger and Bluhm 2004; Bluhm et al. 2010). David et al. (2015) observed that the under-ice metazoan community structure differed between a densely ice-covered 'Nansen Basin regime' (corresponding to the Atlantic regime in the present study), and a more open 'Amundsen Basin regime' (the Shelf-influenced regime in the present study) in summer 2012. Our observation that sea-ice concentration was an important factor structuring the epipelagic metazoan community (Table 3) is in agreement with a multi-annual study in the Western Arctic Ocean finding that the contribution of sea-ice concentration to the variability in zooplankton community structure ranked highest together with bathymetry among numerous investigated environmental parameters (Hunt et al. 2014). In the epipelagic metazoan community ordination, crossing gradients of sea-ice properties (SIC) and shelf influence (S.ML, Si) indicated that, in combination with sea-ice influence, the epipelagic metazoan community structure responded to shelf influence (Fig. 4d). Most high-Arctic zooplankton studies focused on horizontal and vertical differences in community structure in relation to large, physically defined water masses and bathymetrically defined habitats (e.g., Mumm et al. 1998; Kosobokova and Hirche 2000; Wassmann et al. 2015). The shelf-influence gradient (S.ML/Si) of our CCA resembled such a hydrographical pattern (Fig. 4d).

In the Eurasian Basin, plankton communities are strongly influenced by Atlantic species advected through the Fram Strait and the Barents Sea (Wassmann et al. 2015). While in our research area, the advection of Atlantic species is tied to the distribution of Atlantic water flowing eastward along the continental slope at depths below 100 m, surface waters of Polar origin are associated with the westward Transpolar Drift transporting sea ice from Siberia towards the Fram Strait. Advection of Polar species with surface waters thus probably contributed partly to the sea ice-associated gradient in protist and metazoan community structure. The sea ice itself may have advected species from the Siberian shelf, as has been found for sea-ice protists by Hardge et al. (2017a), and for polar cod *Boreogadus saida* by David et al. (2016). Besides the physical properties of sea ice, the presence of ice algae may have attracted certain zooplankton and sympagic species, and contributed to a sea-ice-driven trend in under-ice and epipelagic metazoan community composition. Ice algae were an important carbon source of abundant metazoan species in summer 2012, accounting for up to about 50% of the carbon demand in the pelagic copepods *Calanus* spp., and over 90% in the sympagic amphipod *Apherusa glacialis* (Kohlbach et al. 2016).

Hydrographical structures, sea-ice properties and advection patterns were major drivers of community composition. Several of these drivers were intrinsically linked to seasonal changes in both habitats, impeding a clear disentanglement of seasonal change and environmental drivers. In 2012, the sampling period extended over 9 weeks from summer to the onset of winter (Table 1). Seasonal changes were indicated by decreasing temperatures in the mixed layer (T.ML), increasing mixed layer depth (MLD) and high sea-ice concentrations (SIC) towards the end of the sampling period (Fig. 2). In the under-ice habitat, seasonal processes, such as the increased exchange of protist communities between water column and sea ice during the onset of freezing (Hardge et al. 2017b) and the seasonal downward migration of copepods (David et al. 2015) probably influenced community structure at locations I–K (Fig. 4a, c). In the epipelagic habitat, seasonal change of community composition appeared less pronounced, as the hydrographically similar earliest and latest locations B and K grouped closely together in the CCA (Fig. 4b, d). This indicates that seasonal change of community composition was most pronounced at the ice–water interface due to the more extreme physical changes at the surface, e.g. from melting conditions to freeze-up.

Trophic community structure

Variability of sea-ice properties was an important driver of the taxonomic community structure in both protists and metazoans (Table 3, Fig. 4). This pattern, however, was not mirrored in the trophic structure of the communities. In all four communities, a stronger dominance of the most heterotrophic trophic group (protists: heterotrophs; metazoans: carnivores) was associated with sampling locations of the shelf-influenced and Polar regimes with low nitrate + nitrite concentrations (NO_x) (Fig. 5). Conversely, the dominance of the most heterotrophic trophic group was negatively related with NO_x in both protist communities and in epipelagic metazoans (Table 4). When primary production is limited by nutrient depletion, heterotrophic processes can be expected to increase in relative importance, because autotrophs and their herbivorous grazers cannot realise their full growth potential relative to their heterotrophic competitors and predators. Basedow et al. (2010) explained an increase in mean trophic levels of the zooplankton community from a bloom- to a post-bloom situation in the Barents Sea by a switch from a dominance of small herbivorous zooplankton to a dominance of carnivorous zooplankton, combined with a change in the diet of omnivorous grazers, such as *Calanus* spp. Our results show that similar processes take place in the central Arctic Ocean. A dominance of heterotrophic processes has been linked with nutrient limitation in several ecosystems of the Western Arctic Ocean bordering the Canada Basin, due to either hydrographical structures (e.g. shelf versus basin), or seasonal succession (Cota et al. 1996; Levinsen et al. 1999; Nielsen and Hansen 1999; Forest et al. 2014). The Canada Basin is a mostly oligotrophic environment, because nutrient input through the Bering Strait and by riverine input is used up on the shelf (Tremblay et al. 2015). In contrast, the Eurasian Basin receives substantial nutrient input through the Fram Strait, which is redistributed by the surface currents, leading to strong gradients. Because of these more intensive nutrient dynamics in the Eurasian Basin, changes in the trophic structure of the ecosystem due to changing nutrient distribution can be expected to be more pronounced. Therefore, we consider the Eurasian Basin a well-suited model system to study the interacting effects of sea-ice distribution and nutrient availability on the ecosystem of the central Arctic Ocean.

Our analysis of trophic structure faces several caveats that are founded in the quantification of protist community structure by OTUs rather than abundances or biomass, and in limited knowledge about the trophic ecology of various protist and metazoan taxa. Generally, it is difficult to relate sequence abundances of protists to cell number or biomass, because the number of target gene copies varies between protist species (Prokopowich et al. 2003; Zhu et al. 2005; Godhe et al. 2008; Egge et al. 2013). A microscopic analysis of two subsurface water samples (locations C and H; Online Resource ESM3) found that diatoms constituted 3–5% of the protist biomass, which was in agreement with the low share of diatom sequences and biomass in our study region (Roca-Martí et al. 2016; Hardge et al. 2017b). Microscopic analysis further confirmed the dominance of dinoflagellates in OTU abundances (Hardge et al. 2017b), but indicated that the relative biomass of ciliates could have been higher by a factor of 2–3 compared to the relative OTU abundance. Furthermore, we likely underestimated the abundance of haptophytes due to insufficient coverage of the 18S rRNA gene primer set used (Balzano et al. 2012; Bradley et al. 2016). In spite of these limitations, we assume that relative differences in OTU abundance patterns between environmental regimes realistically reflect the intrinsic variability of the system investigated here, because the potential bias of relative OTU abundances compared to relative abundance or biomass affected all samples equally. In our approach to analyse the trophic structure of the two protist communities we classified dinoflagellates as mixotrophs, because many dinoflagellates can switch between a photo-autotrophic and a heterotrophic mode of life. Dinoflagellates in autotrophic mode, however, are rare in Arctic oceanic ecosystems during late summer (Levinsen et al. 1999; Nielsen and Hansen 1999), and they constituted less than 0.1% of the dinoflagellate biomass in the microscopic analysis (Online Resource ESM3). Likewise, we classified *Calanus* copepods as herbivores, although they can prey substantially on microzooplankton (Ohman and Runge 1994; Levinsen et al. 2000; Campbell et al. 2009). Bulk stable isotope data from *Calanus* spp. from our sampling campaign showed that mean $\delta^{15}N$ values ranged between 2.7–3.5 and 3.0–3.8‰ above the trophic baselines of ice algae and phytoplankton in *C. glacialis* and *C. hyperboreus*, respectively (Kohlbach et al. 2016). Assuming a mean $\delta^{15}N$ enrichment of 3.4‰ per trophic level (Minagawa and Wada 1984), the two most abundant *Calanus* copepods in our study would be considered herbivores. Yet, even a conservative approach considering *Calanus* spp. as omnivores would not change the general pattern of an increased dominance of carnivores in locations with low NO_x values compared to locations with high NO_x values (Fig. 5c, d).

The ecosystem investigated in this study has been characterised as a system with low primary productivity (Fernández-Méndez et al. 2015), supporting a food web that was nonetheless capable of sustaining a significant population of polar cod *Boreogadus saida* (David et al. 2016; Kohlbach et al. 2017). In high-Arctic ecosystems, primary productivity is usually limited to a short period in springtime, from the onset of light intrusion through sea-ice, until the available nutrient stocks are consumed to depletion (e.g. Hill et al. 2013). This springtime bloom starts with ice algae and continues in the water column under thinning sea ice, and in

ice-free areas. During the survey period of our study, large amounts of fresh ice algal material on the seafloor indicated that an ice-algae bloom period had occurred in parts of the investigation area only shortly before our sampling (Boetius et al. 2013; Roca-Martí et al. 2016). During our sampling campaign, the food demand of abundant herbivorous grazers alone exceeded primary production of both ice algae and phytoplankton (David et al. 2015; Kohlbach et al. 2016). This suggests that in the Eurasian Basin the predominantly heterotrophic food web observed in this study was largely fuelled by an early-season ice algae production peak.

In the central Arctic Ocean ecosystem, the already existing natural dominance of heterotrophic organisms during late summer could be significantly enhanced when nutrients are further depleted. A tentative comparison of key ecosystem parameters and -functions indicates that in summer 2012 sampling locations in the more heterotrophic, NO_x-poor shelf-influenced and Polar regimes were associated with considerably lower median ice algae primary production, metazoan biomass, secondary production, carbon demand, and carbon export, compared to sampling locations in the less heterotrophic, nutrient-rich Atlantic regime (Table 5). In spite of lower metazoan biomass, the median ratio of metazoan carbon demand versus primary production was twice as high in the Polar regime as in the Atlantic regime, emphasising the strong heterotrophic character of the food web in nutrient-poor conditions. In the NO_x-poor regimes, a lower export flux was predominantly related to low algal production, but may have been further diminished by the high grazing pressure of heterotrophic protists, transforming potentially exported particulate carbon into dissolved carbon by respiration and excretion (Forest et al. 2014). Furthermore, low abundances of herbivorous zooplankton caused only a low flux of fast-sinking faecal pellets (Lalande et al.

Table 5 Ecological key parameters of the study area during PS80

	Parameter	Unit	Shelf-influenced	Polar	Atlantic	Total	Source
Ice algae (incl. melt ponds)	Chlorophyll *a* biomass	mg m^{-3}	0.29 (0.24–0.51)	1.05 (0.40–2.54)	0.43 (0.36–0.50)	0.57 (0.30–1.38)	This study
	Carbon biomass[a]	mg C m^{-3}	14.5 (12.0–25.5)	52.5 (20.0–127.0)	21.5 (18.0–25.0)	28.5 (15.0–69.0)	This study
	Primary production	mg C m^{-2} d^{-1}	0.30 (0.26–0.45)	0.65 (0.38–2.05)	8.01 (4.51–11.50)	0.86 (0.53–3.08)	Fernández-Méndez et al. (2015)
Phytoplankton	Chlorophyll *a* biomass	mg m^{-3}	0.26 (0.22–0.29)	0.21 (0.15–0.26)	0.17 (0.14–0.20)	0.19 (0.15–0.23)	This study
	Carbon biomass[a]	mg C m^{-3}	13.00 (11–14.5)	10.50 (7.5–13)	8.50 (7–10)	9.50 (7.5–11.5)	This study
	Primary production	mg C m^{-2} d^{-1}	28.00 (17.00–44.00)	8.50 (1.88–23.75)	28.00 (26.50–29.50)	18.0 (4.63–28.75)	Fernández-Méndez et al. (2015)
Under-ice metazoans	Biomass	mg m^{-2}	4.40 (3.86–7.11)	9.93	17.35 (5.48–16.40)	6.72 (4.10–17.30)	This study
	Carbon biomass[b]	mg m^{-2}	1.76 (1.54–2.84)	3.97	6.94 (2.19–6.56)	2.61 (1.64–6.92)	This study
	Secondary Production[c]	mg C m^{-2} d^{-1}	0.02 (0.02–0.03)	0.05	0.08 (0.03–0.08)	0.03 (0.02–0.08)	This study
	Carbon demand[d]	mg C m^{-2} d^{-1}	0.08 (0.08–0.12)	0.19	0.33 (0.12–0.32)	0.13 (0.08–0.32)	This study
Epipelagic metazoans	Biomass	mg m^{-2}	1972 (1463–3412)	1611 (1250–1738)	3121 (2876–3491)	1972 (1661–3121)	This study
	Carbon biomass[b]	mg m^{-2}	789 (585–1365)	644 (500–695)	1248 (1150–1396)	789 (664–1248)	This study
	Secondary Production[c]	mg C m^{-2} d^{-1}	9.47 (7.02–16.38)	7.73 (6.00–8.34	14.98 (13.80–16.75)	9.47 (7.97–14.98)	This study
	Carbon demand[d]	mg C m^{-2} d^{-1}	37.86 (28.08–65.52)	30.93 (24–33.36)	59.92 (55.2–67)	37.86 (31.88–59.92)	This study
Export	Carbon flux	mg C m^{-2} d^{-1}	40.0 (27.5–45)	27.5 (11.3–47.5)	70.0 (42.5–85.0)	45.0 (15.0–50.0)	Lalande et al. (2014)

Values are medians; interquartile ranges are shown in parentheses

[a]Assuming a C:Chl ratio of 50:1 (Hansen et al. 1996)

[b]Assuming a carbon content of 40% by dry mass (Thibault et al. 1999)

[c]Assuming a production:biomass ratio of 1.2% (Forest et al. 2014)

[d]Assuming a gross growth efficiency of about ~ 25% (Forest et al. 2011)

2014). This indicates that a potential spatial and/or temporal increase of nutrient-depleted areas in the central Arctic Ocean may be associated with profound, potentially negative, changes in key ecosystem functions.

Conclusions

Our results demonstrate that, besides hydrographical conditions, sea-ice influence can be an important driver of the taxonomic structure of protist and metazoan communities, both in the under-ice and the epipelagic habitats of the central Arctic Ocean. Nutrient concentration, however, was the single important driver of the trophic structure in these communities, showing that low-nutrient concentrations in the epipelagic and under-ice habitat of the Arctic Ocean were associated with increasing heterotrophy. Understanding how nutrient limitation enhances heterotrophy in ecosystems, and quantifying the potential impact this has on ecosystem functions, is fundamental for the development of future scenarios of the changing Arctic ecosystems. The relationships of taxonomic and trophic community structure with sea-ice properties, hydrography and nutrient concentrations presented in this snapshot of the ecosystem in the historical sea-ice minimum year 2012 may be indicative of the future central Arctic Ocean. For modelling future Arctic ecosystems, it is important to consider that taxonomic biodiversity can respond to different drivers than trophic diversity.

Acknowledgements This study was conducted under the Helmholtz Association Research Programme *Polar regions And Coasts in the changing Earth System II* (PACES II), Topic 1, WP 4 and is part of the Helmholtz Association Young Investigators Groups *Iceflux*: Ice-ecosystem carbon flux in polar oceans (VH-NG-800) and PLANKTOSENS (VH-NG-500). SUIT was developed by Wageningen Marine Research (formerly IMARES) with support from the Netherlands Ministry of EZ (Project WOT-04–009-036) and the Netherlands Polar Program (Project ALW 866.13.009). I.P. received financial support from the TRANSDRIFT project; BMBF project #03G0833B. We would like to thank Captain Uwe Pahl and the crew of *Polarstern* expedition PS80 for their support in the field work. We thank Jan Andries van Franeker (IMARES) for kindly providing the Surface and Under-Ice Trawl (SUIT) and Michiel van Dorssen for technical support with work at sea. We are grateful for the support by Erika Allhusen, Christiane Lorenzen, Sandra Murawski, Kerstin Ötjen and Martina Vortkamp with laboratory analyses. We thank Karel Bakker for kindly providing the nutrient data. BAL and DK were partly funded by the Natural Sciences and Engineering Research Council of Canada Visiting Fellowships.

Author contributions HF was the main author of this paper, supervised the collection of environmental data, under-ice metazoan and epipelagic metazoan samples, and accomplished the data analyses. CD conducted laboratory analyses of under-ice metazoans. JE conducted laboratory analyses of epipelagic metazoan samples and provided Online Resources. KH provided protist community data based on OTU analysis and contributed to data analysis. DK provided size and weight data of under-ice metazoans. BAL collected and validated environmental data and provided Fig. 1. BN supervised epipelagic metazoan analysis. E-MN provided count data of phytoplankton samples and advised on aspects of phytoplankton ecology. IP provided chlorophyll and other environmental datasets. KM initiated the study and advised on aspects of molecular-based biodiversity and ecology. All authors contributed significantly to the drafting of this research article.

Funding This study was conducted under the Helmholtz Association Research Programme *Polar regions And Coasts in the changing Earth System II* (PACES II), Topic 1, WP 4 and is part of the Helmholtz Association Young Investigators Groups *Iceflux*: Ice-ecosystem carbon flux in polar oceans (VH-NG-800) and PLANKTOSENS (VH-NG-500). SUIT was developed by Wageningen Marine Research (formerly IMARES) with support from the Netherlands Ministry of EZ (Project WOT-04–009-036) and the Netherlands Polar Program (Project ALW 866.13.009). I.P. received financial support from the TRANSDRIFT project; BMBF project #03G0833B. BAL and DK were partly funded by the Natural Sciences and Engineering Research Council of Canada Visiting Fellowships.

Compliance with ethical standards

Conflict of interest The authors declare that the research was conducted in the absence of any commercial or financial relationships that could be construed as a potential conflict of interest.

Ethical approval All applicable international, national, and institutional guidelines for the use of animals were followed. This article does not contain any studies with human participants performed by any of the authors.

References

Ardyna M, Gosselin M, Michel C, Poulin M, Tremblay J (2011) Environmental forcing of phytoplankton community structure and function in the Canadian High Arctic: contrasting oligotrophic and eutrophic regions. Mar Ecol Prog Ser 442:37–57

Arrigo KR, van Dijken GL (2011) Secular trends in Arctic Ocean net primary production. J Geophys Res 116:C09011

Arrigo KR, van Dijken GL (2015) Continued increases in Arctic Ocean primary production. Prog Oceanogr 136:60–70

Ashjian CJ, Campbell RG, Welch HE, Butler M, Van Keuren D (2003) Annual cycle in abundance, distribution, and size in relation to hydrography of important copepod species in the western Arctic Ocean. Deep Sea Res Pt I 50:1235–1261

Balzano S, Marie D, Gourvil P, Vaulot D (2012) Composition of the summer photosynthetic pico and nanoplankton communities in the Beaufort Sea assessed by T-RFLP and sequences of the 18S rRNA gene from flow cytometry sorted samples. ISME J 6:1480–1498. https://doi.org/10.1038/ismej.2011.213

Basedow SL, Tande KS, Zhou M (2010) Biovolume spectrum theories applied: spatial patterns of trophic levels within a mesozooplankton community at the polar front. J Plankton Res 32:1105–1119. https://doi.org/10.1093/plankt/fbp110

Bauch D, Torres-Valdes S, Polyakov I, Novikhin A, Dmitrenko I, McKay J, Mix A (2014) Halocline water modification and along-slope advection at the Laptev Sea continental margin. Ocean Sci 10:141–154. https://doi.org/10.5194/os-10-141-2014

Bluhm B, Gradinger R, Schnack-Schiel SB (2010) Sea ice meio- and macrofauna. In: Thomas DN, Dieckmann G (eds) Sea ice. Blackwell Publishing, Oxford, UK, pp 357–394

Bluhm BA, Gebruk AV, Gradinger R, Hopcroft RR, Huettmann F, Kosobokova KN, Sirenko BI, Weslawski JM (2011) Arctic

marine biodiversity: asn update of species richness and examples of biodiversity change. Oceanography 24:232–248. https://doi.org/10.5670/oceanog.2011.75

Bluhm BA, Kosobokova KN, Carmack EC (2015) A tale of two basins: an integrated physical and biological perspective of the deep Arctic Ocean. Prog Oceanogr 139:89–121. https://doi.org/10.1016/j.pocean.2015.07.011

Boetius A, Albrecht S, Bakker K, Bienhold C, Felden J, Fernández-Méndez M, Hendricks S, Katlein C, Lalande C, Krumpen T, Nicolaus M, Peeken I, Rabe B, Rogacheva A, Rybakova E, Somavilla R, Wenzhöfer F, Party RPA (2013) Export of algal biomass from the melting Arctic sea ices. Science 339:1430–1432. https://doi.org/10.1126/science.1231346

Bokulich NA, Subramanian S, Faith JJ, Gevers D, Gordon JI, Knight R, Mills DA, Caporaso JG (2013) Quality-filtering vastly improves diversity estimates from Illumina amplicon sequencing. Nat Methods 10:57–59

Bradley IM, Pinto AJ, Guest JS (2016) Design and evaluation of Illumina MiSeq-compatible, 18S rRNA gene-specific primers for improved characterization of mixed phototrophic communities. Appl Environ Microb 82:5878–5891. https://doi.org/10.1128/Aem.01630-16

Budge S, Wooller M, Springer A, Iverson S, McRoy C, Divoky G (2008) Tracing carbon flow in an arctic marine food web using fatty acid-stable isotope analysis. Oecologia 157:117–129

Campbell RG, Sherr EB, Ashjian CJ, Plourde S, Sherr BF, Hill V, Stockwell DA (2009) Mesozooplankton prey preference and grazing impact in the western Arctic Ocean. Deep Sea Res Pt Ii 56:1274–1289. https://doi.org/10.1016/j.dsr2.2008.10.027

Caporaso JG, Kuczynski J, Stombaugh J, Bittinger K, Bushman FD, Costello EK, Fierer N, Peña AG, Goodrich JK, Gordon JI (2010) QIIME allows analysis of high-throughput community sequencing data. Nat Methods 7:335–336

Codispoti LA, Kelly V, Thessen A, Matrai P, Suttles S, Hill V, Steele M, Light B (2013) Synthesis of primary production in the Arctic Ocean: III. Nitrate and phosphate based estimates of net community production. Prog Oceanogr 110:126–150. https://doi.org/10.1016/j.pocean.2012.11.006

Cota GF, Pomeroy LR, Harrison WG, Jones EP, Peters F, Sheldon WM, Weingartner TR (1996) Nutrients, primary production and microbial heterotrophy in the southeastern Chukchi Sea: Arctic summer nutrient depletion and heterotrophy. Mar Ecol Prog Ser 135:247–258. https://doi.org/10.3354/meps135247

David C, Lange B, Rabe B, Flores H (2015) Community structure of under-ice fauna in the Eurasian central Arctic Ocean in relation to environmental properties of sea-ice habitats. Mar Ecol Prog Ser 522:15–32. https://doi.org/10.3354/meps11156

David C, Lange B, Krumpen T, Schaafsma F, van Franeker JA, Flores H (2016) Under-ice distribution of polar cod *Boreogadus saida* in the central Arctic Ocean and their association with sea-ice habitat properties. Polar Biol 39:981–994. https://doi.org/10.1007/s00300-015-1774-0

Edler L (1979) Recommendations on methods for marine biological studies in the Baltic Sea. Phytoplankton and chlorophyll. Baltic Marine Biologists Working Group 9

Egge E, Bittner L, Andersen T, Audic S, de Vargas C, Edvardsen B (2013) 454 pyrosequencing to describe microbial eukaryotic community composition, diversity and relative abundance: a test for marine haptophytes. PLoS ONE 8:e74371

Ehrlich J (2015) Diversity and distribution of high-Arctic zooplankton in the Eurasian Basin in late summer 2012. Master Thesis. Centrum für Naturkunde (CeNaK), Hamburg

Evans CA, O'Reilly JE, Thomas JP (1987) Part 1, A Handbook for the measurement of Chlorophyll a in netplankton and nannoplankton. In: Evans CA, O'Reilly JE, Thomas JP (eds) A Handbook for the measurement of Chlorophyll a and primary production. BIO-MASS scientic series. Texas A & M University, College Station, Tx, pp 3–46

Falk-Petersen S, Gatten RR, Sargent JR, Hopkins CCE (1981) Ecological investigations on the zooplankton community in Balsfjorden, Northern Norway: seasonal changes in the lipid class composition of *Meganyctiphanes norvegica* (M. Sars), *Thysanoessa raschii* (M. Sars), and *T. inermis* (Krøyer). J Exp Mar Biol Ecol 54:209–224. https://doi.org/10.1016/0022-0981(81)90158-1

Fernández-Méndez M, Katlein C, Rabe B, Nicolaus M, Peeken I, Bakker K, Flores H, Boetius A (2015) Photosynthetic production in the central Arctic Ocean during the record sea-ice minimum in 2012. Biogeosciences 12:3525–3549. https://doi.org/10.5194/bg-12-3525-2015

Flores H, van Franeker JA, Siegel V, Haraldsson M, Strass VH, Meesters EHWG, Bathmann U, Wolff WJ (2012) The association of Antarctic krill *Euphausia superba* with the under-ice habitat. PLoS ONE 7:e31775. https://doi.org/10.1371/journal.pone.0031775

Forest A, Tremblay JE, Gratton Y, Martin J, Gagnon J, Darnis G, Sampei M, Fortier L, Ardyna M, Gosselin M, Hattori H, Nguyen D, Maranger R, Vaque D, Marrase C, Pedros-Alio C, Sallon A, Michel C, Kellogg C, Deming J, Shadwick E, Thomas H, Link H, Archambault P, Piepenburg D (2011) Biogenic carbon flows through the planktonic food web of the Amundsen Gulf (Arctic Ocean): a synthesis of field measurements and inverse modeling analyses. Prog Oceanogr 91:410–436. https://doi.org/10.1016/j.pocean.2011.05.002

Forest A, Coupel P, Else B, Nahavandian S, Lansard B, Raimbault P, Papakyriakou T, Gratton Y, Fortier L, Tremblay JE, Babin M (2014) Synoptic evaluation of carbon cycling in the Beaufort Sea during summer: contrasting river inputs, ecosystem metabolism and air-sea CO_2 fluxes. Biogeosciences 11:2827–2856. https://doi.org/10.5194/bg-11-2827-2014

Fujiwara A, Hirawake T, Suzuki K, Imai I, Saitoh SI (2014) Timing of sea ice retreat can alter phytoplankton community structure in the western Arctic Ocean. Biogeosciences 11:1705–1716. https://doi.org/10.5194/bg-11-1705-2014

Godhe A, Asplund ME, Harnstrom K, Saravanan V, Tyagi A, Karunasagar I (2008) Quantification of diatom and dinoflagellate biomasses in coastal marine seawater samples by Real-Time PCR. Appl Environ Microb 74:7174–7182. https://doi.org/10.1128/Aem.01298-08

Gosselin M, Levasseur M, Wheeler PA, Horner RA, Booth BC (1997) New measurements of phytoplankton and ice algal production in the Arctic Ocean. Deep Sea Res II (Top Stud Oceanogr) 44:1623–1644

Gradinger RR, Bluhm BA (2004) In-situ observations on the distribution and behavior of amphipods and Arctic cod (*Boreogadus saida*) under the sea ice of the High Arctic Canada Basin. Polar Biol 27:595–603. https://doi.org/10.1007/s00300-004-0630-4

Hansen B, Christiansen S, Pedersen G (1996) Plankton dynamics in the marginal ice zone of the central Barents Sea during spring: carbon flow and structure of the grazer food chain. Polar Biol 16:115–128

Hardge K, Peeken I, Neuhaus S, Krumpen T, Stoeck T, Metfies K (2017) Sea ice origin and sea ice retreat as possible drivers of variability in Arctic marine protist composition. Mar Ecol Prog Ser 571:43–57. https://doi.org/10.3354/meps12134

Hardge K, Peeken I, Neuhaus S, Lange BA, Stock A, Stoeck T, Weinisch L, Metfies K (2017) The importance of sea ice for exchange of habitat-specific protist communities in the Central Arctic Ocean. J Mar Syst 165:124–138. https://doi.org/10.1016/j.jmarsys.2016.10.004

Hill VJ, Matrai PA, Olson E, Suttles S, Steele M, Codispoti LA, Zimmerman RC (2013) Synthesis of integrated primary production in the Arctic Ocean: II. In situ and remotely sensed estimates.

Prog Oceanogr 110:107–125. https://doi.org/10.1016/j.pocean.2012.11.005

Hop H, Poltermann M, Lonne OJ, Falk-Petersen S, Korsnes R, Budgell WP (2000) Ice amphipod distribution relative to ice density and under-ice topography in the northern Barents Sea. Polar Biol 23:357–367. https://doi.org/10.1007/s003000050456

Hunt BPV, Nelson RJ, Williams B, McLaughlin FA, Young KV, Brown KA, Vagle S, Carmack EC (2014) Zooplankton community structure and dynamics in the Arctic Canada Basin during a period of intense environmental change (2004–2009). J Geophys Res-Oceans 119:2518–2538. https://doi.org/10.1002/2013JC009156

IPCC (2014) Climate change 2014: impacts, adaptation, and vulnerability. Part B: regional aspects. Contribution of working group II to the fifth assessment. Report of the intergovernmental panel on climate change, Cambridge, New York

Kattner G, Lobbes JM, Fitznar HP, Engbrodt R, Nothig EM, Lara RJ (1999) Tracing dissolved organic substances and nutrients from the Lena River through Laptev Sea (Arctic). Mar Chem 65:25–39. https://doi.org/10.1016/S0304-4203(99)00008-0

Kilias E, Wolf C, Noethig E-M, Peeken I, Metfies K (2013) Prostist distribution in the western Fram Strait in summer 2010 based on 454-pyrosequencing of 18S rDNA. J Phycol 49:996–1010. https://doi.org/10.1111/jpy.12109

Kohlbach D, Graeve M, Lange B, David C, Peeken I, Flores H (2016) The importance of ice algae-produced carbon in the central Arctic Ocean ecosystem: food web relationships revealed by lipid and stable isotope analyses. Limnol Oceanogr 61:2027–2044. https://doi.org/10.1002/lno.10351

Kohlbach D, Schaafsma FL, Graeve M, Lebreton B, Lange BA, David C, Vortkamp M, Flores H (2017) Strong linkage of polar cod (*Boreogadus saida*) to sea ice algae-produced carbon: evidence from stomach content, fatty acid and stable isotope analyses. Prog Oceanogr 152:62–74. https://doi.org/10.1016/j.pocean.2017.02.003

Kosobokova K, Hirche HJ (2000) Zooplankton distribution across the Lomonosov Ridge, Arctic Ocean: species inventory, biomass and vertical structure. Deep Sea Res Pt I 47:2029–2060. https://doi.org/10.1016/S0967-0637(00)00015-7

Kraft A, Nöthig E-M, Bauerfeind E, Wildish DJ, Pohle GW, Bathmann UV, Beszczynska-Moller A, Klages M (2013) First evidence of reproductive success in a southern invader indicates possible community shifts among Arctic zooplankton. Mar Ecol Prog Ser 493:291–296. https://doi.org/10.3354/meps10507

Kwok R, Rothrock D (2009) Decline in Arctic sea ice thickness from submarine and ICESat records: 1958–2008. Geophys Res Lett 36:L15501

Lalande C, Nöthig EM, Somavilla R, Bauerfeind E, Shevchenko V, Okolodkov Y (2014) Variability in under-ice export fluxes of biogenic matter in the Arctic Ocean. Glob Biogeochem Cycle 28:571–583

Lange BA, Katlein C, Nicolaus M, Peeken I, Flores H (2016J) Sea ice algae chlorophyll a concentrations derived from under-ice spectral radiation profiling platforms. J Geophys Res 121:8511–8534. https://doi.org/10.1002/2016JC011991

Laxon SW, Giles KA, Ridout AL, Wingham DJ, Willatt R, Cullen R, Kwok R, Schweiger A, Zhang J, Haas C (2013) CryoSat-2 estimates of Arctic sea ice thickness and volume. Geophys Res Lett 40:732–737

Levinsen H, Nielsen TG, Hansen BW (1999) Plankton community structure and carbon cycling on the western coast of Greenland during the stratified summer situation. II. Heterotrophic dinoflagellates and ciliates. Aquat Microb Ecol 16:217–232. https://doi.org/10.3354/ame016217

Levinsen H, Turner JT, Nielsen TG, Hansen BW (2000) On the trophic coupling between protists and copepods in arctic marine ecosystems. Mar Ecol Prog Ser 204:65–77. https://doi.org/10.3354/meps204065

McCullagh P, Nelder JA (1989) Generalized linear models, 2nd edn. Chapman & Hall, New York

Metfies K, von Appen W-J, Kilias E, Nicolaus A, Nöthig E-M (2016) Biogeography and photosynthetic biomass of arctic marine pico-eukaroytes during summer of the record sea ice minimum 2012. PLoS ONE 11:e0148512

Minagawa M, Wada E (1984) Stepwise enrichment of 15 N along food chains: further evidence and the relation between δ15N and animal age. Geochim Cosmochim Acta 48:1135–1140

Mumm N, Auel H, Hanssen H, Hagen W, Richter C, Hirche HJ (1998) Breaking the ice: large-scale distribution of mesozooplankton after a decade of Arctic and transpolar cruises. Polar Biol 20:189–197. https://doi.org/10.1007/s003000050295

Nicolaus M, Katlein C, Maslanik J, Hendricks S (2012g) Changes in Arctic sea ice result in increasing light transmittance and absorption. Geophys Res Lett 39:L24501. https://doi.org/10.1029/2012gl053738

Nielsen TG, Hansen BW (1999) Plankton community structure and carbon cycling on the western coast of Greenland during the stratified summer situation. I. Hydrography, phytoplankton and bacterioplankton. Aquat Microb Ecol 16:205–216. https://doi.org/10.3354/ame016205

Nöthig E-M, Bracher A, Engel A, Metfies K, Niehoff B, Peeken I, Bauerfeind E, Cherkasheva A, Gäbler-Schwarz S, Hardge K (2015) Summertime plankton ecology in Fram Strait—a compilation of long-and short-term observations. Polar Res 34:23349

Ohman MD, Runge JA (1994) Sustained fecundity when phytoplankton resources are in short supply—omnivory by *Calanus finmarchicus* in the Gulf of St. Lawrence. Limnol Oceanogr 39:21–36

Oksanen J, Blanchett FG, Kindt R, Legendre P, Minchin PR, O'Hara RB, Simpson GL, Solymos PM, Stevens MHH, Wagner H (2013) Vegan: community ecology package version 2.0-10. R Foundation for Statistical Computing

Parkinson CL, Comiso JC (2013) On the 2012 record low Arctic sea ice cover: combined impact of preconditioning and an August storm. Geophys Res Lett 40:1356–1361. https://doi.org/10.1002/grl.50349

Poltermann M, Hop H, Falk-Petersen S (2000) Life under Arctic sea ice—reproduction strategies of two sympagic (ice-associated) amphipod species, *Gammarus wilkitzkii* and *Apherusa glacialis*. Mar Biol 136:913–920. https://doi.org/10.1007/s002270000307

Prokopowich CD, Gregory TR, Crease TJ (2003) The correlation between rDNA copy number and genome size in eukaryotes. Genome 46:48–50. https://doi.org/10.1139/G02-103

R Core Team (2017) R: a language and environment for statistical computing. R Foundation for Statistical Computing, Vienna, Austria. https://www.R-project.org/

Rabe B, Wisotzki A, Rettig S, Somavilla Cabrillo R, Sander H (2012) Physical oceanography during POLARSTERN cruise ARK-XXVII/3 (IceArc) PANGEA. Alfred Wegener Institute, Helmholtz Center for Polar and Marine Research, Bremerhaven. https://doi.org/10.1594/PANGAEA.802904

Roca-Martí M, Puigcorbé V, Rutgers van der Loeff MM, Katlein C, Fernández-Méndez M, Peeken I, Masqué P (2016) Carbon export fluxes and export efficiency in the central Arctic during the record sea-ice minimum in 2012: a joint 234Th/238U and 210Po/210Pb study. J Geophys Res 121:5030–5049. https://doi.org/10.1002/2016JC011816

Rudels B, Schauer U, Björk G, Korhonen M, Pisarev S, Rabe B, Wisotzki A (2013) Observations of water masses and circulation with focus on the Eurasian Basin of the Arctic Ocean from the 1990s to the late 2000s. Ocean Sci 9:147–169. https://doi.org/10.5194/os-9-147-2013

Sakshaug E (2004) Primary and secondary production in the Arctic Seas. In: Stein R, MacDonald RW (eds) The organic carbon cycle in the Arctic Ocean. Springer, Berlin, pp 57–81

Serreze MC, Holland MM, Stroeve J (2007) Perspectives on the Arctic's shrinking sea-ice cover. Science 315:1533–1536

Shaw W, Stanton T, McPhee M, Morison J, Martinson D (2009) Role of the upper ocean in the energy budget of Arctic sea ice during SHEBA. J Geophys Res 114:C06012

Simmonds I (2015) Comparing and contrasting the behaviour of Arctic and Antarctic sea ice over the 35 year period 1979–2013. Ann Glaciol 56:18–28

Søreide JE, Leu E, Berge J, Graeve M, Falk-Petersen S (2010) Timing of blooms, algal food quality and *Calanus glacialis* reproduction and growth in a changing Arctic. Glob Chang Biol 16:3154–3163. https://doi.org/10.1111/j.1365-2486.2010.02175.x

Spreen G, Kaleschke L, Heygster G (2008) Sea ice remote sensing using AMSR-E 89-GHz channels. J Geophys Res 113:C02S03

Stoeck T, Bass D, Nebel M, Christen R, Jones MDM, Breiner HW, Richards TA (2010) Multiple marker parallel tag environmental DNA sequencing reveals a highly complex eukaryotic community in marine anoxic water. Mol Ecol 19:21–31. https://doi.org/10.1111/j.1365-294X.2009.04480.x

Stroeve JC, Kattsov V, Barrett A, Serreze M, Pavlova T, Holland M, Meier WN (2012g) Trends in Arctic sea ice extent from CMIP5, CMIP3 and observations. Geophys Res Lett 39:L16502. https://doi.org/10.1029/2012gl052676

Thibault D, Head EJH, Wheeler PA (1999) Mesozooplankton in the Arctic Ocean in summer. Deep Sea Res Pt I 46:1391–1415. https://doi.org/10.1016/S0967-0637(99)00009-6

Tremblay J-É, Anderson LG, Matrai P, Coupel P, Bélanger S, Michel C, Reigstad M (2015) Global and regional drivers of nutrient supply, primary production and CO_2 drawdown in the changing Arctic Ocean. Prog Oceanogr 139:171–196. https://doi.org/10.1016/j.pocean.2015.08.009

van Franeker JA, Flores H, Van Dorssen M (2009) The Surface and Under-Ice Trawl (SUIT). In: Flores H (ed) Frozen Desert Alive—the role of sea ice for pelagic macrofauna and its predators. PhD thesis. University of Groningen, Groningen, pp 181–188

Vergin KL, Beszteri B, Monier A, Thrash JC, Temperton B, Treusch AH, Kilpert F, Worden AZ, Giovannoni SJ (2013) High-resolution SAR11 ecotype dynamics at the Bermuda Atlantic time-series study site by phylogenetic placement of pyrosequences. ISME J 7:1322–1332

Wang M, Overland JE (2009) A sea ice free summer Arctic within 30 years? Geophys Res Lett 36:L07502

Wang SW, Budge SM, Iken K, Gradinger RR, Springer AM, Wooller MJ (2015) Importance of sympagic production to Bering Sea zooplankton as revealed from fatty acid-carbon stable isotope analyses. Mar Ecol Prog Ser 518:31–50

Wassmann P (2011) Arctic marine ecosystems in an era of rapid climate change. Prog Oceanogr 90:1–17. https://doi.org/10.1016/j.pocean.2011.02.002

Wassmann P, Duarte CM, Agusti S, Sejr MK (2011) Footprints of climate change in the Arctic marine ecosystem. Glob Chang Biol 17:1235–1249. https://doi.org/10.1111/j.1365-2486.2010.02311.x

Wassmann P, Kosobokova KN, Slagstad D, Drinkwater KF, Hopcroft RR, Moore SE, Ellingsen I, Nelson RJ, Carmack E, Popova E, Berge J (2015) The contiguous domains of Arctic Ocean advection: trails of life and death. Prog Oceanogr 139:42–65. https://doi.org/10.1016/j.pocean.2015.06.011

Yun MS, Whitledge TE, Stockwell D, Son SH, Lee JH, Park JW, Lee DB, Park J, Lee SH (2016) Primary production in the Chukchi Sea with potential effects of freshwater content. Biogeosciences 13:737–749

Zhu F, Massana R, Not F, Marie D, Vaulot D (2005) Mapping of picoeucaryotes in marine ecosystems with quantitative PCR of the 18S rRNA gene. FEMS Microbiol Ecol 52:79–92. https://doi.org/10.1016/j.femsec.2004.10.006

Online Resource / Electronic Supplementary Material

Effects of sea ice decay and nutrient depletion on taxonomic composition and trophic structure in high-Arctic protist and metazoan communities

Hauke Flores, Carmen David, Julia Ehrlich, Kristin Hardge, Doreen Kohlbach, Benjamin A. Lange, Barbara Niehoff, Eva-Maria Nöthig, Ilka Peeken & Katja Metfies

ESM1. Protist taxa as identified by Operational Taxonomic Units (OTU), and corresponding trophic groups (au=autotroph; ht=heterotroph; mx=micotroph; nc=not classified)

Taxon	Troph. Group
Eukaryota;__	nc
Eukaryota;__Alveolata;__	nc
Eukaryota;__Alveolata;__Ciliophora;__	ht
Eukaryota;__Alveolata;__Ciliophora;__Conthreep;__	ht
Eukaryota;__Alveolata;__Ciliophora;__Conthreep;__Oligohymenophorea;__	ht
Eukaryota;__Alveolata;__Ciliophora;__Conthreep;__Oligohymenophorea;__Homalogastra	ht
Eukaryota;__Alveolata;__Ciliophora;__Conthreep;__Oligohymenophorea;__Paramecium	ht
Eukaryota;__Alveolata;__Ciliophora;__Conthreep;__Oligohymenophorea;__Porpostoma	ht
Eukaryota;__Alveolata;__Ciliophora;__Conthreep;__Oligohymenophorea;__Stokesia	ht
Eukaryota;__Alveolata;__Ciliophora;__Conthreep;__Phyllopharyngea;__	ht
Eukaryota;__Alveolata;__Ciliophora;__Conthreep;__Phyllopharyngea;__Aporthotrochilia	ht
Eukaryota;__Alveolata;__Ciliophora;__Conthreep;__Plagiopylea;__	ht
Eukaryota;__Alveolata;__Ciliophora;__Conthreep;__Prostomatea;__Cryptocaryon	ht
Eukaryota;__Alveolata;__Ciliophora;__Heterotrichea;__Peritromus;__	ht
Eukaryota;__Alveolata;__Ciliophora;__Litostomatea;__	ht
Eukaryota;__Alveolata;__Ciliophora;__Litostomatea;__Haptoria;__	ht
Eukaryota;__Alveolata;__Ciliophora;__Litostomatea;__Haptoria;__Didinium	ht
Eukaryota;__Alveolata;__Ciliophora;__Litostomatea;__Haptoria;__Epiphyllum	ht
Eukaryota;__Alveolata;__Ciliophora;__Litostomatea;__Haptoria;__Loxophyllum	ht
Eukaryota;__Alveolata;__Ciliophora;__Litostomatea;__Haptoria;__Phialina	ht
Eukaryota;__Alveolata;__Ciliophora;__Spirotrichea;__Choreotrichia;__	ht
Eukaryota;__Alveolata;__Ciliophora;__Spirotrichea;__Choreotrichia;__Codonella	ht
Eukaryota;__Alveolata;__Ciliophora;__Spirotrichea;__Choreotrichia;__Metacylis	ht
Eukaryota;__Alveolata;__Ciliophora;__Spirotrichea;__Choreotrichia;__Salpingella	ht

Online Resource ESM1

Taxon	Troph. Group
Eukaryota;__Alveolata;__Ciliophora;__Spirotrichea;__Choreotrichia;__Strobilidium	ht
Eukaryota;__Alveolata;__Ciliophora;__Spirotrichea;__Choreotrichia;__uncultured	ht
Eukaryota;__Alveolata;__Ciliophora;__Spirotrichea;__Hypotrichia;__Anteholosticha	ht
Eukaryota;__Alveolata;__Ciliophora;__Spirotrichea;__Hypotrichia;__Holosticha	ht
Eukaryota;__Alveolata;__Ciliophora;__Spirotrichea;__Hypotrichia;__Oxytricha	ht
Eukaryota;__Alveolata;__Ciliophora;__Spirotrichea;__Oligotrichia;__	ht
Eukaryota;__Alveolata;__Ciliophora;__Spirotrichea;__Oligotrichia;__Laboea	ht
Eukaryota;__Alveolata;__Ciliophora;__Spirotrichea;__Oligotrichia;__Pseudotontonia	ht
Eukaryota;__Alveolata;__Ciliophora;__Spirotrichea;__Oligotrichia;__Strombidium	ht
Eukaryota;__Alveolata;__Ciliophora;__Spirotrichea;__Oligotrichia;__uncultured	ht
Eukaryota;__Alveolata;__Dinoflagellata;__	mx
Eukaryota;__Alveolata;__Dinoflagellata;__BBSRP1;__;__	mx
Eukaryota;__Alveolata;__Dinoflagellata;__Dinophyceae;__;__	mx
Eukaryota;__Alveolata;__Dinoflagellata;__Dinophyceae;__B28;__	mx
Eukaryota;__Alveolata;__Dinoflagellata;__Dinophyceae;__D244;__	mx
Eukaryota;__Alveolata;__Dinoflagellata;__Dinophyceae;__Dinophysiales;__	mx
Eukaryota;__Alveolata;__Dinoflagellata;__Dinophyceae;__Gymnodiniphycidae;__	mx
Eukaryota;__Alveolata;__Dinoflagellata;__Dinophyceae;__Gymnodiniphycidae;__Chytriodinium	mx
Eukaryota;__Alveolata;__Dinoflagellata;__Dinophyceae;__Gymnodiniphycidae;__Cochlodinium	mx
Eukaryota;__Alveolata;__Dinoflagellata;__Dinophyceae;__Gymnodiniphycidae;__FV18-2D9	mx
Eukaryota;__Alveolata;__Dinoflagellata;__Dinophyceae;__Gymnodiniphycidae;__Gyrodinium	mx
Eukaryota;__Alveolata;__Dinoflagellata;__Dinophyceae;__Gymnodiniphycidae;__Karlodinium	mx
Eukaryota;__Alveolata;__Dinoflagellata;__Dinophyceae;__Gymnodiniphycidae;__Lepidodinium	mx
Eukaryota;__Alveolata;__Dinoflagellata;__Dinophyceae;__Gymnodiniphycidae;__Pelagodinium	mx
Eukaryota;__Alveolata;__Dinoflagellata;__Dinophyceae;__Gymnodiniphycidae;__Spiniferodinium	mx
Eukaryota;__Alveolata;__Dinoflagellata;__Dinophyceae;__Gymnodiniphycidae;__Symbiodinium	mx
Eukaryota;__Alveolata;__Dinoflagellata;__Dinophyceae;__Gymnodiniphycidae;__Woloszynskia	mx
Eukaryota;__Alveolata;__Dinoflagellata;__Dinophyceae;__Halostylodinium;__	mx
Eukaryota;__Alveolata;__Dinoflagellata;__Dinophyceae;__NPK60-44;__	mx
Eukaryota;__Alveolata;__Dinoflagellata;__Dinophyceae;__Peridiniphycidae;__	mx
Eukaryota;__Alveolata;__Dinoflagellata;__Dinophyceae;__Peridiniphycidae;__Alexandrium	mx
Eukaryota;__Alveolata;__Dinoflagellata;__Dinophyceae;__Peridiniphycidae;__Glenodiniopsis	mx
Eukaryota;__Alveolata;__Dinoflagellata;__Dinophyceae;__Peridiniphycidae;__Neoceratium	mx
Eukaryota;__Alveolata;__Dinoflagellata;__Dinophyceae;__Peridiniphycidae;__Protoperidinium	mx
Eukaryota;__Alveolata;__Dinoflagellata;__Dinophyceae;__Peridiniphycidae;__Scrippsiella	mx
Eukaryota;__Alveolata;__Dinoflagellata;__Dinophyceae;__Prorocentrales;__Exuviaella	mx
Eukaryota;__Alveolata;__Dinoflagellata;__Dinophyceae;__SCM16C67;__	mx
Eukaryota;__Alveolata;__Dinoflagellata;__Dinophyceae;__SL163A10;__	mx
Eukaryota;__Alveolata;__Dinoflagellata;__Haplozoon;__;__	mx
Eukaryota;__Alveolata;__H67;__;__;__	nc
Eukaryota;__Alveolata;__OLI11255;__;__;__	nc

Taxon	Troph. Group
Eukaryota;__Alveolata;__Protalveolata;__Syndiniales;__	ht
Eukaryota;__Alveolata;__Protalveolata;__Syndiniales;__;__	ht
Eukaryota;__Alveolata;__Protalveolata;__Syndiniales;__Amoebophrya;__	ht
Eukaryota;__Alveolata;__Protalveolata;__Syndiniales;__Duboscquella;__	ht
Eukaryota;__Alveolata;__Protalveolata;__Syndiniales;__SyndinialesGroup	ht
Eukaryota;__Alveolata;__Protalveolata;__Syndiniales;__SyndinialesGroupI;__	ht
Eukaryota;__Alveolata;__Protalveolata;__Syndiniales;__SyndinialesGroupII;__	ht
Eukaryota;__Alveolata;__Protalveolata;__Syndiniales;__SyndinialesGroupIII;__	ht
Eukaryota;__Alveolata;__Protalveolata;__Syndiniales;__SyndinialesGroupV;__	ht
Eukaryota;__Alveolata;__SCM37C52;__;__;__	nc
Eukaryota;__Ancyromonadida;__Ancyromonas;__;__;__	nc
Eukaryota;__Apusomonadidae;__Amastigomonas;__;__;__	nc
Eukaryota;__Apusomonadidae;__IncertaeSedis;__;__;__	nc
Eukaryota;__Centrohelida;__	nc
Eukaryota;__Centrohelida;__Acanthocystidae;__Pterocystis;__;__	nc
Eukaryota;__Chloroplastida;__Chlorophyceae;__	mx
Eukaryota;__Chloroplastida;__Chlorophyceae;__Carteria;__;__	mx
Eukaryota;__Chloroplastida;__Chlorophyceae;__Chloromonas;__;__	mx
Eukaryota;__Chloroplastida;__Chlorophyceae;__Fasciculochloris;__;__	mx
Eukaryota;__Chloroplastida;__Mamiellophyceae;__	mx
Eukaryota;__Chloroplastida;__Mamiellophyceae;__;__;__	mx
Eukaryota;__Chloroplastida;__Mamiellophyceae;__Bathycoccus;__;__	mx
Eukaryota;__Chloroplastida;__Mamiellophyceae;__Crustomastix;__;__	mx
Eukaryota;__Chloroplastida;__Mamiellophyceae;__DSGM-81;__;__	mx
Eukaryota;__Chloroplastida;__Mamiellophyceae;__Micromonas;__;__	mx
Eukaryota;__Chloroplastida;__Prasinophytae;__	mx
Eukaryota;__Chloroplastida;__Prasinophytae;__Pterosperma;__;__	mx
Eukaryota;__Chloroplastida;__Prasinophytae;__Pyramimonas;__;__	mx
Eukaryota;__Chloroplastida;__Trebouxiophyceae;__AN1-3;__;__	mx
Eukaryota;__Chloroplastida;__Trebouxiophyceae;__Chlorella;__;__	mx
Eukaryota;__Chloroplastida;__Trebouxiophyceae;__Radiofilum;__;__	mx
Eukaryota;__Chloroplastida;__uncultured;__;__;__	mx
Eukaryota;__Co	nc
Eukaryota;__Conosa;__Protosteliida;__Protostelium;__;__	nc
Eukaryota;__Cryptophyceae;__Cryptomonadales;__	mx
Eukaryota;__Cryptophyceae;__Cryptomonadales;__Cryptomonas;__;__	mx
Eukaryota;__Cryptophyceae;__Cryptomonadales;__FV18-2G7;__;__	mx
Eukaryota;__Cryptophyceae;__Cryptomonadales;__Geminigera;__;__	mx
Eukaryota;__Cryptophyceae;__Cryptomonadales;__Teleaulax;__;__	mx
Eukaryota;__Cryptophyceae;__Goniomonas;__;__;__	mx
Eukaryota;__Discosea;__Flabellinia;__Vannellida;__Protosteliopsis;__	nc
Eukaryota;__Haptophyta;__Prymnesiophyceae;__	au

Online Resource ESM1

Taxon	Troph. Group
Eukaryota;__Haptophyta;__Prymnesiophyceae;__Phaeocystis;__;__	au
Eukaryota;__Haptophyta;__Prymnesiophyceae;__Prymnesiales;__	au
Eukaryota;__Haptophyta;__Prymnesiophyceae;__Prymnesiales;__Imantonia;__	au
Eukaryota;__Holozoa;__	nc
Eukaryota;__Holozoa;__Choanomonada;__Acanthoecida;__	nc
Eukaryota;__Holozoa;__Choanomonada;__Acanthoecida;__Acanthocorbis;__	nc
Eukaryota;__Holozoa;__Choanomonada;__Acanthoecida;__Diaphanoeca;__	nc
Eukaryota;__Holozoa;__Choanomonada;__Acanthoecida;__Stephanoeca;__	nc
Eukaryota;__Holozoa;__Choanomonada;__Craspedida;__Lagenoeca;__	nc
Eukaryota;__Lobosa;__Tubulinea;__Euamoebida;__Hartmannella;__	nc
Eukaryota;__Rhizaria;__Cercozoa;__	mx
Eukaryota;__Rhizaria;__Cercozoa;__Endomyxa;__Phytomyxea;__	mx
Eukaryota;__Rhizaria;__Cercozoa;__Glissomonadida;__Heteromita;__	mx
Eukaryota;__Rhizaria;__Cercozoa;__NovelClade2;__;__	mx
Eukaryota;__Rhizaria;__Cercozoa;__NovelClade4;__;__	mx
Eukaryota;__Rhizaria;__Cercozoa;__NovelCladeGran-3;__;__	mx
Eukaryota;__Rhizaria;__Cercozoa;__Silicofilosea;__	mx
Eukaryota;__Rhizaria;__Cercozoa;__Silicofilosea;__;__	mx
Eukaryota;__Rhizaria;__Cercozoa;__Silicofilosea;__7-5.4;__	mx
Eukaryota;__Rhizaria;__Cercozoa;__Silicofilosea;__Chlorarachniophyta;__BC52	mx
Eukaryota;__Rhizaria;__Cercozoa;__Silicofilosea;__Chlorarachniophyta;__NOR26	mx
Eukaryota;__Rhizaria;__Cercozoa;__Silicofilosea;__Marimonadida;__Auranticordis	mx
Eukaryota;__Rhizaria;__Cercozoa;__Silicofilosea;__Marimonadida;__NAMAKO-15	mx
Eukaryota;__Rhizaria;__Cercozoa;__Silicofilosea;__p15D09;__	mx
Eukaryota;__Rhizaria;__Cercozoa;__Silicofilosea;__Thaumatomonadida;__	mx
Eukaryota;__Rhizaria;__Cercozoa;__Silicofilosea;__Thaumatomonadida;__Allas	mx
Eukaryota;__Rhizaria;__Cercozoa;__Silicofilosea;__Thaumatomonadida;__D6	mx
Eukaryota;__Rhizaria;__Cercozoa;__Silicofilosea;__Thaumatomonadida;__Gyromitus	mx
Eukaryota;__Rhizaria;__Cercozoa;__Thecofilosea;__	mx
Eukaryota;__Rhizaria;__Cercozoa;__Thecofilosea;__Cryomonadida;__Cryothecomonas	mx
Eukaryota;__Rhizaria;__Cercozoa;__Thecofilosea;__Ebriacea;__Ebria	mx
Eukaryota;__Rhizaria;__Cercozoa;__Thecofilosea;__NIF-3A7;__	mx
Eukaryota;__Rhizaria;__Cercozoa;__Thecofilosea;__NOR26;__	mx
Eukaryota;__Rhizaria;__Cercozoa;__Thecofilosea;__uncultured;__	mx
Eukaryota;__Rhizaria;__Cercozoa;__Thecofilosea;__WHOI-LI1-14;__	mx
Eukaryota;__Rhizaria;__Radiolaria;__	ht
Eukaryota;__Rhizaria;__Radiolaria;__Acantharia;__AcanthareaGroupI;__	ht
Eukaryota;__Rhizaria;__Radiolaria;__Acantharia;__Chaunocanthida;__	ht
Eukaryota;__Rhizaria;__Radiolaria;__Polycystinea;__Nassellaria;__Pseudocubus	ht
Eukaryota;__Rhizaria;__Radiolaria;__Polycystinea;__Spumellaria;__	ht
Eukaryota;__Rhizaria;__Radiolaria;__RADC;__;__	ht

Taxon	Troph. Group
Eukaryota;__Stramenopiles;__	nc
Eukaryota;__Stramenopiles;__;__;__;__	nc
Eukaryota;__Stramenopiles;__Bicosoecida;__Cafeteriidae;__	nc
Eukaryota;__Stramenopiles;__Bicosoecida;__Cafeteriidae;__BCI5F15RM3E05;__	nc
Eukaryota;__Stramenopiles;__Bicosoecida;__Cafeteriidae;__Cafeteria;__	nc
Eukaryota;__Stramenopiles;__Bicosoecida;__Cafeteriidae;__Symbiomonas;__	nc
Eukaryota;__Stramenopiles;__Bicosoecida;__LG08-10;__;__	nc
Eukaryota;__Stramenopiles;__Bicosoecida;__Siluaniidae;__Caecitellus;__	nc
Eukaryota;__Stramenopiles;__Bolidomonas;__;__;__	nc
Eukaryota;__Stramenopiles;__Chrysophyceae;__	au
Eukaryota;__Stramenopiles;__Chrysophyceae;__CCMP1899;__;__	au
Eukaryota;__Stramenopiles;__Chrysophyceae;__Chromulinales;__Spumella;__	au
Eukaryota;__Stramenopiles;__Chrysophyceae;__CladeC;__;__	au
Eukaryota;__Stramenopiles;__Chrysophyceae;__LG01-09;__;__	au
Eukaryota;__Stramenopiles;__Chrysophyceae;__Ochromonadales;__Epipyxis;__	au
Eukaryota;__Stramenopiles;__Chrysophyceae;__Ochromonadales;__Paraphysomonas;__	au
Eukaryota;__Stramenopiles;__Diatomea;__	au
Eukaryota;__Stramenopiles;__Diatomea;__3b-F4;__;__	au
Eukaryota;__Stramenopiles;__Diatomea;__Bacillariophytina;__Bacillariophyceae;__	au
Eukaryota;__Stramenopiles;__Diatomea;__Bacillariophytina;__Bacillariophyceae;__Amphora	au
Eukaryota;__Stramenopiles;__Diatomea;__Bacillariophytina;__Bacillariophyceae;__CCMP2297	au
Eukaryota;__Stramenopiles;__Diatomea;__Bacillariophytina;__Bacillariophyceae;__Cy	au
Eukaryota;__Stramenopiles;__Diatomea;__Bacillariophytina;__Bacillariophyceae;__Haslea	au
Eukaryota;__Stramenopiles;__Diatomea;__Bacillariophytina;__Bacillariophyceae;__Navicula	au
Eukaryota;__Stramenopiles;__Diatomea;__Bacillariophytina;__Bacillariophyceae;__Nitzschia	au
Eukaryota;__Stramenopiles;__Diatomea;__Bacillariophytina;__Bacillariophyceae;__Pinnularia	au
Eukaryota;__Stramenopiles;__Diatomea;__Bacillariophytina;__Bacillariophyceae;__Sellaphora	au
Eukaryota;__Stramenopiles;__Diatomea;__Bacillariophytina;__Mediophyceae;__	au
Eukaryota;__Stramenopiles;__Diatomea;__Bacillariophytina;__Mediophyceae;__Attheya	au
Eukaryota;__Stramenopiles;__Diatomea;__Bacillariophytina;__Mediophyceae;__Chaetoceros	au
Eukaryota;__Stramenopiles;__Diatomea;__Bacillariophytina;__Mediophyceae;__Porosira	au
Eukaryota;__Stramenopiles;__Diatomea;__Coscinodiscophytina;__Coscinodiscids;__Actinocyclus	au
Eukaryota;__Stramenopiles;__Diatomea;__Coscinodiscophytina;__Fragilariales;__	au
Eukaryota;__Stramenopiles;__Diatomea;__Coscinodiscophytina;__Melosirids;__Melosira	au
Eukaryota;__Stramenopiles;__Diatomea;__Coscinodiscophytina;__Rhizosolenids;__Rhizosolenia	au
Eukaryota;__Stramenopiles;__Diatomea;__ME-Euk-FW10;__;__	au
Eukaryota;__Stramenopiles;__Dictyochophyceae;__	nc
Eukaryota;__Stramenopiles;__Dictyochophyceae;__Dictyochales;__Dictyocha;__	nc
Eukaryota;__Stramenopiles;__Dictyochophyceae;__NIF-1D10;__;__	nc
Eukaryota;__Stramenopiles;__Dictyochophyceae;__Pedinellales;__	nc
Eukaryota;__Stramenopiles;__Dictyochophyceae;__Pedinellales;__;__	nc
Eukaryota;__Stramenopiles;__Dictyochophyceae;__Pedinellales;__Pteridomonas;__	nc

5

Online Resource ESM1

Taxon	Troph. Group
Eukaryota;__Stramenopiles;__Dictyochophyceae;__Verrucophora;__;__	nc
Eukaryota;__Stramenopiles;__Labyrinthulomycetes;__	nc
Eukaryota;__Stramenopiles;__Labyrinthulomycetes;__D2P04F01;__;__	nc
Eukaryota;__Stramenopiles;__Labyrinthulomycetes;__D52;__;__	nc
Eukaryota;__Stramenopiles;__Labyrinthulomycetes;__TAGIRI-15;__;__	nc
Eukaryota;__Stramenopiles;__Labyrinthulomycetes;__Thraustochytriaceae;__AB3F14RJ3E10;__	nc
Eukaryota;__Stramenopiles;__MAST-	ht
Eukaryota;__Stramenopiles;__MAST-1;__MAST-1A;__;__	ht
Eukaryota;__Stramenopiles;__MAST-1;__MAST-1B;__;__	ht
Eukaryota;__Stramenopiles;__MAST-1;__MAST-1C;__;__	ht
Eukaryota;__Stramenopiles;__MAST-2;__;__;__	ht
Eukaryota;__Stramenopiles;__MAST-3;__;__;__	ht
Eukaryota;__Stramenopiles;__MAST-7;__;__;__	ht
Eukaryota;__Stramenopiles;__MAST-8;__;__;__	ht
Eukaryota;__Stramenopiles;__MAST-9;__;__;__	ht
Eukaryota;__Stramenopiles;__Pelagophyceae;__	nc
Eukaryota;__Stramenopiles;__Pelagophyceae;__Pelagomonadales;__Pelagomonas;__	nc
Eukaryota;__Stramenopiles;__Pelagophyceae;__Sarcinochrysidales;__SS1-E01-69;__	nc
Eukaryota;__Stramenopiles;__Xanthophyceae;__Tribonematales;__	nc
Eukaryota;__Telonema;__IncertaeSedis;__;__;__	nc

Online Resource / Electronic Supplementary Material

Effects of sea ice decay and nutrient depletion on taxonomic composition and trophic structure in high-Arctic protist and metazoan communities

Hauke Flores, Carmen David, Julia Ehrlich, Kristin Hardge, Doreen Kohlbach, Benjamin A. Lange, Barbara Niehoff, Eva-Maria Nöthig, Ilka Peeken & Katja Metfies

ESM2. Dry weights and trophic groups of under-ice fauna and zooplankton collected during PS80

Taxon	Trophic group	Mean biomass [mg m^{-2}]	Mean ind. DW [mg]	Reference
Under-ice fauna				
Clione limacina	Carnivore	0.508	0.570	Mizdalski, 1988
Limacina helicina	Herbivore	0.003	0.272	Mizdalski, 1988
Polychaeta	Carnivore	< 0.001	0.062	Richter, 1994
Boroecia borealis	Carnivore	0.000	0.256	Conchoecia sp. from Mizdalski (1988)
Calanus finmarchicus	Herbivore	1.050	0.462	0.7 * *C. glacialis* (Ashjian et al., 2003)
Calanus glacialis	Herbivore	0.745	0.660	Ashjian et al., 2003
Calanus hyperboreus	Herbivore	6.142	1.629	Ashjian et al., 2003
Metridia longa	Herbivore	0.167	0.089	Ashjian et al., 2003
Paraeuchaeta glacialis	Carnivore	0.006	6.580	Auel and Hagen, 2005
Pseudocalanus spp.	Herbivore	0.003	0.012	Norrbin et al., 1990
Apherusa glacialis	Herbivore	2.626	4.168	measured
Eusirus holmii	Carnivore	0.176	85.295	measured
Gammarus wilkitzkii	Omnivore	0.168	103.208	measured
Gammaracanthus loricatus	Omnivore	0.003	103.208	measured (as *G. Wilkitzkii)*
Onisimus glacialis	Omnivore	0.560	46.020	measured (as *O. nanseni)*
Onisimus nanseni	Omnivore	0.174	46.020	measured
Themisto libellula	Carnivore	1.041	14.178	measured length-weight relationship
Themisto abyssorum	Carnivore	0.101	12.761	0.9 * l-w rel. from *T. libellula*
Thysanoessa inermis	Herbivore	0.002	20.000	Falk-Petersen, 1981
Euphausiacea	Herbivore	0.000	5.000	Falk-Petersen, 1981
Eukrohnia spp.	Carnivore	0.064	2.151	Donnelly et al., 1994
Sagitta spp.	Carnivore	0.007	4.500	Ikeda and Skjoldal, 1989
Oikopleura vanhoeffeni	Herbivore	0.103	0.200	Richter, 1994

Online Resource ESM2

Taxon	Trophic group	Mean biomass [mg m^{-2}]	Mean ind. DW [mg]	Reference
Mesozooplankton				
Polychaeta	Carnivore	0.819	0.062	Richter, 1994
Ostracoda	Carnivore	15.281	0.250	Mizdalski, 1988
Cirripedia	Omnivore	0.005	0.001	as in *Calanus* nauplii (Richter, 1994)
Calanus hyperboreus	Herbivore	706.997	0.598	Ashjian et al. (2003)
Calanus spp.	Herbivore	507.201	0.462	0.7 * *C. glacialis* (Ashjian et al., 2003)
Calanus nauplii	Herbivore	2.768	0.001	Richter (1994)
Centropages spp.	Herbivore	0.020	0.017	Ikeda et al. (2001)
Paraeuchaeta spp.	Carnivore	160.439	6.580	Auel and Hagen (2005)
Heterorhabdus spp.	Herbivore	0.756	0.089	as in *Metridia* spp. (Ashjian et al., 2003)
Metridia spp.	Herbivore	30.348	0.089	Ashjian et al. (2003)
Temora spp.	Herbivore	0.030	0.016	Ikeda et al. (2001)
Clausocalanidae	Herbivore	8.700	0.003	as in *Oithona* (Richter, 1994)
Oithona spp.	Herbivore	60.405	0.003	Richter (1994)
Oithona nauplii	Herbivore	2.635	0.001	as in *Oncaea* nauplii (Richter, 1994)
Oncaea spp.	Omnivore	0.236	0.002	Richter (1994)
Corycaeus spp.	Omnivore	118.430	0.030	Ikeda et al. (2001)
Microsetella spp.	Herbivore	0.068	0.003	as in *Oithona* (Richter, 1994)
Tisbe spp.	Herbivore	0.030	0.002	as in *Oncaea* (Richter, 1994)
Mormonilla spp.	Herbivore	0.064	0.003	as in *Oithona* (Richter, 1994)
Amphipoda	Carnivore	300.232	6.000	small *T. libellula*
Chaetognatha	Carnivore	425.175	2.151	*Eukrohnia* sp., Donnelly et al. (1994)
Appendicularia	Herbivore	69.605	0.200	Richter (1994)

References:

Ashjian, C.J., Campbell, R.G., Welch, H.E., Butler, M., and Van Keuren, D. (2003). Annual cycle in abundance, distribution, and size in relation to hydrography of important copepod species in the western Arctic Ocean. *Deep-Sea Research Part I-Oceanographic Research Papers* 50**,** 1235-1261.

Auel, H., and Hagen, W. (2005). Body mass and lipid dynamics of Arctic and Antarctic deep-sea copepods (Calanoida, Paraeuchaeta): ontogenetic and seasonal trends. *Deep-Sea Research Part I-Oceanographic Research Papers* 52**,** 1272-1283.

Donnelly, J., Torres, J.J., Hopkins, T.L., and Lancraft, T.M. (1994). Chemical composition of Antarctic zooplankton during austral fall and winter. *Polar Biology* 14**,** 171-183.

Falk-Petersen, S. (1981). Ecological investigations on the zooplankton community of Balsfjorden, northern Norway: Seasonal changes in body weight and the main biochemical composition of *Thysanoessa inermis* (krøyer), *T. Raschii* (M. Sars), and *Meganyctiphanes norvegica* (M. Sars) in relation to environmental factors. *Journal of Experimental Marine Biology and Ecology* 49**,** 103-120.

Ikeda, T., Kanno, Y., Ozaki, K., and Shinada, A. (2001). Metabolic rates of epipelagic marine copepods as a function of body mass and temperature. *Marine Biology* 139**,** 587-596.

Ikeda, T., and Skjoldal, H.R. (1989). Metabolism and elemental composition of zooplankton from the Barents Sea during early Arctic summer. *Marine Biology* 100**,** 173-183.

Mizdalski, E. (1988). Weight and length data of zooplankton in the Weddell Sea in austral spring 1986 (ANT V/3). *Berichte zur Polarforschung (Reports on Polar Research)* 55.

Norrbin, M.F., Olsen, R.E., and Tande, K.S. (1990). Seasonal variation in lipid class and fatty-acid composition of 2 small copepods in Balsfjorden, northern Norway. *Marine Biology* 105**,** 205-211.

Richter, C. (1994). *Regional and seasonal variability in the vertical distribution of mesozooplankton in the Greenland Sea.* PhD PhD thesis, University of Bremen.

3

Online Resource / Electronic Supplementary Material

Effects of sea ice decay and nutrient depletion on taxonomic composition and trophic structure in high-Arctic protist and metazoan communities

Hauke Flores, Carmen David, Julia Ehrlich, Kristin Hardge, Doreen Kohlbach, Benjamin A. Lange, Barbara Niehoff, Eva-Maria Nöthig, Ilka Peeken & Katja Metfies

Microscopic analysis of phyto- and protozooplankton (> 3µm)

Methodology

The taxonomic composition of auto- and heterotrophic unicellular protists larger than 3µm was analysed by light microscopy in two samples from the surface waters (approximately 10-20 m depth) of Location C and Location H. Seawater samples were preserved in hexamethylenetetramine-buffered formalin (final concentration 0.5%) and stored in brown glass bottles. For the microscopic analyses, 50-ml aliquots were transferred to settling chambers where the phytoplankton cells were allowed to settle for 48h. At least 400 cells of the most abundant phyto- and protozooplankton species or groups were counted with an inverted microscope using phase contrast and at four different magnifications (Utermöhl, 1958). Phyto- and protozooplankton cells were identified in most cases to the genus level, counted, and their sizes were measured with a scale bar in the ocular. The carbon content per litre was obtained by multiplying the cell counts/l by the carbon values for individual cells. The phytoplankton carbon content was calculated from cell volume as described in Edler (1979).

Results

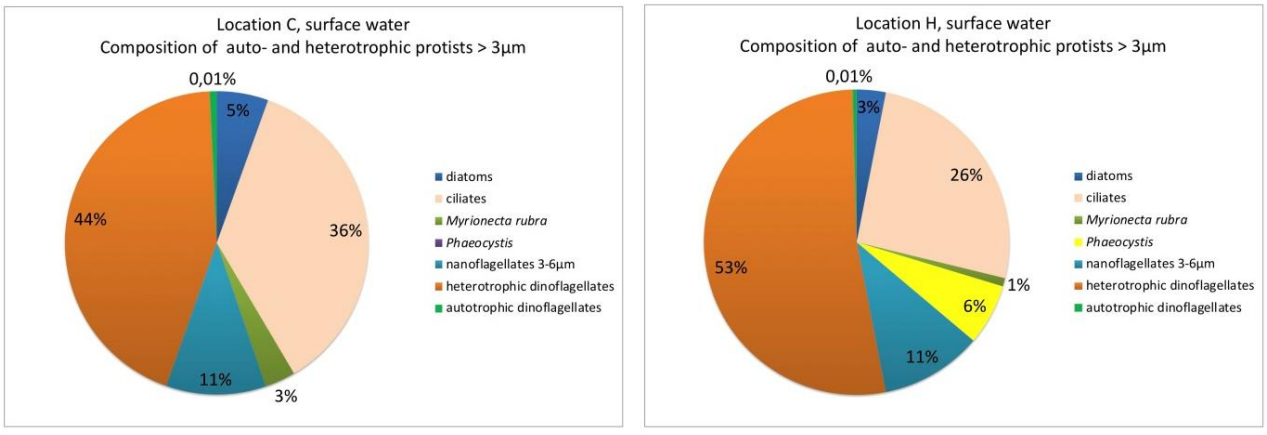

ESM3. Share (% of carbon biomass) of dominating groups within the protistian plankton >3 µm at Locations C (left) and H (right).

References

Edler L (1979) Recommendations on methods for marine biological studies in the Baltic Sea. Phytoplankton and chlorophyll. Baltic Marine Biologists Working Group 9, 38

Utermöhl H (1958) Zur Vervollkommnung der quantitativen Phytoplankton-Methodik. Mitt. int. Ver. theor. angew. Limnol. 9, 1–38 (1958)

Chapter V

Allometric measurements of Arctic and Antarctic zooplankton and nekton

F.L. Schaafsma[1], C. David[2,3], D. Kohlbach[4], M. Vortkamp[5], A. Meijboom[1], **J. Ehrlich**[5,6], G. Castellani[5], B. A. Lange[4], A. Immerz, H. Cantzler, A. van de Putte[7], J. A. van Franeker[1], H. Flores[5]

[1] Wageningen Marine Research, Den Helder, The Netherlands
[2] Department of Biology, Dalhousie University, Halifax, NS, Canada
[3] Woods Hole Oceanographic Institution, Biology Department, Woods Hole, MA, USA
[4] Norwegian Polar Institute, Ecotoxicology, Fram Centre, Tromsø, Norway
[5] Alfred-Wegener-Institute Helmholtz-Centre for Polar- and Marine Research, Bremerhaven, Germany
[6] University of Hamburg, Centre for Natural History (CeNak), Hamburg, Germany
[7] Royal Belgian Institute of Natural Sciences, Brussels, Belgium

In preparation for submission to Polar Biology

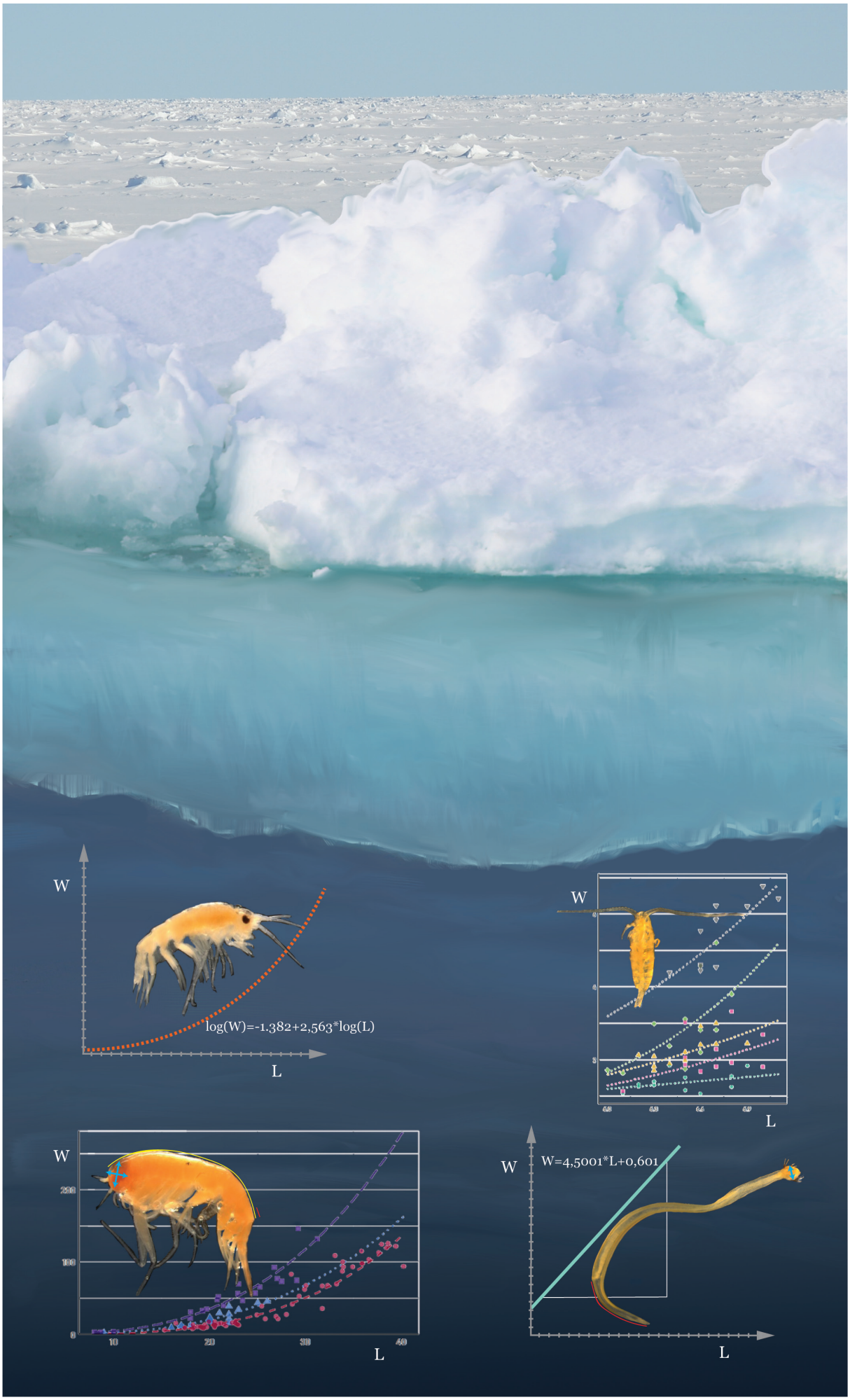
W
log(W)=-1,382+2,563*log(L)
L
W
L
W
200
100
0
10
20
30
40
L
W
W=4,5001*L+0,601
L

Allometric measurements of Antarctic and Arctic zooplankton and nekton

Fokje L. Schaafsma[*,1], Carmen L. David[2,3], Doreen Kohlbach[4], Martina Vortkamp[5], André Meijboom[1], Julia Ehrlich[5,6,] Giulia Castellani[5], Benjamin A. Lange[4], Antonia Immerz, Hannelore Cantzler, Anton van de Putte[7], Jan Andries van Franeker[1], Hauke Flores[5]

*** corresponding author**

[1] Wageningen Marine Research, Ankerpark 27, 1871 AG Den Helder, The Netherlands

[2] Dalhousie University, Department of Biology, Halifax, B3K 4R2, Canada

[3] Woods Hole Oceanographic Institution, Biology Department, Woods Hole, MA 02543, USA

[4] Norwegian Polar Institute, Ecotoxicology/ Sea Ice and Oceans, Fram Centre, 9296 Tromsø, Norway

[5] Alfred-Wegener-Institute Helmholtz-Centre for Polar- and Marine Research, Bremerhaven, Germany

[6] University of Hamburg, Centre for Natural History (CeNak), Hamburg, Germany

[7] Royal Belgian Institute of Natural Sciences, Vautierstraat 29, B-1000 Brussels, Belgium

Abstract

Allometric relationships between body properties of animals are of fundamental interest in biology. Such data can be useful for a wide variety of purposes such as estimation of biomass, growth, population structure, biogeochemical or bioenergetic modelling and carbon flux studies. This study summarizes allometric measurements from zooplankton and nekton, measured on 616 individuals from the Southern Ocean and 2081 individuals from the Arctic Ocean. Animals were collected during three expeditions in the Southern Ocean (winter and summer) and three expeditions in the Arctic Ocean (spring and summer). From the Southern Ocean, species measured include the krill *Euphausia superba*, *Euphausia crystallorophias*, and *Thysanoessa macrura*, the amphipods *Eusirus laticarpus* and *Eusirus microps*, the fishes *Bathylagus antarcticus*, *Electrona antarctica*, *Gymnoscopelus braueri* and *Notolepis coatsi*, the chaetognath *Pseudosagitta gazellae*, the salp *Salpa thompsoni*, and the hydrozoans *Atolla* spp. and *Periphylla periphylla*. From the Arctic Ocean, species measured include the krill *Thysanoessa inermis*, the amphipods *Apherusa glacialis*, *Eusirus holmii*, *Gammarus wilkitzkii*, *Onisimus nanseni*, *Onisimus glacialis*, *Themisto abyssorum,* and *Themisto libellula*, the fish *Boreogadus saida*, the chaetognaths *Eukrohnia hamata*, *Parasagitta elegans,* and *Pseudosagitta maxima*, and the copepod *Calanus hyperboreus*. Relationships between length and wet/dry weight were investigated for most species. Other allometric measurements were used to model relationships between length/weight and body parts, such as carapace (krill), eye and telson (amphipods), head and tail length (chaetognaths) and otoliths (fish). The usefulness and quality of the models is discussed. The information provided by this study fills gaps in available knowledge about species, seasons, and maturity stages. Results include regression models for species, seasons, and maturity stages that are hitherto scarcely available and insights in sources of intra-specific variation.

Key words: Polar Oceans, Length, Weight, Zooplankton, Nekton, Carapace, Otoliths, Telson

Introduction

Measurements on size, weight and other physiological or biochemical properties of species are of fundamental interest in biology and important for the use in ecosystem studies and biogeochemical models. Allometric relationships derived from these measurements can be used for studying a variety of biological and ecological processes, dynamics, and interactions such as morphology, predator-prey relationships, the environmental impact on certain body parameters, and for the comparison of e.g., growth, energy expenditure, population structure and body condition between groups of individuals (Froese, 2006). The direct measurement of many body parameters is often complicated, for example, due to time or logistical constrains. Allometric relationships can, therefore, be useful to fill data gaps or reduce the need for time consuming measurements such as dry weights. In addition, such relationships are often used to estimate biomass and production derived from length/frequency data in hydroacoustic surveys (Siegel, 1992; Geoffroy et al., 2016) and to estimate biomass when using tools that do not allow for direct measurements. Examples of such tools are the Lightframe On-sight Keyspecies Investigation (LOKI) system or ZooScan (Gorsky et al., 2010), which are image-based tools that are being used more frequently for semi-automatically obtaining data on species identification and count (LOKI) and species identification (ZooScan) on a high spatial resolution. Lastly, diet studies often rely on body parts to identify food items and reconstruct an estimated biomass of the ingested food (Van Franeker et al., 2001; Fijn et al., 2012; Leopold et al., 2015; Schaafsma et al., 2017). Regressions of relationships between e.g., length and the size of a certain body part can be helpful for these purposes.

Seasonal, regional and/or annual variation in weight per given length is found for many animals (e.g., Nicol et al., 2000; Froese, 2006; Dubishar et al., 2012) due to, for example, life cycle events, variability in food availability. For many species it has been established that the weight can differ for a certain length depending on developmental stage, due to differences in morphological characteristics. In addition, species tend to redirect their energy from more growth in length to more growth in weight when aging (Van de Putte et al., 2006). Such differences can have a large impact on biomass estimates (e.g., Ashjian et al., 2003). A lack of knowledge on possible sources of variation makes it hard to assess the accuracy of regressions used, and thus the outcome of the analysis. In addition, a lack of information about the length-weight relationships of a species in certain seasons or for certain ages can hamper the ability to obtain accurate biomass estimates for modelling of food webs and studying ecosystems (Kulbicki et al., 2005; Saunders et al., 2020). The meta-analysis of a large number of models can provide important insights into the ecology of well-studied species (Froese, 2006; Ogle, 2016), and the careful inspection of length-weight regressions of individuals of a species collected at different times and places can indicate if general regressions can be used for different ages, seasons or regions (Culver et al., 1985). Therefore,

a lot of data is necessary encompassing different life stages of a species, but also data from different seasons, regions, and years. Especially in the polar regions, data collections are often temporally and spatially limited, warranting the need for the publication of data for a general use. The availability of data from these regions and a concomitant assessment of these data would aid conservation and the management of current and future fisheries, particularly as the polar regions are very vulnerable for climate change.

In the framework of the Dutch and German Iceflux projects, which aimed to study the importance of sea ice in supporting polar marine living resources and the contribution of sea ice-derived carbon to the carbon flux of polar ecosystems, allometric measurements were performed on several Antarctic and Arctic marine animals. These measurements were necessary for studies on, for example, population dynamics (Schaafsma et al., 2016), community structure (David et al., 2015, Ehrlich et al., 2020), biomass and carbon flux (David et al., 2017; Flores et al., 2019; Ehrlich et al. accepted), food-web dynamics (Kohlbach et al., 2016, 2017a; Schaafsma et al., 2017), energy content (Schaafsma et al., 2018) and lipid content (Kohlbach et al., 2017b, 2018, 2019). This paper provides a detailed record of length, weight and other allometric measurements performed on Antarctic and Arctic zooplankton and nekton collected during six expeditions between 2012 and 2017. The aim of this study is to provide information useful to the scientific community by establishing allometric relationships between several units of length and weight. In addition, regressions between total length or weight and body parts such as carapaces (krill), telson length and eye diameter (amphipods), otoliths (fish), tail length and head width (chaetognaths) are investigated. Where possible, comparisons are made between regressions on data from different life stages or years with the aim to further assess the best use of the models, the influence of sex, developmental stage and season on the regressions and what data is necessary for the most accurate estimate of body size or weight.

Methods

Sample collection

Animals were collected during three Antarctic and three Arctic expeditions on board RV Polarstern (Figure 1; Table 1). The Antarctic expeditions took place in the Northern Weddell Sea from August to October 2013 (PS81), off the Filchner-Ronne ice shelf from December 2013 to March 2014 (PS82), and in the Lazarev Sea from December 2014 to February 2015 (PS89). The Arctic expeditions took place in the Eurasian Basin of the Arctic Ocean from August to October 2012 (PS80), and north of Svalbard from May to June 2015 (PS92) and June to July 2017 (PS106/2). Samples were collected in the upper two meters of the water column (both open water and ice-covered water) with a Surface and Under-Ice Trawl (SUIT) or at deeper depth layers with a

Rectangular Midwater Trawl (RMT). Details of sampling and the sampled areas can be found in the respective cruise reports (PS80: Boetius, 2012; PS81: Meyer and Auerwald, 2014; PS82: Knust and Schröder, 2014; PS89: Boebel, 2015; PS92 Peeken, 2016; PS106: Macke and Flores, 2018). Details on environmental conditions at the SUIT sampling stations can be found in Lange et al. (2016, 2017) and Castellani et al. (2020). Environmental parameters collected during SUIT hauls included water column properties (temperature, salinity, chlorophyll *a*), and sea-ice properties (ice cover, ice thickness, snow cover, in-ice chlorophyll *a* and light transmittance).

Measurements

The total length of *Euphausia superba* (Antarctic krill) was measured, to the nearest mm below, from the anterior margin of the eye to the tip of the telson (Discovery method; Marr, 1962). Sexual maturity of *E. superba* collected during PS81 and PS89 was assessed according to Kirkwood (1982) and Makarov and Denys (1981). The Antarctic krill collected during PS82 was sorted into juveniles, males, and females according to CCAMLR (2011). The total length of other Euphausiacea such as *Thysanoessa macrura*, *Euphausia crystallorophias* (ice krill), and *Thysanoessa inermis* was measured from the tip of the rostrum to the tip of the telson. The carapace of all krill species was measured from the tip of the rostrum to the mid-dorsal posterior edge of the carapace.

Gammarid amphipods were measured following the curved dorsal line from the tip of the head to the tip of the telson (Chapelle and Peck, 2004; Krapp et al., 2008; Figure 2a). Hyperiid amphipods were measured from the front of the head to the tip of the telson (Pakhomov and Perissinotto, 1996; Donnelly et al., 2006; Figure 2b). The eye diameter and the telson were measured for the Arctic amphipod species *Apherusa glacialis* and *Themisto libellula*, as shown in Figure 2a and 2b.

The total length (TL) of fish was measured to the nearest mm below, from the tip of the snout to the tip of the caudal fin. The standard length (SL) was measured from the tip of the snout to the posterior end of the last vertebra. For several fish, otoliths were removed after the weight of the individual was measured, and the maximum length and width of the otoliths were noted. Examples are shown in Figure 2c and 2d. For allometric relationship between otolith parameters and measurements of body size, an average value of the left and right otolith per individual was used, as no difference was found between regression models using one or the other in a previous study performed on Southern Ocean myctophid fish (Saunders et al., 2020).

The total length of chaetognaths was measured from the head to the tip of the tail excluding the tail fin (Immerz, 2016). For copepod species, the prosome and the urosome were separately measured. The prosome length was measured from the tip of the cephalosome to the distal lateral end of the last thoracic segment.

In general, all measurements were conducted on preserved specimens, except for *E. superba* collected during PS82 which were measured before preservation. The length and wet weight of frozen individuals were measured after thawing. Dry weight was measured after animals were freeze-dried until complete desiccation. All allometric measurements will be made available in the online tables of the supplementary material in which Darwin Core standard terms (Wieczorek et al., 2012) were used. These tables will include information on the time and location of sample collection, which gear was used to catch the animals and the preservation method (4% buffered formaldehyde or frozen at -20 or -80°C).

Preservation can have an influence on weight and size. Fixation in a formalin solution can cause a loss in wet weight (Wetzel et al., 2005) and shrinkage in length (Wallis et al., 2020). For example, Wallis et al. (2020) estimated the total shrinkage of the krill *T. macrura* to be 1.4 % after 1.5 years in a 10 % formaldehyde solution. In addition, it has been shown that both formalin fixation and freezing can cause loss in dry weight (Williams and Robins, 1982). The extent of the loss, however, depends on the species, the size and developmental stage, and the amount of time the specimen was preserved (Williams and Robins, 1982; Ogle, 2009 and references therein; Wallis et al., 2020). For example, the amount of length or weight reduction after freezing depends on species and did not occur in some (Ogle, 2009 and references therein).

Statistics

Linear relationships between total length, standard length, prosome length, carapace length, telson length, otolith length, eye diameter, head width or tail length and wet weight or dry weight were established on log10-transformed data according to

$$log(W) = log(a) + b\, log(L) \quad (1)$$

corresponding to the power function

$$W = a\, L^b \quad (2)$$

where W is weight and L is length. Regression constants a and b were estimated using least squares regression.

Linear relationships between the different measurements of length or different measurements of weight were established as

$$y = ax + b \quad (3)$$

were y is the response variable and x the explanatory variable. All regression models were plotted and individuals with weight that was double or half the expected weight based on the model were considered outliers and removed (Jellyman et al., 2013). As length-weight relationships can be

affected by size range, life stages with an expected difference in morphology or size/age classes with small numbers were excluded from the model to avoid misleading results (Froese, 2006; Jellyman et al., 2013). Therefore, the reported regression models should be useful for the reported size range or development stage, if not further discussed in the text. To check the linear regression assumptions of the normal distribution and constant variance of measurement errors, a residual plot and a histogram of the model residuals were assessed visually (Ogle, 2016).

The coefficient of determination (R^2), representing the proportion of the variance of a dependent variable that is explained by the independent variable of the regression model, is given as a measure of how well the linear model predicts the measured values. In order to investigate potential intra-specific differences between relationships depending on e.g., sex, developmental stage or season, the slopes and intercepts of linear regressions were compared with ANCOVA (Hartman and Brandt, 1995; Ogle, 2016), using version 4.0.2 of R with the packages "car" (Fox and Weisberg, 2019), "FSA" (Ogle et al., 2020) and "dplyr" (Wickham et al., 2020). The residual standard deviation is given when models were compared with ANCOVA, representing the average amount that the real values of y differ from the predictions provided by the regression line given in model comparisons. The R package "ggplot2" (Wickham, 2016) was used for visualization.

Results

Length – weight regressions

Krill

Measurements performed on krill species included *E. superba* (Antarctic krill), *T. macrura* and *E. crystallorophias* (ice krill) from the Southern Ocean and *T. inermis* from the Arctic Ocean. For *E. superba*, total length and wet weight were measured on specimens caught during austral summer (PS89), and total length, wet weight and dry weight were measured on specimens collected during austral winter (PS81). Regression models of these measurements can be found in Table 2. The length-wet weight models given for austral winter are based on age class 0 (AC0) Antarctic krill < 24 mm consisting of furcilia and juveniles (Schaafsma et al., 2016). The number of sub-adult and adult krill wet weight measurements from PS81 was very low and therefore excluded from the model, they will be, however, provided in the supplementary material. Contrastingly, the total length-dry weight model for PS81 was based on sub-adult and adult krill. Due to morphological differences, age class 0 krill was excluded from this model, and the small number of dry weight measurements on these will be given in the supplementary material. The number of measurements of krill from PS89 allowed for a further analysis of regression models from different developmental stages of which the results will be discussed in a coming paragraph. The relationship between length and dry weight of Antarctic krill caught during another austral summer (PS82) did not result in

reliable models. This could be due to the relatively small sample size of measurements included in the regression analysis which, in addition, encompassed a wide range of stages, including gravid females. In addition, an earlier study found a greater residual variance in dry weight models compared to wet weight models, without any clear explanation (Morris et al., 1988). The measurements will be provided in the supplementary material.

The total length-wet weight relationship of *T. macrura* collected during austral winter is presented in Table 2. The size range indicates that the measured individuals encompassed both juvenile and adult individuals (Nordhausen, 1994). The dry weight of *T. macrura* was measured on 7 individuals caught in austral summer (PS82), which will be available in the supplementary material. Regression models using total lengths and dry weights of *E. crystallorophias* caught in the Filchner region during austral summer (PS82) and of the Arctic krill species *T. inermis*, can also be found in Table 2. The regression model for *T. inermis* did not explain a large part of the measured values (R2 = 0.32, Table 2). This could, again, be due to high residual variance in combination with a low sample size (Cornell and Berger, 1986).

Fish

Measurements were done on the Antarctic fish species *Electrona antarctica*, *Bathylagus antarcticus*, *Gymnoscopelus braueri* and *Notolepis coatsi* and the Arctic species *Boreogadus saida*. Total length-wet weight and total length - standard length relationships are given for *E. antarctica*, *B. antarcticus* and *B. saida* in Table 2. Dry weight was also measured for *E. antarctica* and *B. antarcticus* and related to total length and wet weight (Table 2). Only small numbers of allometric measurements were done on *G.braueri* and *N. coatsi*, which will be provided in the supplementary material. In addition, a small number of dry weight measurements performed on *B saida* can be found there.

Amphipods

Amphipod measurements were done on two species from the Southern Ocean (*Eusirus laticarpus* and *Eusirus microps*) and seven Arctic species, including *Apherusa glacialis*, *Eusirus holmii*, *Gammarus wilkitzkii*, *Onisimus glacialis*, *Onisimus nanseni*, *Themisto abyssorum* and *T. libellula*. A length-wet weight relationship was established for *A. glacialis* caught during spring (PS92) using individuals with a total length between 7.6 and 11.1 mm (Table 2). Although two age classes were found during this expedition, no measurements were done on small individuals and the measured range represents a single cohort or age class. The wet and dry weight of *T. libellula* was measured in several seasons (Table 2). During summer/autumn (PS80) multiple developmental stages were distinguished. Results of intra-specific comparisons will be shown in the concerning paragraph.

Summer measurements of *E. holmii*, *O. glacialis* and the Antarctic *E. laticarpus* (austral summer) showed a relatively high variability in wet weight per total length, resulting in regressions models

that explained a relatively small proportion of the measured individuals (R^2 = 0.47, 0.66 and 0.69, respectively, Table 2). Similar results were found for total length-dry weight models (Table 1). The total length-wet weight model for *O. nanseni* seemed to have a better fit, although the number of measured individuals is relatively small (n = 11, Table 2), and, therefore, could be a result of the natural variance not being well represented by the data (Cornell and Berger, 1986). *O. nanseni* length ranged from 11.6 to 16.6 mm, except for one individual that was 23.9 mm long. Few dry weight measurements were done on *O. glacialis* caught in summer/autumn (PS80) and *E. holmii* caught in summer (PS92), which will be available in the supplementary material, as well as four total length, wet weight, and dry weight measurements of *E. microps* (PS89).

Other species

The total length and dry weight were measured for a number of adult females of the Arctic copepod *Calanus hyperboreus*. Interestingly, the dry weight per length showed very high variation depending on sampling location (Figure 3). Length-wet weight and length-dry weight regressions are given for the chaetognath species *Eukrohnia hamata* collected in Arctic spring (PS92, Table 2). A few measurements of total length, wet and dry weight were performed on the Arctic chaetognath *Pseudosagitta maxima*, the Antarctic chaetognath *Pseudosagitta gazellae* and the Antarctic salp *Salpa thompsoni*, which will be made available in the supplementary material. Wet weight-dry weight relationships are given for two species of scyphozoa (*Atolla* spp. and *Periphylla periphylla*), which were collected in the Weddell Sea in austral summer (PS89, Table 2).

Other allometric relationships

Austral winter (PS81) relationships between carapace length, body length and wet weight are given for age class 0 (furcilia and juveniles) Antarctic krill <24 mm (Figure 4, Table 3). Comparing the regression with a regression using sub-adult and adult data from this season suggested that this would give a different result. There were, however, only a few data points for these latter stages (n = 8), so the regression coefficients of the model for sub-adult and adult krill is likely not reliable and, therefore, not given. The relationship between carapace length, total length, and wet weight of *T. macrura* collected in winter can also be found in Figure 4 and Table 3. Although the size range of *T. macrura* in this analysis is similar to that of *E. superba*, these individuals represent older developmental stages (juvenile to adult).

Telson length and eye diameter were measured for the Arctic amphipods *A. glacialis* and *T. libellula* caught during late summer/autumn (PS80, Table 3). All measurements were a relatively good predictor for total length for *T. libellula*, while the R^2 values for the models on *A. glacialis* measurements were less high, suggesting that they are a less suitable predictor for total length for

this species. For this latter species, the regression using horizontal eye diameter gave the best results based on the coefficient of determination (Table 3).

From the fish species *B. antarcticus*, *E. antarctica* (Southern Ocean) and *B. saida* (Arctic Ocean), the otoliths were measured and related to total length, wet weight, and dry weight (Table 3). One measurement of the otolith length (4.31 mm) of *B. saida* seemed much too small for the given weight of the concerning fish (18.9 g) and was considered an outlier.

The head width and tail length of chaetognaths were measured as a predictor of total length for the Arctic species *E. hamata* and *Parasagitta elegans* (Table 3). Particularly tail length seemed a good predictor of total length, while head width showed higher variability. The distance between the eyes was also measured but was not a good predictor for total length (results not shown).

Intra-specific comparisons

Individuals of Antarctic krill from summer (PS89) were divided in the developmental stages juveniles (covering a length range of 19-40 mm), sub-adult females, adult females (not gravid), sub-adult males and adult males. The regression models were not significantly different between sub-adult and adult females, nor between sub-adult and adult males (Figure 5). Comparing males and females (including both sub-adults and adults), the regression models did not show any difference in slope, but did differ in intercept ($F1, 120 = 8.90$, $p < 0.005$), suggesting that the difference in weight between males and females is constant and does not vary as a function of length. Looking at the regression model for juveniles, no significant difference was found when comparing with females, while the intercept ($F1, 118 = 4.29$, $p = 0.04$), but not the slope, was different when comparing with males (Table 4). None of the gender/stage specific regressions models for *E. superba* differed significantly from the model using all austral summer measurements. The regression model subsets did, however, decrease the residual standard error compared to the model using the complete austral summer dataset. The length-wet weight models compared between furcilia and age-class 0 juveniles sampled during austral winter showed no significant difference.

Total length-dry weight relationships for the krill species *E. crystallorophias* separated by sex and stage did not significantly differ from each other or the model that included all measurements (Figure 6), although the residual standard error decreased slightly when separating sexes (Table 4). No comparison was made with the regression model for juveniles, as the sample size was low.

In order to analyze the difference between ages, the individuals of the fish *E. antarctica* were divided in age classes using the length at age regression (Van de Putte et al., 2006) adapted from the growth curve equation from Greely et al. (1999). Despite that the length-wet weight regression for age class 0 fish looks very different (Figure 7; length-dry weight regressions similar), no statistical differences were found between the slopes of the regression using all data and the slopes of the regressions

separated per age class (ANCOVA, Table 4). Only the intercept of the regression model using age class 1 data differed significantly from the model using all data combined (total length-wet weight: $F_{1,89} = 11.89$, $p < 0.001$; total length-dry weight: $F_{1,56} = 5.19$, $p < 0.03$). This regression did, however, violate the normality assumption.

For the Arctic fish species *B. saida*, total length-dry weight regressions were compared between individuals caught in the under-ice surface during late summer/autumn (PS80) and at the shelf bottom during summer (PS106/2). The regression models had the same slope, but had significantly different intercepts ($F_{1,150} = 3.98$, $p = 0.048$). The majority of the fish from PS80 were in a length range of 52-94 mm (David et al., 2016), likely representing age-0 class (Lønne and Gulliksen, 1989). The fish from PS106/2 were of a larger size class (86-173 mm). A few length and weight measurements were done on fish caught in the under-ice surface during PS92, which will be made available in the supplementary material.

The total lengths and wet weights of *T. libellula* were measured on individuals from spring (PS92) and late summer/autumn (PS80). During PS80, two size classes were found. Based on sex and stage determination of several individuals from this expedition and information on the development of *T. libellula* in the studies of Percy (1993), Koszteyn et al. (1995), and Auel and Werner (2003), amphipods smaller than 12 mm were defined as juveniles and the individuals >15 mm were regarded as a separate age group consisting of immature and mature individuals. The length-wet weight relationship of *T. libellula* from PS80 was neither significantly different between males (n=9) and females (n=17), nor between juveniles and immature/mature individuals (Table 4). Comparing both years (Figure 8a), the total length-wet weight regressions differed significantly in both slopes ($F_{1,114} = 11.17$, $p = 0.001$) and intercepts ($F_{1,115} = 120.95$, $p < 0.00001$). This was also the case for the total length-dry weight regression models of PS80 and PS92 (slope: $F_{1,78} = 6.09$, $p = 0.016$, intercept: $F_{1,79} = 191.62$, $p < 0.00001$; Table 4). Dry weight of individuals collected during summer (PS106/2) were also measured (Figure 8b). The resulting model differed significantly in intercept compared to the models of PS80 ($F_{1,40} = 82.28$, $p < 0.0001$) and PS92 ($F_{1,78} = 43.90$, $p < 0.0001$).

Discussion

In previous studies of euphausiids, the use of length as a predictor of weight was found to be influenced by the differences between sexes, developmental stages, and seasons, for both *E. superba* and *T. macrura* (Morris et al., 1988; Siegel, 1992; Färber-Lorda, 1994). Studying sub-adult and adult Antarctic krill, length-weight regressions (both wet and dry weight) were found to be more accurate when models were separated by sex and stage. However, regarding *E. superba*, comparable accuracy was found when separating the krill into the groups ‘males’, ‘gravid females’, ‘non-gravid females’

and ´spent females´ (the latter in the post-spawning period) according to Siegel (1992), or 'adult males', 'gravid females' and 'standard krill' according to Morris et al. (1988). Similar findings were shown by Atkinson et al. (2006), indicating that the intercepts in the regression models for gravid females and adult males differed from the model combining all stages in summer, which was not the case for other developmental stages, including juveniles. The results indicated that females were heavier than males of the same length (Atkinson et al., 2006). The lack of differences in slope between juvenile, males, and females caught in austral summer (PS89) corresponds with these earlier findings, given that gravid or spent females, which are expected to show morphological differences, were not present. It also must be noted that there were only a few adult males in this study (n = 8). Results suggest, also taking results of previous studies into account, that a single model including juveniles, sub-adult and adult females, and likely sub-adult males, would be sufficient for an accurate prediction of wet weight based on total length for these stages in summer. Siegel (1992) recommends to take the dominant maturity stage into account instead of month when choosing a good length-weight relationship, as there could be interannual and regional variability in the timing of spawning.

Although *E. superba* is a well-studied species and several studies report information on length and weight (overviews in Morris et al., 1988 and Siegel, 1992), most of the information is about post-larval krill. For larval and juvenile Antarctic krill there is much less information, as well as for the months outside summer. Some studies provide a length-wet weight relationship for size ranges that include larvae and juveniles, but do not separate them from sub-adult and adult krill (e.g., references in Siegel, 1992; Daly, 1990). We found no statistical difference between the length-weight regression of furcilia and juvenile caught in winter and larger juveniles caught in summer suggesting there are little differences in morphological traits between these stages. These results would, however, need to be verified using more datasets.

For *T. macrura*, previous summer studies found that the length-weight regressions for sub-adults and adults were not significantly different from each other, although significant differences were found when males and females were separated (Färber-Lorda, 1994). In the present study, the individuals of *T. macrura* were not staged, so a comparison between stages/sexes could not be conducted. For *E. superba*, however, no significant differences were found between the length-weight relationship of males and females during the winter resting stages (Siegel, 1986), and general length/weight relationships are deemed sufficient for the pre-spawning and winter periods (Siegel, 1992). Because the *T. macrura* here were also collected in the winter season, a general regression model is likely sufficient for estimating weight per length of this species, as suggested for *E. superba* (Siegel, 1992). Particularly since, to our knowledge, no other winter models for *T. macrura* are available in the literature.

Summer length-dry weight relationships of *E. crystallorophias* were not statistically different from each other, suggesting that a single regression model can be used to establish dry weight, although separating them did seem to slightly improve the models. In addition, not all developmental stages are represented, and it is likely that gravid and spent females would warrant a separate model similar to *E. superba*. Length-wet weight relationship for individuals caught in summer, with juveniles, males and females separated, can be found in Pakhomov and Perissinotto (1996), although it remains unclear if the regression models were statistically different.

Different length-weight relationships are often found also for different age classes and life stages of fish (Froese, 2006 and references therein). Younger stages grow relatively more in length than in weight, compared to older individuals (Fulton, 1904; Froese, 2006). In addition, seasonal and annual variability can be found, and it is generally recommended that differences between sexes are tested (Froese, 2006). Energy density measurements on *E. antarctica* confirmed that smaller fish invest more energy in becoming larger compared to older individuals (Van de Putte et al., 2006; Schaafsma et al., 2018). However, no statistical differences were found in the regression models when separated by age classes indicating that a general model can be used. Relatively large amounts of data are available on length-weight relationships of fish from the Southern Ocean (e.g., Gon and Heemstra, 1990; Pakhomov et al., 1996; Eastman and DeVries, 2000; Casaux et al., 2003; Kock and Jones, 2005; Reid et al., 2007; Flores et al., 2008; Wei et al., 2017; Escobar-Flores et al., 2020; Saunders et al., 2020), but often no differentiation is made between sexes, developmental stages, or age classes. Several studies investigating *E. antarctica*, show a length-weight relationship similar to the one that included all age classes in this study (e.g., Pakhomov et al., 1996; Saunders et al., 2000; Flores et al., 2008), although the fish in these analyses often include individuals sampled over various seasons.

For polar cod caught during the end of Arctic summer/autumn (PS80), most fish came from the same year class and only five of the measured fish were females. Therefore, a comparison between age classes or sexes was not possible. Fey and Węsławski (2017) did not find any difference between length-wet weight regressions of males and females, analyzed on individuals from 61-240 mm collected in the Svalbard fjords in September/October. In contrast to the fish from PS80 that were caught over the deep basin of the central Arctic Ocean, most fish in previous studies, as well as fish caught during another expedition in this study (PS106/2), were caught in shallow coastal waters (Frost and Lowry, 1981; Finley et al., 1990; Nahrgang et al., 2014; Koenker et al., 2018; Copeman et al., 2020). There was, however, no clear effect of sampling habitat on the length-weight relationship, also when compared to length-weight relationships of other studies. There are indications that there is variation depending on sampling location although this may also be seasonal (Geoffroy et al., 2016 and references therein). Variation in length-weight relationships of polar cod

from different habitats would be interesting to investigate for gaining knowledge on growth and population dynamics, as it is hypothesized that young polar cod descent to deeper water layers or remain in the surface waters depending on timing of hatching (Geoffroy et al., 2016) and hatching time may, thus, have consequences for these parameters.

In earlier studies, the relationship between length and wet weight was found to differ between males and females for the amphipods *A. glacialis* and *G. wilkitzkii* (Poltermann, 2000). This was not the case for *T. libelulla* in this study, which showed no differences between regression models of both sexes. The models suggested an influence of season on dry weight, which increased from spring to end of summer for *T. libellula* (Figure 6b). A variability in length-dry weight relationships between seasons, with lower values in winter, was previously also found for *A. glacialis* and *G. wilkitzkii*, but not for *Onisimus* spp. (Werner and Auel, 2005).

Individuals of *T. libellula* were separated in two age classes according to information from several studies. There are other studies, however, in which *T. libellula* was found to mature at larger sizes. For example, the amphipod was found to mature at approximately 19 - 21 mm, with a maximum length of about 25 mm, at south-eastern Alaska, while they were found to mature when exceeding 35 mm, with a maximum length of approximately 46 mm at Baffin Island, Canadian Arctic. These differences, including the different life cycles of both populations, were attributed to the latitudinal gradient in water temperature (Dunbar, 1946). This suggests large differences in growth and maturation between regions in addition to seasons.

A high variability in dry weight of *C. hyperboreus* like in our study, was found before in several developmental stages (Hirche, 1997; Ashjian et al., 2003). Looking at the data from PS106/2, this can partially be attributed to an increase in weight over time during the expedition. Differences in the extent of the weight increase with an increase in length (slope) between stations, as well as the high variability in weight per given length within a station, might be explained by varying local food availability or life cycle events (e.g., egg maturation and spawning).

For chaetognaths there is also likely a large difference in length-weight regression models between seasons, as a model from autumn (Richter, 1994) showed a much lower value for exponent b (0.165). These animals are known to feed year-round, but studies have indicated that the feeding rate and also growth, are a lot less in the winter months compared to spring and summer (Grigor et al., 2014, 2015). Chaetognaths may form a large part of the zooplankton biomass, and are often the most abundant zooplankton predators, in both the Arctic Ocean and the Southern Ocean (Pakhomov et al., 1999; Kobosokova and Hirche, 2000; Auel and Hagen, 2002; Hopcroft et al., 2005; Flores et al., 2014; David et al., 2017; Ehrlich et al., 2020). In addition, they are prey for many species of fish in both polar regions (Lønne and Gulliksen 1989; Atkinson and Percy, 1992; La Mesa et al., 2004 and

references therein; Walkusz et al., 2011) and recorded in the diets of Arctic bird species (Hartley and Fisher, 1936; Lønne and Gabrielsen, 1992). This makes them an important part of the food web (Pakhomov et al., 1999; Giesecke and Gonlález, 2012), warranting the need for accurate biomass estimates. Ratios of total length versus tail length and head width have been used to distinguish between species and the degree of carnivory of a certain species, respectively (Kobosokova and Isachenko, 2017). Regressions using these parameters can, however, also be useful for reconstructing chaetognath biomass in diet studies. Although tail length seems to be a better predictor for total length, it is likely more common to find heads in the contents of a stomach.

In previous studies, the carapace length of *E. superba* was suggested to be a poor predictor of total length and wet weight when sexes and stages are not separated (Siegel, 1982; Morris et al., 1988; Hill et al., 1990). Therefore, it should be considered that, when carapace length is used to estimate reconstructed length or wet weight, it is not very reliable for growth studies or comparative studies of krill populations in the absence of information on sex and maturity (Morris et al., 1988; Färber-Lorda et al., 1990; Färber-Lorda et al., 1994). Stomach content samples may, however, be heavily digested, leaving the carapace as the only major fragment left (Hill et al., 1990). The relationship between carapace length and total length of *T. macrura* was also found to differ between juvenile, adult male, and adult female individuals collected in a previous summer study (Färber-Lorda et al., 1990). In addition, the carapace length-wet weight relationship differed between sub-adult and adult individuals, but no difference was found between males and females, indicating that morphological differences as a function of wet weight seem to be less pronounced compared to differences as a function of size (Färber-Lorda et al., 1994). Again, most previous studies using carapace length as a predictor for total length and weight used larger juvenile, sub-adult, and adult krill (Siegel, 1982; Färber-Lorda et al., 1990; Hill et al., 1990; Färber-Lorda et al., 1994), and there is little information on the relationship between carapace length and total length or wet weight of age class 0 furcilia and juvenile *E. superba* as presented here.

Otoliths are very useful for the identification of fish species in the food or scats of their predators. Investigations of the relationship between otolith length and fish length indicated that the deviation between measured fish length and estimated fish length using regressions is very small, and that otoliths are thus a reliable predictor for length (Frost and Lowry, 1981). A lot of work has been done on otoliths of Southern Ocean fish, and many regression models are available in literature (e.g., Hecht, 1987; Gon and Heemstra, 1990; Reid, 1996). Also for the Arctic species *B. saida*, several studies showing models relating otoliths to total fish length and weight can be found (Frost and Lowry, 1981; Finley et al., 1990; Harvey et al., 2000; David et al., 2016; Fey and Węsławski, 2017). Direct comparisons between published relationships may be difficult due to the use of different measures for fish length (such as total length, standard length, or fork length).

Conclusions

In general, there is a lack of knowledge on length-weight relationships of certain polar species or the sources of variety in weight at a given length (Froese, 2006). This study provides length-weight regressions of Antarctic and Arctic zooplankton and nekton including less studied developmental stages, and species that are increasingly recognized as important parts of the food web such as chaetognaths and jelly fish. We also provide regression models that are useful in diet studies. Variation for *T. libellula* seems to be due to season rather than age class. Furthermore, there was little difference in models for juvenile krill irrespective of season and no difference between age-classes for *E. antarctica*, although separating developmental stages/age classes did reduce the variation in the residuals. Both species are important prey for many top predators such as birds and seals, and Antarctic krill is commercially harvested, warranting the need for accurate biomass estimates. Regarding the length-weight regressions of polar cod, there is a further need to investigate the source(s) of variability.

Contributions

Samples were collected by F.L. Schaafsma, C. David, D. Kohlbach, M. Vortkamp, A. Meijboom, J. Ehrlich, G. Castellani, B.A. Lange, A. Immerz, H. Cantzler, A. van de Putte, J.A. van Franeker, and H. Flores. Measurements were done by F.L. Schaafsma, C. David, D. Kohlbach, M. Vortkamp, A. Immerz, H. Cantzler, H. Flores. The data were analyzed by F.L. Schaafsma. J. Ehrlich provided sources about taxonomic information. All authors contributed to data validation. The figures were created by F.L. Schaafsma, H. Flores, A. van de Putte, and J. Ehrlich. The first manuscript was written by F.L. Schaafsma with contributions from all authors.

Conflicts of interest/Competing interests

None

Acknowledgements

We thank the Captain and the crew of the Polarstern expeditions PS80, PS81, PS 82, PS89, PS92, and PS106 for their support and guidance. We thank Michiel van Dorssen (Van Dorssen Metaalbewerking) for the support during SUIT sampling and fieldwork. We thank student assistants Nadia Zakharova, Mai Apasiri Klasmeier and Thijs Lichtenbeld for their support in sample analyses. We thank Guido Keijl (WMR) for measuring fish otoliths.

Funding

Antarctic research by Wageningen Marine Research is commissioned by the Netherlands Ministry of Agriculture, Nature and Food Quality (LNV) under its Statutory Research Task Nature & Environment WOT-04-009-047.04. The Netherlands Polar Programme (NPP) managed by the

Dutch Research Council (NWO) funded this research under project nr. ALW 866.13.009. BAL is currently supported from the Norwegian Polar Institute and funding from the Research Council of Norway to projects: CAATEX [280531] and HAVOC [280292]. DK is currently funded by the Research Council of Norway through the project The Nansen Legacy (RCN # 276730) at the Norwegian Polar Institute. HF, GC, CD, MV, and JE were part of the Helmholtz Association Young Investigators Groups *Iceflux*: Ice-ecosystem carbon flux in polar oceans (VH-NG-800). JE was funded by the national scholarship "Promotionsstipendium nach dem Hamburger Nachwuchsfördergesetz (HmbNFG)" by the University of Hamburg.

Supplemental material

Table S 1: List of Arctic and Antarctic species for allometric measurements.

Availability of data and material

All data will be made available in the online supplementary material and will be stored in the publicly accessible databases PANGAEA and the Netherlands Polar Data Center (NPDC).

References

Ashjian CJ, Campbell RG, Welch HE, Butler M, Van Keuren D (2003) Annual cycle in abundance, distribution, and size in relation to hydrography of important copepod species in the western Arctic Ocean. *Deep-Sea Res* I 50:1235–1261. https://doi.org/10.1016/S0967-0637(03)00129-8

Atkinson A, Shreeve RS, Hirst AG, Rothery P, Tarling GA, Pond DW, Korb RE, Murphy EJ, Watkins JL (2006) Natural growth rates in Antarctic krill (*Euphausia superba*): II. Predictive models based on food, temperature, body length, sex, and maturity stage. *Limnol Ocean* 51(2):973-987. https://doi.org/10.4319/lo.2006.51.2.0973

Boebel O. (2015) The Expedition PS89 of the Research Vessel POLARSTERN to the Weddell Sea in 2014/2015. *Berichte zur Polar- und Meeresforschung* 689 pp 151 p. https://doi.org/10.2312/BzPM_0689_2015

Boetius A (2013) The expedition of the research vessel "Polarstern" to the Arctic in 2012 (ARK-XXVII/3). *Berichte zur Polar- und Meeresforschung* 663, pp 166. https://doi.org/10.2312/BzPM_0663_2013

Castellani G, Schaafsma FL, Arndt S, Lange BA, Peeken I, Ehrlich J, David C, Ricker R, Krumpen T, Hendricks S, Schwegmann S, Massicotte P, Flores H (2020) Large-scale variability of physical and biological sea-ice properties in polar oceans. *Front Mar Sci* 7:536. doi: 10.3389/fmars.2020.00536

CCAMLR (2011) Scheme of international scientific observation: scientific observers manual. *CCAMLR*, Hobart.

Chapelle G, Peck LS (2004) Amphipod crustacean size spectra: new insights in the relationship between size and oxygen. *Oikos* 106:167/175.

Culver DA, Boucherle MM, Bean DJ, Fletcher JW (1985) Biomass of freshwater crustacean zooplankton from length-weight regressions. Can I Fish *Aquat Sci* 42:1380-13964.

Daly KL (1990) Overwintering development, growth, and feeding of larval *Euphausia Superba* in the Antarctic marginal ice zone. *Limnol Ocean* 35(7):1564-1576. https://doi.org/10.4319/lo.1990.35.7.1564

David C, Lange B, Rabe B, Flores H (2015) Community structure of under-ice fauna in the Eurasian central Arctic Ocean in relation to environmental properties of sea-ice habitats. *Marine Ecology Progress Series* 522:15-32. https://doi.org/10.3354/meps11156.

David C, Lange BA, Krumpen T, Schaafsma FL, Van Franeker JA, Flores H (2016) Under-ice distribution of polar cod *Boreogadus saida* in the central Arctic Ocean and their association with sea-ice habitat properties. *Pol Biol* 39(6):981-994. https://doi.org/10.1007/s00300-015-1774-0

David C, Schaafsma FL, Van Franeker JA, Lange BA, Brandt A, Flores H (2017) Community structure of under-ice fauna in relation to winter sea-ice habitat properties from the *Weddell Sea. Pol Biol* 40(2):247-261. https://doi.org/10.1007/s00300-016-1948-4

Donnelly J, Sutton TT, Torres JJ (2006) Distribution and abundance of micronekton and macrozooplankton in the NW Weddell Sea: relation to a spring ice-edge bloom. *Pol Biol* 29:280-293. https://doi.org/10.1007/s00300-005-0051-z

Dubischar CD, Pakhomov EA, Von Harbou L, Hunt BPV, Bathmann U (2012) Salps in the Lazarev Sea, Southern Ocean: II. Biochemical composition and potential prey value. *Mar Biol* 159:15–24. https://doi.org/10.1007/s00227-011-1785-5

Ehrlich J, Schaafsma FL, Bluhm BA, Peeken I, Castellani G, Brandt A, Flores H (2020) Sympagic fauna in- and under Arctic pack ice in the annual sea-ice system of the new Arctic. *Front Mar Sci* 7:452. https://doi.org/10.3389/fmars.2020.00452

Ehrlich J, Bluhm BA, Peeken I, Massicotte P, Schaafsma FL, Castellani G, Brandt A, Flores H (accepted for publishing in Elementa) Sea-ice associated carbon flux in Arctic spring.

Escobar-Flores 2020 Estimates of density of mesopelagic fish in the Southern Ocean derived from bulk acoustic data collected by ships of opportunity *Polar Biol* 43, 43–61. https://doi.org/10.1007/s00300-019-02611-3

Färber-Lorda J (1994) Length-weight relationships and coefficient of condition of *Euphausia superba* and *Thysanoessa macrura* (Crustacea: Euphausiacea) in southwest Indian Ocean during summer. *Mar Biol* 118:645–650. https://doi.org/10.1007/BF00347512

Fijn RC, Van Franeker JA, Trathan PN (2012) Dietary variation in chick-feeding and self-provisioning Cape Petrel Daption capense and Snow Petrel Pagodroma nivea at Signy Island, South Orkney Islands, Antarctica. *Mar Ornith* 40: 81–87.

Flores H, David C, Ehrlich J. Hardge K, Kohlbach D, Lange BA, Niehoff B, Nöthig EM, Peeken I, Metfies K (2019) Sea-ice properties and nutrient concentration as drivers of the taxonomic and trophic structure of high-Arctic protist and metazoan communities. *Pol Biol* 42:1377–1395. https://doi.org/10.1007/s00300-019-02526-z

Fox J, Weisberg S (2019). An {R} Companion to Applied Regression, Third Edition. Thousand Oaks CA: Sage. URL: https://socialsciences.mcmaster.ca/jfox/Books/Companion/

Froese R (2006) Cube law, condition factor and weight-length relationships: history, meta-analysis and recommendations. *J Appl Ichthyol* 22(4):241–253. https://doi.org/10.1111/j.1439-0426.2006.00805.x

Fulton TW (1904) The rate of growth of fishes. Twenty-second Annual Report, Part III. *Fisheries Board of Scotland*, Edinburgh, 141–241.

Geoffroy M, Majewski A, LeBlanc M, Gauthier S, Walkusz W, Reist JD, Fortier L (2016) Vertical segregation of age-0 and age-1+ polar cod (*Boreogadus saida*) over the annual cycle in the Canadian Beaufort Sea. *Polar Biol* 39, 1023–1037. https://doi.org/10.1007/s00300-015-1811-z

Hartley CH, Fisher J (1936) The Marine Foods of Birds in an Inland Fjord Region in West Spitsbergen: Part 2. Birds. *J Anim Ecol* 5(2): 370-389.

Hartman KJ, Brandt SB (1995) Estimating energy density of fish. *Trans Amer Fish Soc* 124:347-355

Hecht 1987 A guide to the otoliths of Southern Ocean fishes. S Afr T Nav Antarkt 17:2-86

Jellyman PG, Booker DJ, Crow SK, Bonnett ML, Jellyman DJ (2013) Does one size fit all? An evaluation of length-weight relationships for New Zealand's freshwater fish species, New Zealand *J Mar Freshw Res* 47(4):450-468, https://doi.org/10.1080/00288330.2013.781510

Kohlbach D, Lange BA, Schaafsma FL, David C, Vortkamp M, Graeve M, Van Franeker JA, Krumpen T, Flores H (2017) Ice algae-produced carbon is critical for overwintering of Antarctic krill Euphausia superba. *Front Mar Sci* 4:310. doi: 10.3389/fmars.2017.00310

Kohlbach D, Schaafsma FL, Graeve M, Lebreton B, Lange BA, David C, Vortkamp M, Flores H (2017b) Strong linkage of polar cod (Boreogadus saida) to sea ice algae-produced carbon: Evidence from stomach content, fatty acid and stable isotope analyses. *Prog Ocean* 152:62-74. doi: 10.1016/j.pocean.2017.02.003

Kohlbach D, Lange BA, Graeve M, Vortkamp M, Flores H (2019) Varying dependency of Antarctic euphausiids on ice algae-and phytoplankton-derived carbon sources during summer. *Marine Biology* 166(6):1-17.

Kirkwood JM (1982) A guide to the Euphausiacea of the Southern Ocean. *ANARE Research Notes* 1. Australian Antarctic Division, Kingston.

Knust R, Schröder M (2014) The Expedition PS82 of the Research Vessel POLARSTERN to the southern Weddell Sea in 2013/2014. *Berichte zur Polar- und Meeresforschung* 680, pp 155 p. https://doi.org/10.2312/BzPM_0680_2014

Krapp RH, Berge J, Flores H, Gulliksen B, Werner I (2008) Sympagic occurrence of Eusirid and Lysianassoid amphipods under Antarctic pack ice. *Deep-Sea Res* II 55:1015–1023. https://doi.org/10.1016/j.dsr2.2007.12.018

Kulbicki M, Guillemot N, Amand M (2005) A general approach to length-weight relationships for New-Caledonian lagoon fishes. *Cybium* 29(3):235-252

Lange BA, Katlein C, Nicolaus M, Peeken I, Flores H (2016) Sea ice algae chlorophyll a concentrations derived from under-ice spectral radiation profiling platforms. *Journal of Geophysical Research: Oceans* 121(12):8511-8534.

Lange BA, Katlein C, Castellani G, Fernández-Méndez M, Nicolaus M, Peeken I, Flores H (2017) Characterizing spatial variability of ice algal chlorophyll a and net primary production between sea ice habitats using horizontal profiling platforms. *Frontiers in Marine Science* 4:349.

Leopold MF, Begeman L, Heβe E, Van der Hiele J, Hiemstra S, Keijl G, Meesters EH, Mielke L, Verheyen D, Gröne A (2015) Porpoises: from predators to prey. *J Sea Res* 97:14–23. http://dx.doi.org/10.1016/j.seares.2014.12.005

Macke A, Flores H (2018) The Expeditions PS106/1 and 2 of the Research Vessel POLARSTERN to the Arctic Ocean in 2017. *Berichte zur Polar- und Meeresforschung* 719, pp 171. https://doi.org/10.2312/BzPM_0719_2018

Makarov RR, Denys CJ (1981) Stages of sexual maturity of *Euphausia superba* Dana. BIOMASS Handb 11:2−13.

Marr J (1962) The natural history and geography of the Antarctic krill (*Euphausia superba* Dana). *Discov Rep* 32:37−123.

Meyer B, Auerswald L. (2014) The expedition of the research vessel "Polarstern" to the Antarctic in 2013 (ANT-XXIX/7). *Berichte zur Polar- und Meeresforschung* 674, pp 130. https://doi.org/10.2312/BzPM_0674_2014

Morris DJ, Watkins JL, Ricketts C, Buchholz F, Priddle J (1988) An assessment of the merits of length and weight measurements of Antarctic krill *Euphausia superba* Dana. *Bull Br Antarct Surv* 79: 27–50

Nicol S, Kitchener J, King R, Hosie G, De la Mare WK (2000) Population structure and condition of Antarctic krill (Euphausia superba) off East Antarctica (80-150ºE) during the Austral summer of 1995/1996. *Deep-Sea Res* II 47:2489-2517. https://doi.org/10.1016/S0967-0645(00)00033-3.

Ogle DH (2009) The effect of freezing on the length and weight measurements of ruffe (*Gymnocephalus cernuus*). *Fisheries Research* 99:244–247. https://doi.org/10.1016/j.fishres.2009.06.009

Ogle DH (2016) Chapther 7: weight-length relationships. In: Introductory fisheries analyses with R, Taylor & Francis Group, US, pp 304.

Ogle DH, Wheeler P, Dinno A (2020) FSA: Fisheries Stock Analysis. R package version 0.8.30, https://github.com/droglenc/FSA.

Pakhomov EA, Perissinotto R (1996) Trophodynamics of the hyperiid amphipod *Themisto gaudichaudi* in the South Georgia region during late austral summer. *Mar Ecol Prog Ser* 134:91-100. https://doi.org/10.3354/meps134091

Peeken I. (2016) The Expedition PS92 of the Research Vessel POLARSTERN to the Arctic Ocean in 2015. *Berichte zur Polar- und Meeresforschung* 694, pp 153 p. https://doi.org/10.2312/BzPM_0694_2016

Reid K (1996) A guide to the use of otoliths in the study of predators at South Georgia. *British Antarctic Survey*.

Richter, C., 1994. Regional and seasonal variability in the vertical distribution of mesozooplankton in the Greenland Sea. *Berichte zur Polarforschung* 154, 1–87.

Saunders RA, Lourenço S, Vieira RP, Collins MA, Xavier JC (2020) Length-weight and otolith size to standard length relationships in 12 species of Southern Ocean Myctophidae: A tool for predator diet studies. *J Appl Ichthyol37*(1):140-144. https://doi.org/10.1111/jai.14126

Schaafsma FL, David C, Pakhomov EA, Hunt BPV, Lange BA, Flores H, Van Franeker JA (2016) Size and stage composition of age class 0 Antarctic krill (Euphausia superba) in the ice-water interface layer during winter/early spring. *Polr Biol* 39(9), 1515-1526. https://doi.org/10.1007/s00300-015-1877-7

Schaafsma FL, Kohlbach D, David C, Lange BA, Graeve M, Flores H, Van Franeker JA (2017) Spatio-temporal variability in the winter diet of larval and juvenile Antarctic krill (Euphausia superba) in ice-covered waters. *Mar Ecol Prog Ser* 580, 101-115. https://doi.org/10.3354/meps12309

Schaafsma FL, Cherel Y, Flores H, Van Franeker JA, Lea MA, Raymond B, Van de Putte AP (2018) Review: the energetic value of zooplankton and nekton of the Southern Ocean. *Mar Biol* 165:129. https://doi.org/10.1007/s00227-018-3386-z

Siegel V (1986) Untersuchungen zu Biologie des Antarktischen Krill, *Euphausia superba*, im Bereich der Bransfied Strasse und angrenzender Gebiete. *Mitteilungen Institut für Seefischerei* Hamburg, 38: 1-244.

Siegel V (1992) Review of length-weight relationship for Antarctic krill. *CCAMLR*, WG-KRILL-92/15, pp145-155

Van de Putte A, Flores H, Volckaert F, Van Franeker JA (2006) Energy content of Antarctic mesopelagic fishes: implications for the marine food web. *Polar Biol* 29: 1045–1051. https://doi.org/10.1007/s00300-006-0148-z

Van Franeker, J.A., Williams, R., Imber, M.J. & Wolff, W.J. 2001. Diet and foraging ecology of Southern Fulmar *Fulmarus glacialoides*, Antarctic Petrel *Thalassoica antarctica*, Cape Petrel *Daption capense* and Snow Petrels *Pagodroma nivea* ssp on Ardery Island, Wilkes Land, Antarctica. Chapter 11 (58pp) in: J.A. van Franeker, Mirrors in ice. PhD-Thesis, University of Groningen. Alterra, Texel. ISBN 90-367-1352-8.

Wallis JR, Maschette D, Wotherspoon S, Kawaguchi S, Swadling KM (2020) *Thysanoessa macrura* in the southern Kerguelen region: Population dynamics and biomass. *Deep-Sea Res* II 174:104719. https://doi.org/10.1016/j.dsr2.2019.104719

Wetzel MA, Leuchs H, Koop JHE (2005) Preservation effects on wet weight, dry weight, and ash-free dry weight biomass estimates of four common estuarine macro-invertebrates: no difference between ethanol and formalin. Helgol *Mar Res* 59:206-213. https://doi.org/10.1007/s10152-005-0220-z

Wickham H (2016) ggplot2: Elegant Graphics for Data Analysis. Springer-Verlag New York, 2016.

Wickham H, François R, Henry L, Müller K (2020). dplyr: A Grammar of Data Manipulation. R package version 1.0.2. https://CRAN.R-project.org/package=dplyr

Wieczorek J, Bloom D, Guralnick R, Blum S, Döring M, et al. (2012) Darwin Core: an evolving community-developed biodiversity data standard. *PLoS ONE* 7(1): e29715. https://doi.org/10.1371/journal.pone.0029715

Williams R, Robins D.B. (1982) Effects of preservation on wet weight, dry weight, nitrogen and carbon contents of *Calanus helgolandicus* (Crustacea: Copepoda). *Mar Biol* 71:271–281. https://doi.org/10.1007/BF00397044

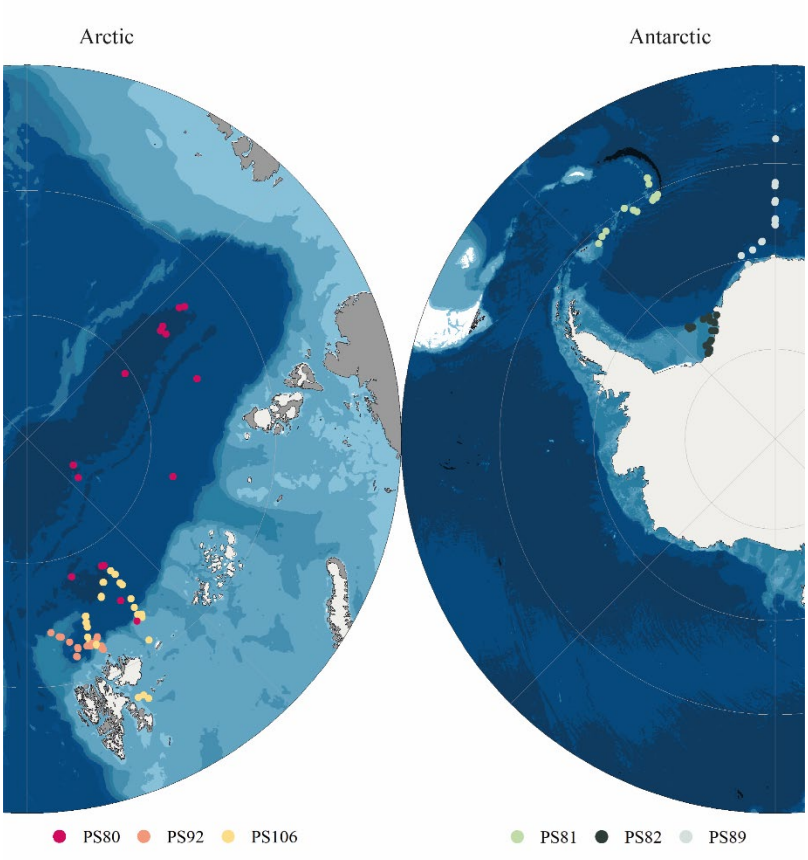

Figure 1: Maps of the study areas and sampled locations during **A)** Arctic Polarstern expeditions PS80, PS92, and PS106/2, and **B)** Antarctic Polarstern expeditions PS81, PS82, and PS89.

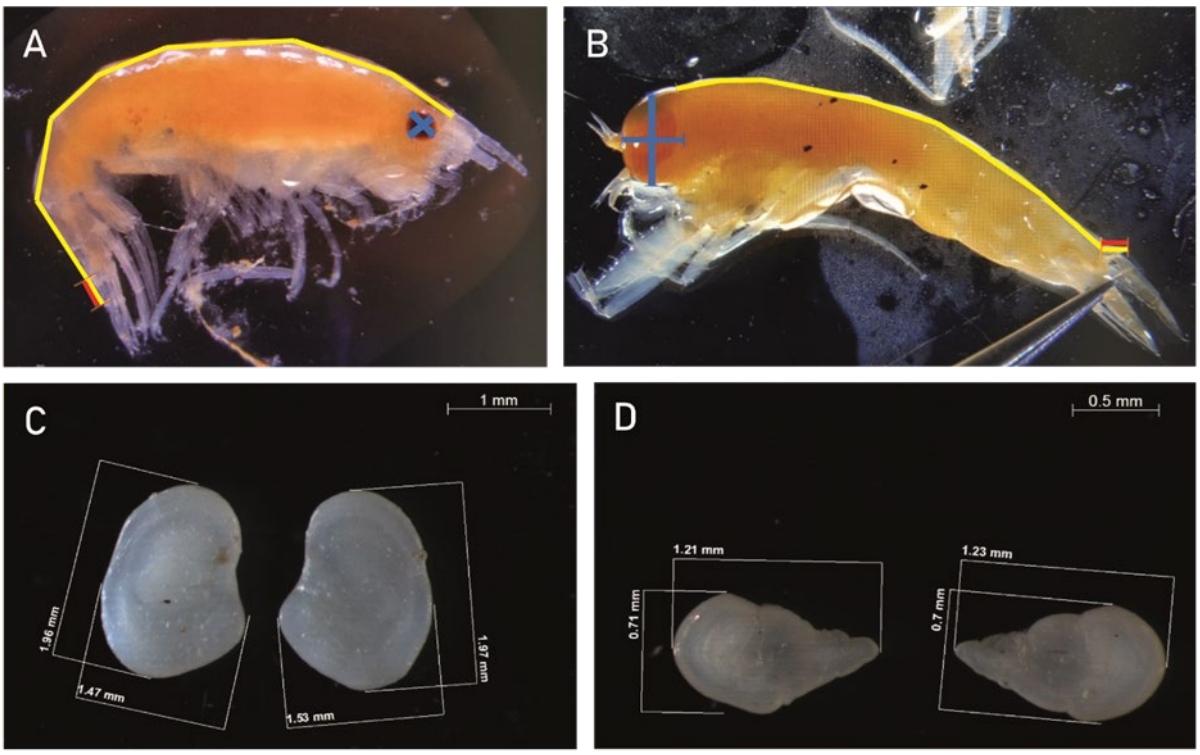

Figure 2: Examples of measurements of the gammarid amphipod *Apherusa glacialis* **A)** and the hyperiid amphipod *Themisto libellula* **B)**, including total length (yellow line), eye length and width (blue line) and telson length (red line), and of measurements on the otoliths of the fishes *Electrona antarctica* **C)** and *Bathylongus antarcticus* **D)**.

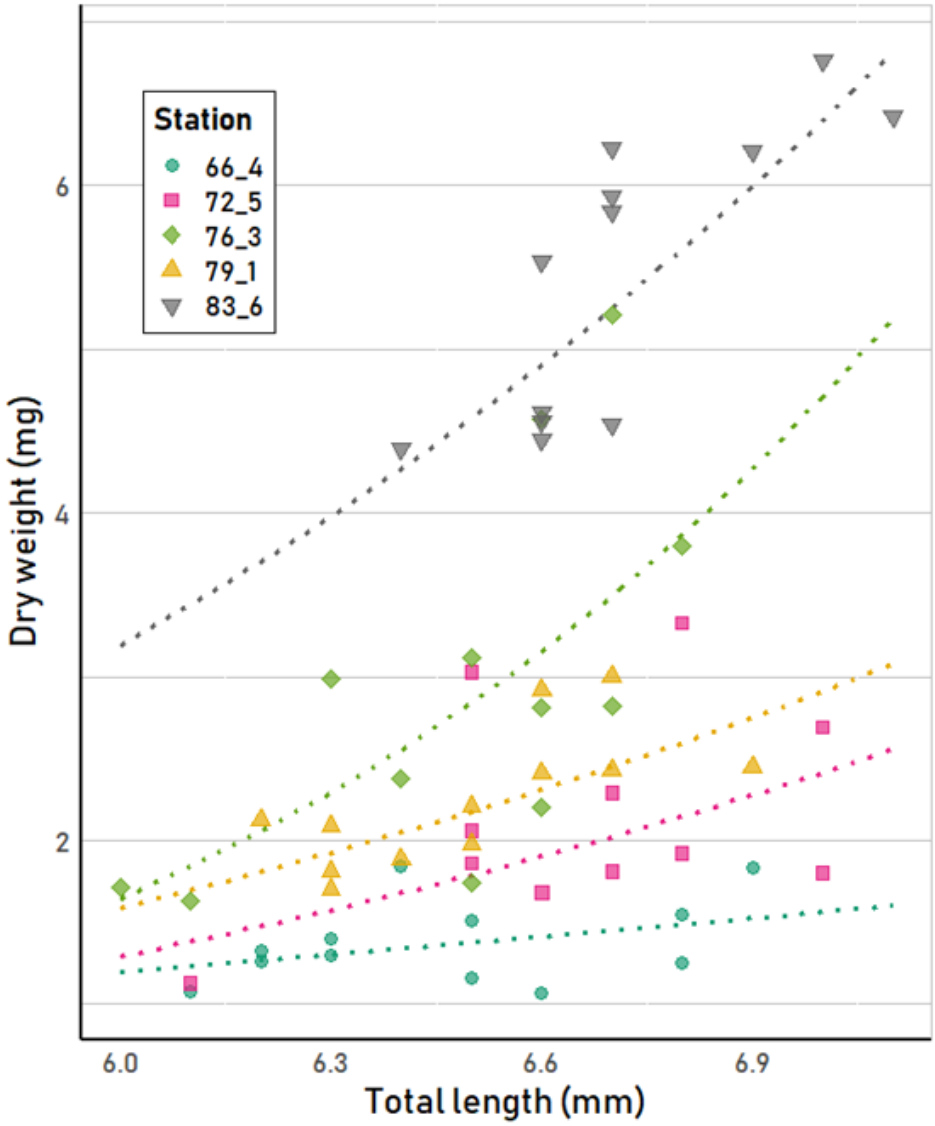

Figure 3: Total length-dry weight relationships of adult females of the copepod *Calanus hyperboreus* caught during summer. Although individuals from 14 stations were measured, the measurements from five stations are shown here to illustrate the variability in dry weight per length at different locations. All measurements can be found in the supplementary material.

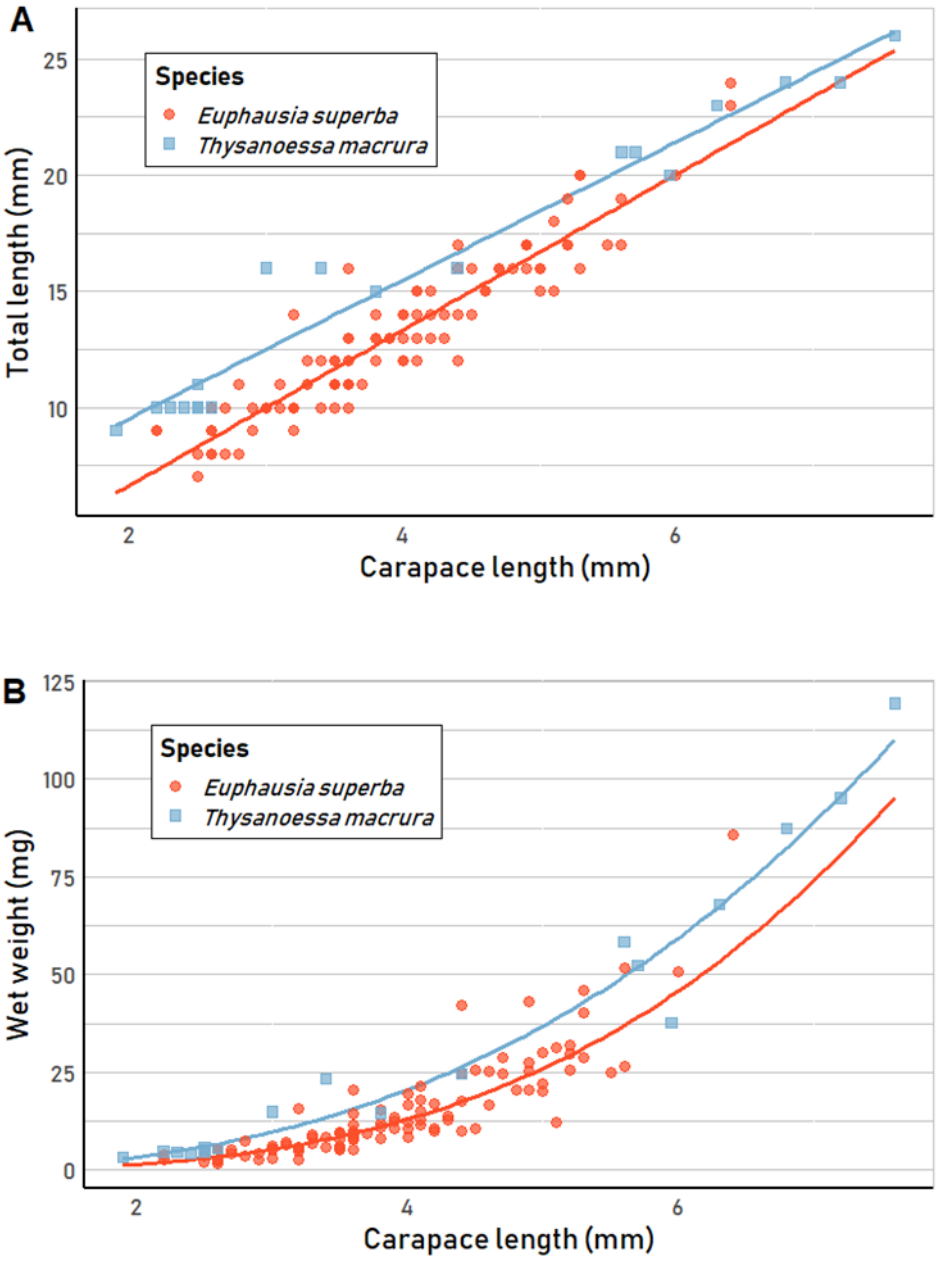

Figure 4: The relationships between carapace length, total length (A), and wet weight (B) of the krill species *Euphausia superba* and *Thysanoessa macrura* caught during austral winter. The size range of *T. macrura* likely represents juvenile and adult individuals, while that of *E. superba* represents furcilia and juveniles in their first winter (age class 0).

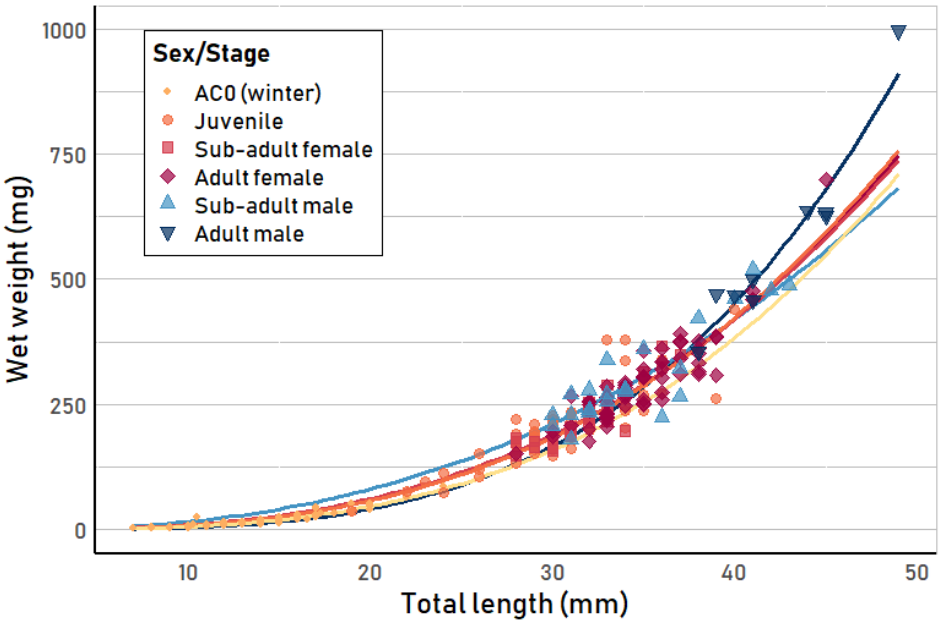

Figure 5: Total length-wet weight relationships of the Antarctic krill *Euphausia superba* separated by sexes and stages. Age class 0 (AC0) individuals encompass furcilia VI and juveniles caught during their first winter. All other sexes/stages were caught in summer (PS89).

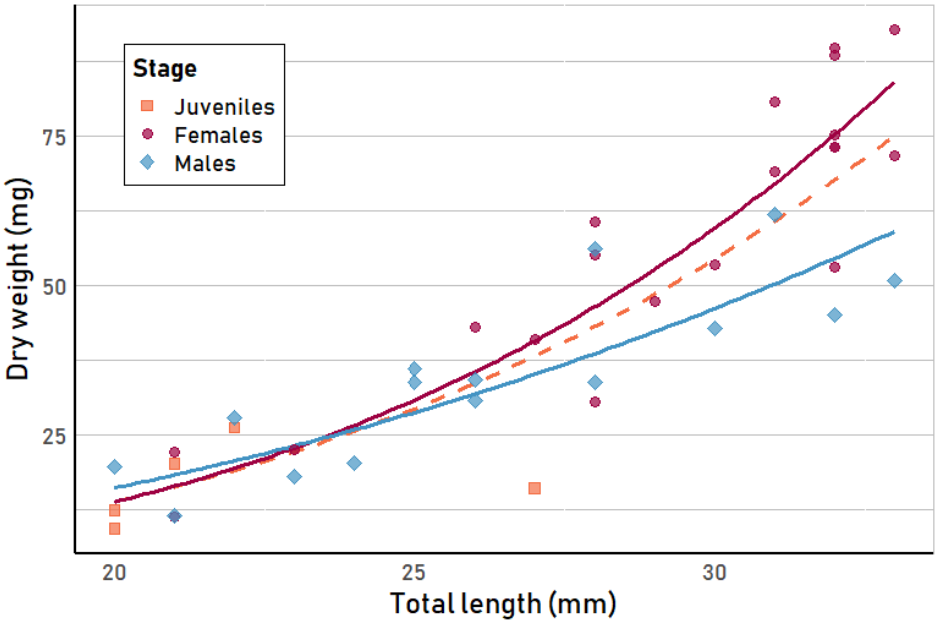

Figure 6: Total length-dry weight relationships of the krill *Euphausia crystallorophias* caught during austral summer including their regression models (dashed line for juveniles, solid lines for females and males).

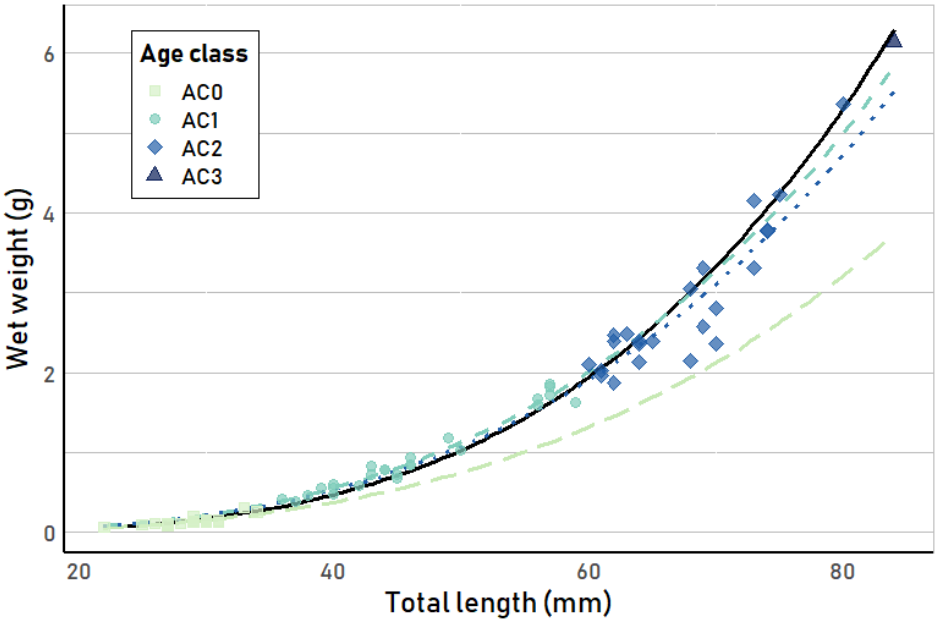

Figure 7: Total length-wet weight relationships of the fish *Electrona antarctica* caught during austral summer separated by age class (AC). The solid black line represents the total length-wet weight relationship of all age classes combined.

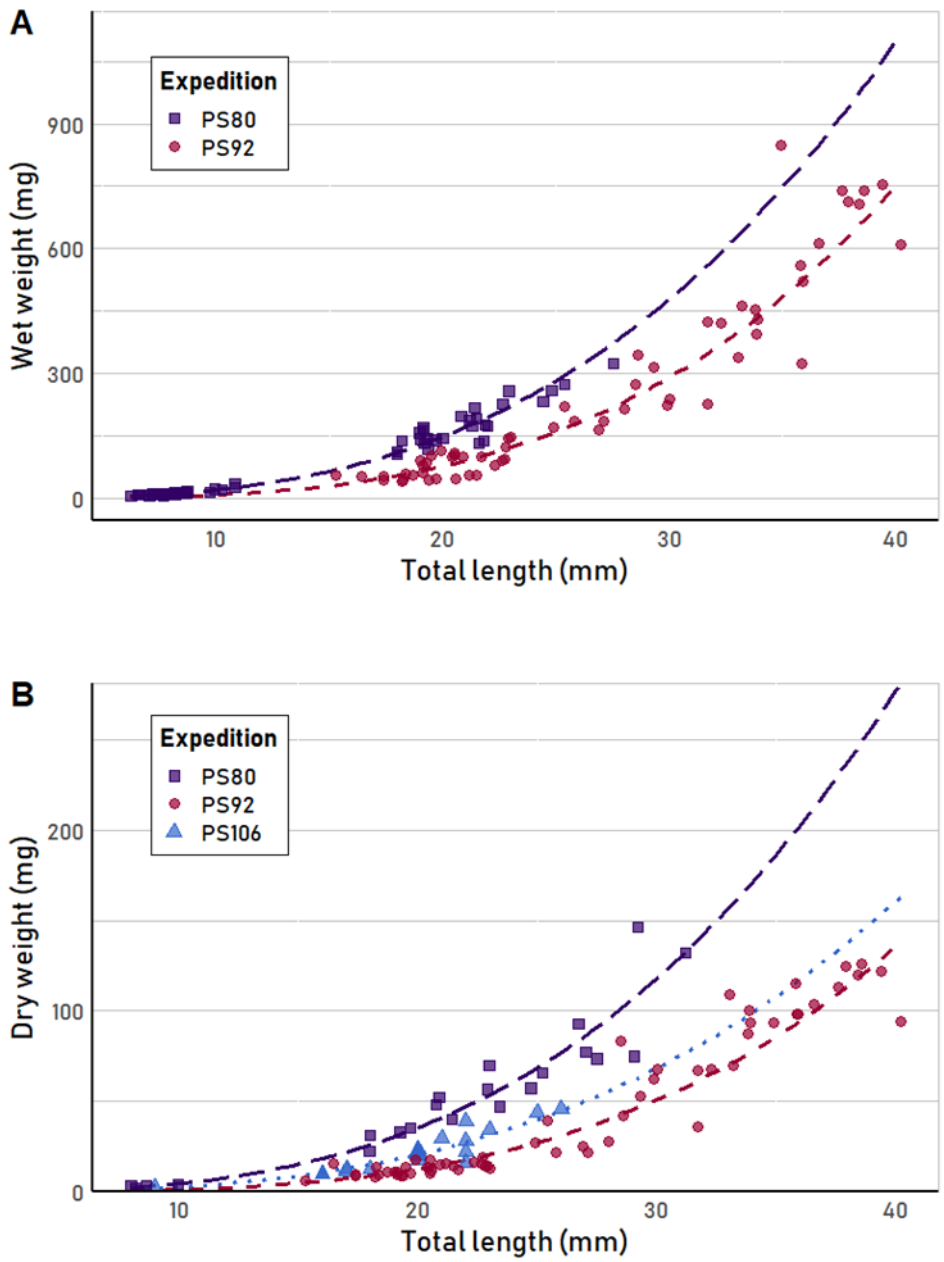

Figure 8: The relationships between total length, wet weight (A), and dry weight (B) of the amphipod *Themisto libellula* caught during the expeditions PS92 in spring, PS106/2 (only dry weight) in summer, and PS80 during end of summer/autumn.

Table 1: Overview of collected data per Antarctic (red, left) and Arctic (purple, right) expedition. Total lengths were recorded for all species except the hydrozoans *Atolla* spp. and *Periphylla periphylla*. For all fish except *Notolepis coatsi* standard length was also measured. Dark coloured squares indicate data that is further used for modelling. Light coloured squares indicate that there is data available, but n is too small for further analysis. WW = wet weight, DW = dry weight and Oth. = other measurements.

Expedition:	PS81			PS82			PS89			Expedition:	PS80			PS92			PS106/2		
Species:	WW	DW	Oth.	WW	DW	Oth.	WW	DW	Oth.	Species:	WW	DW	Oth.	WW	DW	Oth.	WW	DW	Oth.
Atolla spp.										*Apherusa glacialis*									
Bathylagus antarctica										*Boreogadus saida*									
Electrona antarctica										*Calanus hyperboreus*									
Euphausia crystallorophias										*Eukrohnia hamata*									
Euphausia superba										*Eusirus holmii*									
Eusirus laticarpus										*Gammarus wilkitzkii*									
Eusirus microps										*Onisimus nanseni*									
Gymnoscopelus braueri										*Onisumis glacialis*									
Notolepis coatsi										*Parasagitta elegans*									
Periphylla periphylla										*Pseudosagitta maxima*									
Pseudosagitta gazellae										*Themisto abyssorum*									
Salpa thompsoni										*Themisto libellula*									
Thysanoessa macrura										*Thysanoessa inermis*									

Table 2: Regression models of length and weight measurements of a variety of Arctic and Antarctic species. In the Arctic Ocean species were caught during spring (PS92), summer (PS106/2) and late summer/autumn (PS80). The Southern Ocean species were caught during winter (PS81) or summer (PS89). TL = total length, SL = standard length.

Species	Season	Length range (TL)	x	y	n	log a	a	b	R^2
Regression models log(W) = log(a) + b log(L) (W = a L^b)									
ANTARCTIC									
Bathylagus antarcticus	Summer (PS89)	34 – 58 mm	Total length (mm)	Dry weight (mg)	11	-7.398	0.000	3.725	0.983
Bathylagus antarcticus	Summer (PS89)	34 – 58 mm	Total length (mm)	Wet weight (mg)	11	-6.699	0.000	3.797	0.980
Electrona antarctica	Summer (PS89)	22 – 84 mm	Total length (mm)	Wet weight (mg)	68	-5.924	0.000	3.494	0.983
Electrona antarctica	Summer (PS89)	22 – 84 mm	Total length (mm)	Dry weight (mg)	47	-5.934	0.000	3.489	0.986
Eusirus laticarpus	Summer (PS89)	12.5 – 17.7 mm	Total length (mm)	Wet weight (mg)	14	-3.699	0.000	2.113	0.693
Euphausia superba	Winter (PS81)	7 - 22 mm	Total length (mm)	Wet weight (mg)	107	-2.310	0.005	3.048	0.901
Euphausia superba	Winter (PS81)	28 – 55 mm	Total length (mm)	Dry weight (mg)	35	-3.22	0.001	3.252	0.951
Thysanoessa macrura	Winter (PS81)	9 – 26 mm	Total length (mm)	Wet weight (mg)	21	-2.638	0.002	3.306	0.988
ARCTIC									
Apherusa glacialis	Spring (PS92)	7.6 - 11.1 mm	Total length (mm)	Wet weight (mg)	26	-1.382	0.042	2.563	0.731
Apherusa glacialis	Summer (PS106/2)	9.9 – 13.6 mm	Total length (mm)	Dry weight (mg)	27	-2.721	0.002	3.205	0.679
Boreogadus saida	Summer (PS106/2)	86 – 182 mm	Total length (mm)	Wet weight (g)	35	-5.021	0.000	2.929	0.915
*Boreogadus saida**	Sum/Autumn (PS80)	52 – 137 mm	Total length (mm)	Wet weight (g)	119	-5.239	0.000	3.018	0.966
*Eukrohnia hamata**	Spring (PS92)	20.0 – 31.9 mm	Total length (mm)	Wet weight (mg)	26	-3.301	0.001	3.469	0.821
*Eukrohnia hamata**	Spring (PS92)	20.0 – 31.9 mm	Total length (mm)	Dry weight (mg)	26	-3.000	0.001	2.604	0.781
Eusirus holmi	Sum/Autumn (PS80)	30.6 – 37.4 mm	Total length (mm)	Wet weight (mg)	37	-1.116	0.077	2.438	0.466
Eusirus holmi	Sum/Autumn (PS80)	29.8 – 39.2 mm	Total length (mm)	Dry weight (mg)	18	-0.384	0.413	2.149	0.326
Onisimus glacialis	Sum/Autumn (PS80)	12.1 – 19.0 mm	Total length (mm)	Wet weight (mg)	34	-0.228	0.592	1.712	0.660
Onisimus glacialis	Summer (PS106/2)	10.9 – 14.6 mm	Total length (mm)	Dry weight (mg)	14	-1.457	0.035	2.070	0.460
Onisimus nanseni	Sum/Autumn (PS80)	11.6 – 16.6 mm	Total length (mm)	Wet weight (mg)	11	-1.506	0.031	2.743	0.906
Themisto abyssorum	Spring (PS92)	9.5 – 20.3 mm	Total length (mm)	Wet weight (mg)	25	-1.870	0.014	3.102	0.918
Themisto abyssorum	Spring (PS92)	9.5 – 20.3 mm	Total length (mm)	Dry weight (mg)	25	-1.559	0.028	2.143	0.837
Themisto libellula	Sum/Autumn (PS80)	6.3 – 27.5 mm	Total length (mm)	Dry weight (mg)	22	-2.316	0.005	2.970	0.973
Themisto libellula	Spring (PS92)	15.3 – 40.2 mm	Total length (mm)	Wet weight (mg)	60	-2.419	0.004	3.304	0.918
Themisto libellula	Spring (PS92)	15.3 – 40.2 mm	Total length (mm)	Dry weight (mg)	60	-3.345	0.0003	3.419	0.923
Themisto libellula	Summer (PS106/2)	9 – 26 mm	Total length (mm)	Dry weight (mg)	21	-2.552	0.003	2.969	0.932
Thysanoessa inermis	Summer (PS106/2)	20.1 – 26.0 mm	Total length (mm)	Dry weight (mg)	14	-2.796	0.002	3.033	0.324
Regression models y = ax + b									
ANTARCTIC									
Atolla spp.	Summer (PS89)	NA	Wet weight (g)	Dry weight (g)	17	-	0.039	0.395	0.879
Bathylagus antarcticus	Summer (PS89)	34 – 58 mm	Total length (mm)	SL (mm)	11	-	0.989	-2.227	0.987
Bathylagus antarcticus	Summer (PS89)	34 – 58 mm	Wet weight (g)	Dry weight (g)	11	-	0.1553	0.002	0.999
Electrona antarctica	Summer (PS89)	22 – 84 mm	Total length (mm)	SL (mm)	68	-	0.9206	-0.295	0.996
Electrona antarctica	Summer (PS89)	22 – 84 mm	Wet weight (g)	Dry weight (g)	47	-	0.333	-0.026	0.981
Euphausia superba	Winter (PS81)	10.3 – 36 mm	Wet weight (g)	Dry weight (g)	14	-	0.2163	-0.449	0.996
Periphylla periphylla	Summer (PS89)	NA	Wet weight (g)	Dry weight (g)	11	-	0.049	0.225	0.901

ARCTIC									
Boreogadus saida	Summer (PS106/2)	86 – 182 mm	Total length (mm)	SL (mm)	36	-	0.915	-0.744	0.994
Boreogadus saida	Sum/Autumn (PS80)	52 – 137 mm	Total length (mm)	SL (mm)	98	-	0.913	0.197	0.997
Eukrohnia hamata	Spring (PS92)	20.0 – 31.9 mm	Wet weight (mg)	Dry weight (mg)	25	-	0.092	1.355	0.819
Themisto abyssorym	Spring (PS92)	9.5 – 20.3 mm	Wet weight (g)	Dry weight (mg)	25	-	0.095	3.155	0.849
Themisto libellula	Spring (PS92)	15.3 – 40.2 mm	Wet weight (g)	Dry weight (g)	38	-	0.166	-2.869	0.934

* Data previously published in David et al., 2016

[2]model violates homogenous variance assumption

Table 3: Relationship between body parts, total length, and weight of several Southern and Arctic Ocean species.

Species	Season	Function	x	y	n	a	b	R^2
Apherusa glacialis	Summer (PS80)	y = ax + b	Telson (mm)	Total length (mm)	638	19.192	2.094	0.681
		y = ax + b	Eye horizontal (mm)	Total length (mm)	657	16.876	1.340	0.724
		y = ax + b	Eye vertical (mm)	Total length (mm)	657	18.914	1.688	0.667
Bathylagus antarcticus	Summer (PS89)	y = ax + b	Otolith length (mm)	Total length (mm)	11	33.458	-0.623	0.812
		$y = a x^b$	Otolith length (mm)	Wet weight (g)	11	0.1022	4.046	0.869
		$y = a x^b$	Otolith length (mm)	Dry weight (g)	11	0.0169	3.97	0.872
*Boreogadus saida**	Summer (PS80)	y = ax + b	Otolith length (mm)	Total length (mm)	138	24.27	20.713	0.943
		$y = a x^b$	Otolith length (mm)	Wet weight (g)	109	0.521	2.026	0.930
Electrona antarctica	Summer (PS89)	y = ax + b	Otolith length (mm)	Total length (mm)	68	33.767	2.556	0.965
		$y = a x^b$	Otolith length (mm)	Wet weight (g)	69	0.3388	3.283	0.986
		$y = a x^b$	Otolith length (mm)	Dry weight (g)	48	0.0793	3.785	0.974
Eukrohnia hamata	Spring (PS92)	y = ax + b	Head width (mm)	Total length (mm)	70	15.55	2.795	0.726
		y = ax + b	Tail length (mm)	Total length (mm)	186	4.5001	0.601	0.967
Euphausia superba	Winter (PS81)	y = ax + b	Carapace length	Total length (mm)	102	3.348	-0.066	0.867
		$y = a x^b$	Carapace length	Wet weigth (mg)	101	0.169	3.137	0.895
Parasagitta elegans	Spring (PS92)	y = ax + b	Head width (mm)	Total length (mm)	11	23.527	-1.236	0.925
		y = ax + b	Tail length (mm)	Total length (mm)	29	5.2485	0.333	0.923
Themisto libellula	Summer (PS80)	y = ax + b	Telson length	Total length (mm)	490	17.892	1.733	0.95
		y = ax + b	Eye horizontal	Total length (mm)	446	11.206	-3.604	0.89
		y = ax + b	Eye vertical	Total length (mm)	441	8.6115	-5.044	0.927
Thysanoessa macrura	Winter (PS81)	y = ax + b	Carapace length	Total length (mm)	19	2.9757	3.577	0.958
		$y = a x^b$	Carapace length	Wet weigth	19	0.5481	2.615	0.967

*previously published in David et al., 2016

Table 4: Comparison between length-weight regression models of different developmental stages or ages of the Southern Ocean species *Euphausia superba* (summer/autumn PS89), *Euphausia crystallorophias* (summer PS82), and *Electrona antarctica* (summer PS89), and the Arctic Ocean species *Themisto libellula* (summer PS106/2). AC = age class.

Species	Season	Stage	x	y	n	log a	a	b	R^2	df	Res. St. error
Euphausia superba	Summer	All	Total length (mm)	Wet weight (mg)	215	-2.003	0.010	2.895	0.888	213	0.570
	Summer	Juveniles	Total length (mm)	Wet weight (mg)	91	-1.906	0.012	2.828	0.831	89	0.063
	Summer	Sub-adult female	Total length (mm)	Wet weight (mg)	32	-1.989	0.010	2.881	0.806	30	0.045
	Summer	Adult Females	Total length (mm)	Wet weight (mg)	61	-1.835	0.015	2.783	0.826	59	0.048
	Summer	Sub-adult males	Total length (mm)	Wet weight (mg)	22	-1.206	0.062	2.390	0.757	20	0.067
	Summer	Males	Total length (mm)	Wet weight (mg)	9	-2.905	0.001	3.470	0.933	7	0.036
Euphausia crystallorophias	Summer	All	Total length (mm)	Dry weight (mg)	40	-3.246	0.001	3.372	0.803	38	0.124
	Summer	Female	Total length (mm)	Dry weight (mg)	20	-3.559	0.000	3.611	0.860	18	0.092
	Summer	Male	Total length (mm)	Dry weight (mg)	15	-2.162	0.007	2.590	0.731	13	0.109
Electrona antarctica	Summer	All	Total length (mm)	Wet weight (mg)	68	-5.924	0.000	3.494	0.983	66	0.072
	Summer	AC0	Total length (mm)	Wet weight (mg)	19	-5.379	0.000	3.093	0.750	17	0.080
	Summer	AC1	Total length (mm)	Wet weight (mg)	25	-5.331	0.000	3.168	0.964	23	0.041
	Summer	AC2	Total length (mm)	Wet weight (mg)	23	-5.329	0.000	3.155	0.808	21	0.055
	Summer	All	Total length (mm)	Dry weight (mg)	47	-5.934	0.000	3.489	0.986	45	0.071
	Summer	AC0	Total length (mm)	Dry weight (mg)	18	-5.319	0.000	3.053	0.746	16	0.081
	Summer	AC1	Total length (mm)	Dry weight (mg)	13	-5.453	0.000	3.228	0.969	11	0.041
	Summer	AC2	Total length (mm)	Dry weight (mg)	15	-5.139	0.000	3.044	0.706	13	0.063
Themisto libellula	Summer	All	Total length (mm)	Wet weight (mg)	58	-1.595	0.025	2.893	0.988	56	0.071
	Summer	Immature/mature	Total length (mm)	Wet weight (mg)	26	-0.825	0.150	2.314	0.762	24	0.063
	Summer	Juveniles	Total length (mm)	Wet weight (mg)	31	-1.444	0.036	2.723	0.836	29	0.074

Table S 1: List of Arctic and Antarctic species for allometric measurements.

ARCTIC	ANTARCTIC
KRILL	
Thysanoessa inermis (Krøyer, 1846)	*Euphausia superba* Dana, 1850 *Euphausia crystallorophias* Holt & Tattersall, 1906 *Thysanoessa macrura* G.O. Sars, 1883
AMPHIPODS	
Apherusa glacialis (Hansen, 1888) *Eusirus holmii* Hansen, 1887 *Gammarus wilkitzkii* Birula, 1897 *Onisimus nanseni* (G.O. Sars, 1900) *Onisimus glacialis* (G.O. Sars, 1900) *Themisto abyssorum* (Boeck, 1871) *Themisto libellula* (Lichtenstein in Mandt, 1822)	*Eusirus laticarpus* Chevreux, 1906 *Eusirus microps* Walker, 1906
FISH	
Boreogadus saida (Lepechin, 1774)	*Bathylagus antarcticus* Günther, 1878 *Electrona antarctica* (Günther, 1878) *Gymnoscopelus braueri* (Lönnberg, 1905) *Notolepis coatsi* Dollo, 1908
CHAETOGNATHS	
Eukrohnia hamata (Möbius, 1875) *Parasagitta elegans* (Verrill, 1873) *Pseudosagitta maxima* (Conant, 1896)	*Pseudosagitta gazellae* (Ritter-Záhony, 1909)
SALPS	
	Salpa thompsoni Foxton, 1961
HYDROZOANS	
	Atolla Haeckel, 1880 *Periphylla periphylla* (Péron & Lesueur, 1810)
COPEPODS	
Calanus hyperboreus Krøyer, 1838	

3 General discussion and outlook

3.1 Quantifying Biodiversity - an indicator for a changing ecosystem

Numbers of species, trophic levels, or genetic variability are only some of the traits which can be defined as 'biodiversity'. In general, a diverse ecosystem is considered to comprise a variety of organisms that occupy a wide range of ecological niches. Because of this variety of life forms and life strategies, a diverse ecosystem is resilient to changes in the environment (Bernhardt and Leslie, 2013). If conditions change, the possibility is high that some species will adapt and, thus, prevent the ecosystem from collapse. In September 2015, the United Nations (UN) adopted 17 Sustainable Development Goals as part of the 2030 Agenda for Sustainable Development (UN, 2016). The global protection of marine biodiversity is part of goal 14) in the agenda (Figure 7). In addition, the International Oceanographic Commission of the UN (IOC) has launched the Decade of Ocean Science for Sustainable Development (2021 to 2030), in which they encourage scientific research on marine biodiversity and its protection (IOC-Unesco, 2017). The protection of biodiversity, though, requires an understanding of what the natural state of an ecosystem is, to then, determine the response to possible stressors.

Figure 7. UN adopted sustainable development goals, which are part of the 2030 agenda involved goal 14) "Life below water" which includes the aim to protect the marine biodiversity (UN, 2016).

In the Eurasian Basin of the Arctic Ocean, climate-driven changes of faunal biodiversity have increasingly been studied recently (Hop et al., 2020; Ershova et al. 2021). Especially sympagic biota are very susceptible to climate change since they are directly affected not only by a range of environmental parameters, e.g., temperature, salinity, nutrients, but also by the transformation and loss of their habitat itself - the sea ice (Carmack et al., 2015; Polyakov et al., 2017; Krumpen et al., 2019).

The species richness of sympagic multicellular meiofauna is estimated to more than 60 species over the pan-Arctic domain (Bluhm et al., 2017). The taxonomic composition of sea-ice meiofauna varies between regions, seasons, and ice types (Bluhm et al., 2018). Some studies exist about their abundance and distribution in different ice types. Most of them are from landfast ice (Carey and Montagna, 1982; Friedrich, 1997; Michel et al., 2002), whereas Arctic pack-ice studies are underrepresented (Gradinger et al., 1992, 2005; Gradinger, 1999). The knowledge on sea-ice biota is still incomplete and new species of bacteria, microalgae, fungi, and metazoans are continuously found in the sea-ice environment (Piraino et al., 2008; Comeau et al. 2013; Hasset and Gradinger, 2016). One reason for this may certainly be the developing technology of molecular methods, which are increasingly used nowadays (Comeau et al., 2013; Hasset and Gradinger, 2016). In our study we identified a community consisting of 10 sea-ice meiofauna taxa from five phyla in the Eurasian Basin (***Chapter I***). The biodiversity of sea-ice meiofauna taxa showed some distinct differences to earlier studies. The most abundant taxa were well-known inhabitants of the sea-ice realm (Harpacticoida, Ciliophora, copepod nauplii), however, Nematoda, Rotifera, Acoela, and other flatworms were not found in Arctic pack ice in our study (***Chapter I***), though they were frequently occurring taxa in other studies (Gradinger, 1999; Nozais et al., 2001; Gradinger et al., 2005; Bluhm et al., 2018).

Nematoda - the losers of sea-ice meiofauna in the New Arctic?

The absence of Nematoda is especially interesting since this taxon was dominating the sea-ice community in several other studies (Friedrich, 1997; Gradinger, 1999; Schünemann and Werner, 2005) and is with 56 % a frequently occurring taxon across the pan-Arctic domain (Bluhm et al., 2018). The absence of Nematoda, as described in ***Chapter I***, was also observed in other pack-ice studies from the Eurasian Basin in 2015 (Bluhm et al., 2018) and in 2019 and 2020 (Bluhm, personal communication). Thus, it is not a singular observation and can be seen as an indicator for a biodiversity shift to a less diverse sea-ice community. Having a benthic interstitial lifestyle (Tita et al., 1999), Nematoda are frozen into the sea-ice during the ice-formation process in shallow shelf regions and transported in the ice with winds and currents to the deeper regions of the Arctic Ocean. Their absence from Arctic pack ice could be related to the reduced sea-ice coverage but also to the recently observed northward (off-shelf) shifts of sea-ice forming grounds (Krumpen et al., 2019). At the same time, Nematoda were found in higher abundance in nearshore benthic samples during our spring expedition (Grzelak et al., 2020). This would imply that also other benthic taxa, such as Polychaeta, could in the future fail to colonize the sea ice and might disappear from this habitat, too. Subsequently, other pelagic taxa, such as Ciliophora or

pelagic Harpacticoida and their nauplii, would face less competition for resources and could colonize the sea ice even better. If this hypothesis was true, it could explain the high abundance of Harpacticoida and copepod nauplii in ***Chapter I*** compared to other studies (Gradinger et al., 1999; Schünemann and Werner, 2005; Bluhm et al., 2018). Additionally, Nematoda are deposit or carnivorous/omnivorous feeders (Grzelak et al., 2020), therefore a loss of this taxon might have consequences on the predation pressure on e.g., Harpacticoida. Consequently, Harpacticoida abundance would increase and result in a higher grazing pressure on ice algae, as described in more detail in section 3.3. The incomplete knowledge on sympagic Nematoda, though, constrains the evaluation of their role in the sea-ice community and their contribution to the carbon flux. However, biomass-size spectra for the different feeding types of Nematoda species from the Eurasian Basin were only very recently published (Grzelak et al., 2020) and enable future studies to evaluate their contribution to the carbon budget.

Ciliophora - understudied but important for sea-ice diversity

Particularly for sea-ice meiofauna, our knowledge still lags behind in comparison to that of pelagic fauna (e.g., copepods). Implications of climate change for the sea-ice community are, therefore, challenging to anticipate. Past studies often concentrated on particular taxa in the sea-ice and excluded others, which makes it difficult to compare biodiversity studies. For example, Ciliophora were often excluded from analysis (Nozais et al., 2001; Gradinger et al., 2005; Schünemann and Werner, 2005), which might be due to the time consuming analyzing process or their small size, which requires high-powered stereomicroscopes (Figure 8). The fact that Ciliophora were among the dominating taxa in the sea ice in ***Chapter I*** and in other studies (e.g., Gradinger et al., 1999) suggests they are an important contributor to the diversity of the sea-ice community and, I speculate, for its stability. Therefore, I suggest to include Ciliophora in future biodiversity studies. In an ideal way, morphological studies should be complemented by molecular techniques.

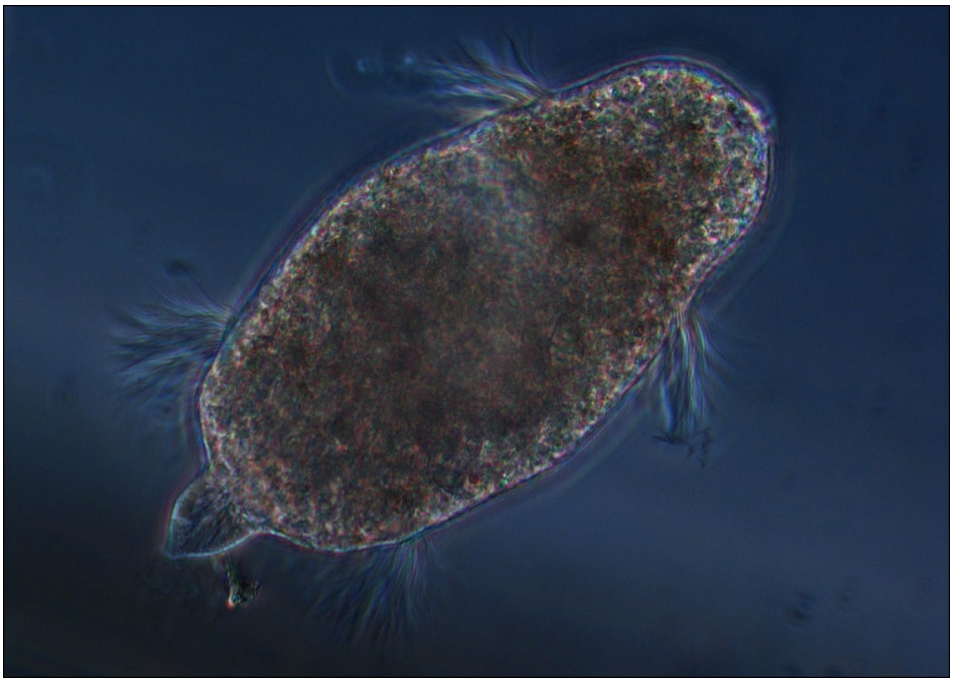

Figure 8. A ciliate from the Arctic pack ice.

Current estimates on the species richness of the under-ice macrofauna suggest more than 40 species, of those 6 – 17 Amphipoda species for the Arctic Ocean (Arndt and Swadling, 2006). To date, little information is available on the large-scale distribution patterns and community structures of the under-ice community. Sampling this unique environment is challenging and has mainly been achieved by SCUBA divers or via pumping through ice holes in the past (Arndt and Pavlova, 2005; Hop et al., 2011). The development of the SUIT has enabled large-scale sampling of the under-ice community for some years. David et al. (2015) presented the first SUIT biodiversity study of the under-ice community in the Eurasian Basin during the historical sea-ice minimum in summer 2012. A comparative summary of the results of David et al. (2015) with those presented in this thesis (***Chapter I***, ***II***, ***III***, and ***IV***) is given in Table 1. The under-ice community in our study was dominated by well-known taxa, such as the three *Calanus* species (*C. finmarchicus*, *C. glacialis, C. hyperboreus*) and copepod nauplii. Characteristics of the under-ice community are discussed in the following.

Diminishing macrofauna of the under-ice community

Amphipoda are among the most studied organisms from the under-ice environment and were often reported to be highly abundant sympagic species until the previous decade (Gradinger and Bluhm, 2004; Werner and Auel, 2005; Hop and Pavlova, 2008; Gradinger et al.,2010). However, their decline throughout the Arctic has recently been reported in some studies (Hop et al., 2011; Berge et al., 2012). Since MYI and pressure ridges provide a longer-lasting habitat for those ice-associated organisms (Gradinger et al., 2010), their

decline is considered to coincide with decreasing sea-ice conditions (Hop et al., 2011; Berge et al., 2012). Especially *Apherusa glacialis* is a species of interest since it is the most dominant of the five common endemic Arctic Amphipoda species (along with *Gammarus wilkitzkii*, *Eusirus holmii*, *Onisimus nanseni,* and *O. glacialis*). How exactly *A. glacialis* uses the under-ice habitat and the underlying water column is still under investigation (e.g., Kunisch et al., 2020). Since thinner sea ice drifts faster, it is hypothesized that *A. glacialis* leave the sea-ice habitat, where they graze on ice algae, to the deeper Atlantic Water to prevent themselves from being transported with the ice and the Transpolar Drift out of the Arctic Ocean (Berge et al., 2012; Schaafsma, 2018; Kunisch et al., 2020). In our study, Amphipoda were among the least abundant under-ice taxa and accounted only for ~ 0.34 % (*A. glacialis* 0.31 %) of the under-ice community abundance (***Chapter I***). Since the presence of *A. glacialis* is dependent on sea-ice conditions, e.g., floe size, presence of MYI, and ridges (Beuchel and Lønne, 2002), a possible reason for their low abundance could be the sea-ice coverage, which was on average 51 %, or the relatively thin FYI in our study (***Chapter I*** and ***II***) (Table 1). More specifically, we hypothesized that *A. glacialis* might no longer be able to drift with the sea ice (formed at the Sibirian shelves) across the Arctic Ocean into our study area. Instead, *A. glacialis* is already released into the central Arctic Ocean because of the increasing decay of sea ice along the Transpolar Drift. Thus, only low abundances were left to recolonize the newly formed ice during its drift towards our study area (***Chapter I*** and ***II***).

Patches of Appendicularia - pattern or coincidence?

Appendicularia were the most abundant (~ 5000 ind. m^{-2}) taxon in our study and contributed ~ 58 % to the under-ice community by abundance (Table 1). Their occurrence was, however, restricted to only a single station in the sampled region which was located on the shelf of Svalbard (***Chapter I***). Some studies reported Appendicularia in the Arctic Ocean before (Mumm, 1993; Kosobokova and Hirche, 2000; Auel and Hagen, 2002; Ershova and Kosobokova, 2019) and our observation confirms accumulating evidence from the Pacific Arctic of increasing occurrence of Appendicularia in the Arctic (Deibel et al., 2005; Lane et al., 2008; Kosobokova and Hopcroft, 2010). However, none of the mentioned studies found them in such high abundances.

Appendicularia are one of the least-studied organisms of the Arctic environment, thus, reasons for their high abundance are hard to pinpoint. The most obvious reason is, therefore, that the SUIT sampled by chance a patch of Appendicularia. Since the SUIT is able to sample the under-ice habitat over several km, the possibility to catch a patch of a certain taxon is higher than by sampling this community with under-ice pumps or SCUBA

divers. This hypothesis is supported by the only other published Arctic SUIT study, which also reported two stations with a dense patch of Appendicularia (David et al., 2015). Since Appendicularia are soft-bodied filter feeders, they might just have followed a patch of phytoplankton on which they fed. In any case, this event shows how a single taxon (or species) has the potential to shift the community composition and, as I discuss in 3.3, the carbon demand for algae produced carbon of a community. It remains to understand, if this event was a coincidence or is the first sign of a pattern. Further large-scale sampling with the SUIT may bring certainty in answering this question. Holistically sampling and analyzing of the sympagic communities is, therefore, crucial to capture the full biodiversity and include patchy distributions in community analysis.

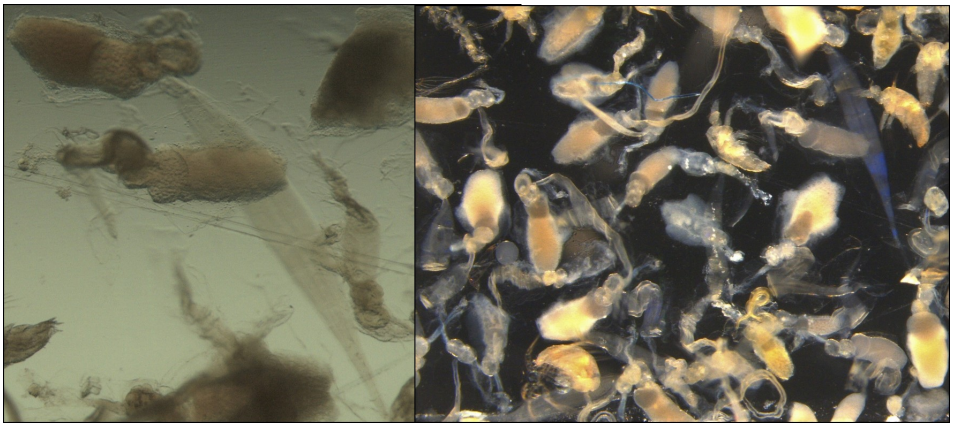

Figure 9. High abundance of Appendicularia in one SUIT sample (station 32) of PS92.

The three guardians of the under-ice community

The three *Calanus* species (*C. hyperboreus*, *C. glacialis*, and *C. finmarchicus*) which dominated the under-ice community at most stations (***Chapter I***) are well-known members of the sympagic community in the Arctic Ocean (Madsen et al., 2001; Hirche and Kosobokova, 2007; David et al., 2015). The high occurrence and abundance of *C. finmarchicus* in our spring study (***Chapter I***) is consistent with the predictions of a replacement of *C. glacialis* by the smaller and less energy-rich *C. finmarchicus* with increasing Atlantification (Bonnet et al., 2005; Richardson, 2008; Polyakov et al., 2017). In the past, the three *Calanus* species were considered to be either "boreal-atlantic" (*C. finmarchicus*), "shelf-neritic" (*C. glacialis*), or "basin-oceanic" (*C. hyperboreus*) (Conover, 1988; Hirche, 1997). This classification, though, was recently challenged when strong correlations were found between the abundance and population structure of *C. glacialis* and *C. hyperboreus* with a number of sea-ice parameters (Ershova et al., 2021). *C. glacialis* was found to be rather a seasonal ice zone associated species than shelf associated (Ershova et al., 2021). Furthermore, in individual-based models, *C. glacialis*

would follow the ice edge further northwards with ongoing reduction of the SIE in the Arctic (Feng et al., 2018; Ershova et al., 2021). These new findings could be significant in terms of the predictions of replacement of *C. glacialis* by *C. finmarchicus* with Atlantification because, I hypothesize, there could be a simultaneous northward shift of *C. glacialis* based on the reducing SIE. In that scenario, *C. finmarchicus* might not 'replace' *C. glacialis*, rather would both species move northward in adaption to their changing environment. This could also explain the findings of the more northern SUIT study from the Eurasian Basin during the historical sea-ice minimum in 2012, where *C. hyperboreus* and *C. glacialis* dominated the under-ice community (***Chapter I***, David et al., 2015) (Table 1).

Table 1. Summarized comparison of sea-ice properties, water properties, biodiversity metrics, and carbon budget information given in *Chapter I*, *II*, *III*, and *IV* of this thesis and in David et al., 2015. *measured at chl *a* max in the mixed layer depth (9 - 34 m); **from this ice algae: 0.6; ***from this ice algae: 1.3

		Chapter I, II and III		*Chapter IV*
	Reference	Ehrlich et al., 2020; Castellani et al., 2020; Ehrlich et al. (accepted after revision)		Flores et al., 2019; David et al., 2015
	Expedition	PS 92		PS 80
	Year	2015		2012
	Season	Spring		Summer
	Region	Eurasian Basin		Eurasian Basin
	Sampling method	**Ice coring**	**SUIT**	**SUIT**
	Fauna	**Sea-ice meiofauna**	**Under-ice fauna**	**Under-ice fauna**
Sea-ice properties	Type	Pack ice, FYI	Pack ice, FYI	Pack ice, FYI
	Thickness [m] (mean)	1.07 - 1.25 (1.16)	1.05 - 3.84 (1.70)	0 - 1.25
	Snow thickness [m] (mean)	0.4-0.9 (0.3)	n.a.	No snow
	Temperature [°C] (mean)	-2.2 - -1.2 (-1.70)	n.a.	n.a.
	Salinity [PSU] (mean)	1.65 - 5.88 (4.47)	n.a.	n.a.
	Coverage [%] (mean)	n.a.	25 – 91 (51)	56 - 100
	Ridges [km^{-1}] (mean)	n.a.	1.4 - 11.4 (4.9)	n.a.
	Chl *a* [mg m^{-2}] (mean)	0.2 - 0.8 (0.4)	0.2 - 0.54 (0.33)	n.a.
	Biomass [mg C m^{-2}] (mean)	10.6 - 41.9 (22.3)	6.3 - 28.5 (17.7)	n.a.
	PP [mg C m-2] (mean)	0.5 - 13.7 (4.8)	3.7 - 34.5 (16.9)	n.a.
Water properties 0 - 2 m	Temperature [°C] (mean)	n.a.	1.3 - 1.8 (1.6)	- 1.76 - - 1.6
	Salinity [PSU] (mean)	n.a.	33.4 - 34.3 (33.8)	29.38 - 32.87
	NO_3^{2-} and NO_2^{3-} [µmol l^{-1}] *	n.a.	n.a.	0.12 - 6.84
	Chl *a* (mean)	n.a.	0.54 - 21.16 (6.97) mg m^{-2}	0.06 - 0.24 mg m^{-3}
	Biomass [mg C m^{-2}] (mean)	n.a.	28.6 - 1,121.4 (352.4)	
	PP [mg C m-2] (mean)	n.a.	1.2 - 114.3 (30.4)	n.a.
Other properties	Bottom depth [m]	n.a.	188 - 2,249	423 - 4,354
	Geographical regions	Yermak Pleateau, Sophia Basin & shelf	Yermak Pleateau, Sophia Basin & shelf	Nansen & Ammundsen Basin
Biodiversity	Taxa richness (total)	2 - 8 (10 taxa, 5 phyla)	7 - 21 (32 taxa, 8 phyla)	8 - 20 (28 species, 10 phyla)
	Shannon diversity	0.60 - 1.53	0.58 - 1.73	0.04 - 2.02
	Pielou's evennes	0.54 - 0.90	0.21 - 0.80	0.02 - 0.69
	Abundance range [ind.m^{-2}]	580 - 17,156	14 - 6,785	0.3 - 69
	Key taxa Abundance	Ciliophora (46 %), copepod nauplii (29 %), Harpacticoida (20 %)	Appendicularia (58 %), copepod nauplii (23 %), *C. finmarchicus*(9 %),	*C. hyperboreus*, *C. glacialis*, *A. glacialis*, *T. libellula*
	Highest impact on the community distribution	Region	Region	Region/ Sea-ice thickness
Carbon budget	Biomass [mg C m^{-2}] (mean) (median)	0.05 - 2.8 (1.1)	3.2 - 62.7 (22.2)	1.64 - 6.92 (2,610)
	Key taxa Biomass	Harpacticoida (92 %), copepod nauplii (4 %), Ciliophora (3 %)	Appendicularia (23 %), *C. finmarchicus* (21 %), *C. hyperboreus* (20 %)	n.a.
	CD [mg C m^{-2} day^{-1}] (mean) (median)	0.06 - 1.5 (0.7) **	0.2 - 29.4 (5.6)***	0.08 - 0.32 (0.13)
	Key taxa CD	Harpacticoida (81 %), copepod nauplii (9 %), Ciliophora (8 %)	Appendicularia (59 %), *C. finmarchicus* (13 %), *C. hyperboreus* (10 %)	n.a.
	SP [mg C m^{-2} day^{-1}] (mean) (median)	0.002 - 0.06 (0.03)	0.04 - 0.75 (0.26)	0.02 - 0.08 (0.03)
	Key taxa SP	Harpacticoida (84 %), Ciliophora (9 %)	Appendicularia (23 %), C. finmarchicus (21 %) *C. hyperboreus* (20 %),	n.a.

3.2 Characterization of the sympagic environment and its influence on the sympagic community

Arctic marine communities are strongly influenced by the dynamic patterns of sea-ice and ocean conditions. Several physical parameters that determine the diversity of species and, therefore, ecosystems in the Arctic Ocean were identified in the Circumpolar Biodiversity Monitoring Program (CBMP) for the Arctic (Gill et al., 2011). According to CBMP, critical ocean parameters include: surface temperature, ocean currents, and frontal boundaries, surface salinity, ocean acidification, and nutrients. Influential sea-ice parameters include: sea-ice cover, sea-ice concentration, sea-ice dynamics, marginal ice zones, landfast ice, and polynyas and leads (Gill et al., 2011). Analyses and interpretations of these core parameters are crucial to understand biodiversity and ecosystem functions in a comprehensive way (Gill et al., 2011).

In ***Chapter II***, datasets of environmental parameters were analyzed for five SUIT campaigns (Arctic and Antarctic) conducted during 2012 and 2017. In this thesis, however, I refer only to the data of expeditions PS92 and PS80 that are relevant for ***Chapter I*** (PS92 in spring 2015) and ***Chapter IV*** (PS80 in summer 2012). The physical datasets for both expeditions included many of the above by CBMP mentioned parameters, e.g., mean ice concentration, mean snow depth, mean total ice thickness, under-ice water temperature, under-ice water salinity, but also other parameters such as insolation, light transmittance, in-ice chl *a*, and under-ice water chl *a*. Also for the sea-ice stations in ***Chapter I*** a range of physical parameters from the sea-ice habitat (mainly from ice-core samples) was measured, including, e.g., sea-ice temperature, bulk salinity, sea-ice chl *a* concentration, snow thickness, and sea-ice thickness. The mentioned environmental data showed a regional pattern for both seasons (***Chapter II***). During the spring expedition PS92 in 2015, the 'Sophia Basin and shelf'-region was characterized by higher under-ice water chl *a* concentrations as well as higher under-ice water temperature and lower salinity than the 'Yermak Plateau'-region (***Chapter II***). During the summer expedition PS80 in 2012, Nansen Basin stations were characterized by higher salinities and lower under-ice water chl *a* concentrations than the Amundsen Basin stations (***Chapter II***). In ***Chapter I*** the above mentioned environmental parameters were assessed for their influence on the sea-ice and under-ice communities:

Geographical regions - the main structuring parameter for sympagic fauna

As in the pan-Arctic study by Bluhm et al. (2018), environmental factors had an overall low explanatory power for the sea-ice meiofauna community (***Chapter I***). The variability in community composition could instead mainly be linked to geographical regions (Yermak

Plateau, Sophia Basin and slope, and shelf) following a quasi-bathymetric gradient. While this pattern was not significant for the sea-ice meiofauna, it was significant for the under-ice fauna (***Chapter I***). Geographic regions and sea-ice thickness were also the main structuring parameters for the under-ice community in ***Chapter IV***. Here the community showed a gradual change from stations located in Nansen Basin to stations in the Amundsen Basin (***Chapter IV***) (Table 1). The finding that bathymetry and sea-ice parameters rank highest with zooplankton community structure is consistent with earlier studies from the Arctic Ocean (Hop and Pavlova, 2008; Hunt et al., 2014). However, the relatively low explanatory power of the tested parameters in our studies indicates that most likely an interplay of several factors influenced the community structure that we were not able to disentangle with our measurements. Sampling over several weeks to months, as mostly done in our studies, covers not only spatial but also temporal variation often inseparable from each other. I, therefore, suggest to design more interseasonal and interregional studies that assure comparability and are crucial for disentangling the influence of spatio-temporal patterns on community structures. Furthermore, the sample sizes might have been too small to adequately assess the complex interplay between physical, geochemical, and biological processes. More analyses together with further development of observational gears and networks, sampling techniques, and improved models are important to meet these challenges and develop reliable forecasts of the future Arctic marine ecosystem.

3.3 Carbon flux through the sympagic community

In the Arctic Ocean, ecosystem functions are still poorly known. This makes it difficult for ecologists to predict food-web dynamics and changes in community structure in future scenarios under climate change. In ***Chapter III***, the role of sympagic biota as a source, sink, and transmitter of carbon in the Arctic ecosystem was evaluated and the dominant taxa in terms of carbon biomass, carbon production, and carbon consumption identified. In addition, the relative roles of ice algae versus phytoplankton for the grazing sympagic fauna were assessed. The results of ***Chapter III*** broaden the understanding of the sea-ice associated ecosystem by providing the first comprehensive carbon budget for the sea-ice meiofauna and under-ice fauna against which future changes can be evaluated.

Ice algae - a fundamental carbon basis of Arctic ecosystems

When sufficient light penetrates the pack ice in early spring, ice algae start to bloom. The phytoplankton bloom normally follows in summer when ice breakup allows sufficient light to reach the water column (Leu et al., 2015). In our study, ice algae presented 27 % of the total primary production (~ 40 mg C m^{-2} day^{-1}) in the Eurasian Basin in spring

(***Chapter III***), which is consistent with another study from the same year and area that reported a share of 30 % in FYI (Fernández-Méndez et al., 2015). Studies from other regions or seasons indicated either that ice-algal production is negligible compared to phytoplankton production (Dupont, 2012; Matrai et al., 2013; Assmy et al., 2017) or that it may contribute as much as half of the total primary production (Gosselin et al., 1997). This shows that the relative proportions of ice-algal versus primary production vary clearly with regions and seasons.

Both ice algae and phytoplankton constitute the basis of the marine food web since they are the main carbon source for sea-ice associated and pelagic grazers. In the last two decades, the role of ice algae as food source has been studied increasingly with the result that they play a role for all compartments of the Arctic ecosystem (Søreide et al., 2006, 2013; Budge et al., 2008; Wang et al., 2015; Kohlbach et al., 2016, 2017). Our study showed that ice algae still contribute strongly to the carbon flow through the sympagic environment (***Chapter III***). The high potential demand of the sympagic fauna for ice-algal carbon, estimated at 30 % of that for phytoplankton, constraints the current spring contribution of ice to the sympagic food web (***Chapter III***). Many organisms are adapted in their feeding, reproduction, and migration patterns to the timing of both blooms (Gradinger, 1999; Søreide et al., 2010; Leu et al., 2011). Especially ice algae are known to provide a high-quality food source for herbivorous species, such as *Calanus* species and *A. glacialis*, weeks before the phytoplankton bloom develops. The ongoing decline in sea ice might, thus, not only change the start and duration of ice-algal and phytoplankton blooms (Arrigo et al., 2008; Arrigo and van Dijken, 2015), but also important vital activities of herbivorous taxa and with them the marine food web that depends on them. *C. glacialis* and *C. hyperboreus*, for example, depend on ice algae as food source since both synchronize their nauplii development with the peak of primary production in spring (Falk-Petersen et al., 2008; Kosobokova and Hirche, 2009; Søreide et al., 2010). The above mentioned changes in the timing of ice-algal and phytoplankton blooms could, therefore, result in mismatches which hamper their reproductive success (Lannuzel et al., 2020).

Figure 10. Ice algae in and under sea ice in Arctic spring during the PS92 expedition.

Sea-ice meiofauna contribution to the sympagic carbon flux was low. Of the mean sympagic biomass of ~ 20 mg C m^{-2} (sea-ice meiofauna and under-ice fauna combined), sea-ice meiofauna accounted only for 5 % (***Chapter III***). Their carbon demand made up only 12 % and their secondary production 9 % of that of the sympagic community, respectively. These results were expected and mirror findings from earlier studies that reported same biomass and carbon demand ranges as well as a negligible grazing impact of sea-ice meiofauna on the Arctic ice-algal spring bloom (Gradinger, 1999; Nozais et al., 2001; Kramer, 2011). Although Ciliophora were among the most abundant taxa in the sea ice (Table 1; ***Chapter I***), their carbon demand contributed only ~ 10 % to that of the sea-ice meiofauna community in spring (***Chapter III***). Nonetheless, Ciliophora can be essential for the sympagic carbon flux since they constitute a common prey item for sympagic predators (Kramer, 2011).

Harpacticoida and Calanus species - the main grazers of ice algae in and under sea ice

In our spring study, sea-ice meiofauna biomass was dominated by Harpacticoida (92 %) at a level which has never before been reported (***Chapter III***). For example, an earlier study estimated a share of Crustacea biomass (including Harpacticoida) to the sea-ice community of 22 % (Gradinger, 1999). The dominance of Harpacticoida in abundance and biomass in our study, also resulted in their large demand for ice-algal carbon (81 % with respect to the sea-ice meiofauna community) (***Chapter III***). In spite of the different dominating taxa in our spring study and in the study of Gradinger (1999), the estimated total grazing impact of the sea-ice meiofauna communities was in the same range. This result suggests that a shift in biodiversity and/or community composition does not necessarily affect the grazing impact of the community as a whole (***Chapter III***).

Figure 11. A harpacticoid copepod from the Arctic pack ice.

Under-ice fauna was the main contributor to the sympagic carbon flux in Arctic spring. Consistent with open water zooplankton studies in the region (Auel and Hagen, 2002; Basedow et al., 2018), the majority (55 %) of under-ice fauna biomass in our study was attributed to the three *Calanus* species, which had similar relative contributions to the under-ice fauna (Table 1, ***Chapter III***). As known grazers on sea-ice algae and phytoplankton (Falk-Petersen et al., 2007; Kohlbach et al., 2016), their high grazing impact (a third of the mean carbon demand of the under-ice fauna) supports the notion that the three *Calanus* species are key drivers of the Arctic marine ecosystem by transferring primary produced carbon to higher trophic levels (e.g., Polar cod) (***Chapter III***) (Budge et al., 2008; Kohlbach et al., 2017). What consequences the above discussed replacement of *C. glacialis* with *C. finmarchicus* will have for the ecological function (e.g., carbon budget) of the under-ice community is not yet entirely clear. The impact might not be as severe, though, because copepod lipid content seems to be more related to habitat conditions than species identity (Renaud et al., 2018).

Figure 12. A female calanoid copepod from the under-ice water (0-2 m).

Mass occurrences - a hyperbiomass event alters the sympagic carbon budget

At one station in our spring study, the exceptionally high abundance of Appendicularia (***Chapter I***) translated into an estimated grazing impact similar to that of all three *Calanus* spp. together (***Chapter III***). Although the carbon demand of the herbivorous fauna in and under Arctic pack ice did not have the potential to control ice-algal or phytoplankton production in the Arctic spring (***Chapter III***), this event shows how patchiness can result in a local boost of carbon demand and therefore lower algae carbon export to other trophic levels. Appendicularia are known to undergo rapid population increases under favorable food conditions caused by their short generation time and rapid growth rates (Deibel et al., 2005; Lane et al., 2008). The observed prolonged phytoplankton growing season in the Arctic (Arrigo et al., 2012; Assmy et al., 2017) could therefore favor Appendicularia abundance. Since they constitute an important food source for Copeoda, Chaetognatha, and fish larvae in other regions (Capitanio et al., 2018), I speculate, that a boost in their biomass would attract carnivorous under-ice fauna and other pelagic predators.

Importance of allometric relationships for biomass estimations

The allometric relationships ascertained for *Themisto* spp. and *Thysanoessa* sp. in ***Chapter V*** made it possible to determine biomasses of these taxa in our studies in ***Chapter III*** and ***Chapter IV***. Such measurements are of fundamental interest when it comes to the calculation of the carbon budget for a given ecosystem, but they also give insights into intra-specific variation. Body size analysis can furthermore provide information about ecosystem functioning, e.g., hydrographical regimes and prevailing sea-ice conditions affect the size structure of benthic Nematoda assemblages in our study area (Grzelak et al., 2020). However, studies addressing allometric relationships of polar zooplankton are scarce (Auel and Werner, 2003; Mumm, 1991; Donelly et al., 1994), probably due to the time-consuming measurements for a large number of individuals. Allometric relationships (e.g., between length and weight) of one species can vary between sexes, stages, and seasons (***Chapter V***). The use of improper allometric relationships (e.g., length-weight relationships of another stage or season) can result in over- or underestimations of the biomass of a given species. Especially for a more comprehensive assessment of communities like in this thesis (***Chapter III*** and ***IV***), more studies about allometric relationships are needed to account for those variations (***Chapter V***). For any of those measurements, it is most important that the specimens are collected and processed in a standardized way, since different preservation methods can cause different results, e.g., through shrinkage of specimens preserved in Formaldehyde solution (Kapiris et al., 1997). Standardized methodology should ideally be complemented in all aspects of taxonomic

identification, measurement techniques, preservation method, and sampling procedures as suggested in the State of the Arctic Marine Biodiversity Report (SAMBR) because only such data would allow proper reproducibility and comparability (CAFF, 2017).

Amphipoda - not the most important grazers of the sympagic environment

Whereas previous studies focused in particular on the grazing impact of sympagic Amphipoda on ice algae (Werner and Auel, 2005; Hop and Pavlova, 2008; Kohlbach et al., 2016; CAFF, 2017), our spring study showed clearly that Amphipoda were among the least important grazers of the sympagic fauna (***Chapter III***). Consistent with the decline of ice Amphipoda in the Atlantic Arctic sector over the past decade (Hop and Pavlova, 2008; CAFF, 2017), the three *Calanus* species had a nine-fold higher ice-algal carbon demand than the amphipod *A. glacialis* in our spring study (***Chapter III***). A similar pattern can be assumed for our summer study where *A. glacialis* and *C. hyperboreus* had similar shares of biomasses, which therefore leads to a similar proportional carbon demand (***Chapter IV***). *A. glacialis* is a sympagic species which is known for its high trophic dependency on the ice-algal production (~ 90 %, Kohlbach et al., 2016) and represents an important food source for other ice-associated species such as Polar cod, seabirds, and seals (Bradstreet and Cross, 1982; Werner, 1997; Kohlbach et al., 2017). Therefore, *A. glacialis* is often emphasized in its key role for transferring carbon from lower to higher trophic levels in the Arctic marine food web (Werner, 1997; Scott et al., 1999; Kohlbach et al., 2016). However, our results show that determining grazing pressure on ice algae should consider all taxa of a certain habitat. A focus on only one key species such as *A. glacialis* might result in an underestimation of the grazing impact of the sympagic community.

Chaetognatha - the dominant carnivores of the sympagic community

Chaetognatha (predominantly *Eukhronia hamata* and *Parasagitta elegans)* constituted 99 % of the carbon demand of the carnivorous under-ice fauna, whereas the demand of other carnivores such as *Themisto* spp., Paraeuchaeta or *Clione limacina* was negligible, though they may have been underrepresented in the net used (***Chapter III***). The secondary production of the sympagic fauna hardly covered the carbon demand of carnivorous under-ice taxa, suggesting they fulfil their carbon demand with more pelagic prey. *E. hamata* and *P. elegans* are known predators of copepods (Kruse et al., 2010; Giesecke and González, 2012) that follow their prey distribution (David et al., 2016). Another important predator, albeit underrepresented in our study (and in SUIT catches in general, David et al., 2016) is young Polar cod (*B. saida*), which feeds on *A. glacialis*, *Calanus* spp. and the harpacticoid *Tisbe* spp. (Kohlbach et al., 2017). It is considered an important species for channeling energy flux from ice algae through *Calanus* species and

Amphipoda to top predators, such as narwhales, belugas and seabirds (Bradstreet and Cross, 1982; Welch et al., 1992). Therefore, *B. saida* is a growing subject of current research (Wang et al., 2015; Kohlbach et al., 2017; Pettitt-Wade et al., 2021). Restricted food availability for carnivores, as present in our study, could possibly disrupt the carbon flux to higher trophic levels, including top predators such as polar bears. For the latter, an even higher energy demand due to increased locomotion costs caused by sea-ice reduction was recently estimated (Pagano and Williams, 2021).

4 Implications for the future and knowledge needs

Understanding how Arctic sea-ice ecosystems respond to environmental change is crucial for marine resource management and conservation efforts. Clearly, Arctic species and ecosystems are exposed to increasing pressure induced by their rapidly changing physical and biological environment, e.g., changing in SIE, a shift from MYI to FYI, and increasing Atlantification (Serreze et al., 2007; Kwok et al., 2009; Ivanov et al., 2012; Landrum and Holland, 2020). These changes have already resulted in documented shifts in Arctic pelagic and benthic marine communities and food webs that affect ecosystem functioning (Dalpadado et al., 2012; Ershova et al., 2015, 2021; Kortsch et al., 2015; Krause-Jensen et al., 2020) and may lead to a new equilibrium of the Arctic ecosystem. Shifts in community composition, abundance, and biomass of sympagic fauna due to changes in the Arctic sea-ice regime were already forecasted in the late 2000's (Falk-Petersen et al., 2007; Bluhm and Gradinger, 2008; Kramer, 2011) and detected in recent studies (***Chapter I*** and ***Chapter III***; CAFF, 2017; Hop et al., 2020). Predictions about future Arctic biodiversity or community compositions, though, are hard to make because of the manifold interplay of factors, which could result in either increasing or decreasing overall biodiversity in the coming decades (Weslawski et al., 2009). However, a likely decrease in biodiversity for the eastern Arctic Ocean is expected (Lannuzel et al., 2020). Changes in community composition might result in no or yet unforeseeable consequences for the carbon budget of sympagic communities as seen in the example of Harpacticoida abundance shift and Nematoda disappearing in sea-ice meiofauna (***Chapter I*** and ***III***) but might also result in hyperbiomass events as seen for Appendicularia in the under-ice fauna (***Chapter I*** and ***Chapter III***). Thus, the influence of community changes on the pathways and magnitude of cryo-pelagic coupling differs accordingly and cannot be generalized (***Chapter III***). It remains to be seen if and to what extent the sympagic community can buffer environmental and biological shifts (Weslawski et al., 2009; Bluhm et al., 2011).

The forecasted shifts in sea-ice biodiversity from Protozoa, Acoela, Harpacticoida, and Nematoda dominated communities in thick pack ice to a more diverse community in

younger, thin FYI (Kramer, 2011) can only partly be confirmed (***Chapter I***). Although Acoela and Nematoda were indeed absent in our study, Harpacticoida were the predominating fauna in the FYI of the Arctic pack ice (***Chapter I***). We, therefore, rather predicted a loss of benthic originating fauna in the pack ice of the Atlantic inflow region, caused by the ongoing shift of sea-ice forming processes in the areas of the Transpolar Drift (Krumpen et al., 2019) (***Chapter I***). The recently identified interruption of the Transpolar Drift is also a possible reason for the reduced Amphipoda (especially *A. glacialis*) abundance in our studies, as discussed above (***Chapter I*** and ***Chapter IV***). To further investigate those issues, future studies should include comparisons of FYI and MYI or long-time sampling of sympagic fauna within one ice type or one region as recently published for sea-ice protists (Hop et al., 2020). Time-series samples of sympagic fauna, which were taken during the recently accomplished annual expedition MOSAiC, are an important step towards needed insights into the sympagic colonization over different seasons. Other organisms of the sea-ice food web, such as bacteria and large sub-ice algal aggregations (Fernández-Méndez et al. 2015) or fungi (Hasset and Gradinger, 2016), also need to be taken into account in future food-web studies in order to investigate their role in the sympagic food web.

Water temperature has been increasing in the inflow regions of both PW and AW forced by increasing air temperatures in Arctic and sub-Arctic regions and is related to further reduction in sea-ice cover (Bluhm et al., 2020; Polyakov et al., 2020b). Also the process of Atlantification in the Eurasian Basin is anticipated to continue over the next decades (Polyakov et al., 2020a). This process has implication for both flora and fauna of the Arctic Ocean. It is, e.g., forecasted to result in an increased pelagic PP in the study region of the Eurasian Basin due to enhanced mixing caused by the weakening of the halocline stratification (Polyakov et al., 2020a,b; Lind and Ingvaldsen, 2012). The increased open water expands the growing conditions of phytoplankton blooms (Arrigo et al., 2008), however, increasing temperatures due to increased AW inflow will also result in increasing metabolic rates that need to be compensated for by enhanced nutrient availability. This aspect exemplifies the tight connection between the physical-chemical and the biological Atlantification. Substantial inflow of *C. finmarchicus* with increasing Atlantification is hypothesized (Bonnet et al., 2005; Richardson, 2008; Polyakov et al., 2017), though this species is already carried along the outer perimeter of the Eurasian Basin with the Arctic circumpolar Boundary Current along the slope (Bluhm et al., 2020). In our study, *C. finmarchicus* was the dominant *Calanus* species (***Chapter I*** and ***Chapter III***), but it is challenging to interpret our abundances as an indication for the hypothesized replacement. Such replacement might or might not have implications for the ecosystem

functioning as explained in detail in this synthesis. As a key feeder on ice algae, *C. glacialis* is timing its seasonal migration and reproduction to the ice-algal bloom (Søreide et al., 2010; Leu et al., 2011). Thus, the enhanced sea-ice melt caused by Atlantification might result in a mismatch between the bloom and developmental stages of *C. glacialis*.

The New Arctic - a perspective

The continuing loss and transformation of sea-ice habitats in the Eurasian Basin of the New Arctic will cause shifts in the sympagic community towards less biodiversity and will favor sub-polar generalists over polar specialists. The decline in biodiversity might lead to a less resilient ecosystem even more sensitive to environmental stressors. Benthic species will steadily vanish from the sea ice and pelagic species that take advantage of less competition for resources (e.g., space and food) will dominate the sea-ice habitat. The key species of both habitats (sea-ice and under-ice water) are herbivores that depend to a significant proportion on ice-algal carbon as early available, high-quality food source. Some species shifts might therefore be driven by changes in ice-algal composition or the declining SIE, especially when sea ice is an obligatory part of their life cycle. Abrupt community changes can have cascading consequences for the carbon budget of the sympagic ecosystem but might also be outbalanced by equivalent replacement (e.g., same biomasses and secondary production rates). Species with pronounced prey-preferences (e.g., certain prey size), will be particularly affected by biodiversity shifts. The winners of the New Arctic will be those species who can adapt fast to the changing environment. However, the interruption of long-term evolved, finely tuned carbon fluxes and dependencies (e.g., reproductive synchronization with the peak of ice-algal bloom) will have consequences for the whole ecosystem. The already burdened Arctic marine ecosystem would suffer even more if anthropogenic stressors such as fisheries, offshore platforms, or tourism are not mitigated or even prohibited. The establishment of marine protected areas would be a first step to protect the Arctic ecosystem. To ensure proper resource conservation and management, it is fundamental to understand the consequences of ecological changes in sea-ice habitats as requested by the Intergovernmental Panel on Climate Change (IPCC). This thesis comprises short-term studies that provide a valuable baseline, but need to be complemented by holistic long-term observations that are indispensable for verification of the ongoing changes and adaptations in the ecosystems of the New Arctic.

References

Aagaard K, Darnall C, Greisman P. 1973. Year-long current measurements in the Greenland-Spitsbergen passage. Deep Sea Research and Oceanographic Abstracts. Elsevier.

Aagaard K, Greisman P. 1975. Toward new mass and heat budgets for the Arctic Ocean. *Journal of Geophysical Research* **80**(27): 3821-3827.

Anderson L, Björk G, Holby O, Jones E, Kattner G, et al. 1994. Water masses and circulation in the Eurasian Basin: Results from the Oden 91 expedition. *Journal of Geophysical Research: Oceans* **99**(C2): 3273-3283.

Ardyna M, Babin M, Gosselin M, Devred E, Rainville L, et al. 2014. Recent Arctic Ocean sea ice loss triggers novel fall phytoplankton blooms. *Geophysical Research Letters* **41**(17): 6207-6212.

Ardyna M, Arrigo KR. 2020. Phytoplankton dynamics in a changing Arctic Ocean. *Nature Climate Change*. doi:10.1038/s41558-020-0905-y.

Arndt CE, Pavlova O. 2005. Origin and fate of ice fauna in the Fram Strait and Svalbard area. *Marine Ecology Progress Series* **301**: 55-66.

Arndt CE, Swadling KM. 2006. Crustacea in Arctic and Antarctic Sea Ice: Distribution, Diet and Life History Strategies. *Advances in Marine Biology* 197-315.

Arrigo KR, van Dijken G, Pabi S. 2008. Impact of a shrinking Arctic ice cover on marine primary production. *Geophysical Research Letters* **35**(19). doi:10.1029/2008gl035028.

Arrigo KR, Perovich DK, Pickart RS, Brown ZW, Van Dijken GL, et al. 2012. Massive phytoplankton blooms under Arctic sea ice. *Science* **336**(6087): 1408-1408.

Arrigo KR, van Dijken GL. 2015. Continued increases in Arctic Ocean primary production. *Progress in Oceanography* **136**: 60-70.

Assmy P, Fernández-Méndez M, Duarte P, Meyer A, Randelhoff A, et al. 2017. Leads in Arctic pack ice enable early phytoplankton blooms below snow-covered sea ice. *Scientific Reports* **7**: 40850.

Auel H, Hagen W. 2002. Mesozooplankton community structure, abundance and biomass in the central Arctic Ocean. *Marine Biology* **140**(5): 1013-1021.

Auel H, Werner I. 2003. Feeding, respiration and life history of the hyperiid amphipod Themisto libellula in the Arctic marginal ice zone of the Greenland Sea. *Journal of Experimental Marine Biology and Ecology* **296**(2): 183-197.

Basedow SL, Sundfjord A, von Appen W-J, Halvorsen E, Kwasniewski S, et al. 2018. Seasonal variation in transport of zooplankton into the Arctic basin through the Atlantic gateway, Fram Strait. *Frontiers in Marine Science* **5**: 194.

Berge J, Varpe Ø, Moline M, Wold A, Renaud P, et al. 2012. Retention of ice-associated amphipods: possible consequences for an ice-free Arctic Ocean. *Biology Letters* **8**(6): 1012-1015.

Bernhardt JR, Leslie HM. 2013. Resilience to climate change in coastal marine ecosystems.

Beszczynska-Möller A, Fahrbach E, Schauer U, Hansen E. 2012. Variability in Atlantic water temperature and transport at the entrance to the Arctic Ocean, 1997–2010. *ICES Journal of Marine Science* **69**(5): 852-863.

Beuchel F, Lønne O. 2002. Population dynamics of the sympagic amphipods Gammarus wilkitzkii and Apherusa glacialis in sea ice north of Svalbard. *Polar Biology* **25**(4): 241-250.

Bluhm BA, Gradinger R. 2008. Regional variability in food availability for Arctic marine mammals. *Ecological Applications* **18**(sp2): S77-S96.

Bluhm BA, Gradinger RR, Schnack-Schiel SB. 2010. Sea ice meio-and macrofauna *Oxford, Wiley-Blackwell* **Sea Ice 2**: 357-393.

Bluhm BA, Gebruk AV, Gradinger R, Hopcroft RR, Huettmann F, et al. 2011. Arctic Marine Biodiversity An Update of Species Richness and Examples of Biodiversity Change. *Oceanography* **24**(3): 232-248.

Bluhm BA, Swadling KM, Gradinger R. 2017. Sea ice as a habitat for macrograzers. *Sea ice*: 394-414.

Bluhm BA, Hop H, Vihtakari M, Gradinger R, Iken K, et al. 2018. Sea ice meiofauna distribution on local to pan-Arctic scales. *Ecology and Evolution* **8**(4): 2350-2364. doi:10.1002/ece3.3797.

Bluhm B, Janout M, Danielson SL, Ellingsen IH, Gavrilo M, et al. 2020. Arctic continental slopes sharp gradients of physical processes affect pelagic and benthic ecosystems.

Bonnet D, Richardson A, Harris R, Hirst A, Beaugrand G, et al. 2005. An overview of Calanus helgolandicus ecology in European waters. *Progress in Oceanography* **65**(1): 1-53.

Bradstreet MS, Cross WE. 1982. Trophic relationships at high Arctic ice edges. *Arctic*: 1-12.

Broccoli A, Manabe S. 1987. The influence of continental ice, atmospheric CO 2, and land albedo on the climate of the last glacial maximum. *Climate dynamics* **1**(2): 87-99.

Brodsky K. 1967. Calanoida of the far eastern seas and polar basin of the USSR Opredeliteli po Faune SSSR 35: 1-442. *Translation: Israel Program for Scientific Translations, Jerusalem*.

Budge S, Wooller M, Springer A, Iverson SJ, McRoy C, et al. 2008. Tracing carbon flow in an arctic marine food web using fatty acid-stable isotope analysis. *Oecologia* **157**(1): 117-129.

CAFF. 2017. State of the Arctic Marine Biodiversity Report Conservation of Arctic Flora and Fauna International Secretariat, Akureyri, Iceland.

Campbell K, Mundy C, Barber D, Gosselin M. 2015. Characterizing the sea ice algae chlorophyll a–snow depth relationship over Arctic spring melt using transmitted irradiance. *Journal of Marine Systems* **147**: 76-84.

Capitanio FL, Spinelli ML, Presta ML, Aguirre GE, Cervetto G, et al. 2018. Ecological Role of Common Appendicularian Species from Shelf Waters Off Argentina. *Plankton Ecology of the Southwestern Atlantic*. Springer: 201-218.

Cardinale BJ, Duffy JE, Gonzalez A, Hooper DU, Perrings C, et al. 2012. Biodiversity loss and its impact on humanity. *Nature* **486**(7401): 59-67.

Carey A, Jr. 1985. RA (ed.): Sea Ice Biota. CRC Press. Boca Raton Florida.

Carey Jr AG, Montagna PA. 1982. Arctic Sea Ice Fauna1 Assemblage: First Approach to Description and Source of the Underice Meiofauna.

Carmack E, Polyakov I, Padman L, Fer I, Hunke E, et al. 2015. Toward quantifying the increasing role of oceanic heat in sea ice loss in the new Arctic. *Bulletin of the American Meteorological Society* **96**(12): 2079-2105.

Caron DA, Gast RJ. 2010. Heterotrophic protists associated with sea ice. *Sea ice* **2**: 327-356.

Collins RE, Rocap G, Deming JW. 2010. Persistence of bacterial and archaeal communities in sea ice through an Arctic winter. *Environmental microbiology* **12**(7): 1828-1841.

Comeau AM, Philippe B, Thaler M, Gosselin M, Poulin M, et al. 2013. Protists in Arctic drift and land-fast sea ice. *Journal of Phycology* **49**(2): 229-240.

Comiso JC. 2012. Large decadal decline of the Arctic multiyear ice cover. *Journal of Climate* **25**(4): 1176-1193.

Conover R. 1988. Comparative life histories in the genera Calanus and Neocalanus in high latitudes of the northern hemisphere. *Hydrobiologia* **167**(1): 127-142.

Conover R, Huntley M. 1991. Copepods in ice-covered seas—distribution, adaptations to seasonally limited food, metabolism, growth patterns and life cycle strategies in polar seas. *Journal of Marine Systems* **2**(1-2): 1-41.

Dalpadado P, Ingvaldsen RB, Stige LC, Bogstad B, Knutsen T, et al. 2012. Climate effects on Barents Sea ecosystem dynamics. *ICES Journal of Marine Science* **69**(7): 1303-1316.

Darnis G, Robert D, Pomerleau C, Link H, Archambault P, et al. 2012. Current state and trends in Canadian Arctic marine ecosystems: II. Heterotrophic food web, pelagic-benthic coupling, and biodiversity. *Climatic Change* **115**(1): 179-205.

David C, Lange B, Rabe B, Flores H. 2015. Community structure of under-ice fauna in the Eurasian central Arctic Ocean in relation to environmental properties of sea-ice habitats. *Marine Ecology Progress Series* **522**: 15-32. doi:10.3354/meps11156.

David C, Lange B, Krumpen T, Schaafsma F, van Franeker JA, et al. 2016. Under-ice distribution of polar cod Boreogadus saida in the central Arctic Ocean and their association with sea-ice habitat properties. *Polar Biology* **39**(6): 981-994.

Deibel D, Saunders P, Acuna J, Bochdansky A, Shiga N, et al. 2005. The role of appendicularian tunicates in the biogenic carbon cycle of three Arctic polynyas. *Response of marine ecosystems to global change: ecological impact of appendicularians*: 327-358.

Dethloff K, Handorf D, Jaiser R, Rinke A, Klinghammer P. 2019. Dynamical mechanisms of Arctic amplification. *Annals of the New York Academy of Sciences* **1436**(1): 184-194.

Doney SC, Ruckelshaus M, Duffy JE, Barry JP, Chan F, et al. 2012. Climate change impacts on marine ecosystems. *Annual Review of Marine Science* **4**(1): 11-37. doi:10.1146/annurev-marine-041911-111611.

Donnelly J, Torres J, Hopkins T, Lancraft T. 1994. Chemical composition of Antarctic zooplankton during austral fall and winter. *Polar Biology* **14**(3): 171-183.

Dupont F. 2012. Impact of sea-ice biology on overall primary production in a biophysical model of the pan-Arctic Ocean. *Journal of Geophysical Research: Oceans* **117**(C8). doi:10.1029/2011jc006983.

Dybwad C, Assmy P, Olsen LM, Peeken I, Nikolopoulos A, et al. 2021. Carbon Export in the Seasonal Sea Ice Zone North of Svalbard From Winter to Late Summer. *Frontiers in Marine Science* **7**(1137). doi:10.3389/fmars.2020.525800.

Ehrenberg C. 1853. Über neue Anschauungen des kleinsten nördlichen Polarlebens. *Monatsber Dtsch Akad Wiss Berlin* **1853**: 522-529.

Eicken H. 2003. From the microscopic, to the macroscopic, to the regional scale: growth, microstructure and properties of sea ice. *Sea ice: an introduction to its physics, chemistry, biology and geology*: 22-81.

Ershova EA, Hopcroft RR, Kosobokova KN, Matsuno K, Nelson RJ, et al. 2015. Long-term changes in summer zooplankton communities of the western Chukchi Sea, 1945–2012. *Oceanography* **28**(3): 100-115.

Ershova EA, Kosobokova KN. 2019. Cross-shelf structure and distribution of mesozooplankton communities in the East-Siberian Sea and the adjacent Arctic Ocean. *Polar Biology* **42**(7): 1353-1367. doi:10.1007/s00300-019-02523-2.

Ershova E, Kosobokova K, Banas N, Ellingsen I, Niehoff B, et al. 2021. Sea ice decline drives biogeographical shifts of key Calanus species in the central Arctic Ocean. *Global Change Biology*.

Falk-Petersen S, Pavlov V, Timofeev S, Sargent JR. 2007. Climate variability and possible effects on arctic food chains: the role of Calanus. *Arctic alpine ecosystems and people in a changing environment*. Springer: 147-166.

Falk-Petersen S, Leu E, Berge J, Kwasniewski S, Nygård H, et al. 2008. Vertical migration in high Arctic waters during autumn 2004. *Deep Sea Research Part II: Topical Studies in Oceanography* **55**(20-21): 2275-2284.

Feng Z, Ji R, Ashjian C, Campbell R, Zhang J. 2018. Biogeographic responses of the copepod Calanus glacialis to a changing Arctic marine environment. *Global Change Biology* **24**(1): e159-e170.

Fernández-Méndez M, Katlein C, Rabe B, Nicolaus M, Peeken I, et al. 2015. Photosynthetic production in the central Arctic Ocean during the record sea-ice minimum in 2012. *Biogeosciences* **12**(11): 3525-3549.

Flores H. 2009. Frozen desert alive. The role of sea ice for pelagic macrofauna and its predators: implications for the Antarctic pack-ice food web Available online:⟨ http://epic awi de/30609/1/Flores_FrozenDesertAlive_std pdf⟩

Flores H, Van Franeker JA, Siegel V, Haraldsson M, Strass V, et al. 2012. The association of Antarctic krill Euphausia superba with the under-ice habitat. *PloS one* **7**(2).

Fortier M, Fortier L, Hattori H, Saito H, Legendre L. 2001. Visual predators and the diel vertical migration of copepods under Arctic sea ice during the midnight sun. *Journal of Plankton Research* **23**(11): 1263-1278.

Friedrich C. 1997. Ökologische Untersuchungen zur Fauna des arktischen Meereises. *Ber zur Polarforschung*.

Giesecke R, González H. 2012. Distribution and feeding of chaetognaths in the epipelagic zone of the Lazarev Sea (Antarctica) during austral summer. *Polar biology* **35**(5): 689-703.

Gill M, Crane K, Hindrum R, Arneberg P, Bysveen I, et al. 2011. CAFF Monitoring Series Report No. 3-Arctic Marine Biodiversity Monitoring Plan (CBMP-MARINE PLAN). CAFF International Secretariat.

Gosselin M, Levasseur M, Wheeler PA, Horner RA, Booth BC. 1997. New measurements of phytoplankton and ice algal production in the Arctic Ocean. *Deep Sea Research Part II: Topical Studies in Oceanography* **44**(8): 1623-1644.

Gradinger R. 1999. Integrated abundance and biomass of sympagic meiofauna in Arctic and Antarctic pack ice. *Polar Biology* **22**(3): 169-177.

Gradinger R, Spindler M, Weissenberger J. 1992. On the structure and development of Arctic pack ice communities in Fram Strait: a multivariate approach. *Polar biology* **12**(8): 727-733.

Gradinger R, Friedrich C, Spindler M. 1999. Abundance, biomass and composition of the sea ice biota of the Greenland Sea pack ice. *Deep Sea Research Part II: Topical Studies in Oceanography* **46**(6-7): 1457-1472.

Gradinger RR, Bluhm BA. 2004. In-situ observations on the distribution and behavior of amphipods and Arctic cod (Boreogadus saida) under the sea ice of the High Arctic Canada Basin. *Polar Biology* **27**(10): 595-603.

Gradinger RR, Meiners K, Plumley G, Zhang Q, Bluhm BA. 2005. Abundance and composition of the sea-ice meiofauna in off-shore pack ice of the Beaufort Gyre in summer 2002 and 2003. *Polar Biology* **28**(3): 171-181.

Gradinger RR, Kaufman MR, Bluhm BA. 2009. Pivotal role of sea ice sediments in the seasonal development of near-shore Arctic fast ice biota. *Marine Ecology Progress Series* **394**: 49-63.

Gradinger R, Bluhm B, Iken K. 2010. Arctic sea-ice ridges—Safe heavens for sea-ice fauna during periods of extreme ice melt? *Deep Sea Research Part II: Topical Studies in Oceanography* **57**(1-2): 86-95.

Gradinger R, Bluhm BA. 2020. First analysis of an Arctic sea ice meiofauna food web based on abundance, biomass and stable isotope ratios. *Marine Ecology Progress Series* **634**: 29-43.

Grainger E, Hsiao SI. 1990. Trophic relationships of the sea ice meiofauna in Frobisher Bay, Arctic Canada. *Polar Biology* **10**(4): 283-292.

Granskog MA, Assmy P, Koç N. 2020. Emerging Traits of Sea Ice in the Atlantic Sector of the Arctic. *Climate Change and the White World*. Springer: 3-10.

Grebmeier JM, Overland JE, Moore SE, Farley EV, Carmack EC, et al. 2006. A major ecosystem shift in the northern Bering Sea. *Science* **311**(5766): 1461-1464.

Grebmeier JM, Moore SE, Overland JE, Frey KE, Gradinger R. 2010. Biological response to recent Pacific Arctic sea ice retreats. *Eos, Transactions American Geophysical Union* **91**(18): 161-162.

Grigor JJ, Marais AE, Falk-Petersen S, Varpe Ø. 2015. Polar night ecology of a pelagic predator, the chaetognath Parasagitta elegans. *Polar Biology* **38**(1): 87-98.

Grzelak K, Gluchowska M, Kędra M, Błażewicz M. 2020. Nematode responses to an Arctic sea-ice regime: morphometric characteristics and biomass size spectra. *Marine Environmental Research* **162**: 105181.

Gulliksen B, Lønne OJ. 1989. Distribution, abundance, and ecological importance of marine sympagic fauna in the Arctic. *Rapp PV Reun Cons Int Explor Mer* **188**: 133-138.

Gulliksen B, Lønne OJ. 1991. Sea ice macrofauna in the Antarctic and the Arctic. *Journal of Marine Systems* **2**(1-2): 53-61.

Haas C, Pfaffling A, Hendricks S, Rabenstein L, Etienne JL, et al. 2008. Reduced ice thickness in Arctic Transpolar Drift favors rapid ice retreat. *Geophysical Research Letters* **35**(17).

Hansen BW, Nielsen TG, Levinsen H. 1999. Plankton community structure and carbon cycling on the western coast of Greenland during the stratified summer situation. III. Mesozooplankton. *Aquatic Microbial Ecology* **16**(3): 233-249.

Hardge K, Peeken I, Neuhaus S, Krumpen T, Stoeck T, et al. 2017. Sea ice origin and sea ice retreat as possible drivers of variability in arctic marine protist composition. *Marine Ecology Progress Series* **571**: 43-57.

Hassett B, Gradinger R. 2016. Chytrids dominate arctic marine fungal communities. *Environmental microbiology* **18**(6): 2001-2009.

Hirche HJ. 1997. Life cycle of the copepod Calanus hyperboreus in the Greenland Sea. *Marine Biology* **128**(4): 607-618. doi:10.1007/s002270050127.

Hirche H-J. 2013. Long-term experiments on lifespan, reproductive activity and timing of reproduction in the Arctic copepod Calanus hyperboreus. *Marine biology* **160**(9): 2469-2481.

Hirche H-J, Kosobokova K. 2007. Distribution of Calanus finmarchicus in the northern North Atlantic and Arctic Ocean—expatriation and potential colonization. *Deep Sea Research Part II: Topical Studies in Oceanography* **54**(23-26): 2729-2747.

Hop H, Poltermann M, Lønne OJ, Falk-Petersen S, Korsnes R, et al. 2000. Ice amphipod distribution relative to ice density and under-ice topography in the northern Barents Sea. *Polar Biology* **23**(5): 357-367.

Hop H, Pavlova O. 2008. Distribution and biomass transport of ice amphipods in drifting sea ice around Svalbard. *Deep Sea Research Part II: Topical Studies in Oceanography* **55**(20-21): 2292-2307.

Hop H, Mundy CJ, Gosselin M, Rossnagel AL, Barber DG. 2011. Zooplankton boom and ice amphipod bust below melting sea ice in the Amundsen Gulf, Arctic Canada. *Polar Biology* **34**(12): 1947-1958. doi:10.1007/s00300-011-0991-4.

Hop H, Vihtakari M, Bluhm BA, Assmy P, Poulin M, et al. 2020. Changes in Sea-Ice Protist Diversity With Declining Sea Ice in the Arctic Ocean From the 1980s to 2010s. *Frontiers in Marine Science* **7**(243). doi:10.3389/fmars.2020.00243.

Hunt BP, Nelson RJ, Williams B, McLaughlin FA, Young KV, et al. 2014. Zooplankton community structure and dynamics in the Arctic Canada Basin during a period of intense environmental change (2004–2009). *Journal of Geophysical Research: Oceans* **119**(4): 2518-2538.

Ivanov VV, Alexeev VA, Repina I, Koldunov NV, Smirnov A. 2012. Tracing Atlantic Water signature in the Arctic sea ice cover east of Svalbard. *Advances in Meteorology* **2012**.

Jakobsson M, Grantz A, Kristoffersen Y, Macnab M. 2003. Bathymetry and physiography of the Arctic Ocean and its constituent seas. *Arctic Ocean Organic Carbon Cycle: Present and Past*. 158.

Jones EP, Anderson LG, Swift JH. 1998. Distribution of Atlantic and Pacific waters in the upper Arctic Ocean: Implications for circulation. *Geophysical Research Letters* **25**(6): 765-768.

Kapiris K, Miliou H, Moraitou-Apostolopoulou M. 1997. Effects of formaldehyde preservation on biometrical characters, biomass and biochemical composition ofAcartia clausi (Copepoda, Calanoida). *Helgoländer Meeresuntersuchungen* **51**(1): 95-106.

Kiko R, Michels J, Mizdalski E, Schnack-Schiel SB, Werner I. 2008. Living conditions, abundance and composition of the metazoan fauna in surface and sub-ice layers in pack ice of the western Weddell Sea during late spring. *Deep Sea Research Part II: Topical Studies in Oceanography* **55**(8-9): 1000-1014.

Kohlbach D, Graeve M, A. Lange B, David C, Peeken I, et al. 2016. The importance of ice algae-produced carbon in the central Arctic Ocean ecosystem: Food web

relationships revealed by lipid and stable isotope analyses. *Limnology and Oceanography* **61**(6): 2027-2044.

Kohlbach D, Schaafsma FL, Graeve M, Lebreton B, Lange BA, et al. 2017. Strong linkage of polar cod (Boreogadus saida) to sea ice algae-produced carbon: evidence from stomach content, fatty acid and stable isotope analyses. *Progress in Oceanography* **152**: 62-74.

Kohlbach D, Hop H, Wold A, Schmidt K, Smik L, et al. 2021. Multiple Trophic Markers Trace Dietary Carbon Sources in Barents Sea Zooplankton During Late Summer. *Frontiers in Marine Science* **7**: 1216.

Kortsch S, Primicerio R, Fossheim M, Dolgov AV, Aschan M. 2015. Climate change alters the structure of arctic marine food webs due to poleward shifts of boreal generalists. *Proceedings of the Royal Society B: Biological Sciences* **282**(1814): 20151546.

Kosobokova K, Hirche H-J. 2000. Zooplankton distribution across the Lomonosov Ridge, Arctic Ocean: species inventory, biomass and vertical structure. *Deep Sea Research Part I: Oceanographic Research Papers* **47**(11): 2029-2060.

Kosobokova K, Hirche H-J. 2009. Biomass of zooplankton in the eastern Arctic Ocean–a base line study. *Progress in Oceanography* **82**(4): 265-280.

Kosobokova KN, Hopcroft RR. 2010. Diversity and vertical distribution of mesozooplankton in the Arctic's Canada Basin. *Deep Sea Research Part II: Topical Studies in Oceanography* **57**(1-2): 96-110.

Kosobokova KN, Hopcroft RR, Hirche H-J. 2011. Patterns of zooplankton diversity through the depths of the Arctic's central basins. *Marine Biodiversity* **41**(1): 29-50.

Kramer M. 2011. The role of sympagic meiofauna in Arctic and Antarctic sea-ice food webs. PhD thesis.

Krause-Jensen D, Archambault P, Assis J, Bartsch I, Bischof K, et al. 2020. Imprint of climate change on pan-Arctic marine vegetation. *Frontiers in Marine Science*.

Krumpen T, Belter HJ, Boetius A, Damm E, Haas C, et al. 2019. Arctic warming interrupts the Transpolar Drift and affects long-range transport of sea ice and ice-rafted matter. *Scientific reports* **9**(1): 5459.

Kruse S, Hagen W, Bathmann U. 2010. Feeding ecology and energetics of the Antarctic chaetognaths Eukrohnia hamata, E. bathypelagica and E. bathyantarctica. *Marine biology* **157**(10): 2289-2302.

Kunisch EH, Bluhm BA, Daase M, Gradinger R, Hop H, et al. 2020. Pelagic occurrences of the ice amphipod Apherusa glacialis throughout the Arctic. *Journal of Plankton Research*. **42**(1): 73-86

Kwok R, Cunningham G, Wensnahan M, Rigor I, Zwally H, et al. 2009. Thinning and volume loss of the Arctic Ocean sea ice cover: 2003–2008. *Journal of Geophysical Research: Oceans* **114**(C7).

Landrum L, Holland MM. 2020. Extremes become routine in an emerging new Arctic. *Nature Climate Change* **10**(12): 1108-1115. doi:10.1038/s41558-020-0892-z.

Lane PV, Llinás L, Smith SL, Pilz D. 2008. Zooplankton distribution in the western Arctic during summer 2002: hydrographic habitats and implications for food chain dynamics. *Journal of Marine Systems* **70**(1-2): 97-133.

Lannuzel D, Tedesco L, Van Leeuwe M, Campbell K, Flores H, et al. 2020. The future of Arctic sea-ice biogeochemistry and ice-associated ecosystems. *Nature Climate Change* **10**(11): 983-992.

Leu E, Søreide J, Hessen D, Falk-Petersen S, Berge J. 2011. Consequences of changing sea-ice cover for primary and secondary producers in the European Arctic shelf seas: timing, quantity, and quality. *Progress in Oceanography* **90**(1-4): 18-32.

Leu E, Mundy C, Assmy P, Campbell K, Gabrielsen T, et al. 2015. Arctic spring awakening–Steering principles behind the phenology of vernal ice algal blooms. *Progress in Oceanography* **139**: 151-170.

Lewis K, van Dijken G, Arrigo K. 2020. Changes in phytoplankton concentration now drive increased Arctic Ocean primary production. *Science* **369**(6500): 198-202.

Lind S, Ingvaldsen RB. 2012. Variability and impacts of Atlantic Water entering the Barents Sea from the north. *Deep Sea Research Part I: Oceanographic Research Papers* **62**: 70-88.

Link H, Chaillou G, Forest A, Piepenburg D, Archambault P. 2013. Multivariate benthic ecosystem functioning in the Arctic–benthic fluxes explained by environmental parameters in the southeastern Beaufort Sea. *Biogeosciences* **10**(9): 5911-5929.

Liu Z. 2012. Dynamics of interdecadal climate variability: A historical perspective. *Journal of Climate* **25**(6): 1963-1995.

Madsen S, Nielsen T, Hansen B. 2001. Annual population development and production by Calanus finmarchicus, C. glacialis and C. hyperboreus in Disko Bay, western Greenland. *Mar Biol* **139**(1): 75-83.

Madsen SD, Nielsen TG, Hansen BW. 2008. Annual population development and production by small copepods in Disko Bay, western Greenland. *Marine Biology* **155**(1): 63-77.

Manabe S, Stouffer RJ. 1980. Sensitivity of a global climate model to an increase of CO2 concentration in the atmosphere. *Journal of Geophysical Research: Oceans* **85**(C10): 5529-5554.

Marquardt M, Kramer M, Carnat G, Werner I. 2011. Vertical distribution of sympagic meiofauna in sea ice in the Canadian Beaufort Sea. *Polar Biology* **34**(12): 1887-1900. doi:10.1007/s00300-011-1078-y.

Marquardt M, Majaneva S, Pitusi V, Søreide JE. 2018. Pan-Arctic distribution of the hydrozoan Sympagohydra tuuli? First record in sea ice from Svalbard (European Arctic). *Polar Biology* **41**(3): 583-588.

Matrai P, Olson E, Suttles S, Hill V, Codispoti L, et al. 2013. Synthesis of primary production in the Arctic Ocean: I. Surface waters, 1954–2007. *Progress in Oceanography* **110**: 93-106.

Matthews J, Hestad L. 1977. Ecological studies on the deep-water pelagic community of Korsfjorden, Western Norway: length/weight relationships for some macroplanktonic organisms. *Sarsia* **63**(1): 57-63.

Melnikov I, Kulikov A. 1980. The cryopelagic fauna of the central Arctic basin. *Biology of the central Arctic Basin Nauka, Moscow*: 97-111.

Meredith M, Sommerkorn M, Cassotta S, Derksen C, Ekaykin A, et al. 2019. Polar Regions. Chapter 3, IPCC Special Report on the Ocean and Cryosphere in a Changing Climate.

Michel C, Nielsen TG, Nozais C, Gosselin M. 2002. Significance of sedimentation and grazing by ice micro-and meiofauna for carbon cycling in annual sea ice (northern Baffin Bay). *Aquatic Microbial Ecology* **30**(1): 57-68.

Mumm N. 1991. Zur sommerlichen Verteilung des Mesozooplanktons im Nansen-Becken, Nordpolarmeer= On the summerly distribution of mesozooplankton in the Nansen Basin, Arctic Ocean. *Berichte zur Polarforschung (Reports on Polar Research)* **92**.

Mumm N. 1993. Composition and distribution of mesozooplankton in the Nansen Basin, Arctic Ocean, during summer. *Polar Biology* **13**(7): 451-461.

Mundy C, Ehn J, Barber D, Michel C. 2007. Influence of snow cover and algae on the spectral dependence of transmitted irradiance through Arctic landfast first-year sea ice. *Journal of Geophysical Research: Oceans* **112**(C3).

Nansen F. 1905. *The Norwegian North polar expedition, 1893-1896: scientific results*. Longmans, Green and Company.

Norkko A, Villnäs A, Norkko J, Valanko S, Pilditch C. 2013. Size matters: implications of the loss of large individuals for ecosystem function. *Scientific reports* **3**(1): 1-7.

Nozais C, Gosselin M, Michel C, Tita G. 2001. Abundance, biomass, composition and grazing impact of the sea-ice meiofauna in the North Water, northern Baffin Bay. *Marine Ecology Progress Series* **217**: 235-250. doi:10.3354/meps217235.

Olli K, Halvorsen E, Vernet M, Lavrentyev PJ, Franzè G, et al. 2019. Food Web Functions and Interactions During Spring and Summer in the Arctic Water Inflow Region: Investigated Through Inverse Modeling. *Frontiers in Marine Science* **6**(244). doi:10.3389/fmars.2019.00244.

Overland JE, Wang M. 2013. When will the summer Arctic be nearly sea ice free? *Geophysical Research Letters* **40**(10): 2097-2101.

Pagano AM, Williams TM. 2021. Physiological consequences of Arctic sea ice loss on large marine carnivores: unique responses by polar bears and narwhals. *Journal of Experimental Biology* **224**(Suppl 1).

Parkinson CL, Comiso JC. 2013. On the 2012 record low Arctic sea ice cover: Combined impact of preconditioning and an August storm. *Geophysical Research Letters* **40**(7): 1356-1361.

Peters RH, Peters RH. 1986. *The ecological implications of body size*. Cambridge university press.

Pettitt-Wade H, Loseto LL, Majewski A, Hussey NE. 2021. Cod movement ecology in a warming world: Circumpolar arctic gadids. *Fish and Fisheries*.

Pfirman S, Colony R, Nürnberg D, Eicken H, Rigor I. 1997. Reconstructing the origin and trajectory of drifting Arctic sea ice. *Journal of Geophysical Research: Oceans* **102**(C6): 12575-12586.

Piraino S, Bluhm B, Gradinger R, Boero F. 2008. Sympagohydra tuuli gen. nov. and sp. nov.(Cnidaria: Hydrozoa) a cool hydroid from the Arctic sea ice. *Marine Biological Association of the United Kingdom Journal of the Marine Biological Association of the United Kingdom* **88**(8): 1637.

Pistone K, Eisenman I, Ramanathan V. 2014. Observational determination of albedo decrease caused by vanishing Arctic sea ice. *Proceedings of the National Academy of Sciences* **111**(9): 3322-3326.

Poltermann M. 2000. Growth, production and productivity of the Arctic sympagic amphipod Gammarus wilkitzkii. *Marine Ecology Progress Series* **193**: 109-116.

Poltermann M, Hop H, Falk-Petersen S. 2000. Life under Arctic sea ice–reproduction strategies of two sympagic (ice-associated) amphipod species, Gammarus wilkitzkii and Apherusa glacialis. *Marine Biology* **136**(5): 913-920.

Polyakov IV, Walsh JE, Kwok R. 2012. Recent changes of Arctic multiyear sea ice coverage and the likely causes. *Bulletin of the American Meteorological Society* **93**(2): 145-151.

Polyakov IV, Pnyushkov AV, Alkire MB, Ashik IM, Baumann TM, et al. 2017. Greater role for Atlantic inflows on sea-ice loss in the Eurasian Basin of the Arctic Ocean. *Science* **356**(6335): 285-291. doi:10.1126/science.aai8204.

Polyakov IV, Alkire MB, Bluhm BA, Brown KA, Carmack EC, et al. 2020a. Borealization of the Arctic Ocean in Response to Anomalous Advection From Sub-Arctic Seas. *Frontiers in Marine Science* **7**(491). doi:10.3389/fmars.2020.00491.

Polyakov IV, Rippeth TP, Fer I, Alkire MB, Baumann TM, et al. 2020b. Weakening of cold halocline layer exposes sea ice to oceanic heat in the eastern Arctic Ocean. *Journal of Climate* **33**(18): 8107-8123.

Poulin M, Daugbjerg N, Gradinger R, Ilyash L, Ratkova T, et al. 2011. The pan-Arctic biodiversity of marine pelagic and sea-ice unicellular eukaryotes: a first-attempt assessment. *Marine Biodiversity* **41**(1): 13-28.

Rabenstein L, Hendricks S, Martin T, Pfaffhuber A, Haas C. 2010. Thickness and surface-properties of different sea-ice regimes within the Arctic Trans Polar Drift: Data from summers 2001, 2004 and 2007. *Journal of Geophysical Research: Oceans* **115**(C12).

Renaud PE, Daase M, Banas NS, Gabrielsen TM, Søreide JE, et al. 2018. Pelagic food-webs in a changing Arctic: a trait-based perspective suggests a mode of resilience. *ICES Journal of Marine Science* **75**(6): 1871-1881.

Richardson AJ. 2008. In hot water: zooplankton and climate change. *ICES Journal of Marine Science* **65**(3): 279-295.

Richter C. 1994. Regional and seasonal variability in the vertical distribution of mesozooplankton in the Greenland Sea. *Berichte zur Polarforschung (Reports on Polar Research)* **154**.

Riebesell U, Schloss I, Smetacek V. 1991. Aggregation of algae released from melting sea ice: implications for seeding and sedimentation. *Polar biology* **11**(4): 239-248.

Rudels B. 2015. Arctic Ocean circulation, processes and water masses: A description of observations and ideas with focus on the period prior to the International Polar Year 2007–2009. *Progress in Oceanography* **132**: 22-67. doi:https://doi.org/10.1016/j.pocean.2013.11.006.

Rudels B, Jones E, Anderson L, Kattner G. 1994. On the intermediate depth waters of the Arctic Ocean. *The polar oceans and their role in shaping the global environment* **85**: 33-46.

Rudels B, Schauer U, Björk G, Korhonen M, Pisarev S, et al. 2013. Observations of water masses and circulation in the Eurasian Basin of the Arctic Ocean from the 1990s to the late 2000s. *OS Special Issue: Ice-Atmosphere-Ocean interactions in the Arctic Ocean during IPY: the Damocles project* **9**(1): 147-169.

Sakshaug E. 2004. Primary and secondary production in the Arctic Seas. *The organic carbon cycle in the Arctic Ocean*. Springer: 57-81.

Schaafsma FL. 2018. Life in de polar oceans: the role of sea ice in the biology and ecology of marine species. PhD thesis, Wageningen University.

Schnack-Schiel SB. 2003. The macrobiology of sea ice. *Sea ice: an introduction to its physics, chemistry, biology and geology*: 211-239.

Schünemann H, Werner I. 2005. Seasonal variations in distribution patterns of sympagic meiofauna in Arctic pack ice. *Marine Biology* **146**(6): 1091-1102.

Scott CL, Falk-Petersen S, Sargent JR, Hop H, Lønne OJ, et al. 1999. Lipids and trophic interactions of ice fauna and pelagic zooplankton in the marginal ice zone of the Barents Sea. *Polar Biology* **21**(2): 65-70.

Serreze MC, Holland MM, Stroeve J. 2007. Perspectives on the Arctic's shrinking sea-ice cover. *science* **315**(5818): 1533-1536.

Solan M, Batty P, Bulling MT, Godbold JA. 2008. How biodiversity affects ecosystem processes: implications for ecological revolutions and benthic ecosystem function. *Aquatic Biology* **2**(3): 289-301.

Søreide JE, Hop H, Carroll ML, Falk-Petersen S, Hegseth EN. 2006. Seasonal food web structures and sympagic–pelagic coupling in the European Arctic revealed by stable isotopes and a two-source food web model. *Progress in Oceanography* **71**(1): 59-87.

Søreide JE, Leu E, Berge J, Graeve M, Falk-Petersen S. 2010. Timing of blooms, algal food quality and Calanus glacialis reproduction and growth in a changing Arctic. *Global change biology* **16**(11): 3154-3163.

Stachowicz JJ, Bruno JF, Duffy JE. 2007. Understanding the effects of marine biodiversity on communities and ecosystems. *Annu Rev Ecol Evol Syst* **38**: 739-766.

Steele M, Boyd T. 1998. Retreat of the cold halocline layer in the Arctic Ocean. *Journal of Geophysical Research: Oceans* **103**(C5): 10419-10435.

Tande K, Båmstedt U. 1985. Grazing rates of the copepods Calanus glacialis and C. finmarchicus in arctic waters of the Barents Sea. *Marine Biology* **87**(3): 251-258.

Tita G, Vincx M, Desrosiers G. 1999. Size spectra, body width and morphotypes of intertidal nematodes: an ecological interpretation. *Journal of the Marine Biological Association of the UK* **79**(6): 1007-1015.

UN. 2016. Transforming our world: The 2030 agenda for sustainable development.

UN. 2017. Resolution A/RES/72/73, Part XI of the Omnibus Resolution for Oceans and the law of the sea.

van Franeker JA, Flores H, Van Dorssen M. 2009. The surface and under ice trawl (SUIT). *Frozen Desert Alive-The role of sea ice for pelagic macrofauna and its predators PhD thesis University of Groningen*: 181-188.

van Leeuwe MA, Tedesco L, Arrigo KR, Assmy P, Campbell K, et al. 2018. Microalgal community structure and primary production in Arctic and Antarctic sea ice: A synthesis. *Elementa: Science of the Anthropocene* **6**.

Wang SW, Budge SM, Iken K, Gradinger RR, Springer AM, et al. 2015. Importance of sympagic production to Bering Sea zooplankton as revealed from fatty acid-carbon stable isotope analyses. *Marine Ecology Progress Series* **518**: 31-50.

Wassmann P, Kosobokova KN, Slagstad D, Drinkwater KF, Hopcroft RR, et al. 2015. The contiguous domains of Arctic Ocean advection: trails of life and death. *Progress in Oceanography* **139**: 42-65.

Weissenberger J, Dieckmann G, Gradinger R, Spindler M. 1992. Sea ice: a cast technique to examine and analyze brine pockets and channel structure. *Limnology and Oceanography* **37**(1): 179-183.

Welch HE, Bergmann MA, Siferd TD, Martin KA, Curtis MF, et al. 1992. Energy flow through the marine ecosystem of the Lancaster Sound region, arctic Canada. *Arctic*: 343-357.

Werner I. 1997. Grazing of Arctic under-ice amphipods on sea-ice algae. *Marine Ecology Progress Series* **160**: 93-99.

Werner I. 2006. Seasonal dynamics of sub-ice fauna below pack ice in the Arctic (Fram Strait). *Deep Sea Research Part I: Oceanographic Research Papers* **53**(2): 294-309.

Werner I, Arbizu PM. 1999. The sub-ice fauna of the Laptev Sea and the adjacent Arctic Ocean in summer 1995. *Polar Biology* **21**(2): 71-79.

Werner I, Auel H. 2005. Seasonal variability in abundance, respiration and lipid composition of Arctic under-ice amphipods. *Marine Ecology Progress Series* **292**: 251-262.

Weslawski J, Kwasniewski S, Stempniewicz L. 2009. Warming in the Arctic may result in the negative effects of increased biodiversity. *Polarforschung* **78**(3): 105-108.

Supplement

Table S 1. List of taxa mentioned in the general introduction and synoptic discussion (alphabetical order).

Taxa
Apherusa glacialis (Hansen, 1888)
Appendicularia Fol, 1874
Boreogadus saida (Lepechin, 1774)
Calanus finmarchicus (Gunnerus, 1765)
Calanus glacialis Jaschnov, 1955
Calanus hyperboreus Krøyer, 1838
Chaetognatha not documented
Ciliophora not documented
Clione limacina (Phipps, 1774)
Ctenophora Eschscholtz, 1829
Dinoflagellata not documented
Eukrohnia hamata (Moebius, 1875)
Foraminifera d'Orbigny, 1826
Harpacticoida G.O. Sars 1903
Mollusca not documented
Nematoda not documented
Oithona Baird, 1843 sp.
Paraeuchaeta Scott, 1909 spp.
Parasagitta elegans (Verrill,1873)
Polychaeta Grube, 1850
Radiolaria Muller, 1858
Rotifera Cuvier, 1817
Themisto Guerin, 1825 spp.
Thysanoessa Brandt, 1851
Tisbe Lilljeborg, 1853 spp.
Xenacoelomorpha Philippe, Brinkmann, Copley, Moroz, Nakano, Poustka, Wallberg, Peterson & Telford, 2011

Acknowledgements

I would like to thank:

My supervisor Angelika Brandt for the ongoing support during the last years and making this PhD possible despite change of University.

My supervisor Hauke Flores for making me a part of the *Iceflux* team, giving me the opportunity to get in touch with this fascinating research field and to attend three Polarstern expeditions that have connected me deeply with the Polar Oceans. For supporting me during the proposal writing processes and for the inspirational comments on various manuscripts.

Bodil Bluhm for introducing me into the research field of sea-ice meiofauna and to make me feel very welcome during my research stay at the UiT. For supporting me when I needed it the most, for guiding me through the jungle of the paper writing process, and for making me believe that I can do it.

Christian Möllmann, Rolf Koppelmann, and Jörg Ganzhorn for their willingness to be my PhD thesis defense committee members.

The dutch squad Bram Fey, Michiel van Dorssen, André Meijboom, and Fokje Schaafsma for the great times during the field work, for all the survival cookies and tons of coffee, for always offering a helping hand, and for the unforgettable Pink Saloon sessions. Especially Fokje, for supporting me during uncertain times and for the fruitful collaboration.

Marina Monti for the support during my study visit at the OGS, and for the nice coffee breaks by the sea in beautiful Trieste.

Dieter Wolf-Gladrow for his sympathetic ear and the good advices.

Claudia Sprengel and Claudia Hanfland from the graduate school POLMAR for all the support and for the opportunities they offer their PhD students.

People who brightened my days at AWI: Tanja Glawatty, Swantje Rogge, Pim Sprong. Doreen Kohlbach and Andreas Rogge for being my favorite roombuddies.

The one and only dudes, Erin Kunisch and Brandon Hasset for making the expedition extra special. This is to the dudes of the poles…

Giulia Castellani for all the walks and talks during the last Corona-months that kept me going, for making Bremen a little sunnier, and for being my favorite sauna and ice-coring buddy during expeditions.

The cheerleaders and sunrays of my life: Sari, Jule, Betty, Evi und Jonas, die fantastischen Drei (Jan, Erik, Mo), Marcus, Renni, Juli. Liebe.

Erik, for simply everything. Dafür, dass du mein Anfeurer, Kaffeedude, Rückzugsort, Nervenschoner und Tanzpausenpartner bist.

Mutsch, Uwe, Marie, Nili und Hanni für eure bedingungslose Unterstützung und Liebe. Peter (und Renate), Kurt und Hannelore, dafür, dass ihr mir die Liebe zur Natur weitergegeben habt.

Eidesstattliche Versicherung/ Declaration on oath

Hiermit erkläre ich an Eides statt, dass ich dir vorliegende Dissertationsschrift selbst verfasst und keine anderen als die angegebenen Quellen und Hilfsmittel benutzt habe.

I hereby declare upon oath that I have written the present dissertation independently and have not used further resources and aids than those stated.

Stadt, Datum
City, date

Unterschrift
Signature

Funding

This Dissertation was mainly funded by the national scholarships “Promotionsstipendium nach dem Hamburger Nachwuchsfördergesetz (HmbNFG)” in 2016 and 2017, both granted by the University of Hamburg.

This Dissertation was partly funded by the national scholarship “Gleichstellungsfond 2017 (4-GLF-2017)”, granted by the University of Hamburg.

The German Academic Exchange Service (DAAD) and the graduate school “POLMAR”
Of the Alfred Wegener Institute Helmholtz Centre for Polar and Marine Research partly funded my study visits at The Arctic University of Norway’s Institute of Arctic and Marine Biology in Tromsø, Norway and at the Istituto Nazionale di Oceanografia e Geofisica Sperimentale (OGS) in Trieste, Italy.

Chapter I (Paper I)

Sympagic Fauna in and Under Arctic Pack Ice in the Annual Sea-Ice System of the New Arctic

Authors:
Julia Ehrlich
Fokje L. Schaafsma
Bodil A. Bluhm
Ilka Peeken
Giulia Castellani
Angelika Brandt
Hauke Flores

This paper was published in Frontiers in Marine Science (2020).
doi: 10.3389/fmars.2020.00452

H. Flores and **J. Ehrlich** designed the sampling of this study. H. Flores, F.L. Schaafsma, and G. Castellani, collected the samples of sea-ice meiofauna and under-ice fauna. **J. Ehrlich** analyzed the sea-ice meiofauna samples under supervision of B.A. Bluhm. **J. Ehrlich** analyzed most of the under-ice fauna samples with support of F.L. Schaafsma. I. Peeken contributed to the biological dataset. G. Castellani and F.L. Schaafsma contributed to the environmental dataset. A. Brandt supervised the taxonomical accuracy of the manuscript. **J. Ehrlich** prepared all figures and tables. **J. Ehrlich** analyzed the data. B.A. Bluhm, F.L. Schaafsma, and H. Flores contributed to data interpretation. **J. Ehrlich** wrote the manuscript. **All** authors contributed to the discussion of various versions of the manuscript.

Julia Ehrlich

Dr. Hauke Flores- Supervisor

Chapter II (Paper II)

Large-Scale Variability of Physical and Biological Sea-Ice Properties in Polar Oceans

Authors:
Giulia Castellani
Fokje L. Schaafsma
Stefanie Arndt
Benjamin A. Lange
Ilka Peeken
Julia Ehrlich
Carmen David
Robert Ricker
Thomas Krumpen
Stefan Hendricks
Sandra Schwegmann
Philippe Massicotte
Hauke Flores

This paper was published in Frontiers in Marine Science (2020).
doi: 10.3389/fmars.2020.00536

G. Castellani processed the data to obtain sea-ice draft and in-ice chl *a*, and prepared most of the figures. S. Arndt processed the RAMSES data to obtain integrated irradiance and radiance values and also to extract the wavelengths. R. Ricker provided the satellite ice concentration data. P. Massicotte provided modeled downwelling irradiance data. I. Peeken supervised the Arctic sea ice biology sampling and processed all HPLC samples. F.L. Schaafsma, H. Flores, and **J. Ehrlich** contributed to develop the structure of the manuscript. F.L. Schaafsma provided information on the snow depth per each SUIT haul. T. Krumpen, S. Hendricks, S. Schwegmann, and B.A. Lange collected the EM-bird data. B.A. Lange processed and plotted the EM-data, provided in-ice chl a estimates for PS80, and carried out the spatial autocorrelation analysis. G. Castellani, H. Flores, **J. Ehrlich**, B.A. Lange, F.L. Schaafsma, and C. David contributed to SUIT data collection. **J. Ehrlich**, F.L. Schaafsma, C. David, and H. Flores contributed to data interpretation in connection with biological data. H. Flores supervised the construction of the SUIT and designed the sampling for all the campaigns and conducted statistical analyses. G. Castellani wrote the first version of the paper. **All** co-authors contributed to the discussion of results and to the preparation of the manuscript.

Julia Ehrlich

Dr. Hauke Flores- Supervisor

Chapter III (Paper III)

Sea-ice associated carbon flux in Arctic spring

Authors:
Julia Ehrlich
Bodil A. Bluhm
Ilka Peeken
Philippe Massicotte
Fokje L. Schaafsma
Giulia Castellani
Angelika Brandt
Hauke Flores

This paper will be accepted in Elementa: Science of the Anthropocene after "moderate revision".

J. Ehrlich, H. Flores, A. Brandt, and B.A. Bluhm designed the study. H. Flores, F.L. Schaafsma, G. Castellani, and I. Peeken collected the samples. **J. Ehrlich** analyzed the sea-ice meiofauna samples under supervision of B.A. Bluhm. **J. Ehrlich** analyzed most of the under-ice fauna samples with the support of F. Schaafsma. I. Peeken determined the chlorophyll *a* concentration in the sea-ice samples. G. Castellani calculated chl *a* concentration in the ice and the 0-2 m water column for all SUIT stations. **J. Ehrlich** calculated the biomass of ice-algae and phytoplankton for all stations. P. Massicotte calculated the primary production of ice algae and phytoplankton for all stations. **J. Ehrlich** calculated the biomass, carbon demand, and secondary production of sea-ice meiofauna and under-ice fauna for all stations. **J. Ehrlich** analyzed the data and prepared all figures and tables. **J. Ehrlich**, B.A. Bluhm, H. Flores, and I. Peeken contributed to data interpretation. **J. Ehrlich** wrote the manuscript. **All** authors contributed to different versions of the manuscript.

Julia Ehrlich

Dr. Hauke Flores- Supervisor

Sea-ice properties and nutrient concentration as drivers of the taxonomic and trophic structure of high-Arctic protist and metazoan communities

Authors:
Hauke Flores
Carmen David
Julia Ehrlich
Kristin Hardge
Doreen Kohlbach
Benjamin A. Lange
Barbara Niehoff
Eva-Maria Nöthig
Ilka Peeken
Katja Metfies

This paper was published in Polar Biology (2019).
doi: 10.1007/s00300-019-02526-z

H. Flores supervised the sample collection of environmental data, under-ice metazoan and epipelagic metazoan samples. **J. Ehrlich** conducted laboratory analyses of epipelagic metazoan samples. C. David conducted laboratory analyses of under-ice metazoans. K. Hardge provided protist community data based on OTU analysis and contributed to data analysis. D. Kohlbach provided size and weight data of under-ice metazoans. B.A. Lange collected and validated environmental data and provided Fig. 1. B. Niehoff supervised the epipelagic metazoan analysis. E.-M. Nöthig provided count data of phytoplankton samples and advised on aspects of phytoplankton ecology. I. Peeken provided chlorophyll and other environmental datasets. H. Flores analyzed the data. **J. Ehrlich** provided online resources for the data analysis. K. Metfies initiated the study and advised on aspects of molecular-based biodiversity and ecology. H. Flores wrote the manuscript. **All** authors contributed significantly to the drafting of this research article.

Julia Ehrlich

Dr. Hauke Flores- Supervisor

Chapter V (Paper V)

Allometric measurements of Arctic and Antarctic zooplankton and nekton

Authors:
Fokje L. Schaafsma
Carmen David
Doreen Kohlbach
Martina Vortkamp
André Meijboom
Julia Ehrlich
Giulia Castellani
Benjamin A. Lange
Antonia Immerz
Hannelore Cantzler
Anton van de Putte
Jan Andries van Franeker
Hauke Flores

This paper is in preparation for submission to Polar Biology.

Samples were collected by F.L. Schaafsma, C. David, D. Kohlbach, M. Vortkamp, A. Meijboom, **J. Ehrlich,** G. Castellani, B.A. Lange, A. Immerz, H. Cantzler, A. van de Putte, J.A. van Franeker, and H. Flores. Samples were analyzed by F.L. Schaafsma, C. David, D. Kohlbach, M. Vortkamp, A. Immerz, H. Cantzler, H. Flores. M.A. Klasmeier and N. Zakharova analyzed samples under supervision of H. Flores. The data were analyzed by F.L. Schaafsma. **J. Ehrlich** provided sources about taxonomic informations. **All** authors contributed to data validation. The figures were created by F.L. Schaafsma, H. Flores, A. van de Putte, and **J. Ehrlich**. The first manuscript was written by F.L. Schaafsma with contributions from **all** authors.

Julia Ehrlich

Dr. Hauke Flores- Supervisor

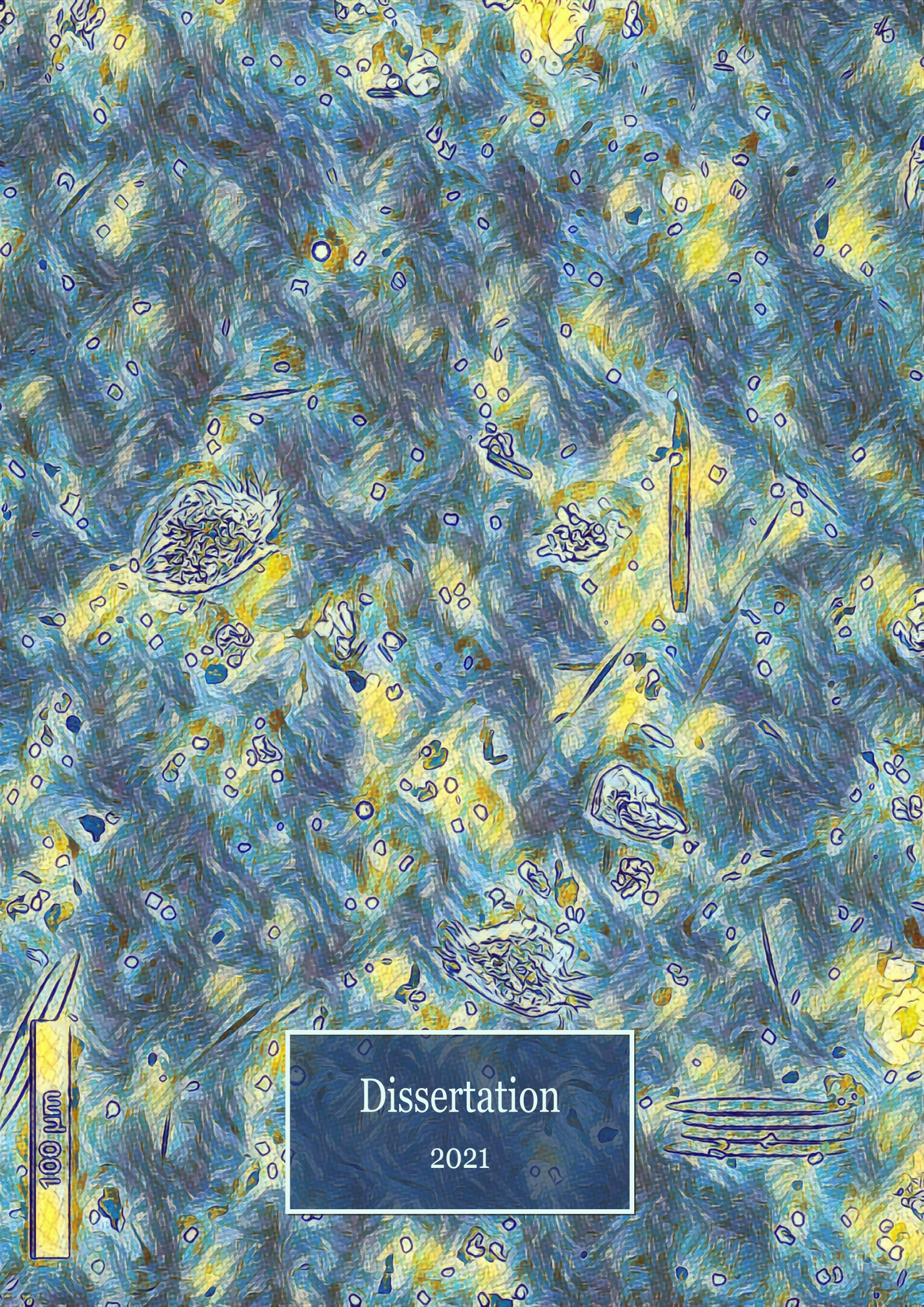

Dissertation

2021